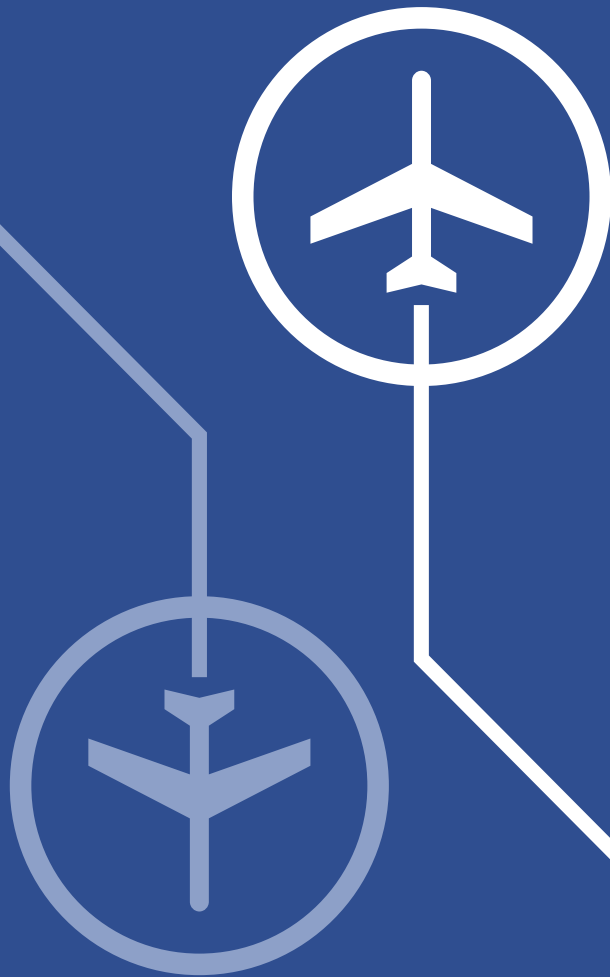


Airborne Conflict Resolution In Three Dimensions

J. Ellerbroek



Airborne Conflict Resolution In Three Dimensions

Joost Ellerbroek

ISBN/EAN 9789461918277

DOI 10.4233/uuid:96c65674-06d4-410c-87c2-b981af95211e

Copyright ©, 2013 by J. Ellerbroek

Airborne Conflict Resolution In Three Dimensions

Proefschrift

ter verkrijging van de graad van doctor
aan de Technische Universiteit Delft,
op gezag van de Rector Magnificus prof. ir. K. C. A. M. Luyben,
voorzitter van het College voor Promoties,
in het openbaar te verdedigen
op dinsdag 10 september 2013 om 15.00 uur

door

Joost ELLERBROEK

ingenieur luchtvaart en ruimtevaart
geboren te Boskoop

Dit proefschrift is goedgekeurd door de promotor:
Prof. dr. ir. M. Mulder

Copromotor: Dr. ir. M. M. van Paassen

Samenstelling promotiecommissie:

Rector Magnificus,	Voorzitter
Prof. dr. ir. M. Mulder,	Technische Universiteit Delft, promotor
Dr. ir. M. M. van Paassen,	Technische Universiteit Delft, co-promotor
Prof. dr. ir. J. M. Hoekstra,	Technische Universiteit Delft
Prof. dr. R. Curran,	Technische Universiteit Delft
Prof. dr. J. M. Flach,	Wright State University, USA
Prof. dr. P. Werkhoven,	Universiteit Utrecht
Ir. N. de Gelder,	Nationaal Lucht- en Ruimtevaart Laboratorium NLR
Prof. dr. ir. J. A. Mulder,	Technische Universiteit Delft, reservelid

Het onderzoek beschreven in dit proefschrift is financieel ondersteund door het *European Organisation for the Safety of Air Navigation (EUROCONTROL)*, binnen het Research Grant scheme for Innovative Studies, grant nr. 08-120917-C, en door het *Nationaal Lucht- en Ruimtevaartlaboratorium NLR*.

Summary

Airborne Conflict Resolution in Three Dimensions

Joost Ellerbroek

The advent of automation in the cockpit has greatly affected the nature of the tasks on the flight deck, as well as requirements on the flight crew. Although the introduction of automation in aircraft undeniably improved performance and safety, it also increased complexity in the cockpit. In addition to knowledge of basic flight information, pilots are nowadays also required to keep track of how their automated systems work. This requires a coordination of tasks between automation and human actors, and a transparency of automation that can currently not always be guaranteed.

The focus of this thesis is on the concept of airborne separation, which is proposed as part of both European and American plans for the future air-traffic management system. Such a system of airborne separation implies either partial or full delegation of separation responsibility from the controller to the aircrew. This should reduce workload for the controller on the ground, and consequently increase airspace capacity, but will also lead to a profound change on the flight deck. These plans will, in order to be realized, have substantial consequences for the degree of automation, both on the ground and in the cockpit.

To assist the flight crew with the airborne separation task, current plans propose that novel automation should be available, which provides both conflict detection and explicit resolution advisories. The flight crew will, in principle, only have to monitor the functioning of the automation, and select and apply the resolutions that it provides. They will, however, still have final responsibility for ensuring that any change of trajectory is conflict free, and that their automation is functioning properly. Maintaining a central role for the human operator is therefore a prominent part in all of the future air-traffic management plans.

Because these plans emphasize a high degree of automation, it becomes more important than ever that automation and instrumentation are transparent, and promote a high level of situation awareness. Although automation can benefit flight safety and pilot workload, it can also reduce flight crew involvement in the decision making process, with a reduction in situation awareness as a result. Ironically, the introduction of such automation therefore hampers a pilot's ability to properly reflect on the functioning of that same automation. The work in this thesis therefore aimed to investigate what information would be required for appropriate interaction between pilots and airborne separation automation, and how this information should be presented, such that it maximizes the transparency of automation and promotes proper situation awareness for the pilot.

An important aspect with these problems of automation transparency is that, regardless of specific implementation of any automated system, the complexity of the system of airborne separation as a whole, as well as that of the automated system itself, will always be directly related to the complexity of the work domain in which the system should function. An understanding of the work domain is therefore a prerequisite for understanding of the automation. In the context of airborne separation, this work domain is a complex, open system, governed by multi-dimensional and often closely inter-related parameters for airspace users and objects, all moving relative to each other, each trying to satisfy their own individual goals.

In this thesis it is argued that capturing the inherent work domain information in a functional representation should be the basis for automating

the task of airborne separation. To accomplish this, a constraint-based approach, inspired by Ecological Interface Design (EID), was employed, to provide the basis for a transparent interface to automation. This method aims to make the structure of the work domain salient, and in addition to providing a basis for automation design, should yield an interface that facilitates transparency of automation, and should support operators in constructing situation awareness.

A thorough analysis of the work domain preceded the interface designs in this thesis. This analysis identified functionalities, constraints, and relationships between elements in the work domain. The Abstraction Hierarchy (AH) was an important tool in this analysis. Its hierarchical structure, and the emphasis on relationships and dependencies between elements on levels and between levels, make the AH a valuable tool to determine the structure of the work domain, and to determine what information is required for appropriate interaction between pilots and airborne separation automation. The transition from such a work-domain analysis to an effective interface design, however, remains a prominent challenge in this approach. As with any interface design method, determining an appropriate visual form does not have a clearly defined recipe in EID. Together with continuing insights from experiments and research, this makes that the step from a work-domain analysis to an effective interface design is not an instantaneous one, but rather one where analysis, design and evaluation follow each other in an iterative process.

The displays presented in this thesis should therefore also be seen in light of the concepts that preceded them. They are two-dimensional displays, that present planar projections of the own aircraft three-dimensional maneuver space, in combination with the more traditional Horizontal and Vertical Situation Displays. These projections represent simplified, two-dimensional versions of the maneuver space. Because of this planar projection, both displays inescapably discard information about the inevitable three-dimensionality of the problem. The aim of the concepts in this thesis was, therefore, to find a representation that captures as much as possible the relevant information of the multi-dimensional separation problem.

In order to determine how to reduce the complexity of this multi-dimensional problem, this thesis considered what kind of other tasks are performed in the work domain. This means that aside from the task of airborne separation itself, also the implications of interaction with existing tasks (e.g., path planning) were examined. The two resulting concepts take two fundamentally different approaches to this visualization problem. The first concept presented an egocentric (semi-)perspective display, whereas for the second concept a co-planar approach was followed. The final comparative analysis between these two concepts favors the co-planar display, based on two arguments: First, experiments presented in this thesis, as well as those performed in other studies, showed that pilots have a strong preference for single-axis resolution maneuvers. While this does not imply that one-dimensional representations should be used, it does argue for a co-planar over a perspective display, because only a co-planar representation provides an undistorted view on the constraints along each axis. A second argument for a co-planar display can be drawn from the design of each of the constraint-based separation assistance displays. They illustrate that traffic constraints can become complex, yet precise judgment of these constraints is valuable for safe and efficient conflict resolution. They also illustrate that the planar projections of the constraints show an intuitive relation with the absolute geometry of the conflict, which benefits situation awareness.

Despite the focus on automation transparency in the design of the display concepts, in the experiments, emphasis was placed on manual conflict resolution. The reasons for this are that in nominal conditions, evaluation of an automation support tool would be trivial, as subjects would not be encouraged to participate in the assessment of conflict situations. It are the unanticipated situations where well-informed pilots, supported by good interfaces, prove their worth, but these are by definition impossible to evaluate. As an alternative, therefore, the interface concepts were evaluated as if automated resolution had already failed, and the pilots' resolution decisions were used to give insight in how the information on the display is used by pilots, and how it affects their situation awareness. This way, the pilots' ability to comprehend automated resolutions is evaluated by observing how well they make decisions themselves, based on the available information.

The results from these evaluations show that, regardless of the limited level of training that the participants received, they are able to use the visualizations to find efficient resolutions. Because these kinds of displays make several complex relationships directly perceivable, they relieve pilots from cognitive work. This transforms what would otherwise be a task that requires knowledge-based problem solving, into a simple task of perception and observation, where pilots can apply basic skills and predefined rules to safely and efficiently resolve a conflict. This allows pilots to perform well, even with a limited amount of training.

These results also show a persistent type of behavior, where after reaching a conflict-free state, the majority of the subjects returned to their original track in several small steps, following the edge of the constraint area as closely as possible. This behavior can be attributed to showing precise constraints: when maneuver limits are visualized with high precision, human operators will use that precision to maximize their efficiency. This 'hunting' behavior, however, in some instances also led to small judgment errors, which in the current context can lead to losses of separation.

It has to be noted, however, that any attempt to measure the relevant components of pilot behavior, performance, and situation awareness will always depend on the context in which the measurements are made. Predicting how a new interface would influence situation awareness in real-world situations, from measurements in a synthetic experimental environment, will therefore not always produce accurate results, even when subjects in the experiment are domain experts, and have been properly trained. Despite these limitations, and the sometimes less desired pilot behavior shown in the experiments, it is encouraging that with a very limited amount of training, pilots are able to use the displays to become more aware of their surroundings, and that they can use this information to perform the task of conflict resolution, to optimize their maneuvers, and –most importantly– to effectively reason about the conflicts they encounter. It is this deeper understanding of the work domain which will be essential for transparent interaction between operator and automation.

Contents

Summary	v
1 Introduction	1
1-1 The future of the airspace system: unmanaged airspace	2
1-2 Problem definition	4
1-3 Research approach	5
1-4 Research scope	6
1-5 Thesis outline	9
1-6 Bibliography	11
2 Background	17
2-1 Introduction	18
2-2 The horizontal separation assistance display	19
2-3 The influence of turn dynamics on horizontal constraints . . .	21
2-4 The influence of intent on horizontal constraints	23
2-4-1 Separation methods for pre- and post-TCP constraints	24

2-4-2	Calculation of post-TCP constraints	25
2-5	The vertical separation assistance display	26
2-6	Related work: Relative travel constraints	29
2-7	Related work: Separation display concepts	30
2-7-1	Expected miss-distance display	30
2-7-2	Non-veridical maneuver space display	32
2-7-3	Predictive ASAS	33
2-7-4	The HIPS display	37
2-7-5	The 3-D Cockpit Situation Display	40
2-8	Discussion	41
2-9	Bibliography	43
I	Design	49
3	Constant-velocity conflict resolution	51
3-1	Introduction	52
3-2	WDA for airborne separation	55
3-2-1	AH for airborne separation	56
3-2-2	Internal constraints	58
3-2-3	External constraints	59
3-3	Functional presentation of constraints	61
3-3-1	Traffic constraints	62
3-3-2	Production and maneuvering constraints	70
3-4	The display concept	72
3-4-1	Elements of the display	72

3-4-2	Dynamic behavior of the display	73
3-5	Practical application	74
3-6	Discussion	77
3-7	Bibliography	79
4	Co-planar representation of 3-D constraints	87
4-1	Introduction	88
4-2	Three-dimensional data visualization	90
4-2-1	Motivation for a co-planar display concept	91
4-2-2	Comparison with other three-dimensional displays	92
4-3	Functional presentation of constraints	93
4-3-1	Velocity action space	94
4-3-2	Internal constraints	95
4-3-3	External constraints	97
4-3-4	Planar constraint projections	101
4-3-5	Interactions between projection planes	102
4-4	Concept	105
4-4-1	Traditional display elements	106
4-4-2	Velocity action-space overlays	107
4-4-3	Conflict urgency visualization	110
4-4-4	Visual momentum	111
4-4-5	Comparison with previous concepts	111
4-5	Relationships between the AH and this concept	114
4-6	Practical application	115
4-7	Discussion	117

4-8	Conclusions	119
4-9	Bibliography	120
II	Evaluation	127
5	Evaluating the co-planar display concept	129
5-1	Introduction	130
5-2	The interface	132
5-3	Measuring situation awareness	134
5-4	Experiment I: Active conflict resolution	135
5-4-1	Apparatus and aircraft model	136
5-4-2	Independent variables	137
5-4-3	Experiment design and procedure	138
5-4-4	Subjects and instructions to subjects	139
5-4-5	Dependent measures	139
5-4-6	Experiment hypotheses	140
5-5	Experiment I: Results	140
5-5-1	Resolution strategy	141
5-5-2	Safety	143
5-5-3	Performance	145
5-6	Experiment II: Passive SA assessment	147
5-6-1	Apparatus	147
5-6-2	Independent variables	148
5-6-3	Experiment design and procedure	148
5-6-4	Subjects and instructions to subjects	149

5-6-5	Dependent measures	149
5-6-6	Experiment hypotheses	150
5-7	Experiment II: Results	150
5-7-1	Situation awareness scores	151
5-7-2	Response time	153
5-7-3	Post-experiment questionnaire	154
5-8	Discussion	156
5-9	Conclusions	159
5-10	Bibliography	160
6	Implicit coordination in manual airborne separation	165
6-1	Introduction	166
6-2	The interface	168
6-2-1	Functional presentation of constraints	168
6-2-2	Using the interface	172
6-2-3	Implicit coordination for manual control	172
6-3	Experiment	175
6-3-1	Apparatus and aircraft model	175
6-3-2	Experiment design and procedure	176
6-3-3	Subjects and instructions to subjects	179
6-3-4	Dependent measures	180
6-3-5	Experiment hypotheses	181
6-4	Results	182
6-4-1	Solution type and level of cooperation	182
6-4-2	Safety	187

6-4-3	Performance	187
6-4-4	Situation awareness	189
6-5	Discussion	190
6-6	Future work and recommendations	194
6-7	Conclusions	195
6-8	Bibliography	195
7	Fast-time simulations of manual conflict resolution	199
7-1	Introduction	200
7-2	Coordination rules	202
7-2-1	Coordination using rules of the air	204
7-2-2	Coordination using minimum path deviation	206
7-2-3	Combined coordination rules	207
7-3	Simulation set-up	207
7-3-1	Simulation design	208
7-3-2	Decision logic	211
7-3-3	Independent variables	212
7-3-4	Dependent measures	212
7-4	Results	213
7-4-1	Solution type and level of cooperation	213
7-4-2	Performance	221
7-5	Discussion	226
7-6	Conclusions	228
7-7	Bibliography	229

8 Discussion and conclusions	235
8-1 Design of an airborne separation assistance display	236
8-1-1 Interfacing humans, automation, and work	236
8-1-2 Visual form	237
8-2 Experimentation and evaluation	240
8-2-1 Evaluating automation transparency	241
8-2-2 Evaluating an expert tool	241
8-3 Limitations and recommendations	245
8-4 Conclusions	247
8-5 Bibliography	248
 Appendices	 255
 A Horizontal and vertical projected constraints	 257
A-1 Defining a conflict	257
A-2 Derivation of the horizontal forbidden area	259
A-3 Horizontal resolution maneuvers	260
A-4 Derivation of the vertical forbidden area	262
 B Constant-speed constraints	 265
B-1 Parametric description of three-dimensional traffic constraints	266
B-2 Constant-ownspeed constraints	266
B-3 Constant relative speed constraints	267
 C Horizontal and vertical reduced constraints	 269
C-1 Conical cutting plane	269

C-2	Horizontal flat cutting plane	271
C-3	Vertical cutting plane	272
D	Discrete event maneuver equations	273
D-1	Straight flight	273
D-2	Unaccelerated turns	274
D-3	Accelerated turns	275
D-4	Bibliography	276
	Abbreviations	277
	Symbols	281
	Samenvatting	285
	Acknowledgments	291
	Biography	293

We envision information in order to reason about, communicate, document, and preserve that knowledge – activities nearly always carried out on two-dimensional paper and computer screen. Escaping this flatland and enriching the density of data displays are the essential tasks of information design. Such escapes grow more difficult as ties of data to our familiar three-space world weaken, and as the number of dimensions increases.

– Edward R. Tufte, “Envisioning Information”, pp. 33 (1990)

The past century has been a time where technological (r)evolutions succeeded each other at an increasingly rapid pace. The aviation domain specifically has seen tremendous change, with the introduction of a multitude of electronic systems, complex automation, and multi-function interfaces on the flight deck. In just a few decades aircraft went from push-pull rods and analog gauges, to fly-by-wire controlled systems, with glass cockpits, and an extensive Flight-Management System (FMS) [2–5]. An end to these changes is not in sight.

Especially the advent of automation in the cockpit has greatly affected the nature of the tasks on the flight deck, as well as requirements on the flight crew [3, 6, 7]. Although the introduction of automation in aircraft undeniably improved performance and safety, it also increased complexity in the cockpit. In addition to knowledge of basic flight information, pilots are nowadays also required to keep track of how their automated systems work. This requires a coordination of tasks between automation and human actors, and a transparency of automation that can currently not always be guaranteed [6, 8–14].

1-1 The future of the airspace system: unmanaged airspace

In 2005, following similar plans in the United States [15, 16], the European commission defined a set of high level goals for the future of the European airspace system that will, in order to be realized, have even more far-reaching consequences for the degree of automation both on the ground, and in the cockpit. These goals envision a 3-fold increase in capacity, a level of safety performance that is increased by a factor of 10, a 10% reduction in environmental impact, and a cost reduction for Air-Traffic Management (ATM) services to airspace users of at least 50%. In 2007, these commitments were formalized with the creation of the Single European Sky ATM Research Joint Undertaking (SESAR-JU), a consortium of several European air transport stakeholders [17].

The current SESAR ATM master plan, released October 2012, defines more modest goals for 2020: a 27% increase in capacity, and an associated improvement in safety such that the total number of accidents does not grow despite traffic growth, a 2.8% environmental impact reduction, and a 6% reduction in ATM services cost [18]. The ATM master plan defines several key features for the realization of these improvements, such as a move from fixed airways to Trajectory-Based Operations (TBO), where aircraft can apply preferred routes that best meet their objectives, collaborative planning between parties involved in flight management, and new technologies that provide accurate airborne navigation and optimized spacing between aircraft.

More rigorous plans with respect to increasing capacity are planned beyond 2020. These plans propose partial and full delegation of separation responsibility from the controller to the aircrew, as a way to reduce controller workload, and consequently increase airspace capacity. In case of partial delegation, a controller would delegate separation responsibility by transferring the corresponding separation task to the respective flight crew. This delegated responsibility would be limited to separation between the designated aircraft and a specific number of reference aircraft. The transfer of responsibility would also be limited in duration, space, and scope, and has to be accepted by the aircrew to whom separation responsibility is delegated [19]. The goal of this partial delegation is to reduce controller workload, by maintaining *strategic* control of the airspace for the controller, while transferring specific *tactical* tasks (that are consistent with the controller's strategy) to the flight deck [20, 21]. Aside from reducing controller workload, airborne spacing and separation can also improve precision and efficiency, as the relevant parameter (i.e., spacing or separation distance) can be controlled directly*.

Airborne self-separation applications represent the case of full delegation, where the flight crew is responsible for proper separation from *all* other aircraft. There are several possible scenarios where this could be the case: unmanaged airspace, managed airspace that is restricted to suitably equipped aircraft, and mixed equipage managed airspace. Unmanaged airspace can be applicable in areas with low traffic density, where the risk of collision is sufficiently small. In mixed equipage managed airspace, some aircraft would receive a separation service from an Air Navigation Service Provider (ANSP), while other, suitably equipped aircraft would fly approved trajectories, but monitor their own separation.

To assist the flight crew with the task of airborne separation, they will be supported by novel automation that provides both conflict detection and explicit resolution advisories. The flight crew will, in principle, only have to monitor the functioning of the automation, and select and apply the

*When managing spacing or separation, pilots have direct control over the aircraft, allowing them to respond quickly to changes in the traffic situation. An air traffic controller, however, has several aircraft to manage, and will often have less opportunities to manage each aircraft's spacing in detail. Also, a controller can only change the trajectory of an aircraft by issuing a command to the respective aircrew.

resolutions that it provides. The flight crew will, however, still be ultimately responsible for ensuring that any change of trajectory is conflict free, and that their automation is functioning properly. SESAR, therefore, maintains a central role for the human operator in their future ATM plans.

1-2 Problem definition

The long-term plans for partially and fully delegated airborne separation that are proposed in programmes such as SESAR and NextGen will introduce a profound shift in the tasks and requirements on the flight crew, and will increase complexity on the flight deck, compared to current levels. In their new separation task, pilots will be expected to supervise a highly automated and complex system, for which even normal events are sparse (at the current level of traffic density, on average, less than one conflict would occur per flight* [22, 24, 25]). Although automation provides the resolutions, pilots will ultimately remain responsible for the validity of that resolution. They should therefore be able to monitor the proper functioning of the automation, and they should be able to intervene in case the automation fails. In other words, pilots should be able to detect, and act upon very infrequent situations that were not anticipated in the design of the automation.

Because current plans for airborne separation emphasize a high degree of automation, it becomes more important than ever that automation and instrumentation are transparent, and promote a high level of situation awareness. Although automation can benefit flight safety and pilot workload [3, 10, 26–29], it can also reduce flight crew involvement in the decision making process, with a reduction in situation awareness as a result. Ironically, the introduction of such automation therefore hampers a pilot's ability to properly reflect on the functioning of that same automation [27, 30–35]. This leads to the fundamental question of how the human actors can interact, and share their decision-making with the automation [6, 8, 9, 11, 13, 36–38], and what needs to be presented to optimize human performance from the

*In specific areas, with very dense traffic, this conflict rate increases to around one conflict per hour [22, 23]. More generally, the local conflict rate (the amount of conflicts observed from the perspective of an individual aircraft) is directly proportional to the amount of flights within a given area, whereas the global conflict rate (as perceived by a centralized observer, i.e., an air traffic controller) scales quadratically with increasing traffic density [22, 23].

perspective of situation awareness [39]. These issues form the main topic for this thesis, and the problem statement can be formulated as follows:

Problem statement

What information is required for appropriate interaction between pilots and airborne separation automation, and how can this information be presented such that it maximizes the transparency of automation and proper situation awareness for the pilot?

An important aspect with these problems of automation transparency is that, regardless of specific implementation of any automated system, the complexity of the system of airborne separation as a whole, as well as that of the automated system itself, will always be directly related to the complexity of the work domain in which the system should function. An understanding of the work domain is therefore a prerequisite for understanding of the automation. In the context of airborne separation, this work domain is a complex, open system, governed by multi-dimensional and inter-related parameters for airspace users and objects, all moving relative to each other, each trying to satisfy their individual goals. Capturing this information in a functional presentation should be the basis for any airborne separation display.

1-3 Research approach

The concepts presented in this thesis employ a constraint-based approach, inspired by Ecological Interface Design (EID), a proven design paradigm from the domain of process control [40, 41], to provide the basis for a transparent interface to automation, that makes the structure of the work domain salient, and supports operators in their buildup of situation awareness [42, 43].

EID is a method that addresses the cognitive interaction between humans and complex socio-technical systems. Its approach to interface design gives priority to the workers environment, or 'ecology', focusing on how the environment poses constraints on the worker [42, 43]. Ecological displays are designed to allow for direct perception of the possibilities and constraints afforded by the work domain [44, 45]. The theory behind EID puts emphasis on the fact that problems that cannot be anticipated in the design

of automation are inherent to complex and open systems, and that creative human experts therefore continue to be important resources when dealing with these unanticipated events.

The design of an interface for airborne separation assistance will be preceded by a thorough analysis of the work domain, which should identify functionalities, constraints, and relationships between elements in the work domain. An important element in this analysis will be the Abstraction Hierarchy (AH), developed by Rasmussen [46]. The abstraction hierarchy is a work-domain analysis tool that presents a stratified, hierarchical description of the workspace. Each stratum of the hierarchy represents the same system, but on a different level of abstraction. The levels are connected by means-end relationships between the adjacent levels. Along the vertical axis, commonly five levels represent the workspace at decreasing levels of abstraction, starting at the top with the purpose(s) for which the system was designed, all the way down to the spatial topology, properties, and appearance of the components that make up the system on the bottom level [46, 47]. Several studies that conducted a workspace analysis for the air transport domain showed that dividing the horizontal dimension of the AH between items “internal”, and “external” to the aircraft, provides a logical structure for an abstraction hierarchy that describes this domain [48–50].

The hierarchical structure of the AH, and the emphasis on relationships and dependencies between elements on levels and between levels, make the AH a valuable tool to determine the structure of the work domain, and to determine what information is required for appropriate interaction between pilots and airborne separation automation. The transition from such a workspace analysis to an effective interface design remains a prominent challenge in this approach. The step from a work domain analysis to an effective design is not an instantaneous one, but rather one where analysis, design and evaluation follow each other in an iterative process.

1-4 Research scope

The motivation for this research has its basis in the plans for the future of the airspace as foreseen by SESAR. Many of the assumptions and limitations on this research therefore also relate to the promises and assumptions made

in the various stages of the SESAR ATM master plan. The most relevant assumptions are summarized here by topic.

Air-traffic system properties: The display designs and corresponding evaluations limit themselves to unmanaged airspace, where aircraft fly optimized, four-dimensional trajectories, that have been determined and coordinated completely before the actual flight. To resolve traffic (or other) conflicts that result from uncertainties that arise during flight (e.g., bad weather, departure delays), automated systems are in place that detect conflicts, and provide resolution advisories to the pilot. The pilot's task is one of monitoring separation, and selecting and applying resolution advisories, provided by the automation. They should, however, be able to intervene in case the automation fails.

Although airborne separation has applications throughout the flight (self-separation in unmanaged airspace during cruise, self-separation in managed airspace, spacing applications, ...), in this research only self-separation in unmanaged airspace is considered. Also, while future trajectories of other aircraft (intruder intent) can significantly influence maneuver constraints, this research will focus on tactical maneuvering, relying on current state information.

The applicability of separation application is also such, that conflicts below 60 seconds to loss of separation, and conflicts where a loss of separation has already taken place, are not considered. Below 60 seconds, collision avoidance systems like the Traffic Collision Avoidance System II (TCAS2) must take over in order to prevent collision [51]. The display concepts and experiment designs also do not consider the effects of wind. This research acknowledges the fact that wind can affect maneuverability both in terms of aircraft performance and relative motion, but the initial focus of the separation assistance interfaces lies purely with traffic separation, as other factors might distract from this analysis.

Airborne automation and systems: The premise is that an airborne separation application will be developed based principally on information received via Automatic Dependent Surveillance – Broadcast (ADS-B), considering only the currently defined ADS-B message content [52]. It is acknowledged that ADS-B will evolve during the years before airborne separation

applications are actually implemented, but these changes will not play a role in the current research.

Although this research is motivated by the need for a shared representation between automation and the human operator, automated conflict resolution itself does not feature in this research. Experimental evaluations in this research are based on scenarios where resolution advisories are not available, and the pilot has only the work domain visualizations to manually resolve a conflict.

Non-nominal evaluation conditions: The traffic scenarios that will be used in the experimental evaluations in this research mostly represent situations that would not likely occur under normal operations. Conflicts will be on a shorter timescale, and relative orientations are not necessarily representative of commonly occurring conflicts. Instead, conflicts are designed to provide measurable results, and sometimes also to elicit specific behavior. System malfunctions and emergency situations are not considered in the current research.

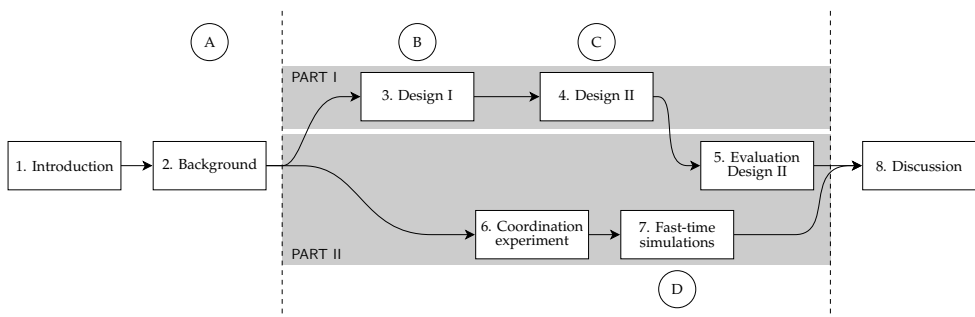


Figure 1.1: Structure of this thesis. In this diagram, each rectangle represents a chapter, each circle represents an appendix. Chapters are sorted chronologically in horizontal direction, and are vertically separated in two parts, where chapters in Part I discuss display designs, and chapters in Part II describe experiments and their results. Chapters in the middle section all correspond to papers that are either published, or submitted. The arrows represent research paths.

1-5 Thesis outline

This thesis consists of eight chapters, shown in chronological order in Figure 1.1. All chapters, except for Chapter 1 (Introduction), Chapter 2 (Background), and Chapter 8 (Discussion), consist of papers that have either been published or submitted. The content of these chapters corresponds directly with the content of the original papers. The titles of the chapters, however, have been adapted to emphasize the structure of the thesis. The chapters are ordered in two parts: The first part considers the interface designs that resulted from this research, the second part covers the evaluation experiments. Figure 1.1 also shows two research paths. Here, the top path represents the main research path of new display designs and their evaluation. The second path represents an additional research direction that was performed in this work (coordination in manual conflict resolution). Each chapter is preceded by a short introduction, that illustrates how it is related to the overall research, and, when applicable, a publication summary, stating the original title of the work, the co-authors, and further publication details.

Chapter 2: Background This chapter provides a summary of the constraint-based separation assistance display concepts that either preceded, or were developed alongside the concepts in this thesis. The first horizontal and vertical display concepts are discussed, as well as methods to visualize the influence of maneuver dynamics and intruder intent. It also gives a brief overview of related research performed by others, and illustrates how their work relates to the work presented in this thesis.

Chapter 3: Constant-velocity conflict resolution This chapter presents a separation assistance display concept that presents traffic constraints in a 'heading - flight-path angle action space'. A pilot preference for constant-velocity maneuvers motivated this choice of design. The resulting display resembles a Primary-Flight Display, with overlays for flight-path vector constraints, and conflict geometry visualization. A work-domain analysis is included in the chapter which was used to identify the constraints and interactions that define traffic conflict resolution in a heading - flight-path angle action space.

Chapter 4: Co-planar representation of 3-D constraints This chapter describes a concept for a co-planar airborne separation display. The decision

for a co-planar display is a departure from the aim of the concept described in Chapter 3, which was to create a single, integrated presentation of the three-dimensional constraints. This chapter therefore describes the motivation for this design change, before presenting the visualization methods and the resulting display concept. The co-planar display concept presents speed, heading, and altitude action possibilities in two planar projections of the three-dimensional maneuver action space. The display also provides visualizations of the interactions between these planes of projection, as well as methods to improve the visual momentum across displays.

Chapter 5: Evaluation of the co-planar concept This chapter presents the results from two experiments that were conducted to evaluate the co-planar display concept introduced in Chapter 4. In both experiments, the co-planar display concept is compared with a display that is very similar, but lacks the visualization of the interaction between projection planes. The first experiment concerns an active conflict resolution task, that investigates how operator performance and behavior are influenced by the visualization. The second experiment consisted of a passive situation awareness assessment. Together, these experiments cover each of the three main categories of situation awareness measures: Explicit, implicit, as well as subjective methods are used to assess situation awareness.

Chapter 6: Implicit coordination in manual conflict resolution Most of the concepts that preceded this research, as well as the concepts presented in this thesis, are evaluated one way or another, with a number of professional pilot subjects, who are asked to resolve conflicts with simulated traffic. Because conflicts are resolved in a decentralized fashion, however, coordination between actors in each conflict is no longer trivial, especially when manual conflict resolution is concerned. This chapter, therefore, describes an experiment that evaluates the horizontal separation assistance display concept described in Chapter 2, in a set of conflict scenarios where all aircraft in each conflict were controlled by actual pilots.

Chapter 7: Fast-time simulations of manual conflict resolution This chapter presents the results of a fast-time batch simulation study, that investigated emergent features of conflict detection and resolution in unmanaged airspace. This simulation study is a follow-up of the experiment described in Chapter 6. Because the particular measures employed in this experiment

required sample group sizes that well exceed a practical experiment setup, a simulation study can be used as a way to extrapolate findings to larger sample sizes.

Chapter 8: Discussion and conclusions This chapter combines results and conclusions from each of the preceding chapters. It aims to obtain an overarching view on the challenges of designing a situation awareness tool for airborne separation, and to illustrate how the concepts developed in this thesis face up to complex, real-world applications. This chapter also discusses the difficulties of evaluating tools designed to be used by experts, especially those created for domains that do not yet exist.

1-6 Bibliography

- [1] **E. R. Tufte.** *Envisioning Information*. Cheshire, CT: Graphics Press, 1990. ISBN 978-0961392116.
- [2] **E. J. Lovesey.** The Instrument Explosion – A Study of Aircraft Cockpit Instruments. *Applied Ergonomics*, 8(1), 23–30, 1977.
- [3] **C. E. Billings.** Human-Centered Aircraft Automation: A Concept and Guidelines. NASA Technical Memorandum TM-103885, NASA Ames Research Center, Moffett Field (CA), 1991.
- [4] **F. J. Abbink.** Integrated Free Flight and 4-D Gate-to-gate Air Traffic Management, Possibilities, Promises and Problems. NLR Technical Paper TP 96239 U, National Aerospace Laboratory, Amsterdam, 1996.
- [5] **C. R. Spitzer.** *The Avionics Handbook*. CRC Press, Boca Raton (FL), 2001.
- [6] **K. Christoffersen** and **D. D. Woods.** How To Make Automated Systems Team Players. In: **E. Salas**, ed., *Advances in Human Performance and Cognitive Engineering Research*, vol. 2, chap. 1, pp. 1—12. Elsevier, 2002. ISBN 0-7623-0864-8.
- [7] **D. L. Damos**, **R. S. John**, and **E. A. Lyall.** Pilot Activities and the Level of Cockpit Automation. *The International Journal of Aviation Psychology*, 15(3), 251–268, 2005.

-
- [8] **D. A. Norman.** The “Problem” of Automation: Inappropriate Feedback and Interaction, not “Over-Automation”. *Philosophical Transactions of the Royal Society of London*, 327(1241), 585–593, 1990. ISSN 0962-8436. doi: 10.1098/rstb.1990.0101.
- [9] **N. B. Sarter** and **D. D. Woods.** Pilot Interaction With Cockpit Automation: Operational Experiences With the Flight Management System. *The International Journal of Aviation Psychology*, 2(4), 303–321, 1992. doi:10.1207/s15327108ijap0204_5.
- [10] **C. E. Billings.** Human-Centered Aviation Automation: Principles and Guidelines. *Nasa Technical Memorandum*, (February), 1996.
- [11] **R. Parasuraman** and **V. Riley.** Humans and Automation: Use, Misuse, Disuse, Abuse. *Human Factors*, 39(2), 230–253, 1997.
- [12] **G. Lintern, T. Waite,** and **D. A. Talleur.** Functional Interface Design for the Modern Aircraft Cockpit. *The International Journal of Aviation Psychology*, 9(3), 225–240, 1999.
- [13] **A. M. Bisantz** and **A. R. Pritchett.** Measuring the Fit Between Human Judgments and Automated Alerting Algorithms: A Study of Collision Detection. *Human Factors*, 45(2), 266–280, 2003.
- [14] **S. W. A. Dekker.** On the Other Side of Promise: What Should We Automate Today? In: **D. Harris**, ed., *Human Factors for Civil Flight Deck Design*, pp. 141–155. Ashgate Pub Ltd, 2004.
- [15] **JPDO.** Concept of Operations for the Next Generation Air Transportation System, Version 2.0. Tech. rep., Joint Planning and Development Office, 2007.
- [16] **Federal Aviation Administration.** Nextgen Implementation Plan 2012. Tech. Rep. March, 2012.
- [17] **SESAR Consortium.** SESAR Definition Phase D3: The ATM Target Concept. Tech. Rep. DLM-0612-001-02-00, Eurocontrol, 2007.
- [18] **SESAR Consortium.** European ATM Master Plan - Edition 2. Tech. rep., SESAR-JU, 2012.

-
- [19] **Federal Aviation Administration and Eurocontrol.** Long-Term ADS-B and ASAS Applications: Operational Role of Airborne Surveillance in Separating Traffic. Tech. rep., 2009.
- [20] **Federal Aviation Administration and Eurocontrol.** Principles of Operation for the Use of Airborne Separation Assurance Systems. Tech. Rep. PO-ASAS-V7.1, Federal Aviation Authorities - Eurocontrol, 2001.
- [21] **International Civil Aviation Organization (ICAO).** Global Air Traffic Management Operational Concept. Tech. rep., ICAO, 2005.
- [22] **S. Ratcliffe.** ‘Free Flight’ for Air Traffic in Europe. *Journal of Navigation*, 52(2), 289—295, 1999.
- [23] **J. M. Hoekstra, R. C. J. Ruigrok, and R. N. H. W. van Gent.** Free flight in a crowded airspace? In: *3rd USA/Europe Air Traffic Management R&D Seminar Napoli*, 2000.
- [24] **K. D. Bilimoria and H. Q. Lee.** Properties of Air-Traffic Conflicts for Free and Structured Routing. In: *AIAA Guidance, Navigation, and Control Conference and Exhibit*, August, 2001.
- [25] **M. R. Jardin.** Air traffic conflict models. In: *4th AIAA Aviation, Technology, Integration, and Operations*, September, pp. 1–13, 2004.
- [26] **J. Reason.** *Human Error*. New York: Cambridge University Press, 1990.
- [27] **E. L. Wiener and R. E. Curry.** Flight-Deck Automation: Promises and Problems. *Ergonomics*, 23(10), 995–1011, 1980.
- [28] **D. A. Boehm-Davis, R. E. Curry, E. L. Wiener, and R. L. Harrison.** Human Factors of Flight-Deck Automation: Report on a NASA-Industry Workshop. *Ergonomics*, 26(10), 953–961, 1983.
- [29] **A. R. Pritchett, B. Vándor, and K. Edwards.** Testing and Implementing Cockpit Alerting Systems. *Reliability Engineering and System Safety* 75, pp. 193–206, 2002.
- [30] **E. J. Bass and A. R. Pritchett.** Human-Automated Judge Learning: A Methodology for Examining Human Interaction With Information Analysis Automation. *IEEE Transactions on Systems, Man, and Cybernetics, part A: Systems and Humans*, 38(4), 759–776, 2008.

- [31] **L. Bainbridge.** Ironies of Automation. In: **J. Rasmussen**, ed., *New Technology and Human Error*. John Wiley and Sons, 1987.
- [32] **M. R. Endsley** and **E. O. Kiris.** The Out-of-the-Loop Performance Problem and Level of Control in Automation. *Human Factors*, 2(37), 381–394, 1995.
- [33] **M. R. Endsley.** Automation and Situation Awareness. In: **R. Parasuraman** and **M. Mouloua**, eds., *Automation and Human Performance: Theory and Applications*, pp. 163–181. Hillsdale, NJ: Erlbaum Associates, 1996.
- [34] **B. McGuinness.** Implications of Cockpit Automation for Crew Situational Awareness. In: *Proceedings of the Conference on Human Performance, Situation Awareness and Automation: User-Centered Design for the New Millennium*, pp. 101–106, 2000.
- [35] **N. B. Sarter** and **D. D. Woods.** Pilot Interaction with Cockpit Automation II: An Experimental Study of Pilot’s Model and Awareness of the Flight Management System. *The International Journal of Aviation Psychology*, 4(1), 1–28, 1994.
- [36] **G. Lintern.** An Affordance-Based Perspective on Human-Machine Interface Design. *Ecological Psychology*, 12(1), 65–69, 2000.
- [37] **B. Hilburn**, **R. Parasuraman**, **P. Jha**, and **K. McGarry.** Emerging Human Factors Issues in Future Air Traffic Management, 2006.
- [38] **A. Q. V. Dao**, **S. Brandt**, **V. Battiste**, **K. P. Vu**, **T. Strybel**, and **W. W. Johnson.** The Impact of Automation Assisted Aircraft Separation on Situation Awareness. In: *Human Interface and the Management of Information. Information and Interaction*, pp. 738–747. Springer, 2009.
- [39] **J. M. Flach**, **M. Mulder**, and **M. M. van Paassen.** The Concept of the Situation in Psychology. In: **S. P. Banbury** and **S. Tremblay**, eds., *A Cognitive Approach to Situation Awareness: Theory and Application*, pp. 42–60. Ashgate, 2004. ISBN 978-0-7546-4198-8.
- [40] **K. J. Vicente.** Ecological Interface Design: Progress and Challenges. *Human Factors*, 44, 62–78, 2002.

- [41] **G. A. Jamieson.** Ecological Interface Design for Petrochemical Process Control: An Empirical Assessment. *IEEE Transactions on Systems, Man, and Cybernetics, part A: Systems and Humans*, 37(6), 906–920, 2007. doi: 10.1109/TSMCA.2007.897583.
- [42] **K. J. Vicente** and **J. Rasmussen.** Ecological Interface Design: Theoretical Foundations. *IEEE Transactions on Systems, Man, and Cybernetics*, 22(4), 589–606, 1992.
- [43] **C. M. Burns** and **J. R. Hajdukiewicz.** *Ecological Interface Design*. CRC Press LLC, FL: Boca Raton, 2004. ISBN 0415283744.
- [44] **J. J. Gibson.** *The Ecological Approach to Visual Perception*. Houghton Mifflin, 1979. ISBN 0-89859-959-8.
- [45] **K. J. Vicente** and **J. Rasmussen.** The Ecology of Human-Machine Systems II: Mediating Direct-Perception in Complex Work Domains. *Ecological Psychology*, 2(3), 207–249, 1990.
- [46] **J. Rasmussen.** The Role of Hierarchical Knowledge Representation in Decision Making and System Management. *IEEE Transactions on Systems, Man, and Cybernetics*, 15(2), 234–243, 1985.
- [47] **A. M. Bisantz** and **K. J. Vicente.** Making the Abstraction Hierarchy Concrete. *International Journal of Human-Computer Studies*, 40, 83–117, 1994.
- [48] **C. Borst**, **H. C. H. Suijkerbuijk**, **M. Mulder**, and **M. M. van Paassen.** Ecological Interface Design for Terrain Awareness. *International Journal of Aviation Psychology*, 16(4), 375–400, 2006.
- [49] **M. M. van Paassen**, **M. H. J. Amelink**, **C. Borst**, **S. B. J. van Dam**, and **M. Mulder.** The Chicken, the Egg, the Workspace Analysis, and the Ecological Interface. In: *International Symposium on Aviation Psychology*. Faculty of Aerospace Engineering, Delft University of Technology, Dayton, USA, 2007.
- [50] **C. Borst**, **F. A. Sjer**, **M. Mulder**, **M. M. van Paassen**, and **J. A. Mulder.** Ecological Approach to Support Pilot Terrain Awareness After Total Engine Failure. *Journal of Aircraft*, 45(1), 159–171, 2008.

- [51] **Radio Technical Commission for Aeronautics.** Minimal Operational Performance Standards for Traffic Alert and Collision Avoidance System 2 (TCAS2) Airborne Equipment. Tech. rep., Federal Aviation Authorities, 2002.
- [52] **Radio Technical Commission for Aeronautics.** Minimum operational performance standards for 1090 MHz extended squitter automatic dependent surveillance-broadcast (ADS-B) and traffic information. Tech. rep., RTCA, Washington D.C., 2006.

This chapter provides a summary of the constraint-based separation assistance display concepts that either preceded, or were developed alongside the concepts in this thesis. The first horizontal and vertical display concepts are discussed, as well as methods to visualize the influence of maneuver dynamics and intruder intent. It also gives a brief overview of related research performed by others, and illustrates how their work relates to the work presented in this thesis.

2-1 Introduction

The concepts presented in this thesis can be considered a part of a line of research that has been active (on and off) since nearly fifteen years. As a response to the proposed system of 'Free Flight', which aimed* to increase efficiency through deregulation of certain parts of the airspace, initial work focused on obtaining a functional model of unmanaged airspace [1–3]. Such a functional model should reveal structure, functions and relationships that are otherwise hidden in the complexity of the system, and can be applied in the design of operator support systems (displays, but also automation, both airborne and ground-based), and in the definition of structure and rules of the unmanaged airspace system as a whole.

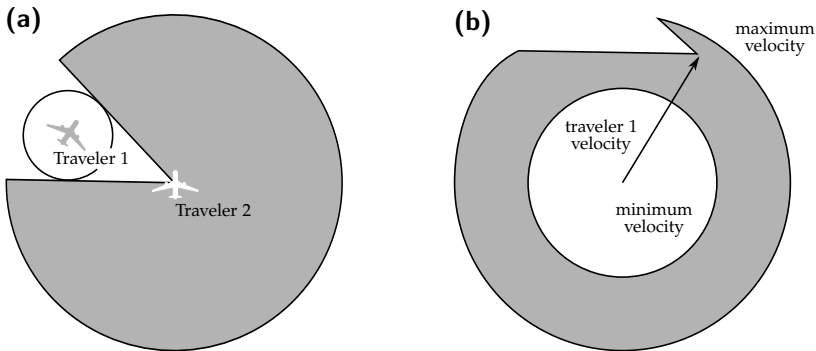


Figure 2.1: Permissible velocities for travelers in unmanaged airspace. The left figure (a) indicates the permissible *relative* velocities for traveler 2. In the right figure (b), this is transformed to permissible *absolute* travel speeds for traveler 2. (Adapted from van Paassen (1999) [1]).

Figure 2.1(a) gives a functional presentation of how the affordances of a part of airspace are affected by the proximity of an obstacle [1]. It shows how locomotion affordances are affected by obstacles (both stationary and moving), in terms of the motion relative to that obstacle. Figure 2.1(b) shows that affordances for the absolute velocity of the traveler can be obtained through vector summation of the area of inadmissible velocities and the velocity of the intruding traveler. This representation turned out to be the

*The concept of Free Flight has, since then, undergone several changes, including its name. In this thesis, the more general term 'unmanaged airspace' will be used instead.

basis for several concepts that were developed in the following fifteen years, including those presented in this thesis.

The first display concept based on this model was in the form of a horizontal separation assistance display, which was based on a Boeing Navigation Display (ND). Later iterations added compensation for non-instant turn dynamics [4, 5], own aircraft and intruder intent [4, 6], and a concept for a vertical separation assistance display [7]. The remainder of this chapter will illustrate these design concepts.

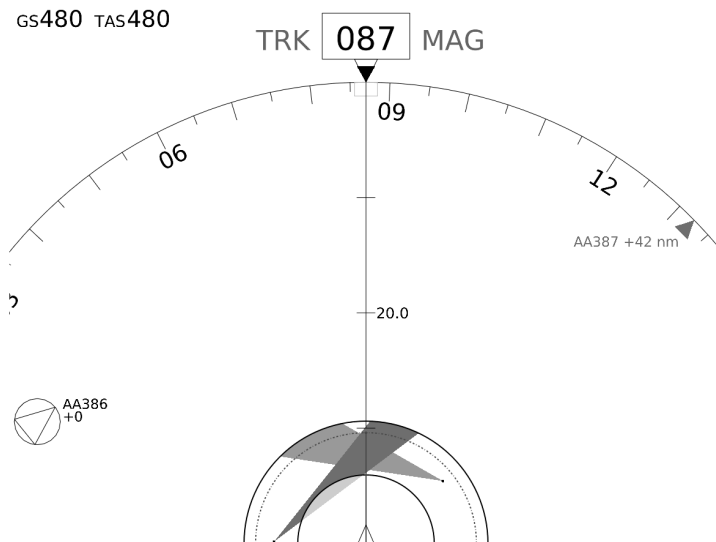


Figure 2.2: The horizontal separation assistance display is based on a classical horizontal situation display, with an added separation assistance overlay (at the bottom of this figure). The overlay provides a functional presentation of the affordances for aircraft airspeed and track angle using a horizontal projection of the three-dimensional velocity-vector affordance space (Taken from Ellerbroek et al. [8]).

2-2 The horizontal separation assistance display

The horizontal separation assistance display is the first practical display implementation that employed the functional model introduced by van Paassen (1999) [1, 5]. Figure 2.2 gives an impression of the display concept, which is based on a classical horizontal situation display. The aim of this concept

is to provide a meaningful, integrated representation of separation-related information in the horizontal plane. This is achieved by combining the existing spatial representation of airspace elements, with a *velocity action space*, that relates own aircraft velocity and heading to several relevant constraints.

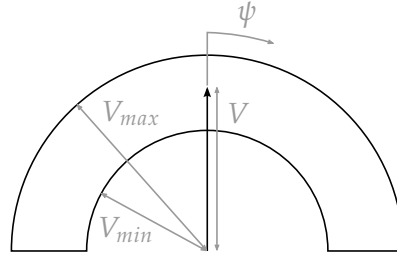


Figure 2.3: The State-Vector Envelope is a vector space that represents combinations of velocity (V) and heading (ψ) that can be obtained by ownship. The minimum (V_{min}) and maximum (V_{max}) obtainable airspeed constraints give it its ring-shaped appearance.

This action space, referred to as the *State-Vector Envelope (SVE)*, is essentially a vector space that contains all possible velocity vectors (i.e., all combinations of velocity and heading). The boundaries of this action space are determined by the aircraft performance limits, see Figure 2.3. The aircraft minimum and maximum operating speeds result in the concentric circular boundaries of the horizontal SVE. A horizontal situation display in expanded mode (as in Figure 2.2) does not show traffic behind the own aircraft. To match this mode, the horizontal state-vector envelope also shows only solutions with $|\Delta\chi| \leq 90^\circ$. Current horizontal situation displays also have modes that show the situation behind the ownship. In such a mode, the horizontal state-vector envelope would be shown as a whole circle, similar to the representation in Figure 2.1(b).

Figure 2.4 shows how the traffic separation constraints can be expressed in a velocity space. In this figure, \mathbf{V}_{rel} represents the motion of ownship, relative to the intruder aircraft:

$$\mathbf{V}_{rel} = \mathbf{V}_{own} - \mathbf{V}_{int} \quad 2.1$$

The figure also shows that when the relative path of ownship intersects with the minimum separation circle, separation will eventually be lost, with a minimum separation of d_{CPA} . It can also be seen that the area between the

two lines tangent to the intruder separation circle represents an instantaneous, complete set of relative velocities that result in an eventual loss of separation. This area is referred to as a *forbidden area*, or *FA*.

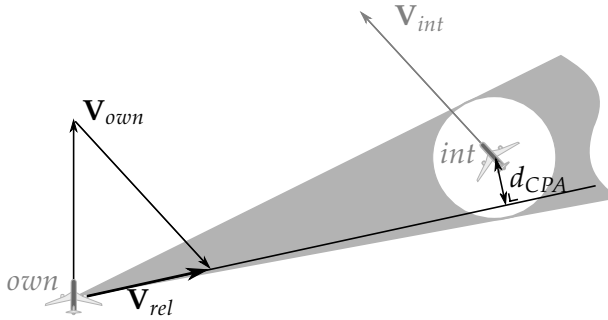


Figure 2.4: Traffic separation constraints can be expressed in a velocity action space, through observation of the relative motion between two aircraft. All relative paths of ownship, that intersect with the separation circle of the intruder aircraft, eventually lead to a loss of separation. Hence, the area between the two lines tangent to the intruder separation circle represents an instantaneous, complete set of conflicting relative velocities. In this figure, *own* is the observed aircraft, and *int* the intruder. \mathbf{V}_{own} is the observed aircraft velocity vector, \mathbf{V}_{int} is the intruder velocity vector, \mathbf{V}_{rel} is the relative velocity vector, and d_{CPA} is the distance at the closest point of approach.

A disadvantage of this relative velocity representation, however, is that it is hard for pilots to relate a velocity constraint zone expressed in *relative space*, to the affordances for control of their own aircraft in *absolute space*. The relation between the relative and absolute space can be made visible by translating the forbidden area and relative velocity vector by the intruder velocity vector. This would be equivalent to adding \mathbf{V}_{int} on both sides of the equal sign in Equation (2.1): the equation is still valid, but the relation between the ownship velocity vector and the relative velocity forbidden area is made explicit.

2-3 The influence of turn dynamics on horizontal constraints

The *velocity space* visualization of the horizontal separation assistance display reveals horizontal maneuver options, under the assumption that maneuver dynamics and duration can be neglected. For short-term conflicts

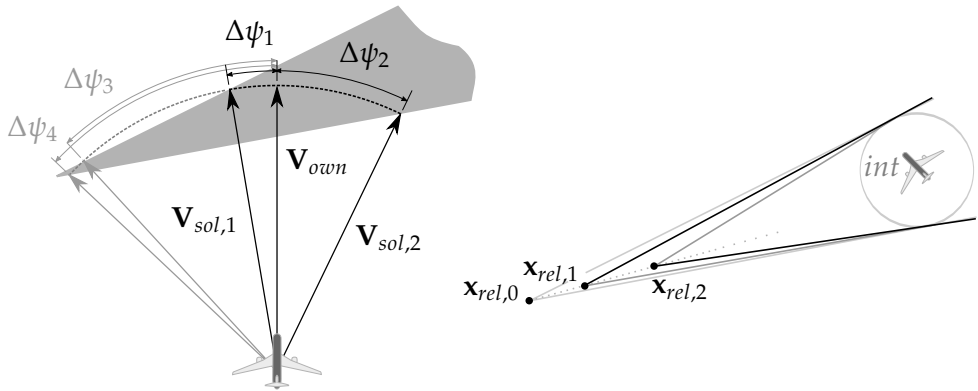


Figure 2.5: Heading maneuver solutions in a traffic conflict.

Figure 2.6: Corrected forbidden area legs derived from extrapolated relative positions.

this assumption is no longer valid, and maneuver duration needs to be taken into account [9]. Compensating maneuver dynamics was therefore the focus of the succeeding design iteration of the horizontal separation display.

The resulting modified concept compensates for turn duration by calculating the forbidden area legs at time $t_{cur} + t_{turn}$. Here, t_{turn} is the maneuver duration for the heading solution that corresponds to the respective forbidden area leg, see Figure 2.5. Depending on the airspeed and the relative position of the intruder, zero, one or two heading solutions can lie along each forbidden area leg. The smallest heading change solution is taken for each leg to obtain a turn duration [10]:

$$t_{turn} = \frac{\Delta\psi}{\dot{\psi}} = \frac{\Delta\psi \cdot V_{TAS}}{g \cdot \tan \phi} \quad 2.2$$

Figure 2.6 shows how the resulting turn durations are used to extrapolate new relative positions. These relative positions are then used to calculate corrected orientations for the corresponding forbidden area legs.

This leg correction is slightly overestimated, as the extrapolation of the new relative position assumes that the relative velocity vector does not

change. Because the resolution maneuver moves the relative velocity vector towards the forbidden area leg, the angular expansion rate of that leg is reduced, and the leg position at the end of the maneuver will be less expanded than initially calculated. A more precise leg position could be derived by iteratively calculating new leg positions and corresponding turn durations. In the modified separation assistance display, however, the lack of precision is used as an added margin.

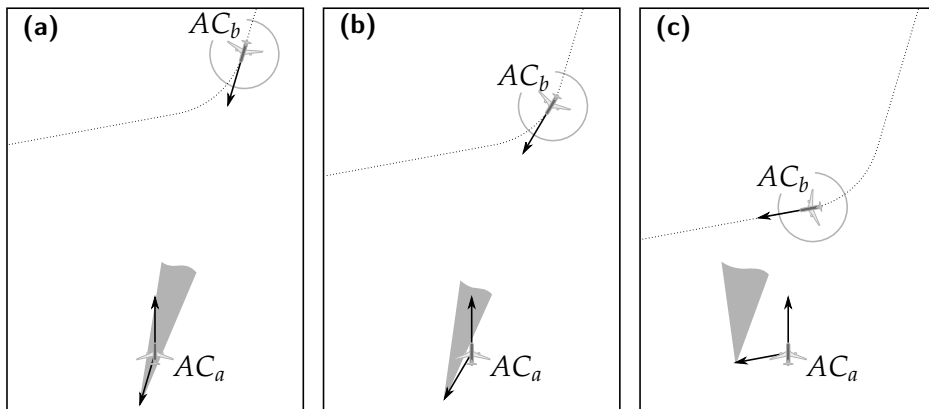


Figure 2.7: The influence of intruder intent on horizontal maneuvering constraints. **(a):** The initial track of aircraft AC_b does not create a conflict with aircraft AC_a . **(b):** When AC_b initiates a turn, a conflict is created with AC_a . Without information about the target state of aircraft AC_b (depicted in **(c)**), the pilot of AC_a does not know whether an evasive maneuver is required to remain sufficiently separated.

2-4 The influence of intent on horizontal constraints

The previously described concept for a horizontal separation assistance display employs only the current states of ownship and intruders to derive constraints imposed by other traffic on ownship maneuvering. This method requires the assumption that ownship and intruder state remain constant in the near future. When this is not the case, the affordance space will change as a function of space and time due to Trajectory Change Points (TCP), and other changes of state or intent, see Figure 2.7. Several studies have illustrated methods to visualize intent in the forbidden areas [6, 11, 12]. Each of these methods makes use of the fact that the dimension along the bisector of

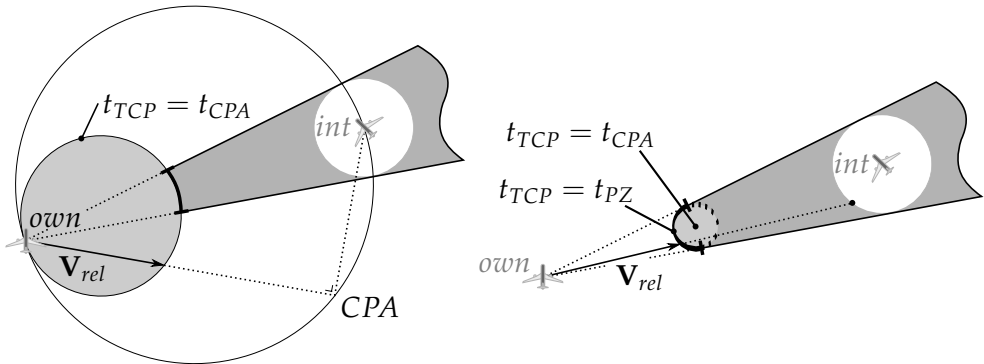


Figure 2.8: Forbidden area division using constant time to closest point of approach. **Figure 2.9:** Forbidden area division using constant time to loss of separation.

the triangular forbidden area is related to the time at which the closest point of approach with the respective intruder will occur, with the triangle origin representing $t_{CPA} = \infty$. A change in state at $t = t_{TCP}$ will therefore result in a change in the forbidden area at the point where $t_{CPA} = t_{TCP}$. The state change at $t = t_{TCP}$ causes the triangular forbidden area based on the current intruder state to become invalid for $t_{TCP} < t < \infty$, i.e., the part nearer to the tip of the triangle no longer represents accurate constraints.

2-4-1 Separation methods for pre- and post-TCP constraints

The visualization methods in [6, 11, 12] provide two methods to select the useful part of the forbidden area. Figure 2.8 illustrates the method used by van Dam et al. [6]. In this method, a set of relative velocities is constructed that lead to a time to closest point of approach that is less than, or equal to the time left for the intruder to reach the trajectory change point. All relative velocity vectors outside this area (the shaded circle in Figure 2.8), but inside the forbidden area will lead to a loss of separation before the intruder reaches the trajectory change point. This part of the forbidden area therefore corresponds to valid constraints, and should be maintained in the visualization.

The second method, elaborated by Hermes et al. [11] and Mercado-Velasco et al. [12], uses time to loss of separation to select the valid part of the forbidden area, see Figure 2.9. This method looks at circles around points of time to collision t_c (points along the bisector of the forbidden area), that are tangent to both forbidden area legs. The relative velocity vectors at points in this circle correspond with relative positions with respect to intruder at the same points in the protected zone circle, for $t = t_c$. The points along the leading edge of the velocity circle (indicated with a thick line in Figure 2.9) therefore correspond to relative velocities that result in a loss of separation at $t = t_c$. Hence, the velocity circle around $t = t_{TCP}$ can be used to select the relevant part of the respective forbidden area.

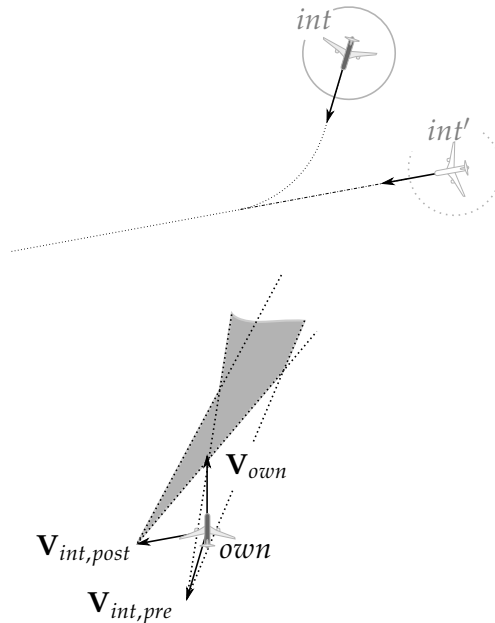


Figure 2.10: Derivation of post-TCP constraints. Here, int is the intruder at the current position, int' is the intruder at the virtual position. $\mathbf{V}_{int,pre}$ is the pre-TCP intruder velocity, and $\mathbf{V}_{int,post}$ is the post-TCP intruder velocity.

2-4-2 Calculation of post-TCP constraints

The post-TCP constraints can be derived by constructing a virtual position of the intruder along the target (post-TCP) track. These virtual points are

placed at such a distance from the start of the actual track, that this ‘virtual intruder’ is at the same distance in time from the TCP compared to the actual position of the intruder, see Figure 2.10. The forbidden area for this ‘virtual intruder’ then gives the *current-time* constraints for the *future* (post-TCP) track of the intruder. This forbidden area can be combined with the current-state forbidden area using one of the two methods described above. Corrections of the forbidden area for intermediate states in the turn can be constructed using additional virtual intruders at virtual tracks tangent to the arc of the turn.

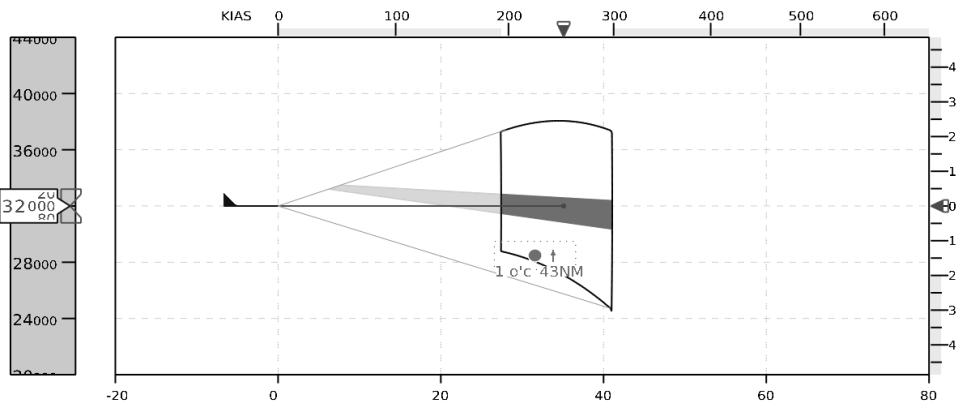


Figure 2.11: The vertical separation assistance display is based on a vertical situation display, with an added separation assistance overlay. Similar to the horizontal concept, the overlay provides a functional presentation of the affordances for aircraft airspeed and flight-path angle using a side-view projection of the three-dimensional velocity-vector affordance space (Taken from Ellerbroek et al. [13]).

2-5 The vertical separation assistance display

For the vertical separation assistance display concept, the same principles of the functional model for horizontal travel have been applied to a side-view projection of the traffic situation. This results in a similar combination of a spatial representation of the airspace elements, with a *velocity action space*, which in this case combines traffic and performance constraints on vertical maneuvering.

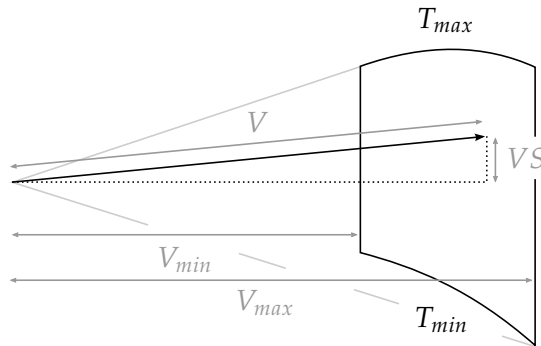


Figure 2.12: The vertical State-Vector Envelope is a vector space that represents combinations of velocity (V) and flightpath angle (γ) that can be obtained by ownship. It is constrained by the minimum (V_{min}) and maximum (V_{max}) obtainable airspeeds. Aircraft performance with maximum (T_{max}) and minimum (T_{min}) thrust settings determine maximum steady climb and descent, respectively.

The vertical action space shows the affordances for vertical maneuvering in terms of airspeed and vertical speed, see Figure 2.12. Similar to its horizontal counterpart, the boundaries of this action space are determined by aircraft performance limits. The vertical edges result from the limits on aircraft airspeed. The minimum speed line can refer to the stall speed of the aircraft, or the minimum operating speed, but the visualization can also show a combination of these speeds. Similarly, the maximum speed line can refer to the never-exceed speed, but also the maximum operating speed, or a combination.

The curved edge at the top of the action space visualizes the maximum obtainable steady climb at each velocity. These climb angles are achieved with maximum throttle settings. Depending on the phase of flight, these settings represent Maximum Takeoff Thrust (MTO), Maximum Climb Thrust (MCL), or Maximum Continuous Thrust (MCT). The relationship between the flight-path angle and the engine thrust is obtained by dividing the amount of excess thrust by the weight of the aircraft [10]:

$$\sin \gamma = \frac{T - D}{W} \quad 2.3$$

The bottom edge indicates steady descent at idle thrust for each velocity. For the initial concept of the vertical separation display, it was assumed that

idle thrust corresponds to ‘unpowered’ or ‘gliding’ flight, where T equals 0. The descent angles for each velocity can then be obtained by solving the following polynomial for γ [10]:

$$0 = \frac{\rho_{SSL}\sigma C_{D0}}{2(W/S)} V^4 + \gamma V^2 + \frac{2K(W/S)}{\rho_{SSL}\sigma} \quad 2.4$$

It should be noted that in reality there is still a certain amount of thrust at idle throttle, which should be taken into account when determining steady maximum descent.

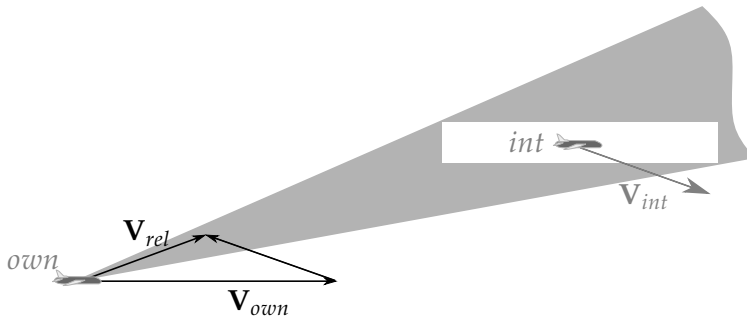


Figure 2.13: Traffic constraints on vertical maneuvering can also be expressed in a velocity action space, through observation of the relative vertical motion. When viewed from the side, the intruder protected zone appears rectangular. The area between the two lines tangent to the outside corners of the intruder protected zone represents an instantaneous, complete set of conflicting relative velocities. In this figure, *own* is the observed aircraft, and *int* the intruder. \mathbf{V}_{own} is the observed aircraft velocity vector, \mathbf{V}_{int} is the intruder velocity vector, and \mathbf{V}_{rel} is the relative velocity vector.

Figure 2.13 shows how the constraints on vertical maneuvering, as imposed by other traffic, can be constructed from the conflict geometry. When viewed from the side, the intruder protected zone appears as a rectangular area, 10 nmi wide, and 2,000 feet high. Similar to the horizontal traffic constraints, a triangular *forbidden area* can be constructed by observing that the area between two lines tangent to the far corners of the intruder protected zone corresponds to the set of vertical relative velocity vectors that result in a conflict between ownship and the respective intruder. As with the forbidden areas in the horizontal separation assistance display, the vertical forbidden areas are also translated by the intruder velocity vector in the final visualization. This way, the constraints can be directly related to ownship maneuvers, and constraints from multiple intruders combine visually

to reveal resolution options that simultaneously solve all detected conflicts, without creating a new conflict with other (detected) traffic.

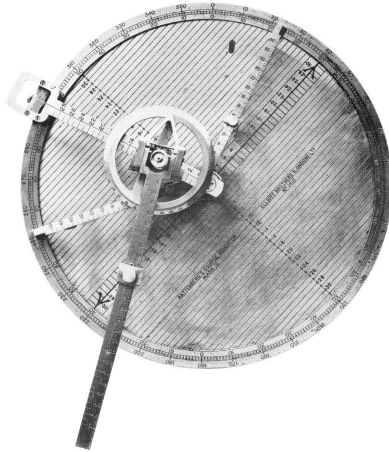


Figure 2.14: The Battenberg course indicator (Taken from *OU 5274: Remarks on Handling Ships* (1934)).

2-6 Related work: Relative travel constraints

The concepts for relative travel visualization used in this study are not new. Already in 1892, Prince Louis of Battenberg, then naval advisor in the British Navy, invented the *Battenberg Course Indicator*, a mechanical device that allowed seamen to investigate relative orientation and motion between ships, see Figure 2.14 [15, 16]. By manipulating a set of bars and sliders, the device can be used to visually perform vector summations, to determine missing angles and lengths in distance and speed triangles*. More recent work also presents visualizations similar to the horizontal display concept presented in Section 2-2, that have been developed as collision avoidance aids for maritime navigation [17–19].

*Consider, for instance, a situation where you want to converge on a specific bearing with another ship, and that you know your own speed, and the speed and bearing of the other ship. In this situation, the course indicator can be used to determine the required course, and the resulting closing speed, i.e., the two missing parameters in the triangle of your own velocity vector, the velocity vector of the other ship, and the relative velocity vector. This triangle is essentially what you construct on the course indicator.

In the field of robotics there have also been several (parallel) investigations on what is now commonly called the *velocity obstacle theory*. Comparable to the *forbidden areas* in this study, a velocity obstacle represents the set of velocities for an actor that will result in a collision with a moving obstacle within a certain timespan, under the assumption that the motion of that obstacle is constant [20–22]. These studies consider horizontal motion only. One of the studies combines the velocity obstacles with own maneuvering constraints [21], similar to the internal constraints that are visualized in the concepts in this thesis.

2-7 Related work: Separation display concepts

Although most current research on airborne separation assistance systems focuses on the development of automated systems that assist pilots with the separation task [23–27], there are also several display concepts that have been developed as aids in the task of self-separation [28–34]. There are two distinct types of conflict representation that are used in these displays: a spatial representation, which is similar to traditional situation displays, and a maneuver-space representation, i.e., visualizing how proximate traffic limits ownship maneuverability in terms of airspeed, heading, and vertical speed. Some displays use only one of these representations, others combine them. A second distinctive factor between displays is whether they show explicit (automated) commands, maneuvering constraints, or a combination of both.

The remainder of this section will discuss five displays. The expected miss-distance display [33] and the non-veridical maneuver space display [34] are both maneuver-space representations. The Predictive ASAS display [30] combines a maneuver-space representation with a spatial representation. The final two displays provide only spatial representations.

2-7-1 Expected miss-distance display

A display format proposed by Gates et al. [33] (see Figure 2.15) presents collision avoidance contours that resemble the display concept presented in Chapter 3. Despite the similarity between Gates' display and the display in Chapter 3, the contours in Gates' display describe a different property of the conflict. Instead of the 'velocity obstacle' approach of the current

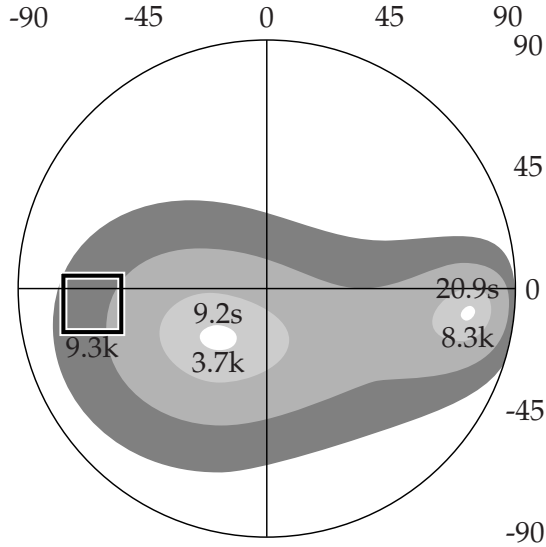


Figure 2.15: Collision avoidance display showing contours of expected miss-distance, adapted from Gates et al. [33]. The values along the horizontal and vertical axes are azimuth and zenith angles of the projection, respectively. The values in the figure are time to closest point of approach in seconds, and expected miss distance in feet $\times 1,000$. The square shows the line of sight to the relevant aircraft, with the relative distance in feet $\times 1,000$.

study, Gates' proposed format considers contours of equal (three-dimensional) Expected Miss-Distance (EMD). With this method, the contour for an expected miss-distance of 5 nautical miles would be equal to the contour of the flight-path vector constraints in the concept presented in Chapter 3. Intruder relative bearing is indicated with a hollow square. The size of this square corresponds to the distance between ownship and intruder.

The main difference between Gates' display concept and the concept presented in Chapter 3, however, lies in the applicable timescale. The EMD display is presented as a collision avoidance display, and therefore aimed at short-term conflicts, whereas the concepts presented in this thesis are aimed at airborne separation, which considers medium to long-term conflicts. This difference is visible in the way information is presented on each display. By showing contours of expected miss-distance, Gates' display reveals maneuvers that maximize separation to avoid a mid-air collision. The separation

assistance concepts, on the other hand, emphasize time to loss of separation, to allow pilots to judge conflicts based on urgency. In terms of expected miss-distance the separation assistance displays only differentiate between values below and values above the minimum separation constraint (i.e., inside or outside the forbidden areas, respectively). The exact value of the expected miss-distance within the separation minimum, here, is less important, as long as there is still enough time to maneuver out of a conflict.

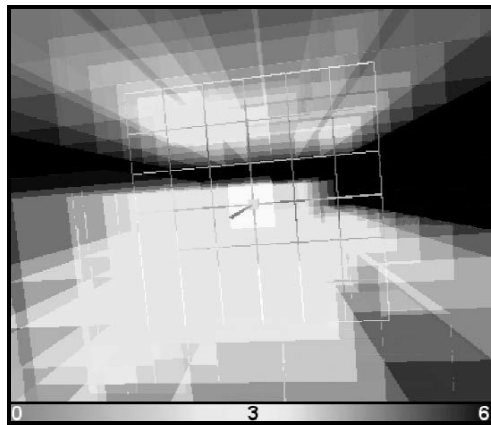


Figure 2.16: Separation assistance display concept that shows a discrete, three-dimensional maneuver space using translucent cubes to represent conflicting states. Adapted from Knecht [34].

2-7-2 Non-veridical maneuver space display

Figure 2.16 shows a display concept by Knecht [34], which also has similarities to the concepts in this thesis. His display concept shows a three-dimensional maneuver space, that is segmented in translucent ‘cubes’. Each cube represents an individual maneuver (i.e., one discrete combination of autopilot settings *velocity*, *heading*, and *vertical speed*). Colored cubes represent conflicting maneuvers, hence selecting a clear cube ensures a conflict-free velocity vector. The fact that each maneuver is visualized with a three-dimensional cube makes this display concept highly non-veridical, which makes it difficult to pair constraints with the intruder aircraft that cause these constraints. It also makes it difficult to predict how a conflict will evolve over time, and how a situation will change when an evasive maneuver is made.

The impact of the high non-veridicality of the display is one of the main aspects that Knecht tried to investigate in the experimental evaluations of this concept.

Even though this display shows constraints which allow pilots to investigate their own maneuver strategies, the fact that the shape of these constraints is not predictable, and that the display does not show how constraints relate to the intruding aircraft that cause these constraints, makes this concept less suitable as a situation awareness tool. This is also the main factor that sets this concept apart from the work presented in this thesis.

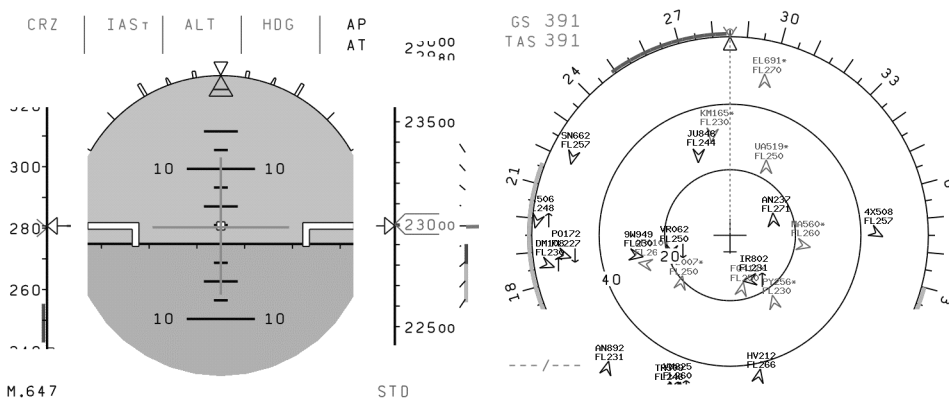


Figure 2.17: The P-ASAS display. Heading constraints are shown in bands along the compass rose on a navigation display. On the primary flight display, velocity constraint bands are added to the speed tape, and vertical speed constraint bands are added to the vertical speed indicator. Figure adapted from Hoekstra [30].

2-7-3 Predictive ASAS

The Predictive ASAS (P-ASAS) display was designed as an addition to an automated conflict detection and resolution system, to correct for deficiencies found in the initial evaluation of this automated system [25, 30]. It added bands of conflicting heading, speed, and vertical rate, to the navigation display, and the speed tape and vertical speed indicator on the primary flight display, respectively, see Figure 2.17. These bands represent predictions for each maneuver possibility whether this maneuver would result in a loss of separation. Each (potential) conflict can correspond with at most one band

on the speed tape and vertical speed indicator, and with at most two bands on the heading compass. Color coding is used to indicate the urgency for each of these bands. The final P-ASAS concept combines this display with the existing automated conflict detection and resolution system.

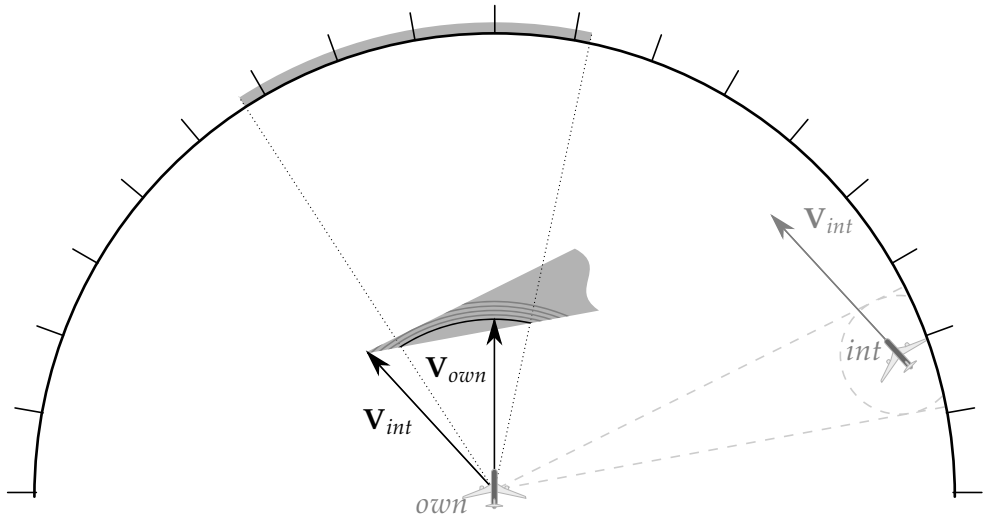


Figure 2.18: Relation between the forbidden areas and the heading bands of the P-ASAS display, for horizontal conflicts. By observing circular sets of velocity vectors for varying values of airspeed, it can be seen that the horizontal forbidden area is a combination of heading bands for all possible values of ownship airspeed.

Figure 2.18 shows how the horizontal bands in the P-ASAS display relate to the horizontal forbidden areas in Section 2-2, when both aircraft are flying level at the same altitude*. The figure illustrates that a horizontal forbidden area can be seen as a set of heading bands for all possible values of ownship airspeed. What the forbidden areas therefore add, compared to the bands on the P-ASAS display, is that they show how velocity and heading constraints (for the horizontal FAs) interact, i.e., how constraints in one dimension vary, when the other parameter is varied. A problem that was acknowledged for the P-ASAS bands, is that it is often difficult to pair constraint bands with their respective intruder aircraft symbols, especially

*Vertical maneuvering and a vertical offset between aircraft in a conflict can result in smaller horizontal constraints, an effect that is taken into account in the calculation of the constraint bands in the P-ASAS display. This effect will be explained further in Chapter 4.

when multiple constraint bands overlap [30]. The forbidden areas, however, have several properties that increase visual momentum between constraints and aircraft symbols, such as the apex of a forbidden area, which represents the intruder velocity vector, and the bisector of the forbidden area, which corresponds to the relative bearing of the intruder, with respect to ownship.

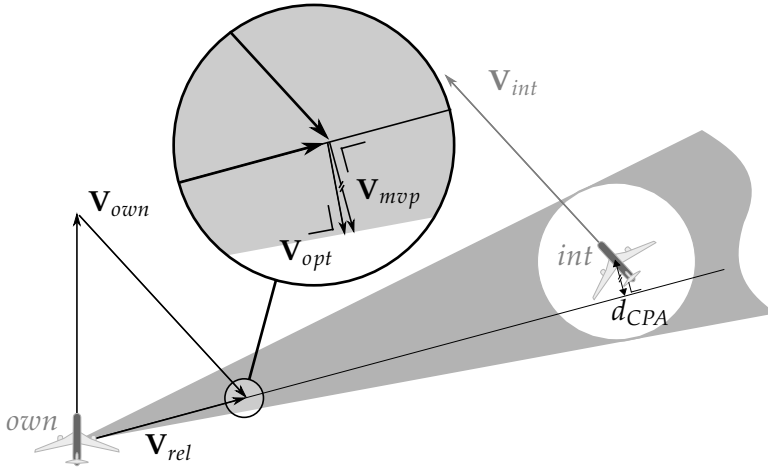


Figure 2.19: Relation between the geometrically optimal solution that is apparent in the horizontal forbidden areas, and the solution that is provided by the Modified Voltage Potential method. The geometrically optimal solution (V_{opt}) is perpendicular to the nearest forbidden area boundary. The MVP-provided solution (V_{mvp}) is perpendicular to the initial relative path.

The resolution advisory method used in the P-ASAS system, the Modified Voltage Potential (MVP) method, uses the predicted future position of both ownship and the intruder aircraft at the closest point of approach, to derive resolution advisories. In this method, avoidance maneuvers are calculated as the vectors starting at the future position of the ownship and ending at the edge of the intruder's protected zone, divided by the time to loss of separation, in the direction of the minimum distance vector (i.e., the vector from the predicted intruder position to the predicted ownship position). The resulting maneuver vector is analogous to the repulsive force between similarly charged particles, hence the name of the method.

Figure 2.19 shows how the solution provided by the MVP method compares to the geometrically optimal solution that is visually apparent in the

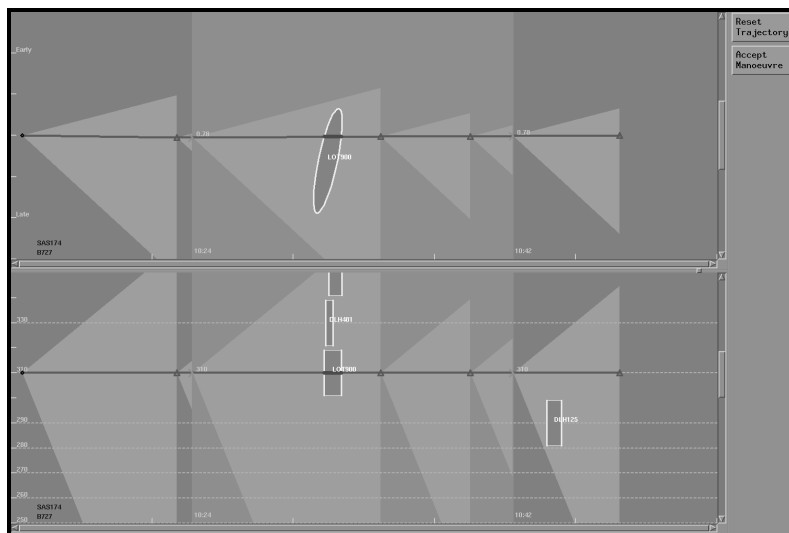
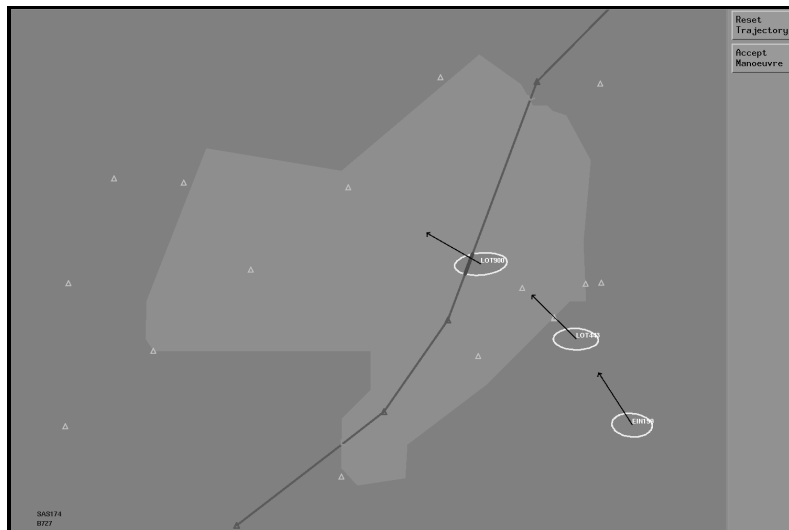


Figure 2.20: The HIPS display. Top: Heading constraints are shown as an overlay on a traditional radar display. Bottom: Two additional displays show constraints for speed and altitude, on a speed-time and altitude-time display, respectively. Figures taken from Meckiff and Gibbs [28].

forbidden area representation. The geometrically optimal solution is perpendicular to the nearest forbidden area boundary, and therefore results in the shortest way out of the conflict. The MVP-provided solution, however, is perpendicular to the initial relative path, and will therefore result in a slightly larger path deviation.

2-7-4 The HIPS display

Although the *Highly Interactive Problem Solver (HIPS)* display was designed as an Air Traffic Controller de-conflicting tool, there are similarities with the concepts in this thesis. The HIPS display combines three two-dimensional graphical representations of aircraft conflicts, that present temporal 'no-go' zones for a chosen subject aircraft [28]. Controllers can manipulate trajectories to avoid these no-go zones, and resolve a conflict.

The display includes three different projections: a horizontal projection, which can be combined with a traditional radar display, a speed-time projection, and an altitude-time projection, see Figure 2.20*. These constraint projections show which values for each parameter will result in a loss of separation, as well as when this loss of separation will occur. On the speed and altitude displays this is shown explicitly on the time axis, on the heading display the current speed is used to calculate at what distance a loss of separation occurs along the own track. Note, though, that each of these constraint zones is only valid when the other two parameters are kept constant.

Compared to the forbidden area concepts in this thesis, the HIPS display does not reveal interactions of constraints between maneuver parameters, but instead gives more detail in the starting time and duration of a loss of separation. For the forbidden areas, the time until loss of separation is visualized in three discrete levels of color coding. The duration of a conflict is not directly perceivable, but can be determined to some extent from the angle between the relative velocity vector and the bisector of the forbidden area. This angle also gives more detail on the severity of a possible loss of separation, as it relates directly to the expected miss-distance. This information is not directly perceivable from the no-go zones of the HIPS display.

*A concept very similar to the horizontal projections in the HIPS display has also been developed as a cockpit display [35]. This concept presents constant-speed no-go zones on the navigation display, in combination with the heading bands from the P-ASAS display.

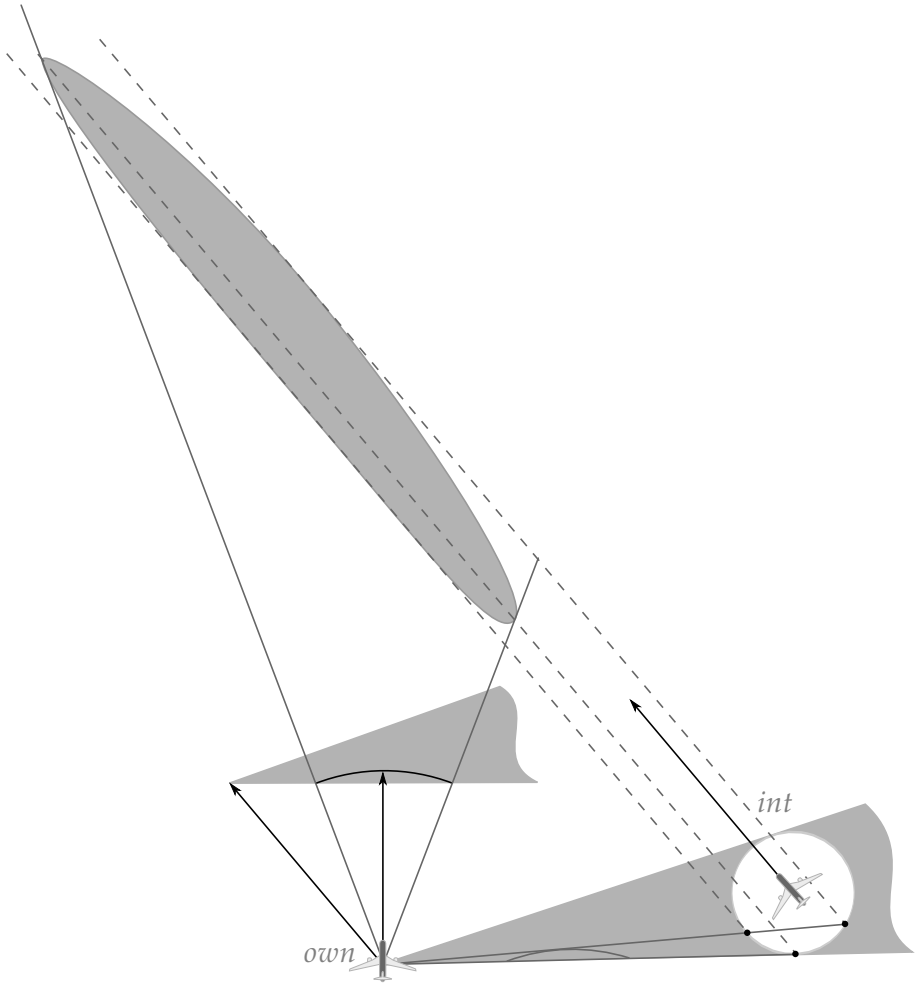


Figure 2.21: Relation between the forbidden areas and the no-go zones of the HIPS display. The extrapolated flight paths of the heading solutions that can be derived from the forbidden area mark the extremes of the spatial no-go zones along the intruder track. For each flight path in between these heading solutions, the intersections between the corresponding relative path and the edges of the intruder protected zone, extrapolate along the intruder trajectory to mark the thickness of the spatial no-go zone.

Figure 2.21 shows how the horizontal no-go zones of the HIPS display relate to the horizontal forbidden areas in Section 2-2. The heading solutions for a given conflict can be derived from the horizontal forbidden area by observing the intersections between the circular set of velocity vectors with constant magnitude, and the forbidden area. The absolute ownship tracks for each heading solution mark the boundaries of the no-go zone along the intruder track. For each of the conflicting headings, the corresponding relative track shows where ownship enters and exits the intruder protected zone. These entry and exit points can be projected along the intruder track, which gives the width of the no-go area. Depending on the amount of heading solutions on the circular set of velocity vectors, there can be zero (0-1 intersections), one (2-3 intersections), or two (4 intersections) no-go zones, as constraints for a single intruder.



Figure 2.22: Three-dimensional cockpit situation display. This display presents traffic, weather, and terrain in a reconfigurable situation display. The pilot can select two-dimensional top and side views, as well as isometric and perspective views that can be panned, zoomed, and rotated. Figure taken from Battiste et al. [32].

2-7-5 The 3-D Cockpit Situation Display

The three-dimensional Cockpit Situation Display (CSD) in Figure 2.22 is a reconfigurable situation display developed at NASA Ames [29, 31, 32]. The display presents traffic, weather, and terrain information in an adjustable view. Pilots can select two-dimensional views, as well as isometric and perspective three-dimensional views, that can be panned, zoomed, and rotated. The display is intended as a primary tool for interaction with the flight management system, and automated conflict resolution systems. Conflicts are indicated by changing the color of the ownship symbol, and the respective intruder aircraft symbol. For more urgent conflicts, also the 'brightness' (a halo is shown around the respective aircraft symbol) of both aircraft symbols is increased, and the predicted conflict position can be presented with overlapping separation circles along the ownship and intruder track.

The pilot can interact with the display using a mouse or a touchpad, to change settings of the display, and to interact with the automation. The flight plan can be changed by adding or modifying waypoints in a list, where the changes can be reviewed graphically on the display. Existing waypoints can also be modified by selecting and dragging the waypoint on the display. For traffic conflicts, an automated list of explicit resolutions, sorted by efficiency, is presented to the pilot [36]. Pilots can either select one of these resolutions, or make a custom modification to the flight plan, to resolve the conflict. In the latter case, pilots can either change their flight plan, or deviate from the flight plan by selecting heading and speed on the autopilot Mode Control Panel (MCP). If the flight plan is modified, the Route Analysis Tool (RAT) can be used to 'probe' for possible conflicts along the modified trajectory. In case of an evasive maneuver using the autopilot, a comparable 'vector probe' is used to probe for conflicts along an arbitrary heading. Both probes operate through on-line Monte Carlo simulations of surrounding traffic [31].

Although these probes do allow pilots to investigate alternatives to the maneuvers advised by the automation, they do so in a way that can be unpredictable, i.e., pilots can only see whether an alternate course is conflict-free when they select it. Figure 2.23 illustrates this issue: it shows that when only a visualization of the predicted conflict is provided, it is not immediately clear what magnitude of a particular maneuver would suffice

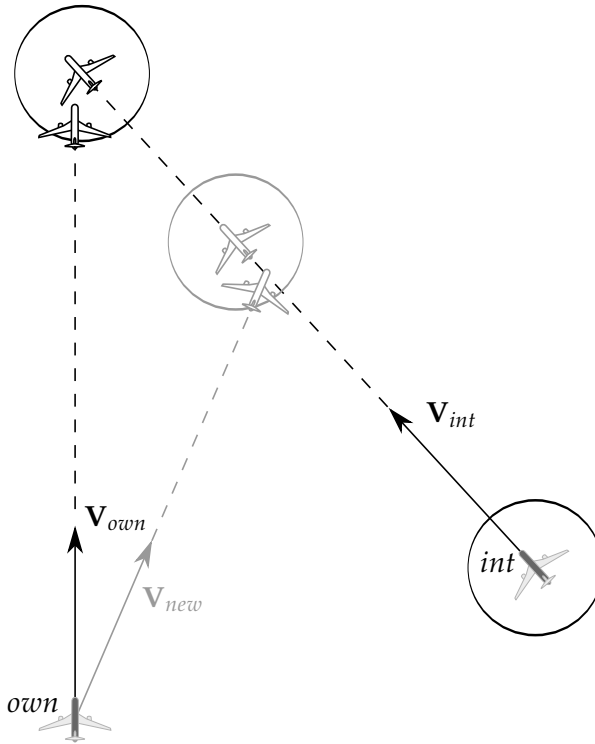


Figure 2.23: Possible result of a conflict probe. It can be seen that even when ownship maneuvers clear of the area of the original conflict, other sets of trajectories may exist that also result in a conflict with the same intruder. These sets are not necessarily contiguous.

to solve the conflict, or if there is a conflict-free trajectory available at all, in the direction in which the pilot is investigating.

2-8 Discussion

The separation assistance displays that preceded the concepts in this thesis, presented in the first five paragraphs of this chapter, are all forms of maneuver-space visualizations, combined with a spatial representation of the airspace. These displays visualize how elements in the work domain restrict the maneuverability of the own vehicle, and, due to the combination with a spatial representation, maintain an intuitive overview of the structure of the surrounding airspace.

The other concepts that have been presented as potential displays of traffic information make different decisions about which representations should be employed. Whereas a few concepts do incorporate some form of constraint visualization, others combine only a plain spatial representation with an automated conflict detection and resolution system, which provides the aircrew with explicit commands.

An oft-made argument for such explicit command displays is that they suffer relatively little from display clutter, and that the presentation of explicit commands reduces workload. In addition, automation has the potential of providing the most efficient and consistent conflict resolution options. The most important drawback of displays that show only explicit resolution commands, however, is that they hide the rationale behind the automation. These displays do not support human information seeking, and, in case of automation malfunction, the pilot is not supported in recognizing failure, nor in seeking alternatives. In these situations, performance can even be worse than when completely unaided [37].

Constraint displays, on the other hand, give a continuous view on maneuver options and limitations, which allow pilots to evaluate their resolution maneuvers. Depending on how constraints are visualized, these displays can reveal the structure of, and relations within the work domain, and can therefore provide a useful basis for illustrating automation logic. By showing higher level information and relations, these displays also allow pilots to investigate the validity of the data. An important drawback of constraint displays is that they can result in more display clutter, compared to showing only explicit commands. According to Tufte's views on the use of details ("To clarify, add detail"), however, this is not necessarily a drawback for a well-designed display [38].

Within the current constraint-based separation assistance displays, a further distinction can be made between those that present state-based constraints, such as the P-ASAS display, the maneuver-space display, and the concepts in this thesis, and those that give a spatial or temporal representation of constraints, such as the HIPS display. Where the state-based constraint displays provide a one-to-one mapping between constraints and the aircraft's maneuver parameters, temporal representations of constraints provide more information regarding where in space, and when a conflict will

occur, as well as the duration of the conflict. Compared to the concepts in this thesis, this additional information comes at the cost of (amongst others) not showing the interactions between maneuver parameters.

The remainder of this thesis will argue for a state-based constraint visualization, such as it is used in the preceding horizontal and vertical separation assistance displays, because it shows the relevant separation information in such a way that the structure of, and relations within the work domain are also visualized. A work-domain analysis (Chapter 3) is used to identify this structure, and key relationships within the work domain. These properties invariably form the premise on which both automation and the human operator should base their actions. A display that helps pilots gain a deeper understanding of the functions and relations within the work domain [39–41], will therefore be invaluable to pilots when they need to judge the automation's functioning [37], as well as in situations where they have to rely on their own problem-solving skills to resolve a conflict.

2-9 Bibliography

- [1] **M. M. van Paassen.** Functions of Space and Travellers. In: *Proceedings of 18th European Annual Conference on Human Decision Making and Manual Control*. Faculty of Aerospace Engineering, Delft University of Technology, 1999.
- [2] **R. M. de Neef and M. M. van Paassen.** Functional Modeling of Airspace. In: *Conference on Human Decision Making and Manual Control*. Orsted DTU, Automation, 2001.
- [3] **A. L. M. Abeloos, J. J. Egging, M. Mulder, M. M. van Paassen, and A. R. Pritchett.** Evaluating an Adaptive, Intelligent Flight Deck Interface for Aircraft Warning Systems. In: *International Symposium on Aviation Psychology*, 2003.
- [4] **S. B. J. van Dam, M. Mulder, and M. M. van Paassen.** Airborne Self-Separation Display with Turn Dynamics and Intruder Intent-Information. In: *IEEE International Conference on Systems, Man and Cybernetics*. IEEE, Montreal, Canada, 2007.

-
- [5] **S. B. J. van Dam, M. Mulder, and M. M. van Paassen.** Ecological Interface Design of a Tactical Airborne Separation Assistance Tool. *IEEE Transactions on Systems, Man, and Cybernetics, part A: Systems and Humans*, 38(6), 1221–1233, 2008.
- [6] **S. B. J. van Dam, M. Mulder, and M. M. van Paassen.** The Use of Intent Information in an Airborne Self-Separation Assistance Display Design. In: *AIAA Guidance, Navigation, and Control Conference and Exhibit*, 2009.
- [7] **F. M. Heylen, S. B. J. van Dam, M. Mulder, and M. M. van Paassen.** Design and Evaluation of a Vertical Separation Assistance Display. In: *AIAA Guidance, Navigation, and Control Conference and Exhibit*. Honolulu (HI), 2008.
- [8] **J. Ellerbroek, M. Mulder, and M. M. van Paassen.** Evaluation of a Separation Assistance Display in a Multi-Actor Experiment. In: *Proceedings of the 16th International Symposium on Aviation Psychology*, 2011.
- [9] **R. A. Paielli.** Modeling Maneuver Dynamics in Air Traffic Conflict Resolution. *Journal of Guidance Control and Dynamics*, 26(3), 407–415, 2003.
- [10] **S. K. Ojha.** *Flight Performance of Aircraft*. AIAA Education Series, 1995. ISBN 978-1563471131.
- [11] **P. Hermes, M. Mulder, M. M. van Paassen, J. H. L. Boering, and H. Huisman.** Solution-Space-Based Complexity Analysis of the Difficulty of Aircraft Merging Tasks. *Journal of Aircraft*, 46(6), 1995–2015, 2009.
- [12] **G. A. Mercado-Velasco, M. Mulder, and M. M. van Paassen.** Analysis of Air Traffic Controller Workload Reduction Based on the Solution Space for the Merging Task. In: *AIAA Guidance, Navigation, and Control Conference and Exhibit*, 2010.
- [13] **J. Ellerbroek, K. C. R. Brantegem, M. M. van Paassen, and M. Mulder.** Design of a Co-Planar Airborne Separation Display. *IEEE Transactions on Human-Machine Systems*, 43(3), 277–289, 2013. doi: 10.1109/TSMC.2013.2242888.

- [14] **Unknown.** OU5274: Remarks on Handling Ships. Tech. rep., Great War Primary Document Archive, 1934.
- [15] **F. S. Miller** and **A. F. Everett.** *Instructions for the Use of Martin's Mooring Board and Battenberg's Course Indicator.* Authority of the Lords of Commissioners of the Admiralty, 1903.
- [16] **I. S. S. Mackay.** Some Navigational Techniques for Use with Marine Radar. *Journal of Navigation*, 9(04), 445–448, 1956.
- [17] **T. Degre** and **X. Lefevre.** A collision avoidance system. *Journal of Navigation*, 34, 294–302, 1981.
- [18] **E. Pedersen, K. Inoue,** and **M. Tsugane.** Simulator studies on a collision avoidance display that facilitates efficient and precise assessment of evasive manoeuvres in congested waterways. *The Journal of Navigation*, 56(03), 411–427, 2003.
- [19] **C. K. Tam, R. Bucknall,** and **A. Greig.** Review of Collision Avoidance and Path Planning Methods for Ships in Close Range Encounters. *The Journal of Navigation*, 62(03), 455–476, 2009.
- [20] **L. Tychonievich, D. Zaret, J. Mantegna, R. Evans, E. Muehle,** and **S. Martin.** A Maneuvering-Board Approach to Path Planning with Moving Obstacles. In: *Proceedings of the 11th international joint conference on Artificial intelligence-Volume 2*, pp. 1017–1021. Morgan Kaufmann Publishers Inc., 1989.
- [21] **P. Fiorini** and **Z. Shiller.** Motion Planning in Dynamic Environments Using Velocity Obstacles. *The International Journal of Robotics Research*, 17(7), 760–772, 1998. doi:10.1177/027836499801700706.
- [22] **A. Chakravarthy** and **D. Ghose.** Obstacle Avoidance in a Dynamic Environment: A Collision Cone Approach. *Systems, Man and Cybernetics, Part A: Systems and Humans, IEEE Transactions on*, 28(5), 562–574, 1998. doi:10.1109/3468.709600.
- [23] **J. K. Kuchar** and **L. C. Yang.** A Review of Conflict Detection and Resolution Modelling Methods. *IEEE Transactions on Intelligent Transportation Systems*, 1(4), 179–189, 2000.

- [24] **R. Ghosh** and **C. J. Tomlin**. Maneuver Design for Multiple Aircraft Conflict Resolution. In: *Proceedings of the American Control Conference*, pp. 672–676. Chicago (IL), 2000.
- [25] **J. M. Hoekstra**, **R. N. H. W. van Gent**, and **R. C. J. Ruigrok**. Designing for Safety: the Free Flight Air Traffic Management Concept. *Reliability Engineering and System Safety*, 75, 215–232, 2002.
- [26] **L. Pallottino**, **E. M. Feron**, and **A. Bicchi**. Conflict Resolution Problems for Air Traffic Management Systems Solved With Mixed Integer Programming. *IEEE Transactions on Intelligent Transportation Systems*, 3(1), 3–11, 2002. ISSN 15249050. doi:10.1109/6979.994791.
- [27] **D. J. Wing**, **R. A. Vivona**, and **D. A. Roscoe**. Airborne Tactical Intent-Based Conflict Resolution Capability. In: *9th AIAA Aviation, Technology, Integration, and Operations*, 2009.
- [28] **C. Meckiff** and **P. Gibbs**. PHARE Highly Interactive Problem Solver. Tech. Rep. 273/94, Eurocontrol, 1994.
- [29] **R. Azuma**, **H. Neely**, **M. Daily**, and **M. Correa**. Visualization of Conflicts and Resolutions in a “Free Flight” Scenario. In: *Proceedings of IEEE Visualization*, pp. 433–436, 1999.
- [30] **J. M. Hoekstra**. *Designing for Safety: The Free Flight Air Traffic Management Concept*. Ph.D. thesis, Delft University of Technology, The Netherlands, 2001.
- [31] **R. Canton**, **M. Refai**, **W. W. Johnson**, and **V. Battiste**. Development and Integration of Human-Centered Conflict Detection and Resolution Tools for Airborne Autonomous Operations. In: *International Symposium on Aviation Psychology*, pp. 115–120, 2005.
- [32] **V. Battiste**, **W. W. Johnson**, **N. H. Johnson**, **S. Granada**, and **A. Q. V. Dao**. Flight Crew Perspective on the Display of 4D Information for En Route and Arrival Merging and Spacing. *Human-Computer Interaction: Interaction Platforms and Techniques*, pp. 541–550, 2007.
- [33] **D. J. Gates**, **E. A. Gates**, **M. Westcott**, and **N. L. Fulton**. Stereo Projections of Miss Distance in Some New Cockpit Display Formats. *Journal of Aircraft*, 45(5), 1725–1735, 2008. ISSN 0021-8669. doi:10.2514/1.35574.

-
- [34] **W. R. Knecht.** Testing a Multidimensional Nonveridical Aircraft Collision Avoidance System. *Human Factors*, 50(4), 565–575, 2008. doi: 10.1518/001872008X288600.
- [35] **W. A. Bas.** *Design and Evaluation of a Cockpit Human Machine Interface for a Future Air Traffic Management Concept.* Master’s thesis, Delft University of Technology, 2002.
- [36] **Flight Deck Research Group.** 3D-CDTI USER MANUAL v2.1. Tech. rep., NASA Ames, 2004.
- [37] **E. J. Bass** and **A. R. Pritchett.** Human-Automated Judge Learning: A Methodology for Examining Human Interaction With Information Analysis Automation. *IEEE Transactions on Systems, Man, and Cybernetics, part A: Systems and Humans*, 38(4), 759–776, 2008.
- [38] **E. R. Tufte.** *Envisioning Information.* Cheshire, CT: Graphics Press, 1990. ISBN 978-0961392116.
- [39] **K. J. Vicente** and **J. Rasmussen.** Ecological Interface Design: Theoretical Foundations. *IEEE Transactions on Systems, Man, and Cybernetics*, 22(4), 589–606, 1992.
- [40] **K. Christoffersen**, **C. N. Hunter**, and **K. J. Vicente.** A Longitudinal Study of the Effects of Ecological Interface Design on Deep Knowledge. *International Journal of Human-Computer Studies*, 48, 729–762, 1998.
- [41] **C. M. Burns** and **J. R. Hajdukiewicz.** *Ecological Interface Design.* CRC Press LLC, FL: Boca Raton, 2004. ISBN 0415283744.

Part I

Design

Constant-velocity conflict resolution

This chapter presents a separation assistance display concept that presents traffic constraints in a 'heading - flight-path angle action space'. A pilot preference for constant-velocity maneuvers motivated this choice of design. The resulting display resembles a Primary-Flight Display, with overlays for flight-path vector constraints, and conflict geometry visualization. A work-domain analysis is included in the chapter which was used to identify the constraints and interactions that define traffic conflict resolution in a heading - flight-path angle action space.

- Paper title** Design of an Airborne Three-Dimensional Separation Assistance Display
- Authors** J. Ellerbroek, M. Visser, S. B. J. van Dam, M. Mulder, M. M. van Paassen
- Published in** IEEE Transactions on Systems, Man, and Cybernetics, part A, Vol. 41, No. 6, September 2011, pp. 863–875

Abstract: *In the context of the NextGen and SESAR future airspace programmes, this paper describes a concept for an Airborne Separation Assistance (ASAS) display, that is designed to aid pilots in their task of self-separation, by visualizing the possibilities for conflict resolution that the airspace provides. This work is part of an ongoing research towards an ecological design of a separation assistance interface that can present all the relevant properties of the spatio-temporal separation problem. A work-domain analysis is described from which several perspective projections of traffic properties and travel constraints are derived. A display concept is proposed that presents heading and altitude action possibilities in a flight-path angle - track angle action space. Key issues in the current design are discussed, with recommendations for future work.*

3-1 Introduction

In today's airspace, increasing amounts of traffic are pushing the limits of capacity and safety. To facilitate continuing growth, new air-traffic management concepts are under development, which allow a more flexible use of airspace [1, 2]. These new concepts promote a shift towards airborne determination of user-preferred trajectories, where airspace capacity is expected to increase, while controller workload decreases. However, with this shift of the separation task to the flight deck, it is expected that pilots will need assistance to perform this task safely and efficiently.

The development of a support system requires a thorough analysis of what level of automation is required to meet with the overall system demands of safety, capacity and efficiency of flight. Crucial in this analysis will be the question of how these tasks should be allocated between humans and automation, and how the human actors can interact, and share their decision-making with the automation [3–5]. The interaction between automation and the human actor also requires transparent functioning of the automated system. The interface should provide operators with information regarding their own performance, as well as that of the automation, so that operators' self-confidence and trust correspond with the capabilities of the system, and promote appropriate use of automation [6–8].

Although several display concepts have been developed as aids in the task of self-separation [9–13], most current research on Airborne Separation Assurance Systems (ASAS) focuses on the development of automated systems that assist pilots with the separation task [11, 14–17]. Generally, these

systems provide the pilot with explicit, 'ready-to-use' resolutions to a separation conflict. Although they lead to lower pilot workload [18], these systems also hide the cognition behind the resolution advisory [19]. Without additional information, such systems may lead to low situation awareness (SA): the pilot is not fully aware anymore of exactly what is going on, and is unable to reason about the functioning of the automation, and other constraints and relationships within the environment under control [20–22]. This may lead to inappropriate reliance on the automation, which can have a significant impact on the overall levels of safety and efficiency. Under-reliance may lead to situations where the pilot prefers manual control over an automated (valid) resolution, leading to higher operator workload, and a possible reduction in performance and safety. On the other hand, over-reliance may cause pilots to use the automation in ways for which it was not designed, or to accept resolutions even when the automation is in error [6, 23].

In the air transport domain, lack of situation awareness is currently considered to be one of the the main causes for human error, responsible for at least seventy percent of the incidents and accidents that occur [24]. As airborne separation systems move towards more automation, it will become more important than ever that automation and instrumentation promote a high level of situation awareness. This leads to the fundamental question of 'what' needs to be presented to optimize human performance from the perspective of situation awareness [25]. In other words, how does one design for situation awareness? The work presented in this paper will employ a constraint-based approach, inspired by Ecological Interface Design (EID), a proven design paradigm from the domain of process control [26, 27], to design for SA [28, 29].

EID is a method that addresses the cognitive interaction between humans and complex socio-technical systems. Its approach to interface design gives priority to the workers environment, or 'ecology', focusing on how the environment poses constraints on the worker [28, 29]. Ecological displays are designed to allow for direct perception of the possibilities and constraints afforded by the work domain [30, 31]. This way, EID aims to support each level of cognitive control [32], while not forcing the operator to control at a higher level than necessary. By visualizing hidden constraints and relationships, ecological interfaces can transform what would otherwise be a cognitive task, into a perceptual task.

An ecological airborne separation assistance display then, should support pilot decision making in the task of self-separation, rather than only providing an automated resolution. In the domain of process control, EID had the freedom to define a new interface for the operator. For air travel, however, pilots already make use of an existing, natural ecology (i.e., the ecology of locomotion). The key in designing an airborne separation support tool will be to not replace, but to enhance this existing ecology, by visualizing hidden affordances*, and exploiting the operator's natural adaptation to the ecology [34–39].

Preceding the design of an ecological display, a thorough analysis of the work domain is required, which should identify functionalities, constraints, and means-end relationships within that work domain. The main tools for this analysis are the Abstraction Hierarchy (AH), and the Skills, Rules, Knowledge taxonomy (SRK), both developed by Rasmussen [32, 40]. To make the transition from a workspace analysis to an effective interface design, functional visualizations of the affordances and constraints in the work domain need to be derived, so that they can be perceived and fluently transformed into goal-directed behavior, supporting the natural coupling between perception and action [41, 42].

This paper presents the results of a work-domain analysis of a self-separation airspace, and a concept for a separation assistance display. The analysis employs tools such as the Abstraction Hierarchy to obtain a clear image of how the work-domain shapes the affordances for a pilot in his task of self-separation. The display concept is the third in an ongoing design process towards an integrated, three-dimensional separation assistance interface, that presents an unambiguous, complete view of the airspace affordances, in an unmanaged traffic environment. The two previous concepts, the horizontal separation assistance display [38], and the vertical separation assistance display [39], presented maneuvering affordances in a heading-speed, and a flight-path angle (FPA) - speed action space, respectively. In a comparable fashion, the current concept will present maneuvering affordances in a FPA - track angle action space.

*James J. Gibson defined affordances as opportunities for action, provided by an object or by the environment. An affordance is considered always in relation to the actor, and therefore dependent on the actor's capabilities [30, 33]. For instance, with respect to an engine, air affords propulsion, but with respect to a wing, air affords lift.

The paper is structured as follows: the following two sections will, respectively, present the results of a work-domain analysis, and illustrate the construction of functional visualizations of the constraints that followed from this analysis. The fourth section will introduce a concept of a separation assistance interface. The fifth section describes how the display concept can be used in more complex conflict situations. This paper concludes with a discussion on the key issues of the current display concept, with recommendations for future work.

3-2 Work Domain Analysis for airborne separation

The work domain under analysis in this study is limited to Trajectory-Based Operations (TBO) with self-separation. These operations involve trajectory (re-)planning on the flight-deck, in order to assure conflict-free flight in unmanaged, i.e., self-separated airspace. In the currently proposed future airspace concepts, the preferable mode of operation is one where automated 4D trajectory prediction and control are applied throughout the flight [2, 17, 43].

In this situation, the pilot's task will be one of monitoring separation, and selecting and applying resolution advisories, provided by the automation. The pilot should, however, be able to judge the fidelity of a proposed resolution, and be able to intervene in case the automation fails. Good situation awareness is therefore of paramount importance, and, in this study the Abstraction Hierarchy (AH) will be employed to determine the relevant aspects of the work domain on several levels of abstraction. It will also serve to illustrate how the constraints and affordances on the different levels of abstraction interact with each other.

The abstraction hierarchy is a work-domain analysis tool that presents a stratified, hierarchical description of the workspace. Each stratum of the hierarchy represents the same system, but on a different level of abstraction. The levels are connected by means-end relationships between the adjacent levels. Along the vertical axis, commonly five levels represent the workspace at decreasing levels of abstraction, starting at the top with the purpose(s) for which the system was designed, all the way down to the spatial topology, properties, and appearance of the components that make up the system on the bottom level [40, 44]. In previous studies on a workspace analysis for

the air transport domain, it showed that dividing the horizontal dimension of the AH between items ‘internal’, and ‘external’ to the ownship, provides a logical structure for an AH that describes this domain [35, 36, 45].

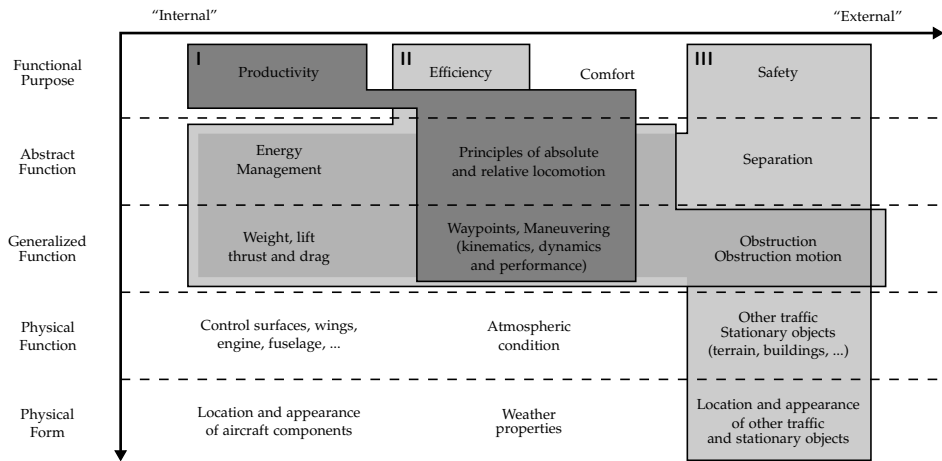


Figure 3.1: Abstraction Hierarchy for the Separation Assistance Display. The analysis presented in this paper focuses on three functional goals. These goals, and the relevant means-ends relationships between levels have been highlighted in three groups in the hierarchy: (I) Productivity, (II) Efficiency, and (III) Safety.

3-2-1 An Abstraction Hierarchy for airborne separation

Figure 3.1 shows an abstraction hierarchy for the workspace relevant to TBO and self-separation. In this hierarchy, the most relevant goals have been highlighted, along with the corresponding means-ends relationships. In the AH, these goals are defined at the functional purpose level. In the case of ASAS self-separation applications, these are flying safely, productively, comfortably and efficiently through unmanaged airspace. For this analysis, it is assumed that safety can be assured by maintaining sufficient separation from potentially hazardous objects, such as other aircraft and terrain. In the current context, this means adhering to the defined separation minima between aircraft [46]. While they are relevant for assuring safe flight, issues such as staying within the flight envelope are kept out of the analysis. Although more complex in reality, in this paper it is defined that work is

considered productive, as long as the distance to the destination is decreasing. For flight in general, comfort poses constraints such as upper limits on maneuver accelerations. The realization of efficiency is much more complicated, however, as it can be defined in many ways, such as fuel efficiency, or minimum path deviation. These constraints are therefore beyond the scope of this paper.

The abstract function level describes the underlying relationships that govern the realization of the purposes of the system. In the case of air travel, this level contains the general physical laws that dictate flight, absolute and relative locomotion, and the geometrical properties of the separation problem [45]. Although for aircraft that follow a pre-defined, four-dimensional path, aircraft intent can influence the constraints that are derived on this level, the current study will only employ the current states to derive these constraints. Previous studies did incorporate the effect of intent on maneuver affordances [47], however, this is beyond the scope of the current study.

The generalized function level describes how the functions at the abstract function level are achieved, independent of the actual implementation of the system. Properties such as aircraft weight, lift, thrust and drag, and the maneuvering performance of the aircraft all impose internal constraints on the maneuver space of an aircraft. External obstructions further constrain this maneuver space, and dictate the (lack of) separation. On the bottom of the abstraction hierarchy, the physical form and functions are described by modeling the internal layout of aircraft components, and external airspace properties such as other traffic, weather, and terrain. The physical function level describes the various components, and their capabilities, and at the physical form level the appearance and location of components, the airspace, and other aircraft are described. The relevant internal and external constraints which can be derived from this abstraction hierarchy will be described in more detail below.

In this paper, the workspace content and boundaries are limited to trajectory planning functions in direct relation with conflict resolution and prevention during cruise flight. Functions related to aircraft control and stability, like staying within the flight envelope, and accounting for passenger comfort, are largely kept out of the analysis. The time horizon in which the

workspace is analyzed is determined by the applicability of conflict management, and is approximately between 60 seconds and 10-20 minutes. Below 60 seconds, collision avoidance systems like the Traffic Collision Avoidance System II (TCAS II) must take over in order to prevent collision [48]. An upper threshold of 20 minutes is chosen because the vast majority of conflict resolution and recovery maneuvers take place in less than 20 minutes [17].

The scope of the current research is also restricted to the visualization of constraints that relate to tactical maneuvering, influences of ownship and intruder intent [47] are beyond the scope of this paper.

3-2-2 Internal constraints

The internal aircraft constraints that are relevant for this work domain analysis are mainly described on the abstract function and the generalized function levels of the work domain model. They relate to the various limitations on the performance of the aircraft, such as bank limits, turn dynamics, available engine power, stall, structural considerations, buffet characteristics, and requirements on emissions and passenger comfort. These limitations result in several constraints relevant to the task of trajectory planning, such as maximum turn rates, maximum and minimum operating speeds, fastest and steepest steady climb and descent, and the steepest steady climbing and descending turn.

Another important, although not directly perceivable constraining factor is the energy state of the aircraft: For an aircraft, speed and altitude share the same energy space. The mechanism that underlies the coordination of the controls, is the management of the aircraft's energy state (abstract function level, Figure 3.1). Speed and altitude are directly related to the kinetic and potential energy of the aircraft. The total amount of energy is determined by the throttle, whereas the elevator is used to control the exchange of kinetic and potential energy. The total energy state of an aircraft essentially determines the affordances for maneuvering in terms of speed and altitude [34, 36]. Together, these internal constraints determine the part of the airspace that is reachable within a certain timespan.

3-2-3 External constraints

In unmanaged airspace, the reachable area that was defined by the internal aircraft constraints is further constrained by external factors, such as weather, terrain, other traffic, and the boundaries of the unmanaged airspace. In this analysis, the focus lies on the constraints imposed by other traffic. Traffic constraints are shaped by a minimum horizontal and vertical separation between any two aircraft, that should be adhered to at all times. With common values of 5 nautical miles horizontal, and 1,000 feet vertical separation, this results in a three-dimensional *Protected Zone (PZ)*: A flat, three-dimensional disc around each aircraft, that should remain clear of other traffic, see Figure 3.2 [49, 50].

Intrusion of this space is referred to as a loss of separation. A conflict is defined as a future loss of separation, within a certain observation timespan (e.g., 5 minutes). In Figure 3.3, a traffic conflict is illustrated from the perspective of ownship. This and subsequent figures depict a conflict situation between the ownship and one intruder aircraft. Although the principles presented in this analysis also hold for multiple intruder aircraft [38], this paper only uses single intruder conflict situations to illustrate the proposed concept, for the sake of clarity. In Figure 3.3, the ownship is flying with velocity V_{own} , and will eventually lose separation with the intruder aircraft, if no further action is taken. The point where separation is at a minimum is called the Closest Point of Approach (CPA). It can be seen that even when the ownship turns away from the conflict location, resulting in V_{new} in Figure 3.3, separation can still be lost.

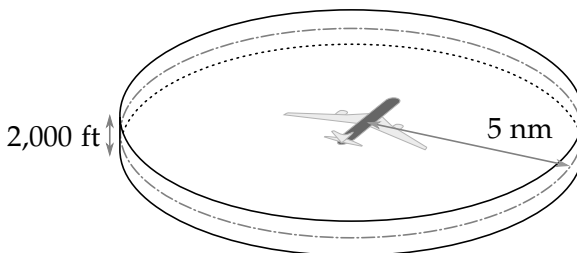


Figure 3.2: The Protected Zone is defined as a disc-shaped area around each aircraft that should remain clear of other traffic.

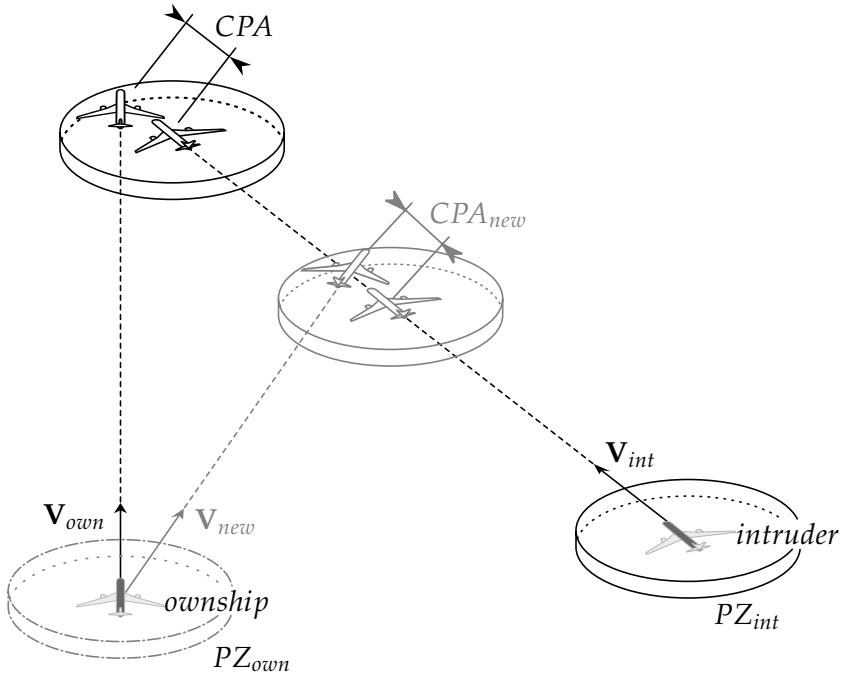


Figure 3.3: A future loss of separation. It can be seen that even when ownship maneuvers around the area of the original conflict, separation can still be lost.

This adverse effect can be eliminated by examining the conflict situation in a relative velocity field [38, 39, 42]. Under the assumption that intruder and ownship state remain unchanged in the near future, a conflict can be predicted using the speed of ownship, relative to the intruder aircraft:

$$\mathbf{V}_{rel} = \mathbf{V}_{own} - \mathbf{V}_{int}$$

3.1

Figure 3.4 shows a conflict in the relative velocity field. When the line extended from the relative velocity vector crosses the intruder protected zone, a loss of separation will occur in the near future. By drawing lines through the ownship position, that are tangent to the intruder PZ, a three-dimensional wedge-shaped area can be defined, which marks the constraints that other traffic imposes on ownship relative motion with respect to an intruder aircraft (Figure 3.4).

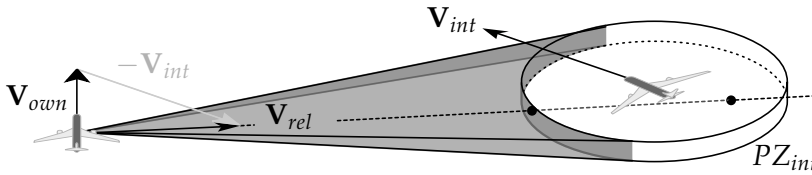


Figure 3.4: A conflict situation expressed in a relative velocity field. Ownship and intruder are in conflict when the line that extends from the relative velocity vector crosses the intruder PZ. The wedge shape indicates the instantaneous set of constraints for the relative velocity vector.

Unlike the absolute, spatial representation in Figure 3.3, this representation only varies as a function of time (i.e., the wedge will expand as a function of the closing speed of the intruder aircraft, with respect to ownship). This means that for the current time, the three-dimensional wedge shape represents the complete set of relative velocity vectors that would result in a loss of separation.

3-3 Functional presentation of constraints

Although a work-domain analysis provides insight in the structure and content of the work domain, it still requires a translation of this analysis into a practical interface design. Functional presentations of constraints and relations in a system should formulate the behavior of that system in terms that are relevant to achieving its ends. For trajectory planning, this implies that the goal-relevant affordances must be visualized in such a way, that the pilot's perception of these cues directly triggers desired goal-directed steering actions. A visualization is required that not only is compatible with the various identified constraints, but should also be able to reveal the *relations* between these constraints.

In the context of airborne separation, the behavior of the system is highly complex, as it is governed by the multi-variable, non-linear dynamics of several aircraft, moving relative to each other. Because such a system has too many degrees of freedom to combine in a usable interface, a different description is required. This description should relate inputs that match common flight practice, to the goals and affordances of the system. In cruise flight, pilots control their aircraft by manipulating velocity, track angle, and

altitude settings, using the autopilot, or by modifying the planned route in the Flight Management System. A successful separation assistance interface should relate these variables and their operational limits to the affordances of the airspace.

3-3-1 Traffic constraints

Figure 3.3 already illustrated that presenting conflicts in absolute space is problematic: The closest point of approach is not constant, as it depends on the relative motion of two aircraft. It changes as a function of ownship and intruder velocity and heading. Therefore, steering away from a conflict based on the presentation in Figure 3.3 will also move the CPA, and might not resolve the conflict at all. In other words, although a conflict presentation like the one in Figure 3.3 provides the pilot with a visualization of the affordance of ‘conflict’, it does not show the affordance of ‘avoidance’, and is therefore an unsuitable conflict avoidance representation [38].

With the design of a horizontal and a vertical separation assistance display, previous studies illustrated that the affordance of avoidance can be consistently represented in a relative velocity field [38, 39] (Figure 3.4). A disadvantageous aspect of the relative velocity field, however, is that it is hard for pilots to relate their affordances of control in *absolute space*, to a velocity constraint zone expressed in *relative space*. In previous research, van Dam [38] showed that this relation can be made visible, by translating the constraint zone and relative velocity vector by the intruder velocity vector, as shown in Figure 3.5. This would be equivalent to adding V_{int} on both sides of the equal sign in Equation (3.1): the equation is still valid, but in the visualization (Figure 3.5), the relation between the ownship velocity vector and the relative velocity constraint zone is made explicit.

The three-dimensional area in Figure 3.5 represents the instantaneous constraints that the intruder position and velocity vector impose on the affordances for ownship locomotion (identifying the means-end relationship between obstruction on the generalized function level, and locomotion and separation on the abstract function level of the AH). It not only reveals the *individual* affordances for ownship velocity, Flight-Path Angle (FPA), and track angle, but also the interaction between the constraints of these three locomotion variables.

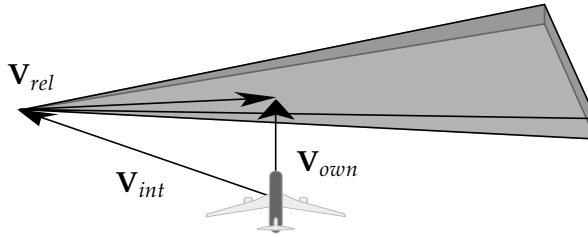


Figure 3.5: Constraints on ownship velocity, expressed in an absolute velocity field. Ownship and intruder are in conflict when the tip of the ownship velocity vector is inside the three-dimensional constraint wedge.

For the visualization of the three-dimensional workspace on a two-dimensional screen, two options can be distinguished: perspective displays and co-planar displays, each with their own benefits and drawbacks. A co-planar display corresponds more closely to the interfaces that are already present in the current flight-deck, whereas perspective displays have been found to have more “pictorial realism”: they correspond more closely to the three-dimensional world [51, 52]. A drawback of co-planar displays in the current context is that some of the information on the interaction between locomotion constraints is lost, when these constraints are presented using separate horizontal and vertical projections. Perspective displays, on the other hand, suffer from perspective distortions, which can induce errors in judging distances on the display [53, 54]. The presentation of 3D structures such as the constraint zones also suffers from problems of occlusion: when viewed from a fixed angle, the front facing side of the structure hides the internal details of the structure.

Earlier designs of separation assistance displays reduced the complexity of the problem by relating several key controllable variables to a planar projection of the three-dimensional conflict situation. For instance, the horizontal separation assistance display presents the affordances for aircraft airspeed and track using a horizontal projection of the conflict situation [38], whereas the vertical separation assistance display relates airspeed and vertical speed to a vertical projection of the constraints [39]. An often heard comment from professional airline pilots, in the evaluation of these previous designs, was, that while it featured as a valid and equal option in both displays, velocity changes are rarely used when resolving a conflict [50, 55].

Based on this feedback, this study investigates a cylindrical projection of an FPA-track angle action space, which will be derived using spherical cutting planes based on constant velocity. The remainder of this section will discuss the applied projection method, and the derivation of affordance zones using the spherical cutting planes, respectively.

Projecting constraint areas onto a 2D display

According to Gibson, a (human) observer perceives the three-dimensional world as an optic array of solid visual angles, that correspond to distinct geometrical parts of the environment [30]. A perspective projection, such as the Synthetic Vision Display (SVD), can be regarded as a window (with a limited field of view) to this optic array. For such projections, the station point (the apex of the perspective projection) [53] corresponds to the point of observation, and horizontal and vertical coordinates in the projection correspond to the horizontal and vertical visual angles, respectively [37].

When the goal of the interface is to present the affordances of the *complete* surrounding airspace, the field of view of an SVD becomes a limiting factor. An ideal method should employ the egocentric natural perspective of an SVD, but in a way that is not restricted to its limited field of view. Several options can be considered. For instance, a section of the display could act as a ‘rear-view-mirror’, to visualize the environment behind the observer. This method, however, would essentially still result in a co-planar representation.

The current concept will therefore use an approach, where the relation between the visual angles and the screen coordinates is defined using an equidistant cylindrical projection, with a horizontal visual angle range of $\phi \in [-180^\circ, 180^\circ]$, and a vertical visual angle range of $\theta \in [-90^\circ, 90^\circ]$. This projection results in a single, continuous presentation of the entire surroundings, which directly relates horizontal and vertical visual angles, to horizontal (x) and vertical (y) screen coordinates, respectively:

$$x = \theta, y = \phi$$

3.2

This method of projection results in size and shape distortions for large vertical visual angles. However, the influence of this effect on the perception of the relevant combined internal and external constraints can be considered small, as the flight-path angle γ will never be very large for commercial

aircraft. For sake of clarity of the presented affordance cues, the line of sight of the projection is aligned with the current aircraft ground-track, but is stationary with respect to roll and pitch angles of the aircraft, keeping vertical angle offset θ_0 fixed. This results in an earth-referenced, 'outside-in' representation of the surroundings, as opposed to the more classical inside-out presentation employed in the current Primary Flight Display (PFD), and the SVD [56].

In the current concept, this projection method will be employed to project two affordance cues onto a wide-screen display that presents the airspace affordances in an FPA-track angle action space. The derivation of these cues will be described below. The first visualization provides the ownship flight-path vector constraints. The second visualization is constructed to inform the pilot on the geometry of each individual conflict. It visualizes relative intruder position and movement, and the urgency of a conflict. The derivations below will employ a virtual projection spherical surface, centered around ownship at an (arbitrary) distance, D_{proj} (see e.g., Figure 3.6), to illustrate the projections.

Ownship velocity direct constraints

The first projection is based on an intersection between the three-dimensional constraint zone (Figure 3.5) and a spherical cutting plane with the current ownship velocity magnitude as radius, see Figure 3.6. Based on pilot feedback that expressed a preference against the use of speed changes when resolving conflicts, it is assumed at this stage that velocity is kept constant. Future design iterations will investigate what exactly can be done in order to include a visualization of the effects of changes in ownship velocity.

Figure 3.6 gives an example of how a spherical shell, with a radius of constant ownship velocity would intersect with the 3D constraint wedge from Figure 3.5. The resulting area, S_{own} , is marked in light-grey in Figure 3.6. The next step is then to project this constraint area on the perspective sphere described in the previous section, see Figure 3.6. The resulting projection, S'_{own} , shows the constraints for the ownship Flight-Path Vector (FPV), that are imposed by the intruder's relative position and motion, for the current velocity of ownship. Note that the constraint areas from multiple intruder

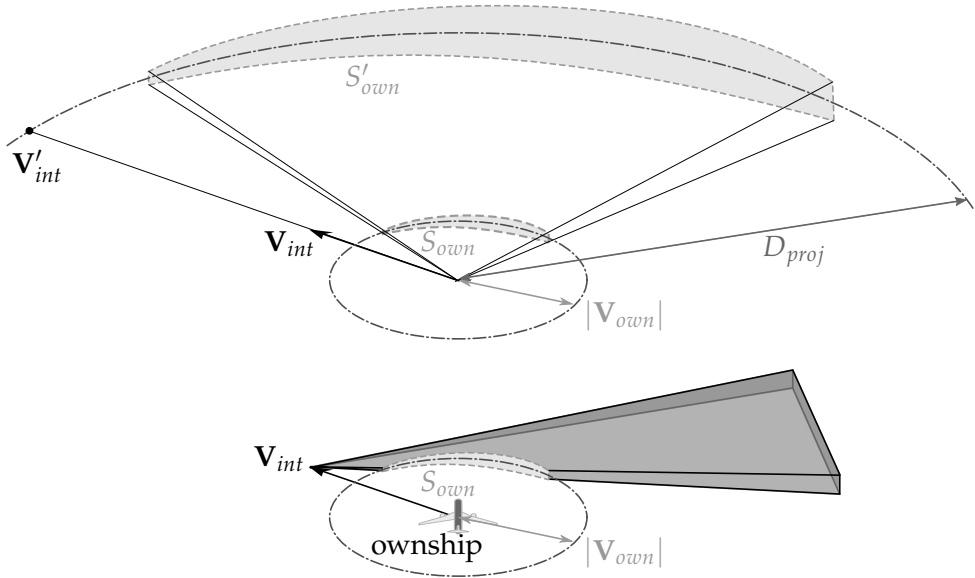


Figure 3.6: The flight-path vector constraint at constant ownship velocity, S_{own} , is given by the intersection between a spherical shell, with a radius of constant ownship velocity, and the three-dimensional FPV constraint zone. Projection of this constraint area yields the visualization of the flight-path vector constraints, S'_{own} .

aircraft can be combined, in order to obtain a complete, instantaneous FPV action space, that addresses all current (possible) conflicts [38].

A display format was proposed by Gates et al. [57], that presents collision avoidance contours that resemble the flight-path vector avoidance contours in the current study. Although the contours presented here and the display presented by Gates et al look similar, they describe a different property of the conflict. The current study distinguishes between horizontal and vertical separation minima, and incorporates these in a visualization of flight-path vector affordances based on constant velocity. Gates' proposed format, however, does not directly consider visualization of affordances, but rather displays contours of equal (three-dimensional) Expected Miss-Distance (EMD).

Figure 3.7 shows several shapes that the two-dimensional projection of the flight-path vector constraint area can take. Figure 3.7(a) shows the result

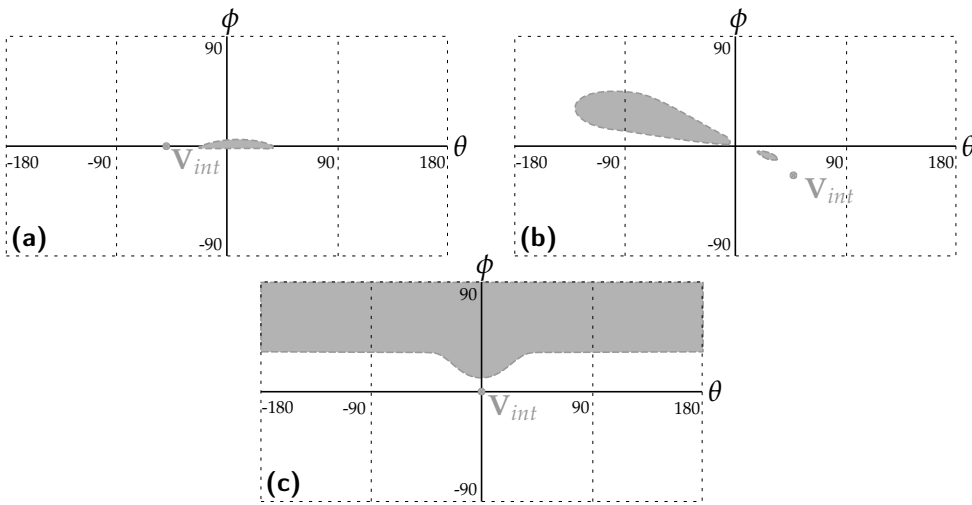


Figure 3.7: Some examples of the projected flight-path vector constraint. **(a):** Basic example of a conflict, where the intruder crosses at an acute angle. **(b):** Velocity sphere intersecting wedge twice ($V_{int} > V_{own}$). **(c):** Intruder overtaking ownship, at a higher flight level.

of the example projection from Figures 3.4-3.6. In this case, the intruder aircraft is situated to the right of ownship, flying at the same altitude. If ownship is flying level, ownship and intruder will eventually lose separation if no further action is taken. Figure 3.7(b) shows a situation where the ownship velocity-sphere intersects the constraint-wedge twice. This can happen when an intruder is flying at a greater velocity than ownship, and intruder and ownship's tracks will be crossing sharply ($\Delta\psi \simeq 90^\circ$). Figure 3.7(c) shows a situation where an intruder is overtaking ownship from directly behind, flying at a higher altitude. Because the intruder is close to ownship, almost all climbing maneuvers would lead to a loss of separation.

Conflict geometry projection

While the flight-path vector constraint projection performs well at presenting constraints that the pilot can directly relate to the locomotion affordances of the aircraft, it does not show the specifics of each conflict: it is difficult to determine which intruder is causing a conflict, and how such a conflict would evolve. A second projection is constructed, therefore, to illustrate the

geometry of individual conflicts. It combines a projection of intruder relative velocity constraints, and of the intruder protected zone, using the same projection surface as was used for the flight-path vector constraint zone.

The relative velocity constraints can be obtained using the intersection of a sphere, with its radius equal to the magnitude of the relative velocity vector $\mathbf{V}_{rel,int} = \mathbf{V}_{int} - \mathbf{V}_{own}$, and the three-dimensional wedge shape from Figure 3.8. The resulting shape, indicated as $S_{rel,int}$ in Figure 3.8, represents all velocities with equal magnitude of the intruder relative to ownship that correspond with possible future loss of separation. Next, this area is projected onto the projection sphere described in Section 3-3-1, together with the current relative speed, $\mathbf{V}_{rel,int}$, and the contour of the intruder PZ, see Figure 3.8.

In this figure, $\mathbf{V}'_{rel,int}$ is the projected relative velocity vector, $S'_{rel,int}$ is the projection of the relative velocity constraint area, and PZ'_{int} is the projection of the protected zone of the intruder. In the two-dimensional presentation on the display, the location on the display of each of these combined projections illustrates the direction of the line-of-sight to the respective intruder. The altitude difference between ownship and the intruder is further emphasized by the curvature of the projected intruder PZ. The curvature in this projection is caused by the circular shape of the protected zone, and changes as a function of the vertical position of the intruder, relative to the ownship. Together with the projection of the relative velocity vector, $\mathbf{V}'_{rel,int}$, the constraint area $S'_{rel,int}$ gives an indication of how a possible conflict would evolve. If the projection of the relative speed vector lies within constraint area $S'_{rel,int}$ the intruder and ownship are in conflict. The direction of $\mathbf{V}'_{rel,int}$ indicates how ownship and the intruder will pass each other, whereas its proximity to the boundary of the constraint area shows how closely they will pass each other. Furthermore, with respect to the size of the intruder's projected PZ, the size of the relative velocity constraint zone can be used as an indication for the closing rate between intruder and ownship.

As a result of the projection onto the projection sphere of the relative velocity vector, it is no longer distinguishable whether $\mathbf{V}_{rel,int}$ is aimed towards, or away from ownship. To resolve this ambiguity on the display, four

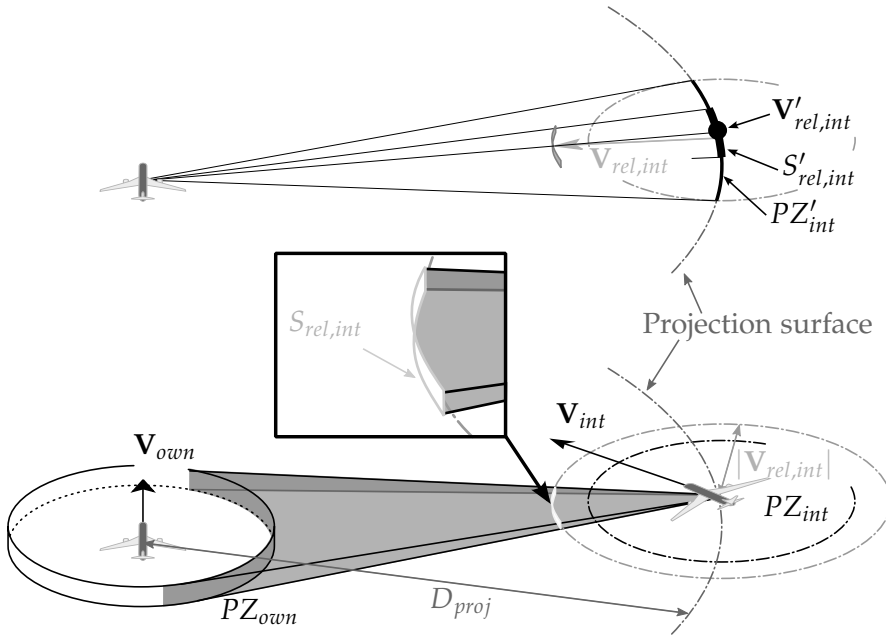


Figure 3.8: Projection of the relative intruder velocity constraints ($S'_{rel,int}$), the relative intruder velocity vector ($V'_{rel,int}$), and of the protected zone geometry (PZ'_{int}), result in the visualization of the 'puck'.

lines are drawn from the boundaries of the puck towards the tip of the relative velocity vector, when $V_{rel,int}$ is aimed towards ownship. These lines are absent when $V_{rel,int}$ is aimed away from ownship.

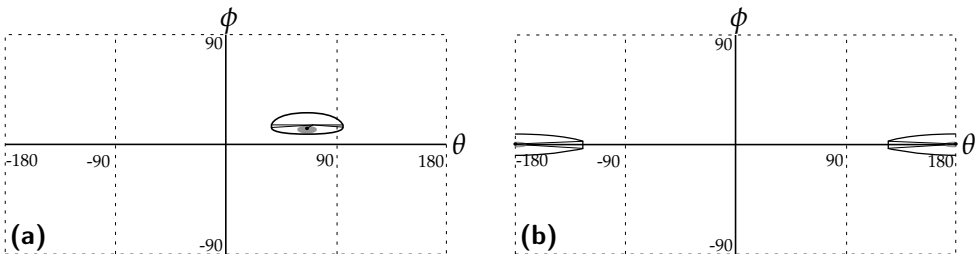


Figure 3.9: Some examples of the 'puck'. **(a):** An intruder passing safely behind and over ownship. **(b):** An intruder overtaking ownship.

The two-dimensional presentation of this projection results in a (ice-hockey) puck-like shape. Figure 3.9 shows two examples of what this 'puck' may look like, for different situations. In Figure 3.9(a), an intruder is flying in front of, and to the right of ownship, at a higher altitude than ownship. The projected relative velocity vector points outside of the relative velocity constraint zone, indicating that ownship and intruder are not in conflict. The direction of the relative velocity vector reveals that the intruder will eventually pass behind and above ownship, if neither aircraft maneuvers.

In Figure 3.9(b), the intruder is flying behind ownship, on the same course, but at a higher velocity. The relative velocity vector is such that it points directly at ownship, and therefore is located in the center of the 'puck'. This means that in this situation a collision would occur, if no further action is taken. Note that when both the ownship as well as the intruder aircraft are equipped with the same interface, their representations would be very similar: the appearance of the 'puck' would be identical, only at a different location on the screen.

Note that the current derivations of the puck and the flight-path vector avoidance zone assume instant state changes. It can be shown that this is a safe assumption when a predicted conflict is still in the far future [58, 59]. However, maneuver dynamics will start to play a larger role when conflicts become more imminent: in the case of tactical maneuvers (within 10 minutes of a predicted conflict), unmodeled dynamics will cause significant errors, particularly speed maneuvers [58]. To compensate for these inaccuracies, future iterations of the interface concept will incorporate maneuver dynamics in the presentation of airspace affordances.

3-3-2 Production and maneuvering constraints

For the horizontal separation assistance display concept, productivity was considered in terms of destination approximation, which for the projection in the horizontal separation assistance display translated into relative track angle constraints of $\pm 90^\circ$ around the desired track [38]. For the current concept these limits can also be marked on the display. It is further assumed that altitude change resolutions do not affect the production goal, as the horizontal trajectory is maintained, and delays caused by vertical maneuvers are minimal.

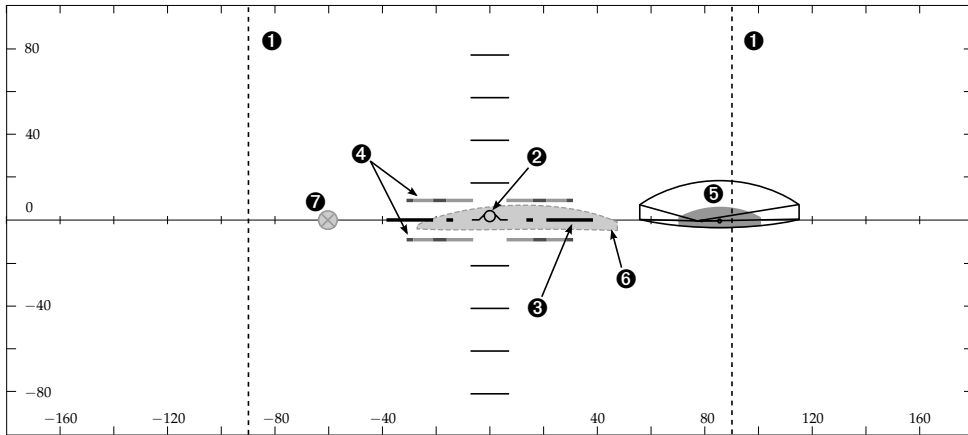


Figure 3.10: The interface design concept showing the example situation. The separation assistance elements numbered in this figure are: **1**: heading production constraints, **2**: flight-path vector, **3**: energy angle, **4**: steepest steady climb/descent, **5**: the 'puck', **6**: FPV constraint zone, and **7**: intruder flight-path vector.

The constraints for vertical maneuvering have been described intensively in [37]. For the current application, the climb and glide performance are considered at a constant airspeed. While potential - kinetic energy exchanges might indeed form interesting maneuvering possibilities for conflict resolution, they are beyond the scope of the current study.

Climbing and gliding constraints at a constant airspeed can be determined as a function of the maximum thrust, the glide ratio (or aerodynamic efficiency), and the roll angle. At a given altitude, these constraints translate into a maximum and a minimum flight-path angle γ . In an angular projection such as described in Section 3-3-1, these constraints can be indicated with lines of constant vertical visual angle.

In order to perform a steady climb or descent, a pilot has to manage the energy state of the aircraft. More precisely, he/she has to keep the kinetic energy rate to zero, and the potential energy such, that it matches the desired flight-path angle. In previous work, Amelink [34] described how the total energy rate of an aircraft can be expressed as a total energy angle, γ_E . When shown in conjunction with the flight-path angle, γ , the total energy angle also reveals the individual kinetic and potential energy rates to the pilot.

3-4 The display concept

Figure 3.10 illustrates the first design prototype of the separation assurance interface, which presents the separation assistance display elements introduced in the previous section, on an equidistant cylindrical projection of the airspace surrounding ownship.

3-4-1 Elements of the display

In this concept, the horizontal axis represents the full track angle range, ± 180 degrees, and behaves like a compass. This means that when ownship changes heading, the separation elements on the display shift horizontally, corresponding to the change in heading. The production constraints from the work-domain analysis are visualized by indicating the ± 90 degree limits with vertical lines ❶. The vertical axis of the current concept presents the vertical visual angle, in an earth-fixed frame of reference, ranging from -90 to 90 degrees.

Vertical ownship maneuvers are visualized with the vertical offset of the flight-path vector symbol ❷, from the center-line of the display. Together with the flight-path angle, the energy angle is shown as well ❸, i.e., the flight-path the pilot can select to realize a steady climb or descent. The steepest steady climb and descent for the current velocity are shown with the dashed lines ❹. Together, they relate to the function of energy management, and with the constraints they relate to the safety goal.

Intruder aircraft that are in conflict with ownship, or can get into conflict with ownship within the prediction horizon, are shown using the puck ❺. For each intruder aircraft within detection range, one puck is shown on the interface. The center of the puck represents the line of sight to the intruder. The arrow and its four lines indicate the direction and (projected) magnitude of the relative velocity of the intruder. When the lines are present the intruder is moving towards ownship, when they are absent the intruder is moving away from ownship. The size of the puck depends on the distance to the ownship (smaller is further away).

The shaded area in the puck represents the constraints for the velocity of the intruder, relative to ownship. If the tip of the relative velocity vector is located inside this area, and has the four lines attached, a loss of separation

will occur within the look-ahead horizon. The puck primarily relates to the safety goal, and shows relations between obstruction (motion), relative motion, and separation from the AH.

Constraints on ownship flight-path vector are shown with a shaded area ⑥. Note that this area is only valid for the current speed. Conflict urgency can be indicated by (locally) varying the color of the flight-path constraint area. In case of multiple intruders, constraint areas can be combined. In situations where areas with different conflict urgency levels overlap, the color of the shaded area is determined based on the highest urgency. ⑥ shows the affordance of conflict, as well as the affordance of avoidance, and relates to the safety goal, as well as to the efficiency goal (through the shortest way out principle [38]). Intruder flight-path vectors are shown as dots on the display ⑦. Moving the ownship flight-path vector towards one of these dots to resolve a conflict will lead to a very inefficient resolution, as this maneuver will cause ownship to fly parallel to the intruder [38].

3-4-2 Dynamic behavior of the display

Because the display projections depend not only on relative speed, but also on relative position of the intruder aircraft, the projection elements will change their shape over time, even when no corrective action is performed to resolve a conflict. Consequently, different conflict geometries will result in a different emergence of shapes. It is expected that after prolonged use of such a display, pilots will recognise patterns in this behavior. These patterns become familiar cues that can trigger rule-based actions [32].

Figure 3.11 shows an example dynamic scenario in planview, where one intruder aircraft passes behind ownship. In the example, ownship is flying level, heading north, at an altitude of 20,000ft, with a groundspeed of 390 kts. The intruder is initially flying at 36,000ft, but descending with a vertical speed of 2000 ft/min, and a groundspeed of 525 kts. Initially, the intruder is flying just behind, and east of ownship, with a track angle of 330° , at a distance of 36 nmi. The resulting $V_{rel,int}$ is directed just behind ownship, resulting in the intruder passing behind ownship during the course of the scenario. Figure 3.12 illustrates the emerging behavior of the flight-path constraint area in the example scenario. Figure 3.12(a) shows the situation at $t = 0$. The intruder is illustrated with the puck, and the constraint area

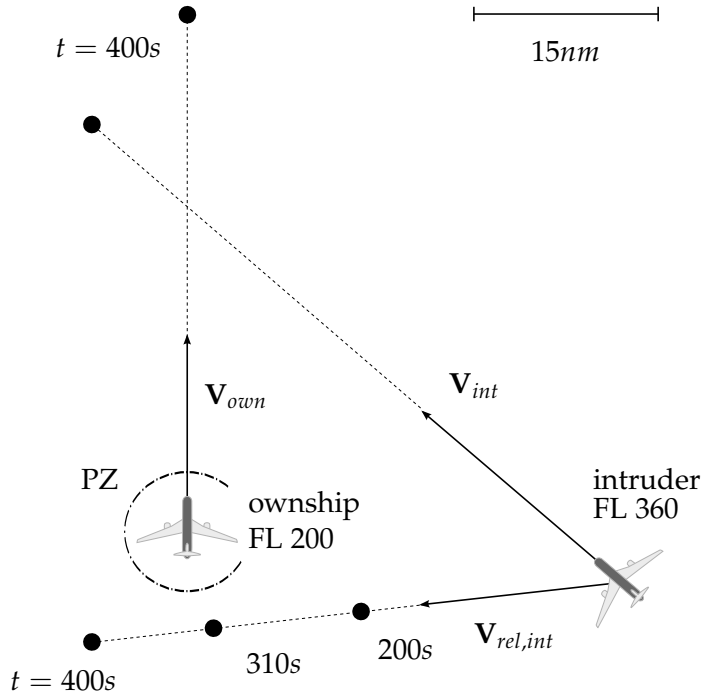


Figure 3.11: Planview of example dynamic scenario.

for the ownship Flight-Path Vector (FPV) is split into two parts. Both FPV constraint areas grow over time, up to the point that the larger of the two is stretched over the sides of the interface, as illustrated in Figure 3.12(b)-(c). In Figure 3.12(d), the larger area ‘opens up’, and stretches over the whole top of the display. In Figure 3.12(d), the small and large constraint areas start to grow towards each other, until they merge in Figure 3.12(e). After that, the stretched area shrinks again and becomes smaller, up to the point where it finally disappears (Figure 3.12(j)), i.e., there is no possibility left to get into conflict with the intruder, at the current velocity.

3-5 Practical application

The appropriateness of the concept for real-world applications depends on how well the proposed constraint projections extend to complex situations. Scenario’s such as multiple intruder conflicts, and complex trajectories will

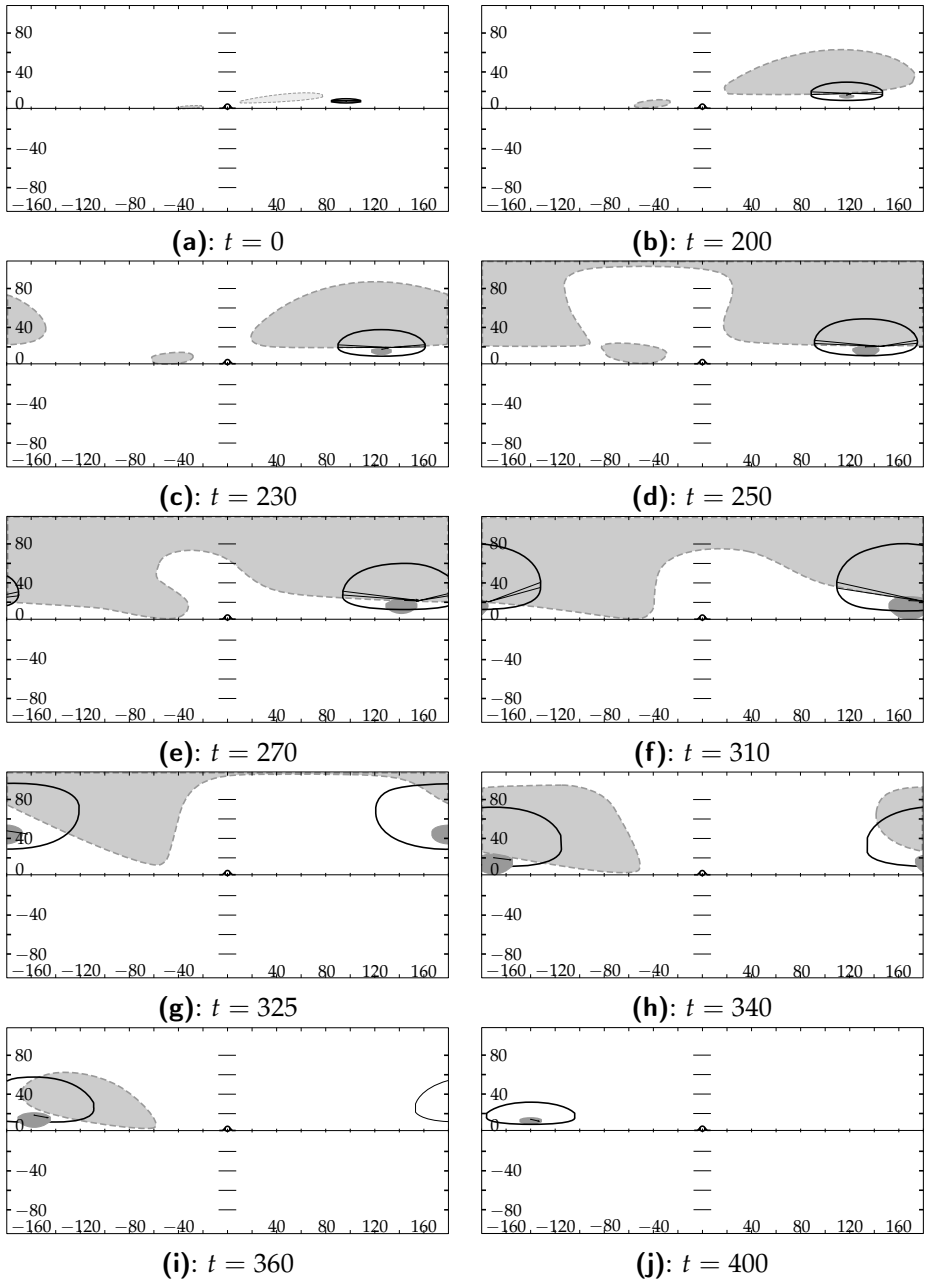


Figure 3.12: Example of a descending intruder aircraft passing behind ownship at distinct times.

ultimately determine the success of the concept. This section describes how the current concept behaves in more complex situations, and possibilities for extending the concept.

When multiple conflicts occur simultaneously, each of the conflicting aircraft would be represented on the display with its own 'puck', and corresponding FPV constraint area. Because each constraint area represents a set of state vectors that result in a conflict with that aircraft, a combination of conflict areas from multiple aircraft, superimposed onto each other, represents the set of states that would lead to a conflict with one or more of these aircraft. As a result, any state outside of this combined constraint area is a solution to *all* of the current conflicts. When such a global solution is unavailable or undesirable, conflicts will have to be solved in sequence.

This, in turn, requires the operator to determine an appropriate sequence in which to solve the conflicts, introducing the need to visualize the priority of each conflict. Color coding of the flight-path vector constraint area can be used to indicate time to loss of separation for a particular conflict. Two options are available: the first option gives a single color to a constraint area belonging to a certain intruder aircraft, where the color corresponds to the time to LoS with the current state vector. A second option would make use of the fact that every point in a constraint area corresponds to a certain state vector, which in turn corresponds to a certain time to loss of separation. This way, each point in a conflict area would be colored individually. The color of an individual constraint area then communicates the priority of the corresponding conflict.

The current approach of presenting the airspace affordances, i.e., presenting them as constraints on the current state, has several benefits: it shows a clear picture of how traffic influences the pilot's maneuvering possibilities (in terms of possible, conflict-free states), and it can be used to create combined visualizations for multiple state dimensions (e.g. the horizontal separation assistance display showing combined heading/speed affordances, the vertical separation assistance display FPA/speed, and the current concept presenting combined FPA/heading affordances). These displays support the pilot on Endsley's first two levels of SA (perceiving situational elements, and comprehending the meaning of the perceived variables, and their significance with regard to the system goals), and to a certain extent also on

the third level of SA (projecting the current state, or a target state into the future) [60]. When intent (ownership and intruder) is taken into account, however, projection is no longer a trivial extrapolation in time of the aircraft state vector. Instead, the affordance space changes as a function of space and time due to Trajectory Change Points (TCP), and other changes of state or intent.

Van Dam already showed for the horizontal case, that the dimension along the bisector of the triangular forbidden area determines the time at which the closest point of approach with the respective intruder will occur [47], with the triangle origin representing $t_{CPA} = \infty$. Using this property, the part of the triangle where $t_{CPA} > t_{TCP}$ can be discarded. Extrapolations of the future track can be used to show constraints due to intruder state beyond the trajectory change point. A similar method can be used to include intent in the current concept.

3-6 Discussion

The work presented in this paper is part of an ongoing study on the design of a trajectory planning aid. The intended goal is to obtain a graphical interface, that supports pilots in their new task of airborne reconfiguration of a pre-planned trajectory, in case of traffic conflicts in unmanaged airspace. For a pilot to function consistently well in this new task, the interface should promote a high level of situation awareness, supporting the pilot in routine, as well as unforeseen situations. This study adopts an EID-inspired, constraint-based approach, where results from a work-domain analysis on multiple levels of abstraction are used to develop a visual representation of the travel constraints.

To improve situation awareness, and support appropriate trust in, and interaction with automated systems, it is necessary for the automation to be transparent and understandable to the operator. An ecological interface tries to achieve this by revealing more about the functioning of the work domain[61]. The current interface concept tries to realize this by showing the implications of other traffic for the affordances of locomotion in *relative space*, and how they relate to ownership performance constraints in *absolute space*. When used in combination with an automated system that provides explicit resolutions, the display helps improve operator trust and understanding of

an automated resolution, by helping him understand how constraints shape possible resolutions.

Previous work from this study resulted in two concepts of separation assistance displays: the horizontal separation assistance display presents a horizontal projection of the constraints and affordances, which resulted in a speed-track angle action space overlay on the Navigation Display (ND)[38]. This display has since then been extended, by showing the effects of maneuver dynamics and ownship and traffic intent on the presentation of the affordance space [47, 59]. The vertical separation assistance display works in a similar fashion, but instead of showing a horizontal projection of the locomotion constraints, it uses a vertical constraint projection to create an FPA-speed action space that is presented on a Vertical Situation Display (VSD) [39].

Both these displays provide a projection of a certain action space. The action, here, is the action of locomotion of an aircraft in three-dimensional space, which can be defined by flight parameters track angle, flight-path angle, and velocity. For this three-dimensional action space, the horizontal and vertical separation assistance displays can be regarded as two orthogonal views on the three-dimensional affordance space. The FPA-track angle affordance zone presented in this paper, then, would be the remaining third view. Considering the preference of airline pilots to keep the airspeed constant [50, 55], it can be hypothesized that the FPA-track angle combination should be the preferred option of these three projections. This should be addressed in a comparative experiment.

One of the main design challenges, is to make use of an aircraft pilot's existing ecology. For travel planning and avoidance, pilots already make use of the outside view and existing cockpit instruments, to perceive the affordances of the airspace. The challenge is therefore not to replace, but to enhance this perception. One way to do this is to find a compatible display to adapt with the separation assistance elements. This method is employed in the previous concepts: the horizontal separation assistance display used the ND to present the travel affordances, and the vertical separation assistance display projected the situation on the VSD.

The current concept would be most compatible with the Primary Flight Display (PFD), since they both present their information in the track angle

/ flight-path angle space. However, a problem with this combination is that a PFD presents its information in an “inside-out” fashion (i.e., the aircraft symbol is stationary, whereas the horizon moves). This is an unfavorable situation when separation avoidance elements are shown on this display. Because these elements are related to the orientation of the ownship, they will move and rotate with the horizon, making them more difficult to interpret. Other options would, then, be auxiliary displays such as the Electronic Flight Bag (EFB).

A consequence of the current choice of cutting-planes is that the visualized affordances relate to ownship motion in terms of track angle and vertical speed changes, however, they do not show the affordances in terms of ownship velocity. Although pilot feedback in the evaluation experiments of the previous concepts already indicated that velocity changes are not preferred, and therefore rarely used when resolving conflicts, the ‘perfect ecological interface’ would ideally present the affordances for *all* of the pilot’s maneuvering options. Also, speed changes might be required to satisfy other goals than safety, for instance to compensate for time deviation along track, to adhere to time constraints at the next waypoint. In terms of requirements following from the efficiency goal, a pilot may for instance also consider a constant-throttle vertical maneuver, where velocity cannot be assumed constant.

It is clear that the step from work domain analysis to display concept is far from a trivial one, and more than one iteration between analysis and design will be required to work towards a fully functional, and mature design [45]. In these iterations, concessions are unavoidable when trying to present four-dimensional work-domain properties on a two-dimensional surface.

3-7 Bibliography

- [1] **JPDO**. Concept of Operations for the Next Generation Air Transportation System, Version 2.0. Tech. rep., Joint Planning and Development Office, 2007.
- [2] **SESAR Consortium**. SESAR Definition Phase D3: The ATM Target Concept. Tech. Rep. DLM-0612-001-02-00, Eurocontrol, 2007.

-
- [3] **D. A. Norman.** The “Problem” of Automation: Inappropriate Feedback and Interaction, not “Over-Automation”. *Philosophical Transactions of the Royal Society of London*, 327(1241), 585–593, 1990. ISSN 0962-8436. doi: 10.1098/rstb.1990.0101.
- [4] **N. B. Sarter** and **D. D. Woods.** Pilot Interaction With Cockpit Automation: Operational Experiences With the Flight Management System. *The International Journal of Aviation Psychology*, 2(4), 303–321, 1992. doi:10.1207/s15327108ijap0204_5.
- [5] **G. Lintern.** An Affordance-Based Perspective on Human-Machine Interface Design. *Ecological Psychology*, 12(1), 65–69, 2000.
- [6] **J. D. Lee** and **N. Moray.** Trust, Control Strategies and Allocation of Function in Human-Machine Systems. *Ergonomics*, 31(10), 1243–1270, 1992.
- [7] **J. D. Lee** and **N. Moray.** Trust, Self-Confidence, and Operators’ Adaptation to Automation. *International Journal of Human-Computer Studies*, 40(1), 153–184, 1994.
- [8] **B. M. Muir.** Trust in Automation. 1: Theoretical Issues in the Study of Trust and Human Intervention in Automated Systems. *Ergonomics*, 37(11), 1905–1922, 1994.
- [9] **C. Meckiff** and **P. Gibbs.** PHARE Highly Interactive Problem Solver. Tech. Rep. 273/94, Eurocontrol, 1994.
- [10] **R. Azuma**, **H. Neely**, **M. Daily**, and **M. Correa.** Visualization of Conflicts and Resolutions in a “Free Flight” Scenario. In: *Proceedings of IEEE Visualization*, pp. 433–436, 1999.
- [11] **J. M. Hoekstra**, **R. N. H. W. van Gent**, and **R. C. J. Ruigrok.** Designing for Safety: the Free Flight Air Traffic Management Concept. *Reliability Engineering and System Safety*, 75, 215–232, 2002.
- [12] **R. Canton**, **M. Refai**, **W. W. Johnson**, and **V. Battiste.** Development and Integration of Human-Centered Conflict Detection and Resolution Tools for Airborne Autonomous Operations. In: *International Symposium on Aviation Psychology*, pp. 115–120, 2005.

- [13] **W. R. Knecht**. Testing a Multidimensional Nonveridical Aircraft Collision Avoidance System. *Human Factors*, 50(4), 565–575, 2008. doi: 10.1518/001872008X288600.
- [14] **J. K. Kuchar** and **L. C. Yang**. A Review of Conflict Detection and Resolution Modelling Methods. *IEEE Transactions on Intelligent Transportation Systems*, 1(4), 179–189, 2000.
- [15] **R. Ghosh** and **C. J. Tomlin**. Maneuver Design for Multiple Aircraft Conflict Resolution. In: *Proceedings of the American Control Conference*, pp. 672–676. Chicago (IL), 2000.
- [16] **L. Pallottino**, **E. M. Feron**, and **A. Bicchi**. Conflict Resolution Problems for Air Traffic Management Systems Solved With Mixed Integer Programming. *IEEE Transactions on Intelligent Transportation Systems*, 3(1), 3–11, 2002. ISSN 15249050. doi:10.1109/6979.994791.
- [17] **D. J. Wing**, **R. A. Vivona**, and **D. A. Roscoe**. Airborne Tactical Intent-Based Conflict Resolution Capability. In: *9th AIAA Aviation, Technology, Integration, and Operations*, 2009.
- [18] **J. M. Hoekstra**, **R. N. H. W. van Gent**, and **J. Groeneweg**. Airborne Separation Assurance Validation With Multiple Humans-In-The-Loop. In: *Proceedings of the 5th USA - Europe ATM Seminar*, 2003.
- [19] **A. R. Pritchett**. Human-Computer Interaction in Aerospace. In: *The Human-Computer Interaction Handbook: Fundamentals, Evolving Technologies and Emerging Applications*, pp. 861–882. Lawrence Erlbaum Associates, Inc., Mahwah, NJ, USA, 2003. ISBN 0-8058-3838-4.
- [20] **E. L. Wiener** and **R. E. Curry**. Flight-Deck Automation: Promises and Problems. *Ergonomics*, 23(10), 995–1011, 1980.
- [21] **L. Bainbridge**. Ironies of Automation. In: **J. Rasmussen**, ed., *New Technology and Human Error*. John Wiley and Sons, 1987.
- [22] **M. R. Endsley**. Automation and Situation Awareness. In: **R. Parasuraman** and **M. Mouloua**, eds., *Automation and Human Performance: Theory and Applications*, pp. 163–181. Hillsdale, NJ: Erlbaum Associates, 1996.

- [23] **R. Parasuraman** and **V. Riley**. Humans and Automation: Use, Misuse, Disuse, Abuse. *Human Factors*, 39(2), 230–253, 1997.
- [24] **M. R. Endsley**, **B. Bolte**, and **D. G. Jones**. *Designing for situation awareness: an approach to user centered design*. Taylor and Francis, 2003. ISBN 0-748-40967-X.
- [25] **J. M. Flach**, **M. Mulder**, and **M. M. van Paassen**. The Concept of the Situation in Psychology. In: **S. P. Banbury** and **S. Tremblay**, eds., *A Cognitive Approach to Situation Awareness: Theory and Application*, pp. 42–60. Ashgate, 2004. ISBN 978-0-7546-4198-8.
- [26] **K. J. Vicente**. Ecological Interface Design: Progress and Challenges. *Human Factors*, 44, 62–78, 2002.
- [27] **G. A. Jamieson**. Ecological Interface Design for Petrochemical Process Control: An Empirical Assessment. *IEEE Transactions on Systems, Man, and Cybernetics, part A: Systems and Humans*, 37(6), 906–920, 2007. doi: 10.1109/TSMCA.2007.897583.
- [28] **K. J. Vicente** and **J. Rasmussen**. Ecological Interface Design: Theoretical Foundations. *IEEE Transactions on Systems, Man, and Cybernetics*, 22(4), 589–606, 1992.
- [29] **C. M. Burns** and **J. R. Hajdukiewicz**. *Ecological Interface Design*. CRC Press LLC, FL: Boca Raton, 2004. ISBN 0415283744.
- [30] **J. J. Gibson**. *The Ecological Approach to Visual Perception*. Houghton Mifflin, 1979. ISBN 0-89859-959-8.
- [31] **K. J. Vicente** and **J. Rasmussen**. The Ecology of Human-Machine Systems II: Mediating Direct-Perception in Complex Work Domains. *Ecological Psychology*, 2(3), 207–249, 1990.
- [32] **J. Rasmussen**. Skills, Rules, Knowledge; Signals, Signs, Symbols, and Other Distinctions in Human Performance Models. *IEEE Transactions on Systems, Man, and Cybernetics*, 13, 257–266, 1983.
- [33] **J. J. Gibson**. The Theory of Affordances. *Perceiving, Acting and Knowing: Toward an Ecological Psychology*, pp. 67–82, 1977.

- [34] **M. H. J. Amelink, M. Mulder, M. M. van Paassen, and J. M. Flach.** Theoretical Foundations for a Total Energy-Based Perspective Flight-Path Display. *The International Journal of Aviation Psychology*, 15, 205–231, 2005.
- [35] **C. Borst, H. C. H. Suijkerbuijk, M. Mulder, and M. M. van Paassen.** Ecological Interface Design for Terrain Awareness. *International Journal of Aviation Psychology*, 16(4), 375–400, 2006.
- [36] **C. Borst, F. A. Sjer, M. Mulder, M. M. van Paassen, and J. A. Mulder.** Ecological Approach to Support Pilot Terrain Awareness After Total Engine Failure. *Journal of Aircraft*, 45(1), 159–171, 2008.
- [37] **C. Borst, M. Mulder, and M. M. van Paassen.** Design and Simulator Evaluation of an Ecological Synthetic Vision Display. *Journal of Guidance, Control and Dynamics*, 33(5), 1577–1591, 2010. doi:10.2514/1.47832.
- [38] **S. B. J. van Dam, M. Mulder, and M. M. van Paassen.** Ecological Interface Design of a Tactical Airborne Separation Assistance Tool. *IEEE Transactions on Systems, Man, and Cybernetics, part A: Systems and Humans*, 38(6), 1221–1233, 2008.
- [39] **F. M. Heylen, S. B. J. van Dam, M. Mulder, and M. M. van Paassen.** Design and Evaluation of a Vertical Separation Assistance Display. In: *AIAA Guidance, Navigation, and Control Conference and Exhibit*. Honolulu (HI), 2008.
- [40] **J. Rasmussen.** The Role of Hierarchical Knowledge Representation in Decision Making and System Management. *IEEE Transactions on Systems, Man, and Cybernetics*, 15(2), 234–243, 1985.
- [41] **G. Lintern, T. Waite, and D. A. Talleur.** Functional Interface Design for the Modern Aircraft Cockpit. *The International Journal of Aviation Psychology*, 9(3), 225–240, 1999.
- [42] **M. M. van Paassen.** Functions of Space and Travellers. In: *Proceedings of 18th European Annual Conference on Human Decision Making and Manual Control*. Faculty of Aerospace Engineering, Delft University of Technology, 1999.

- [43] **Radio Technical Commission for Aeronautics**. Airborne Conflict Management: Application Description V2.5. Tech. Rep. RTCA SC-186, Federal Aviation Authorities, 2002.
- [44] **A. M. Bisantz** and **K. J. Vicente**. Making the Abstraction Hierarchy Concrete. *International Journal of Human-Computer Studies*, 40, 83–117, 1994.
- [45] **M. M. van Paassen**, **M. H. J. Amelink**, **C. Borst**, **S. B. J. van Dam**, and **M. Mulder**. The Chicken, the Egg, the Workspace Analysis, and the Ecological Interface. In: *International Symposium on Aviation Psychology*. Faculty of Aerospace Engineering, Delft University of Technology, Dayton, USA, 2007.
- [46] **Federal Aviation Administration** and **Eurocontrol**. Principles of Operation for the Use of Airborne Separation Assurance Systems. Tech. Rep. PO-ASAS-V7.1, Federal Aviation Authorities - Eurocontrol, 2001.
- [47] **S. B. J. van Dam**, **M. Mulder**, and **M. M. van Paassen**. The Use of Intent Information in an Airborne Self-Separation Assistance Display Design. In: *AIAA Guidance, Navigation, and Control Conference and Exhibit*, 2009.
- [48] **Radio Technical Commission for Aeronautics**. Minimal Operational Performance Standards for Traffic Alert and Collision Avoidance System 2 (TCAS2) Airborne Equipment. Tech. rep., Federal Aviation Authorities, 2002.
- [49] **Radio Technical Commission for Aeronautics**. Final Report of the RTCA Board of Directors' Select Committee on Free Flight. Tech. rep., RTCA, 1995.
- [50] **J. M. Hoekstra**. *Designing for Safety: The Free Flight Air Traffic Management Concept*. Ph.D. thesis, Delft University of Technology, The Netherlands, 2001.
- [51] **C. D. Wickens**. The When and How of Using 2-D and 3-D Displays for Operational Tasks. In: *Proceedings of the Human Factors and Ergonomics Society*, pp. 403–406, 2000.

- [52] **A. L. Alexander, C. D. Wickens, and D. H. Merwin.** Perspective and Coplanar Cockpit Displays of Traffic Information: Implications for Maneuver Choice, Flight Safety, and Mental Workload. *The International Journal of Aviation Psychology*, 15, 1–21, 2005.
- [53] **M. W. McGreevy and S. R. Ellis.** The Effect of Perspective Geometry on Judged Direction in Spatial Information Instruments. *Human Factors*, 28(4), 439–456, 1986.
- [54] **M. L. Bolton and E. J. Bass.** Using Relative Position and Temporal Judgments to Identify Biases in Spatial Awareness for Synthetic Vision Systems. *The International Journal of Aviation Psychology*, 18(2), 183–206, 2008.
- [55] **R. Appleton, M. Mulder, and M. M. van Paassen.** Comparison of Two Interfaces for Supporting Pilots in Airborne Self-Separation Tasks. In: *AIAA Guidance, Navigation, and Control Conference and Exhibit*. AIAA, Keystone (CO), USA, 2006.
- [56] **S. N. Roscoe, L. Corl, and R. S. Jensen.** Flight Display Dynamics Revisited. *Human Factors*, 23(3), 341–353, 1981.
- [57] **D. J. Gates, E. A. Gates, M. Westcott, and N. L. Fulton.** Stereo Projections of Miss Distance in Some New Cockpit Display Formats. *Journal of Aircraft*, 45(5), 1725–1735, 2008. ISSN 0021-8669. doi:10.2514/1.35574.
- [58] **R. A. Paielli.** Modeling Maneuver Dynamics in Air Traffic Conflict Resolution. *Journal of Guidance Control and Dynamics*, 26(3), 407–415, 2003.
- [59] **S. B. J. van Dam, M. Mulder, and M. M. van Paassen.** Airborne Self-Separation Display with Turn Dynamics and Intruder Intent-Information. In: *IEEE International Conference on Systems, Man and Cybernetics*. IEEE, Montreal, Canada, 2007.
- [60] **M. R. Endsley.** Toward a Theory of Situation Awareness in Dynamic Systems. *Human Factors*, 37(1), 32–64, 1995.
- [61] **K. Christoffersen, C. N. Hunter, and K. J. Vicente.** A Longitudinal Study of the Effects of Ecological Interface Design on Deep Knowledge. *International Journal of Human-Computer Studies*, 48, 729–762, 1998.

Co-planar representation of 3-D constraints

This chapter describes a concept for a co-planar airborne separation display. The decision for a co-planar display is a departure from the aim of the concept described in Chapter 3, which was to create a single, integrated presentation of the three-dimensional constraints. This chapter therefore describes the motivation for this design change, before presenting the visualization methods and the resulting display concept. The co-planar display concept presents speed, heading, and altitude action possibilities in two planar projections of the three-dimensional maneuver action space. The display also provides visualizations of the interactions between these planes of projection, as well as methods to improve the visual momentum across displays.

- Paper title** Design of a Co-Planar Airborne Separation Display
- Authors** J. Ellerbroek, K. C. R. Brantegem, M. M. van Paassen, M. Mulder
- Published in** IEEE Transactions on Human-Machine Systems, Vol. 43, No. 3, May 2013, pp. 277–289

Abstract: *This paper describes a concept for a co-planar airborne self-separation display, that is designed to aid pilots in their separation task, by visualizing the possibilities for conflict resolution that the airspace provides. This work is part of an ongoing research towards the design of a constraint-based three-dimensional separation assistance interface that can present all the relevant properties of the spatio-temporal separation problem. A display concept is proposed that presents speed, heading and altitude action possibilities in two planar projections of the maneuver action-space. The interface also visualizes how these projections interact with each other.*

4-1 Introduction

In the current Air-Traffic Management (ATM) concepts for unmanaged airspace, aircraft will fly optimized, four-dimensional trajectories, that have been determined and coordinated completely before the actual flight [1, 2]. To resolve traffic (or other) conflicts that result from uncertainties that arise during flight (e.g., bad weather, departure delays), automated systems will be used to detect conflicts, and provide resolution advisories to the pilot.

Although automation provides the resolutions, pilots will ultimately be responsible for the validity of that resolution. They should therefore be able to monitor the traffic situation, and the proper functioning of the automation, and should be able to intervene in case the automation fails. In other words, pilots should be able to detect, and act upon very infrequent situations that were not anticipated in the design of the automation. It is therefore of paramount importance for automation to be transparent and understandable to the operator [3–6].

The work presented in this paper is part of an ongoing study on the design of a three-dimensional separation assistance interface. The study employs a constraint-based approach, inspired by Ecological Interface Design (EID). EID is a proven design paradigm from the domain of process control [7, 8], that has in recent years also been applied in several aviation-related interface concepts [9–16]. In this approach, work-domain analysis tools such as the Abstraction Hierarchy (AH) are used to identify relevant constraints and relations on multiple levels of abstraction [17, 18]. An extensive analysis of the work domain relevant to airborne separation was performed during the design of previous constraint-based concepts [12, 13, 16]. This paper will

summarize the relevant constraints and relations that were identified in the analysis, which stands at the basis of the concept presented in this paper. For a more exhaustive description of the actual work-domain analysis, the reader is referred to the previous publications.

The aim of this study is to create an interface that realizes proper support for airborne separation, by showing the implications of other traffic for the affordances [19, 20] of locomotion, and how they relate to limitations of the own aircraft [12, 13]. The interface presented in this study does not explicitly relate to specific automation functions. Instead, it visualizes work domain information, which invariably forms the premise on which both automation and the human operator should base their actions. By going beyond visualizations that relate only to the automation logic, these displays help pilots gain a deeper understanding of the functions and relations within the work domain [17, 18, 21], which will be invaluable to pilots when they need to judge the automation's functioning [22]. These displays should provide support in routine as well as unforeseen situations, where pilots may have to rely on their own problem-solving skills to resolve a conflict.

This study has led to three display concepts [12, 13, 16]. Each of these concepts presents a planar projection of the own aircraft's three-dimensional maneuver space. All three projections represent simplified, two-dimensional versions of the maneuver space. They inescapably discard information, a problem that is inherent to the presentation of multi-dimensional data on a two-dimensional surface [23, 24]. Our ultimate goal is therefore to find a representation that mitigates as much as possible the problems of presenting multi-dimensional data on a two-dimensional surface.

Several studies have investigated the effects of three-dimensional visualization methods for airborne traffic information displays [25–27]. They compare between perspective and (co-)planar displays that give a basic representation of traffic. For the current work, however, the focus lies not only on representing traffic, but also on what such traffic means to pilots in terms of achieving functional goals, and how it relates to other functions and constraints in the work domain. This will pose different demands on the method of presentation.

This paper argues for a co-planar representation, on the basis of previous concepts and the corresponding work-domain analysis. It will describe how

to mitigate the problems that arise when information which is intrinsically three dimensional is distributed across two two-dimensional displays, and how to show the interactions that can occur between the two planar presentations. The decision for a co-planar display is a departure from the aim of the previous concept[16], which was to create a single, integrated perspective presentation of the three-dimensional constraints. The following section will therefore discuss the rationale for choosing a co-planar display. Section 4-3 introduces functional presentations for relevant work-domain constraints. The fourth section describes the co-planar display concept. A fifth section illustrates how the visualizations in the display concept link back to the work-domain analysis. The paper concludes with a discussion of the benefits, drawbacks, and remaining challenges of this concept.

4-2 Three-dimensional data visualization

For the visualization of a three-dimensional space on a two-dimensional screen, two options can be distinguished: perspective displays and co-planar displays, each with their own benefits and drawbacks [23, 24]. The decision to choose either of these two methods will depend on the task requirements for the resulting display. A co-planar display has uniform, undistorted axes in its viewing planes, which benefits precise position and angle judgments. Perspective displays, on the other hand, have more “pictorial realism”: they correspond more closely to the three-dimensional world [26, 28, 29]. Perspective displays can also employ texture and shading to increase realism, and improve spatial awareness [30]. Perspective displays might therefore be preferred when the task requires complex shape understanding. St. John et al. also differentiate between tasks that involve only separated spatial dimensions, and tasks that involve integrated spatial dimensions, where co-planar displays are better suited for the former, and perspective displays for the latter [24].

A drawback of co-planar displays in the current context is that some of the information on the interaction between locomotion constraints is lost, when these constraints are presented using separate horizontal and vertical projections. Also, distributing the information across two displays requires the pilot to mentally integrate the information from both displays. Perspective displays, on the other hand, suffer from perspective distortions, which

can induce errors in judging distances and angles on the display [27, 31, 32]. The presentation of three-dimensional structures also suffers from problems of occlusion: when viewed from a fixed angle, the front facing side of the structure hides the internal details of the structure.

4-2-1 Motivation for a co-planar display concept

In the design of a separation assistance display concept, the choice between visualizations should depend on the specifics of the separation task, and how it is performed. From previous studies and experiments, several arguments can be found for the use of a co-planar display. First, experiments performed in this study, as well as other studies, showed that pilots have a strong preference for single-axis resolution maneuvers [26, 33–36]. Second, the design of previous constraint-based separation assistance displays illustrated that traffic constraints can become complex, yet precise judgment of these constraints is valuable for safe and efficient conflict resolution. They also illustrate that the planar projections of the constraints show an intuitive relation with the absolute geometry of the conflict, which benefits situation awareness. Perspective distortion makes this relation less visible in a perspective projection, a problem that also hampered the previous concept for a perspective three-dimensional interface[16]. Although that concept employed constant-velocity cutting planes to reduce the complexity of the constraint visualization, it did not reproduce the intuitive visual relation with the spatial representation of the conflict.

Two of the three current constraint-based separation assistance displays will be used as a basis for the co-planar concept [12, 13, 16]. The three current display concepts provide three orthogonal projections of the maneuver space: a top-down projection [12], a side-view projection [13], and a front-facing, ego-centric equidistant cylindrical projection [16]. The first two are presented on the Horizontal Situation Display (HSD), and Vertical Situation Display (VSD), respectively. The third concept does not have an equivalent existing display in the cockpit. Because the first two concepts feature the most intuitive maneuver space projections, and as they correspond closest to current re-planning tasks and displays, these will be used in the co-planar display concept. Each of the two original display concepts assumes that a traffic conflict lies exactly in its plane, and the challenge in the design of the

co-planar concept discussed in this paper lies in showing the interactions that exist between the projection planes of the co-planar display. This will be discussed in Section 4-3.

4-2-2 Comparison with other three-dimensional displays

Although most current research on airborne separation assistance systems focuses on the development of automated systems that assist pilots with the separation task [37–41], there are also several display concepts that have been developed as aids in the task of self-separation [39, 42–44]. There are two distinct types of conflict representation that are used in these displays: a spatial representation, which is similar to traditional situation displays, and a maneuver-space representation, i.e., visualizing how proximate traffic limits ownship maneuverability in terms of airspeed, heading, and vertical speed. Some displays use only one of these representations, others combine them. An important benefit of spatial representations is that they offer an intuitive overview of the situation, familiar to anyone who has ever used a map. Maneuver-space displays, on the other hand, are useful because they reveal a direct link between constraints or commands, and the applicable maneuver dimensions.

A second distinctive factor between displays is whether they show explicit (automated) commands, or constraints on maneuvering. Benefits of explicit command displays are that they suffer relatively little from display clutter, and that they reduce workload. Automation also has the potential of providing the most efficient conflict resolution options. The most important drawback of displays that show only explicit resolution commands is that they hide the rationale behind automation. These displays do not support human information seeking, and, in case of automation failure, pilots are not supported in recognizing failure, nor in seeking alternatives. In these situations, performance can even be worse than when completely unaided [22].

Constraint displays, on the other hand, give a continuous view on maneuver options and limitations, which allow pilots to evaluate their own resolution maneuvers. Depending on how constraints are visualized, these displays can show the structure of, and relations within the work domain, and can therefore provide a useful basis for illustrating automation logic. By showing higher level information and relations, these displays also allow

pilots to investigate the validity of the data. An important drawback of constraint displays is that they can result in more display clutter, compared to showing only explicit commands. According to Tufte's views on the use of details ("To clarify, add detail"), however, this is not necessarily a drawback for a well designed display [45].

The existing concepts described in [39, 42, 44] show that the concepts presented in the current study are not the only displays that show constraints on maneuvering instead of only presenting explicit commands. The concept presented in [42] provides a spatial representation of constraints in the form of no-go areas on horizontal and vertical map displays. A different approach was taken in [39], where constraints are indicated with colored conflict-bands on the compass, the speed tape and the vertical speed indicator on the Primary Flight Display, the HSD, and the VSD. The concept described in [44] introduces a new display that presents constraints in a perspective, three-dimensional maneuver space.

The concepts in the current study aim to improve upon such constraint-based concepts by visualizing the structure of the work domain, and by illustrating the relations between lower-level elements and higher-level information. The remainder of this paper will describe how properties of the own aircraft and the surrounding traffic are related to each other, and to higher-level constraints and functions, in a way that is made visually apparent on the display.

4-3 Functional presentation of constraints

For airborne trajectory planning and self-separation, several relevant constraints have been identified [12, 13, 16]. These constraints fall broadly into two categories: constraints internal to the own aircraft, and constraints external to the aircraft.

The internal constraints relevant to the problem of separation relate to the various limitations on aircraft performance. In addition to these internal limitations, the maneuver space is further constrained by external factors such as weather, terrain, other traffic, and airspace boundaries (such as those from restricted airspace areas). For airborne separation, the focus obviously lies on the constraints imposed by other traffic.

Functional presentations of these constraints, and the relations between these constraints, should provide a description that is compatible to the means that are available to the controller. For trajectory planning, this implies that the description should relate the goals and affordances of the system, to inputs that match common flight practice. In cruise flight, pilots control their aircraft by manipulating velocity, track angle*, and altitude settings, using the autopilot or by modifying the planned route in the Flight-Management System (FMS). A successful separation assistance interface should relate these control variables and their operational limits to the affordances of the airspace.

4-3-1 Velocity action space

A modern glass cockpit supports trajectory planning through the Horizontal Situation Display and the Vertical Situation Display, which show horizontal and vertical projections of task-relevant information such as the planned route, terrain, weather, and other traffic. While these visualizations clearly identify the elements of the airspace that constrain the maneuver options of the aircraft, they do not show how these elements shape the possibilities for pilot action. Because the operator action space is not shown in a meaningful way, it remains difficult to relate higher level goals and constraints to the available actions and inputs.

The design philosophy employed in this study proposes to achieve this by combining the existing spatial representation of airspace elements, with a *velocity action space*, that relates own aircraft maneuver variables velocity, track angle and vertical speed, to the identified internal and external constraints [12, 16]. This action space is defined as the reachable subset of the three-dimensional vector space that contains all possible velocity vectors (i.e., all combinations of velocity, track angle and vertical speed).

*Track angle differs from aircraft heading in the presence of wind. Heading indicates in which direction the aircraft nose is pointing, as indicated e.g. on the magnetic compass. The track angle gives the direction in which the aircraft is *flying*. With no wind, these angles are equal. With cross-wind, however, there will be an offset between heading and track (the drift angle).

When zero wind is assumed, an aircraft velocity vector in this vector space can be defined as follows:

$$\mathbf{V} = V_{TAS} \cdot \begin{bmatrix} \cos(\chi) \cos(\gamma) \\ \sin(\chi) \cos(\gamma) \\ \sin(\gamma) \end{bmatrix}, \quad 4.1$$

where V_{TAS} is the (true) airspeed of the aircraft, χ the track angle, and γ the flight-path angle, or climb angle of the aircraft. Vertical maneuvering is more commonly expressed in vertical speed, which can be derived from V_{TAS} and γ : $VS = V_{TAS} \sin(\gamma)$. The presence of wind can be of influence on the velocity action space representation, but only when ownship and intruder aircraft experience significantly different wind conditions. It is therefore kept out of the current analysis.

4-3-2 Internal constraints

The reachable area that defines the velocity action space is bounded by constraints that are internal to the own aircraft. These constraints relate to the various limitations on the performance of the aircraft, such as bank limits, maneuver dynamics, available engine thrust, stall, structural considerations, buffet characteristics, and requirements on productivity, emissions and passenger comfort. These limitations result in several constraints relevant to the task of trajectory planning, such as maximum turn rates, maximum and minimum operating speeds, fastest and steepest steady climb and descent, and the steepest steady climbing and descending turn. Some of these constraints also show interactions: For example, in turning flight, increasing the bank angle will also affect the minimum velocity and the maximum attainable climb angle [46].

Figure 4.1(a) and Figure 4.1(b) illustrate how these constraints can be visualized in the horizontal and vertical plane, respectively. The horizontal maneuver space is shaped by the limitations on airspeed, which reduce it to the ring-shaped area in Figure 4.1(a).

Vertical maneuvering is also constrained by airspeed limitations, as well as by the steady climb and descent performance. Figure 4.1(b) shows how these constraints combine in the vertical plane. The vertical edges of the action space result from the limits on airspeed. The curved edges at the top

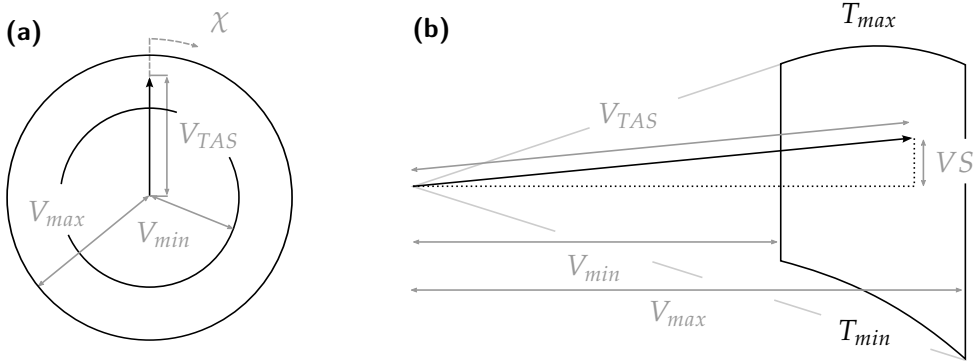


Figure 4.1: The three-dimensional *velocity action space* illustrated in two planar projections. **(a):** Horizontal maneuvering can be expressed in combinations of airspeed (V_{TAS}) and track angle (χ). The minimum (V_{min}) and maximum (V_{max}) obtainable airspeeds are the main constraints for horizontal maneuvering. **(b):** Vertical maneuvering can be expressed in combinations of airspeed (V_{TAS}) and vertical speed (VS). It is also constrained by the minimum (V_{min}) and maximum (V_{max}) obtainable airspeeds. Aircraft performance with maximum (T_{max}) and minimum (T_{min}) thrust settings determine maximum steady climb and descent, respectively.

and bottom of the vertical action space visualize the maximum obtainable steady climb and descent at each velocity, respectively. The resulting contour is also known as the *flight envelope* of the aircraft (refer to [13] for the derivation of this contour).

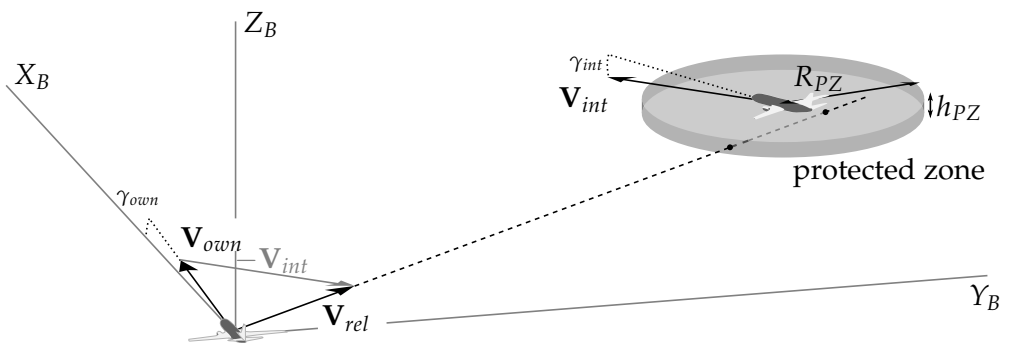


Figure 4.2: A conflict situation. Ownship and intruder are in conflict when the line that extends from the relative velocity vector (\mathbf{V}_{rel}) crosses the intruder Protected Zone (PZ). The PZ is a flat, three-dimensional disc around each aircraft, that should remain clear of other traffic. Common dimensions for this PZ are $R_{PZ} = 5 \text{ nmi}$ and $h_{PZ} = 2,000 \text{ ft}$.

4-3-3 External constraints

In unmanaged airspace, the reachable area that is enclosed by the internal aircraft constraints is further restricted by several external factors, such as weather, terrain, and traffic. For a self-separation interface the focus obviously lies on the constraints imposed by other traffic. These traffic constraints are shaped by a minimum horizontal and vertical separation between any two aircraft, that should be adhered to at all times. With common values of 5 nautical miles horizontal, and 1,000 feet vertical separation, this results in a three-dimensional *Protected Zone (PZ)*: A flat, three-dimensional disc around each aircraft, that should remain clear of other traffic (illustrated for the intruder aircraft in Figure 4.2) [33, 47]. Intrusion of this space is referred to as a loss of separation. A conflict is defined as a predicted future loss of separation, within a certain time horizon [48]. For this concept, the time horizon was set between 60 seconds and 10 to 20 minutes [16].

Although ownship and intruder intent can influence the constraints imposed by the intruder, the current study will only employ the current states to derive these constraints. Previous studies did incorporate the effect of intent on maneuver affordances [49–51], however, this is beyond the scope of the current study. Under the assumption that intruder and ownship state remain unchanged in the near future, a conflict can be predicted using the speed of ownship, relative to the intruder:

$$\mathbf{V}_{rel,own} = \mathbf{V}_{own} - \mathbf{V}_{int} \quad 4.2$$

Relative velocity vector $\mathbf{V}_{rel,own}$ indicates how ownship moves *with respect to the intruder aircraft**, see Figure 4.3. When the relative track of ownship (the line extended from the relative velocity vector) crosses the intruder protected zone, a loss of separation will occur in the near future, see Figure 4.2.

For any given traffic geometry, a set of relative velocity vectors \mathcal{V}_{FA} can be defined that would result in a conflict between the involved aircraft (i.e., all possible relative velocity vectors where the resulting relative tracks cross

*Note that the relative motion of intruder symbols on a traffic display is opposite to this relative velocity: There, the own aircraft symbol is standing still, and intruder aircraft symbols move relative to the own symbol on the display. The current concept observes relative motion from the perspective of ownship ($\mathbf{V}_{rel,own}$) in order to find constraints on own maneuvering.

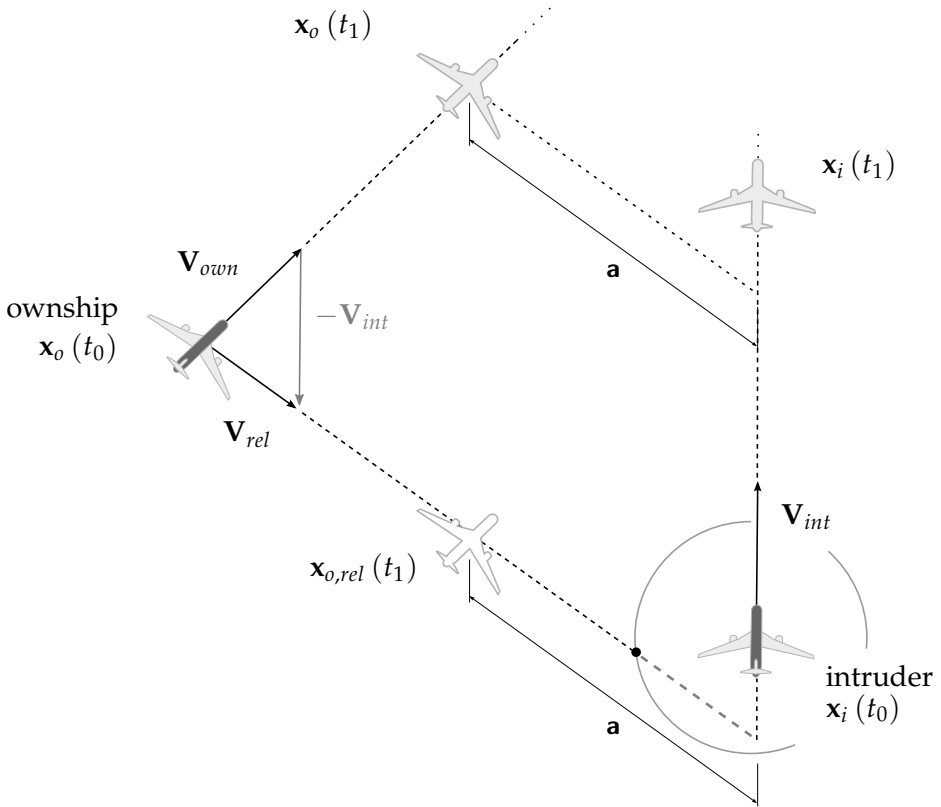


Figure 4.3: Relation between ownship motion relative to the intruder, and the absolute motion of ownship and intruder. Ownship and intruder are shown at time t_0 and t_1 . $\mathbf{x}_{o,rel}$ shows how ownship has moved *relative* to the intruder. Line **a** shows that the change in orientation between ownship and intruder along the relative path is equal to the change along the absolute paths.

the intruder PZ). Figure 4.4 gives an illustration of \mathcal{V}_{FA} . It is a construct of two slanted cones, connected by straight sections. Both cones have their apex at the ownship location, and their curvature is aligned with the upper and lower circles of the intruder PZ. Cross-section (a) in Figure 4.4 illustrates the effect of the thickness of the intruder protected zone: if the PZ had been flat, \mathcal{V}_{FA} would have been a single slanted cone, and cross-section (a) would have been an ellipse. The thickness of the PZ introduces straight sections in the shape of \mathcal{V}_{FA} , and in cross-section (a).

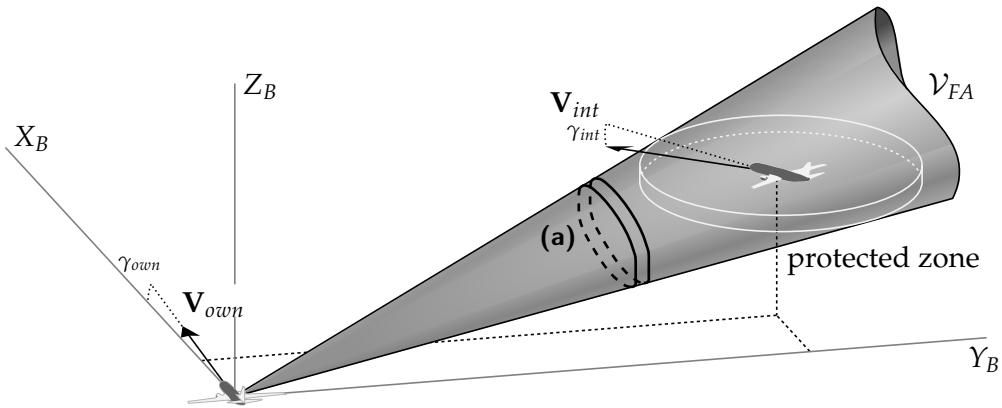


Figure 4.4: The three-dimensional forbidden area \mathcal{V}_{FA} consists of a conical area that is aligned with the edges of the intruder protected zone, as seen from the ownship, and has its apex situated at the center of ownship. Cross-section (a) shows how the thickness of the protected zone changes the shape of the forbidden area from what would otherwise be a pure slanted cone, to a combination of two slanted cones, connected by a straight section.

The three-dimensional vector set \mathcal{V}_{FA} marks the constraints that other traffic imposes on ownship (relative) motion with respect to that intruder aircraft, and will be referred to as the *three-dimensional forbidden area* in the remainder of this paper. This representation only varies as a function of time[†]. This means that for the current time, the three-dimensional forbidden area represents the complete set of relative velocities that would result in a loss of separation.

The concepts preceding the current study illustrated that the relation between the forbidden areas and the own velocity vector can be made visible by translating the forbidden area and relative velocity vector by the intruder velocity vector, see Figure 4.5 [12, 16]. This would be equivalent to adding \mathbf{V}_{int} on both sides of the equal sign in Equation (4.2). The shifted forbidden area represents the constraints imposed by an intruder aircraft in a way that directly relates to the ownship maneuver options. An added benefit,

[†]When neither aircraft maneuver, the opening angle of the forbidden area will expand or contract only as a function of the closing speed of the intruder aircraft, with respect to ownship. When ownship and intruder are not on a collision course, the orientation of the forbidden area will also change as both aircraft pass each other.

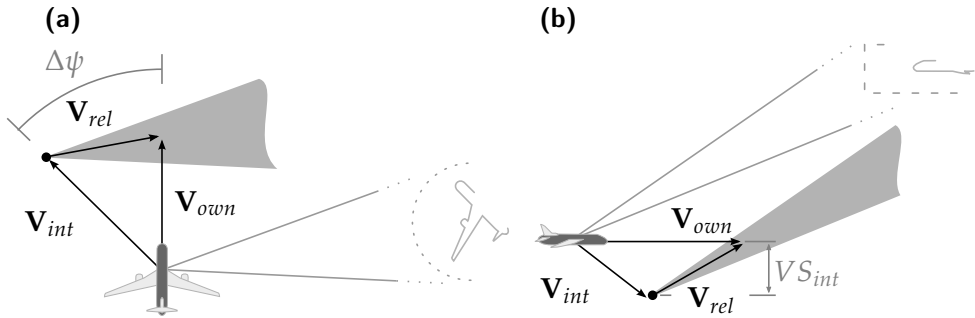


Figure 4.5: Constraints on ownship velocity, expressed in an absolute velocity field. **(a)** illustrates horizontal intruder constraints, **(b)** illustrates vertical constraints. ownship and intruder are in conflict when the tip of the ownship velocity vector is inside the three-dimensional forbidden area. The apex of the shifted area corresponds with the intruder velocity vector, and can be used on the display to determine for instance relative track, and intruder vertical speed. The forbidden area bisector shows relative bearing of the intruder.

illustrated in Figure 4.5, is that the apex of the shifted forbidden area corresponds with the intruder velocity vector, and that the direction of the bisector of the forbidden area is equal to the relative bearing of the corresponding intruder, properties that can be useful when assessing a conflict.

Note that this derivation of the forbidden area assumes instant state changes[‡]. It can be shown that this is a safe assumption when a predicted conflict is still in the far future [52, 53]. However, maneuver dynamics will start to play a larger role when conflicts become more imminent: in the case of tactical maneuvers (within 10 minutes of a predicted conflict), unmodeled dynamics will cause significant errors, particularly speed maneuvers [52]. The previous horizontal display concept compensated for this by observing the constraint area at time $t_{cur} + t_{turn}$. Here, t_{turn} is the maneuver duration for the heading solution that corresponds to the respective forbidden area leg. A new relative position is extrapolated using the current aircraft velocities, which in turn is used to calculate the corrected position for the forbidden area leg. This method can also be applied to the current concept.

[‡]In reality, a heading or speed change that is taken to resolve a conflict will take a certain amount of time. In that time, the constraint area will have grown slightly, and it might occur that what initially seemed a valid solution, will in fact not resolve the conflict, due to the expansion of the constraint area during the course of the maneuver.

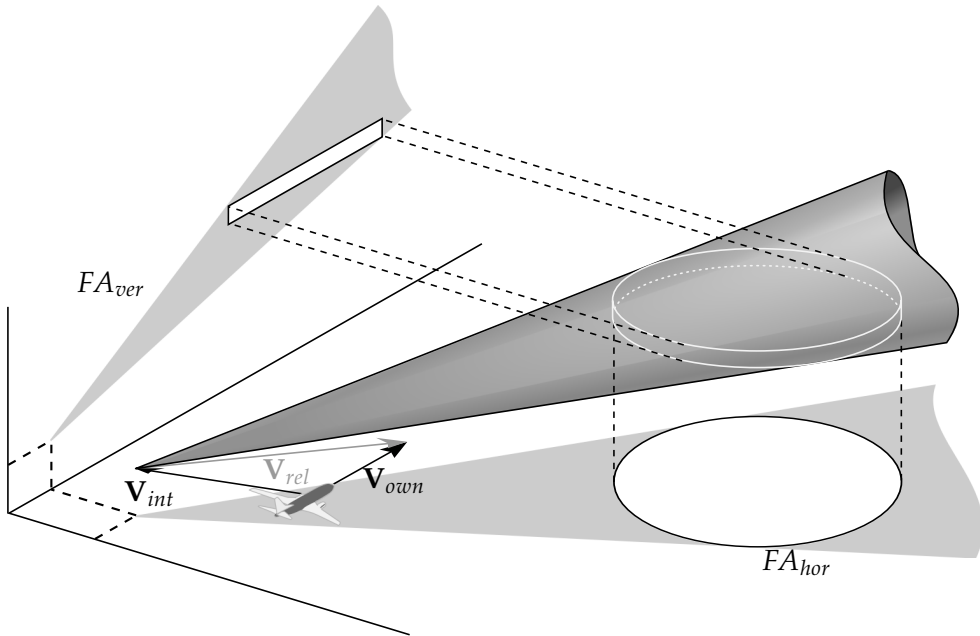


Figure 4.6: Translated three-dimensional forbidden area and horizontal and vertical projections. FA_{hor} is the horizontal projection of the three-dimensional forbidden area, and presents constraints for ownship track and horizontal velocity. FA_{ver} is the vertical projection of the same area, and presents constraints for vertical motion.

4-3-4 Planar constraint projections

There are several visualization techniques for three-dimensional constructs such as the forbidden area, each with its specific benefits and drawbacks [23]. The drawback these methods have in common, however, is loss of context. This, however, is unavoidable, as some form of reduction is necessary to present multi-dimensional data on a two-dimensional surface [23, 24]. The challenge is to determine crucial parts of the context, and to find a visualization that maintains the relevant information.

The previous horizontal and vertical constraint displays both show an orthogonal projection of the three-dimensional forbidden area (illustrated in Figure 4.6). These projections take the three-dimensional shape, and discard the coordinate that is orthogonal to the projection plane. The resulting

shapes are triangular, with the triangle apex at the (projected) ownship position, and its legs aligned with the edges of the projected protected zone.

In Figure 4.6, FA_{hor} is the horizontal projection of the three-dimensional forbidden area, and presents the constraints on relative track and horizontal velocity, for all values of vertical speed combined. FA_{ver} is the vertical projection of the three-dimensional forbidden area, and presents the constraints on relative vertical motion, for all values of the ownship track angle combined.

The orthogonal projections, then, provide a global contour of the forbidden area in their respective dimensions. Visualization of these contours has many benefits. Most importantly, the relation between the triangular contour and the geometry of the conflict is easily interpretable. The triangles reveal several key parameters of a conflict, such as spatial proximity, intruder bearing, intruder heading and velocity, and relative velocity, and how these parameters relate to each other. These cues also help to relate the forbidden areas to the traditional intruder symbols on the display [36].

However, because the projections show constraints for all values of the orthogonal coordinate, the constraints can be conservative when the conflict does not lie exactly in that plane. For instance, a certain combination of speed and track angle may lie in a horizontally projected forbidden area, but can still be conflict-free if there is enough vertical separation, or if vertical separation is obtained before a horizontal loss of separation occurs. This distinction cannot be made with the projected forbidden areas alone.

4-3-5 Interactions between projection planes

What these projections fail to show, then, is how the orthogonal planes interact with each other. The horizontal projection does not reflect vertical separation and maneuvering, and vice versa. Cutting plane visualization partly reveals this interaction, by showing a part (a 'slice') of the three-dimensional shape, for a given constant value of the third dimension [23]. In combination with the planar projection of the three-dimensional shape, it reveals which part of the projection is valid, for a specific point along the dimension that is orthogonal to the projection plane. The result of a cutting-plane intersection will therefore always be a subset of the planar projection of the three-dimensional shape.

Figure 4.7 shows a horizontal cutting plane, that intersects with the three-dimensional constraint area for a certain given value of ownship vertical speed, i.e., the vertical offset of the cutting plane is equal to ownship vertical speed. The resulting 'slice' of the constraint area represents horizontal velocity constraints, taking into account the relative vertical motion and orientation. This reduced forbidden area is a subset of the horizontal projection of the three-dimensional constraint zone (also illustrated in Figure 4.7). When ownship and intruder are not vertically separated, and the relative vertical speed is equal to zero, the horizontal reduced forbidden area will be equal in shape and size to the projected horizontal forbidden area.

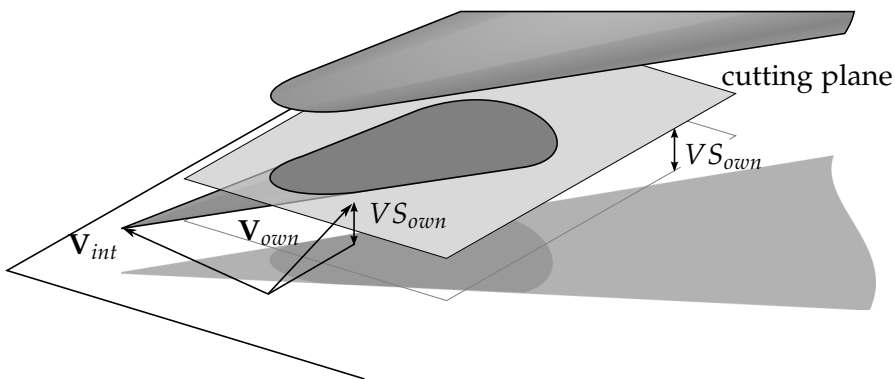


Figure 4.7: The horizontal reduced constraint area is given by the intersection of the three-dimensional constraint area, and a horizontal cutting plane, offset vertically by the ownship vertical speed. The horizontal reduced area illustrates exact constraints on horizontal maneuvering, also for conflicts with non-zero relative vertical distances and velocities.

Figure 4.8 shows a vertical cutting plane, aligned with the ownship track, that intersects with the three-dimensional constraint area. The resulting slice of the constraint area presents vertical velocity constraints, taking into account how a conflict is oriented in the direction orthogonal to the ownship track (i.e., intruder cross-track distance and relative intruder track angle). This reduced forbidden area will always be a subset of the vertical (side-view) projection of the three-dimensional constraint zone (see also Figure 4.8). When ownship and intruder are flying with zero cross-track distance and relative track angle $\Delta\chi = 180^\circ$ or $\Delta\chi = 0^\circ$ (ownship and intruder

are flying head-on or are overtaking, respectively), the vertical reduced forbidden area will be equal in shape and size to the projected vertical forbidden area.

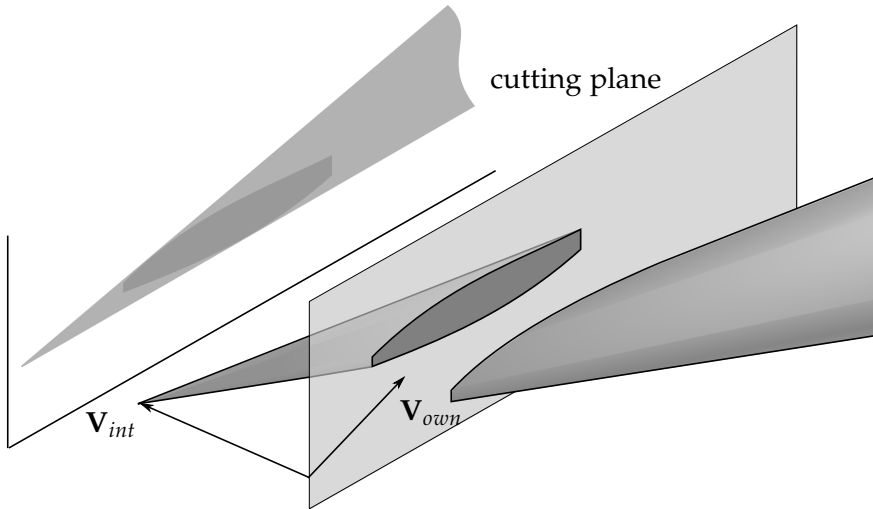


Figure 4.8: The vertical reduced constraint area is given by the intersection of the three-dimensional constraint area, and a vertical cutting plane, aligned with the ownship track. The vertical reduced area illustrates exact constraints on vertical maneuvering, also for conflicts with non-zero cross-track distances and velocities.

Because these reduced forbidden areas depend on the variable that is perpendicular to their plane of projection, they effectively reveal an important part of the interaction between the planes of projection. The reduced areas are invariant with respect to state changes that lie in their own plane of projection, and therefore provide a consistent set of two-dimensional constraints, under the assumption that the third (perpendicular) variable is kept constant. In this case, the reduced areas only vary with time, similar to the forbidden area projections.

When the perpendicular variable is varied, the reduced area will always change in a predictable fashion. If the change in that variable is away from the tip of the three-dimensional forbidden area, the reduced area will also move away from the tip of the triangle in its respective projection. Similarly,

if the change moves the velocity vector closer to the tip of the three-dimensional forbidden area, the reduced area will move towards the tip of the triangle in its respective projection. Also, because the planar projections effectively result in a two-dimensional contour of the forbidden area at its widest point, projections of the reduced areas can never extend beyond the boundaries of the projected forbidden area.

Aside from interactions that result from shortcomings of methods for showing three-dimensional data on multiple, two-dimensional surfaces, interactions can also be found between several aircraft locomotion variables, and their limits. A very direct interaction can be found between the aircraft's bank angle, and its climb performance and stall speed: Increasing the bank angle will increase the stall speed, and reduce the maximum climb angle. On a larger time scale, altitude changes will have an effect on minimum and maximum operating speeds, and on climb and descent performance [46].

These interactions can partly be captured in the visualization when the visualized constraints are dynamically calculated for the current values of the flight variables that influence it. There are, however, situations possible where dynamically calculated constraints do not suffice. Consider for instance a situation where a traffic conflict is solved by assuming a vertical speed that is close to the maximum climb performance. It can happen that although initially this climbing solution seemed to be a valid solution, the reduction in climb performance due to increasing altitude invalidates this solution option. This is, however, beyond the scope of the current study.

4-4 Concept

Figure 4.9 illustrates a design concept for a separation assistance interface, that presents separation-related affordance cues on a co-planar display. The combination of a Horizontal Situation Display and a Vertical Situation Display was chosen for this co-planar display concept, because these displays are omnipresent in the modern flight deck. These two displays also provide the most intuitive maneuver space projections, and they correspond closest to current re-planning tasks.

In this display concept, the three-dimensional traffic situation is visualized in two orthogonal, two-dimensional views: a top-down view (①), and

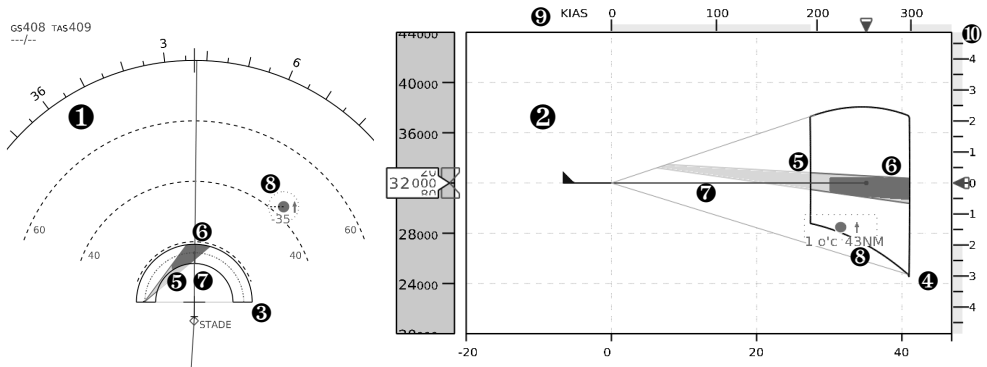


Figure 4.9: Concept for a co-planar separation assistance display. This figure shows a Horizontal Situation Display (1) and a Vertical Situation Display (2), with added separation assistance overlays. 3 and 4 are the horizontal and vertical State-Vector Envelope, respectively. 5 is the projected forbidden area both on the HSD and the VSD. 6 is the reduced forbidden area on both displays. 7 Represents the ownship state vector, 8 is a TCAS-symbol indicating the relative location of the intruder aircraft. 9 is a speed tape, showing current IAS, selected IAS, and simplified traffic constraints. 10 is a vertical speed tape, showing the current and selected vertical speed in feet per minute, and simplified traffic constraints.

a side view (2). Both views present an ownship-centered moving map, that shows spatial information such as the FMS route and intruder aircraft positions. In addition, constraints on ownship maneuvering are shown on both displays through velocity action-space overlays (3, 4).

The top-down view presents information in a polar coordinate system: spatial information is expressed in relative bearing and distance, and the velocity action-space shows constraints for combinations of track angle and airspeed. The side view uses a Cartesian coordinate system: spatial information is expressed in along-track distance and relative altitude. Here, the velocity action-space shows constraints for combinations of airspeed and vertical speed.

4-4-1 Traditional display elements

The moving-map presentations on the HSD and VSD are not new: the HSD is present in all modern cockpits, and also the VSD is becoming more common. To match current practice, intruder aircraft are represented on both displays using TCAS-like symbology* (⑨) [54]: an unfilled diamond indicates a non-conflicting intruder, a filled diamond indicates a conflicting intruder, with more than five minutes to a loss of separation. This is considered a low-priority conflict. A conflict is considered medium priority when a loss of separation is between three to five minutes away, indicated with a solid circle as intruder symbol. A high priority conflict is less than three minutes away, and is indicated with a solid square.

Separation margins are indicated around each intruder on both displays, which results in a circle on the HSD, and a flat rectangle on the VSD, see Figure 4.10. On the HSD, the intruder's horizontal speed vector is shown with a dotted trend line. The length of this line is scaled such, that it equals the radius of the separation circle if the horizontal speed of the intruder is equal to the ownship horizontal speed.

A small up/down arrow is shown next to the intruder symbol, when the vertical speed of that intruder exceeds 500 ft/min. A signed number below the intruder symbol indicates the vertical offset in flight levels (1 flight level equals 100 feet), see Figure 4.10(a). On the VSD, the intruder TCAS symbol is accompanied by a label that shows the relative bearing in hours o' clock, and the distance in nautical miles. An up/down arrow is shown to the right of the TCAS symbol when the vertical speed of that intruder exceeds 500 ft/min, see Figure 4.10(b).

In addition to the map view, the vertical display also includes a speed tape, and a vertical speed tape. The speed tape (⑩) shows current Indicated Air Speed (IAS), selected IAS, and simplified speed constraints in knots. The vertical speed tape (⑪) shows the current and selected vertical speed, and simplified vertical speed constraints, in feet per minute.

*Note that this is not necessarily the best intruder visualization. Intruder symbology design, however, is beyond the scope of the current study. TCAS symbology was therefore chosen to match current practice.

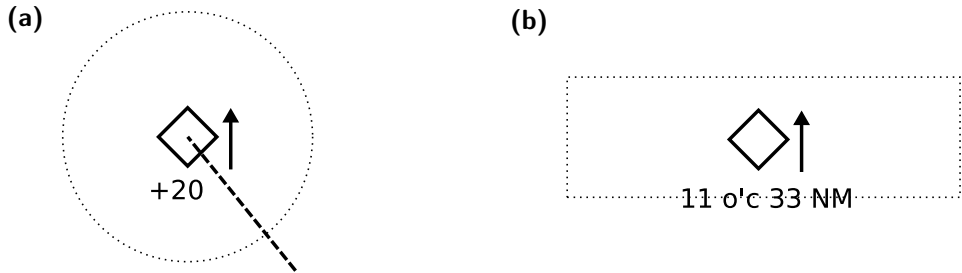


Figure 4.10: Intruder aircraft symbology. Intruders are visualized using TCAS-style symbology: unfilled diamonds for non-conflicting aircraft, filled diamonds for low-priority conflicts, filled circles for medium-priority conflicts, and filled squares for high-priority conflicts. **(a):** Intruder symbology as shown on the HSD. The TCAS symbol is shown together with the separation margin, a speed vector, a vertical speed arrow, and a flight-level offset. **(b):** Intruder symbology as shown on the VSD. The TCAS symbol is shown together with the separation margin, a vertical speed arrow, the relative bearing in hours o' clock, and the intruder distance in nautical miles.

4-4-2 Velocity action-space overlays

The horizontal State-Vector Envelope (SVE) (⑤) shows the affordance space for horizontal maneuvering in terms of track angle and airspeed, see Figure 4.11(a). Because a horizontal situation display in expanded mode (as in Figure 4.9) does not show traffic behind the own aircraft, the horizontal state-vector envelope also shows only solutions with $|\Delta\chi| \leq 90^\circ$. Current horizontal situation displays also have modes that show the situation behind the ownship. In such a mode, the horizontal state-vector envelope would be shown as a whole circle. The vertical State-Vector Envelope (④) is illustrated in Figure 4.11(b), and shows the affordance space for vertical maneuvering in terms of airspeed and vertical speed.

Intruder aircraft that are within detection range will further reduce the available maneuver space in the horizontal and vertical State Vector Envelopes. The reduced forbidden areas (⑥), derived in the previous section, give the most precise representation of these constraints, see Figure 4.11. On the HSD, a reduced forbidden area gives the constraints imposed by an

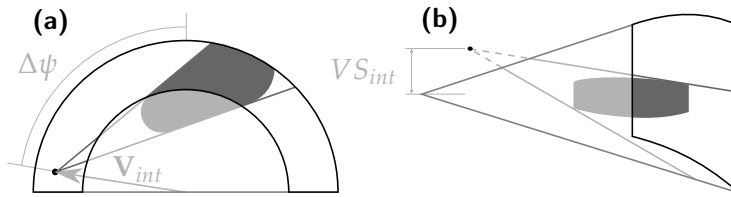


Figure 4.11: The horizontal **(a)** and vertical **(b)** State-Vector Envelopes. The forbidden areas correspond to one intruder, who is situated below, to the front and to the right of ownship, crossing ownship from right to left, and climbing at a shallow climb angle. **(a):** The circular boundaries that constrain the horizontal maneuver space represent the aircraft minimum and maximum operating speeds. The intruder track is offset from the ownship track by $\Delta\psi$. The triangle apex represents the intruder velocity \mathbf{V}_{int} . **(b):** The vertical maneuver space is bounded by minimum and maximum operating speeds, and by minimum and maximum steady-state climb. The vertical offset of the triangle apex corresponds to the intruder vertical speed, VS_{int} .

intruder on ownship track angle and airspeed, for the current value of ownship vertical speed. On the VSD, a reduced forbidden area gives intruder-imposed constraints on ownship airspeed and vertical speed, for the current ownship heading.

Note that each intruder adds a forbidden area to the available maneuver space. These forbidden areas, however, work in a cumulative fashion: selecting a ‘clear’ area solves all detected conflicts, without creating a new conflict. In the current concept, the derivation of the constraint areas uses only state information, and will therefore only be valid when there are no imminent trajectory changes. Although the influence of intent information has been considered in previous concepts [49–51], this is out of the scope of the current study.

The reduced forbidden areas result from the intersection between a flat cutting plane, and the three-dimensional forbidden area: a compound of two slanted conical shapes, aligned with the top and bottom of the intruder protected zone. The shapes that result from this intersection range from circles, to ovals, to open-ended hyperbolic curves, see Figure 4.11.

Ref. [36] describes how the triangular shapes that result from planar projection of the forbidden area can be used to derive several relevant cues

about the spatial configuration of a conflict. These cues make it easier to relate forbidden areas to intruder symbols on the map view, but also provide more information on the urgency of a conflict, and how different resolutions would affect the traffic situation. In other words, while the reduced forbidden areas provide more precise constraint visualization, they sacrifice important cues that link several display elements together. The current concept therefore combines the reduced forbidden areas with the outline of the corresponding projected forbidden areas (⑤). In addition to the added situational information, these outlines also provide an outer limit on the shape and size of the reduced forbidden area, when a perpendicular flight parameter is modified.

The current ownship airspeed, track angle and vertical speed are presented on the two displays by two velocity vectors (⑦) that extend from the origin of the SVE to a certain point in the velocity vector space. On both displays, the length of these vectors is equal to the ownship airspeed. On the vertical situation display, the ownship vertical speed results in a rotation $\gamma = \arcsin(VS/V_{TAS})$ of the velocity vector. Because the horizontal situation display is oriented *track-up*, the horizontal velocity vector has a fixed, vertical orientation. A dot, four kts wide, attached at the tip of each velocity vector, acts as a margin for maneuver selection [36].

In combination with the reduced forbidden areas, the velocity vectors show the affordance of avoidance: placing either of the velocity vectors outside all of the forbidden areas results in a conflict-free trajectory. Intruder flight-path vectors are also shown as dots at the tip of the corresponding forbidden area triangle. On the horizontal display, the distance from the tip of a triangle to the center of the SVE is equal to the airspeed of the corresponding intruder, see Figure 4.11(a). On the vertical display, however, this distance is equal to the in-track component of the intruder airspeed, $V_{vert,int} = V_{TAS,int} \times \cos(\chi_{int} - \chi_{own})$. Here, $V_{TAS,int}$ is the intruder airspeed, χ_{int} is the intruder track angle, and χ_{own} the ownship track angle. Moving the ownship velocity vector towards one of these dots to resolve a conflict will lead to a very inefficient resolution, as it will cause ownship to fly parallel to the intruder [12].

4-4-3 Conflict urgency visualization

In addition to varying intruder symbology, conflict urgency is also indicated using color coding for all of the display elements that correspond to one intruder. This means that the aircraft symbols on both displays, as well as the forbidden area triangles and reduced forbidden areas on both displays are colored according to the urgency of the conflict between ownship and the corresponding intruder. Similar to the TCAS system, four levels of urgency have been defined for the current concept[54]. The lowest urgency level corresponds with intruder aircraft that are currently not in conflict with ownship. For these intruders, the display elements are colored white. The second level of urgency corresponds with a conflicting intruder, with a loss of separation further than five minutes away. This is defined as a low-urgency conflict, and display elements are colored yellow. A medium-urgency conflict corresponds with a loss of separation between three and five minutes, and is colored orange on the display. A high-urgency conflict indicates a loss of separation within less than three minutes, and is colored red on the display.

4-4-4 Visual momentum

When more than one intruder aircraft needs to be shown on the display, it becomes more important for the display to provide ways to link the several visual elements on the display to an intruder and to each other. Visual cues that facilitate this link increase visual momentum: they facilitate the integration of information across multiple displays, and between elements on each display [55]. This integration is essential for proper SA, as the elements on both displays are intrinsically tied together. Manipulation in one plane will often affect constraints in the other plane. Visualizing which elements belong together should aid pilots when assessing these relations.

Woods introduces functional data overlap as a method that *“improves the visual momentum across multiple displays by ‘presenting pictorially the functional relationships that cut across display frame boundaries’ ”*. In other words, visual momentum can be improved by showing particular information on both displays, and by visualizing relationships between information on both displays. The color coding that is used to indicate conflict urgency is an obvious way to improve visual momentum. The shape and orientation of the

conflict zones, however, also provide ways to identify display elements that belong together. Examples are the distance to an intruder, which also determines the opening angle of the corresponding forbidden areas, the predicted intruder flight path determines the location of the tip of the horizontal triangle, and the vertical speed, that determines the vertical position of the tip of the triangle on the vertical display.

4-4-5 Comparison with previous concepts

The main difference between the current co-planar display concept and the previous separate horizontal and vertical display concepts, is the visualization of the interactions that can occur between the planes of projection. The horizontal display shows constraints on horizontal maneuvering, under the assumption that intruding aircraft are flying level, within minimum vertical separation. Similarly, the vertical display shows constraints on vertical maneuvering, assuming zero cross-track distance and maneuvering. These projected constraints become increasingly conservative when conflicts deviate from these assumptions. The reduced forbidden areas show more precise constraints by taking the conflict orientation orthogonal to each projection into account.

Figure 4.12 illustrates how the constraints imposed by an intruding aircraft change when the corresponding conflict geometry can no longer be defined in a single plane of projection. All four examples in Figure 4.12 show how conflict constraints would be visualized on the new display. Note that on the original two displays the visualization would be similar, but that all triangles would always be completely filled.

The first conflict, shown in Figure 4.12(a), corresponds to an intruder that is both on the same track and the same level as ownship, and both aircraft are flying level. In this case, neither the assumptions for the original horizontal display, nor those for the original vertical display are violated. As a result, the constraints imposed by the intruder are presented as completely filled triangles on the new display, completely identical to what the visualization for this conflict would be on the original displays.

Figure 4.12(b) shows how the constraints change when the intruding aircraft starts to climb. Because the intruder is still on the same track as

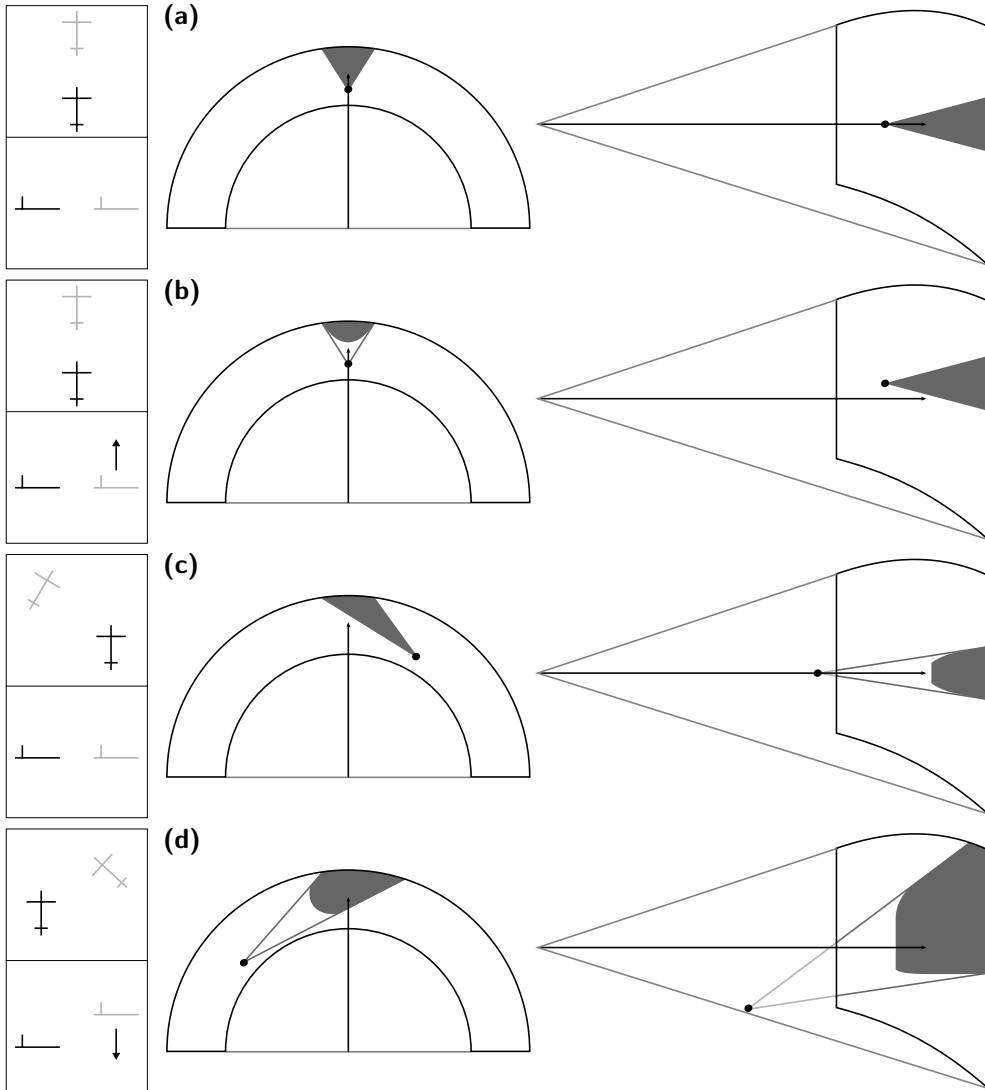


Figure 4.12: Example scenarios. An overview of each scenario is given on the left. The black aircraft symbols represent ownship, the gray symbols represent the intruder. **(a)** Ownship is behind and overtaking the intruder, both are flying level, at equal altitude. **(b)** Intruder is climbing. **(c)** Both are flying level, but the intruder is to the left of ownship, crossing to the right. **(d)** Intruder is to the right of ownship, crossing to the left, descending from a higher altitude.

ownership, the assumptions for the original vertical display still hold, and the presented vertical constraints are still identical to how they would be presented on the original vertical display. The horizontal constraints, however, change as a result of the vertical maneuver of the intruder. Where the original horizontal display would show a conflict, the reduced forbidden areas reveal that ownership would have to accelerate to get into conflict.

Figure 4.12(c) shows how the vertical constraints change when the intruder is on a different track than ownership. Similar to the situation in Figure 4.12(b), the original vertical display would show a conflict, while in reality the intruder passes in front of ownership before they get too close. Figure 4.12(d) shows that both the horizontal and the vertical presentation of constraints change when the intruder is both off level and off track. In this example ownership and intruder are still in conflict. The presentation in Figure 4.12(d) shows that maneuvers exist that solve the conflict, while still being in both the horizontal and vertical triangles. Such solutions would be impossible to derive from the original two displays.

4-5 Relationships between the AH and this concept

The constraint-based approach that was adopted in this study used work-domain analysis tools such as the Abstraction Hierarchy to identify constraints and relationships on multiple levels of abstraction [17, 18]. Although the work-domain analysis for this concept has not changed significantly since the previous concept, looking at how the visualizations in the current concept are related to that work-domain analysis can provide a useful review of the concept, as well as relevant insights for future design iterations and experiments. This section will therefore briefly describe how the different elements of the display link back to the functions, constraints and relationships in the abstraction hierarchy (Fig. 1 in [16]). Ref. [16] describes the work-domain analysis in more detail.

The velocity action-space overlays proposed in the display concept form the main additions to the horizontal and vertical situation displays. These overlays give a consistent view on the relations between locomotion inputs and the primary functions of productivity, efficiency and safety, and they show how these relationships are influenced by the identified constraints.

Together with the velocity vectors, the horizontal and vertical state-vector envelopes relate to the safety goal, by showing how internal constraints (available power, structural limits, ...) limit possible velocity vectors. In combination with the horizontal FMS track on the map display, the horizontal SVE relates to the production goal through the destination approximation constraint (deviations from track that are larger than $\Delta\chi = 90^\circ$ move the aircraft away from its destination).

The reduced forbidden area relates to the safety goal by showing the affordance of conflict, (the own velocity vector inside a reduced forbidden area indicates a conflict). Together with the internal maneuvering constraints from the SVE, it shows the affordance of avoidance: any vector within the SVE that is not inside any reduced forbidden area is a possible solution to a conflict. The reduced forbidden area also relates to the efficiency goal, through the 'shortest way out' principle [12]. The smallest vector change out of a reduced area will also result in the smallest path deviation. Note, however, that path deviation in the horizontal plane does not directly compare to path deviation in the vertical plane.

The forbidden area outlines link lower-level elements to higher level constraints. Together with the intruder symbols on the map displays, they link conflict and separation on the abstract function level to obstruction (motion), relative motion, and traffic location on the generalized and physical function levels. The tip of the triangle conveys intruder motion (the tip is offset from the center of the SVE by the intruder velocity vector), and the triangle bisector communicates intruder relative bearing, and therefore helps to link forbidden areas to their respective intruders.

4-6 Practical application

An important argument in the current study is that in order to support operators in unforeseen situations, displays should go beyond visualizations that relate only to the automation logic. The interface should provide a window to the reasoning and functioning of the automation, by visualization of the affordances of the work domain, and by making clear how these affordances relate to the actions and advisories of the automation. The appropriateness of these displays for real-world applications, however, also depends on how

well the concepts extend to complex situations, such as multiple intruder conflicts, complex trajectories, and of course situations where the automation is failing. This has also been considered for preceding concepts, and many of the properties illustrated in those studies apply to the current concept as well [12, 16].

Van Dam, for instance, illustrated that the forbidden areas work in a cumulative fashion [12]. Because each forbidden area reveals absolute maneuvering constraints, imposed by an intruder aircraft, a combination of forbidden areas from multiple aircraft, superimposed onto each other, will represent the set of states that would lead to a conflict with any one (or more) of these aircraft. As a result, any state outside of this combined constraint area is a solution to *all* of the current conflicts. This property is inherent to the presentation of constraints in an absolute velocity space.

Ellerbroek illustrated that conflicts can be solved in sequence, when the priority of each conflict is visualized using color coding of each forbidden area [16]. The current concept uses single colors for each forbidden area, where the color corresponds to the time to loss of separation, given the current state of ownship and intruder. A possible improvement could make use of the fact that every point in a forbidden area corresponds to a certain state vector, which in turn corresponds to a certain time to loss of separation. This way, each point in a forbidden area can be colored individually. In addition to visualization of the priorities of conflicts given the current state, the interface can then also reveal the viability of possible intermediate solutions in complex traffic situations.

One of the issues with co-planar displays is that the operator has to combine information from two displays to obtain a complete mental picture of the situation. Although the projected forbidden areas already provide strong links between the different elements on the displays, a crowded airspace can still make it difficult to make these links, especially when workload is already high. One of the techniques Woods proposes to improve this, is to provide across-display *perceptual landmarks* [55]. A common color, for instance, can provide a perceptual link between items on different displays that belong together. The priority color coding already partly fulfills this function, but can be improved with a selection system, where the display elements that correspond to one intruder are highlighted upon selection.

The current concept employs the current states to derive the constraints imposed by other traffic. This method holds under the assumption that ownship and intruder state remain constant in the near future. When this is not the case, the affordance space will change as a function of space and time due to Trajectory Change Points (TCP), and other changes of state or intent. Several studies have illustrated methods to visualize intent in the forbidden areas [49–51]. Each of these methods makes use of the fact that the dimension along the bisector of the triangular forbidden area is related to the time at which the closest point of approach with the respective intruder will occur, with the triangle origin representing $t_{CPA} = \infty$. A change in state at $t = t_{TCP}$ will therefore result in a change in the forbidden area at the point where $t_{CPA} = t_{TCP}$. A similar method can be used to include intent in the current concept, by extending one of these methods to three dimensions.

Although current ATM concepts for unmanaged airspace suggest a traffic display to be used as a situation awareness tool for automated self-separation systems, constraint-based displays are not limited to this level of support. Because the displays visualize work-domain constraints and relations, they support the pilot on multiple levels of control, from fully automated conflict resolution, to manual pilot decision making.

4-7 Discussion

The work presented in this paper is part of an ongoing study on the design of a trajectory planning aid. The goal is to obtain a graphical interface that supports pilots in their new task of airborne reconfiguration of a pre-planned trajectory, in case of traffic conflicts in unmanaged airspace. The current work focuses on ways to visualize three-dimensional data on a two-dimensional display. A co-planar display concept has been proposed, that is based on the previous top-down and side-view display concepts.

There are several reasons why a combination of a Horizontal Situation Display (HSD) and a Vertical Situation Display (VSD) was chosen for the co-planar display concept. First, these two displays provide the most intuitive maneuver space projections, and support the most straightforward resolution strategies, such as single-axis maneuvers, and combinations of speed and heading or vertical speed. A practical factor is also that these displays

are already available on a modern flight deck, and they correspond closest to current re-planning tasks.

In previous research, the visualization of constraints on the display implicitly assumed that conflict geometries were flat: the constraints shown on the horizontal interface assume zero vertical separation and no vertical maneuvering, and the side-view display assumes that there is no cross track separation with intruder aircraft. When these assumptions are violated these displays will present overly conservative constraints. Simply combining these displays, therefore, is not sufficient to create an effective co-planar solution. Aside from the fact that good visual momentum demands visual cues that link both displays together, each individual display also requires modifications so that the presented constraints remain valid when a conflict can no longer be defined in just one plane. A co-planar display should reveal how individual planes interact with each other, and provide pilots with a consistent and intuitive view on what can be a complex, three-dimensional traffic situation.

The current concept, therefore, re-implements as much as possible the strong points of the previous, single-plane displays. The triangular shapes that result from planar projection of the three-dimensional traffic constraints provide strong and intuitive cues about the conflict geometry, reveal how different elements on the display belong together, and can help pilots keep an overview in complex traffic situations with multiple intruders. These projections are complemented with precisely derived constraints, that are also valid in combined cross-track and off-level conflict situations.

Although full, simultaneous three-dimensional maneuvering is still not consistently supported, it can be argued that this is a minor sacrifice when choosing a co-planar display over a perspective display: Several studies indicate that pilots prefer single-axis maneuvers [26, 33–36]. Also, the benefits (e.g., in terms of efficiency) of three-axis maneuvers over two- or one-axis maneuvers are rarely ever significant.

A possible downside of the constraint-based presentation in this concept is that in a densely populated airspace, the state-vector envelope can become crowded with forbidden areas, making it less suitable (or unsuitable) as a situation awareness tool. Although this is an undesired situation, a de-cluttering algorithm will increase automation complexity, and reduce

transparency of actions towards the operator. This will be the topic of a future study.

Current ATM concepts for the future of the structure of the airspace suggest a highly optimized, and –in certain parts of the airspace– decentralized system, with a high degree of automation. In the decentralized parts of airspace, aircraft will fly optimized, predetermined trajectories, where automation will be used to resolve problems that result from uncertainties during the flight. The concepts suggest that a display of traffic information should be added to help the aircrew judge these kinds of situations, and solve problems when they arise. The current study uses a constraint-based approach to design an interface that supports traffic situation awareness.

When used in combination with an automated system that provides explicit resolutions, such a display should improve operator trust and understanding of an automated resolution, by helping him understand how constraints shape possible resolutions. Note that this visualization is independent of the specific implementation of conflict resolution automation. Instead, it visualizes work domain information, which invariably forms the premise on which both automation and the human operator should base their actions. This method of visualization also provides an opportunity to create a visualization that is consistent across different levels of automation.

This method of display design, however, also implies that there are certain demands on the design of the automation. The interaction between automation and the human actor requires transparent functioning of the automated system. When a resolution advisory cannot consistently be explained by the information on a display, for instance because it takes additional (hidden) constraints into account, a pilot can hardly be asked to judge the fidelity of this resolution. Consistency between interface and automation, therefore, requires a common model of the work domain, from which the automation derives a resolution, and which the interface visualizes to the operator. This consistency will be crucial for human actors to share their cognition and decision-making with the automation.

4-8 Conclusions

A separation assistance display was proposed, that presents constraints on horizontal and vertical maneuvering, in a velocity action space that is overlaid on both a horizontal and a vertical situation display. A two-dimensional co-planar presentation was chosen because it offers an intuitive, undistorted and precise view on the constraints and the traffic situation. It also corresponds more closely to current-day flight-deck interfaces, as well as to pilot resolution preferences.

A follow-up paper (see Chapter 5) will present a set of experiments that evaluate this concept in terms of safety, performance, and situation awareness, in manual conflict resolution tasks. Future design iterations will focus on display clutter, intent, and on the interaction with different automated resolution modes.

4-9 Bibliography

- [1] **Radio Technical Commission for Aeronautics.** Airborne Conflict Management: Application Description V2.5. Tech. Rep. RTCA SC-186, Federal Aviation Authorities, 2002.
- [2] **SESAR Consortium.** SESAR Definition Phase D3: The ATM Target Concept. Tech. Rep. DLM-0612-001-02-00, Eurocontrol, 2007.
- [3] **D. A. Norman.** The “Problem” of Automation: Inappropriate Feedback and Interaction, not “Over-Automation”. *Philosophical Transactions of the Royal Society of London*, 327(1241), 585–593, 1990. ISSN 0962-8436. doi: 10.1098/rstb.1990.0101.
- [4] **N. B. Sarter and D. D. Woods.** Pilot Interaction With Cockpit Automation: Operational Experiences With the Flight Management System. *The International Journal of Aviation Psychology*, 2(4), 303–321, 1992. doi:10.1207/s15327108ijap0204_5.
- [5] **G. Lintern, T. Waite, and D. A. Talleur.** Functional Interface Design for the Modern Aircraft Cockpit. *The International Journal of Aviation Psychology*, 9(3), 225–240, 1999.

- [6] **A. Q. V. Dao, S. Brandt, V. Battiste, K. P. Vu, T. Strybel, and W. W. Johnson.** The Impact of Automation Assisted Aircraft Separation on Situation Awareness. In: *Human Interface and the Management of Information. Information and Interaction*, pp. 738–747. Springer, 2009.
- [7] **K. J. Vicente.** Ecological Interface Design: Progress and Challenges. *Human Factors*, 44, 62–78, 2002.
- [8] **G. A. Jamieson.** Ecological Interface Design for Petrochemical Process Control: An Empirical Assessment. *IEEE Transactions on Systems, Man, and Cybernetics, part A: Systems and Humans*, 37(6), 906–920, 2007. doi: 10.1109/TSMCA.2007.897583.
- [9] **N. Dinadis and K. J. Vicente.** Designing Functional Visualizations for Aircraft System Status Displays. *The International Journal of Aviation Psychology*, 9(3), 241–269, 1999.
- [10] **C. Borst, H. C. H. Suijkerbuijk, M. Mulder, and M. M. van Paassen.** Ecological Interface Design for Terrain Awareness. *International Journal of Aviation Psychology*, 16(4), 375–400, 2006.
- [11] **C. Borst, F. A. Sjer, M. Mulder, M. M. van Paassen, and J. A. Mulder.** Ecological Approach to Support Pilot Terrain Awareness After Total Engine Failure. *Journal of Aircraft*, 45(1), 159–171, 2008.
- [12] **S. B. J. van Dam, M. Mulder, and M. M. van Paassen.** Ecological Interface Design of a Tactical Airborne Separation Assistance Tool. *IEEE Transactions on Systems, Man, and Cybernetics, part A: Systems and Humans*, 38(6), 1221–1233, 2008.
- [13] **F. M. Heylen, S. B. J. van Dam, M. Mulder, and M. M. van Paassen.** Design and Evaluation of a Vertical Separation Assistance Display. In: *AIAA Guidance, Navigation, and Control Conference and Exhibit*. Honolulu (HI), 2008.
- [14] **A. van der Eijk, C. Borst, A. C. In 't Veld, M. M. van Paassen, and M. Mulder.** Assisting Air Traffic Control in Planning and Monitoring Continuous Descent Approach Procedures. *Journal of Aircraft*, 49(5), 1376–1390, 2012. doi:10.2514/1.C031686.

- [15] **C. Borst, M. Mulder, and M. M. van Paassen.** Design and Simulator Evaluation of an Ecological Synthetic Vision Display. *Journal of Guidance, Control and Dynamics*, 33(5), 1577–1591, 2010. doi:10.2514/1.47832.
- [16] **J. Ellerbroek, M. Visser, S. B. J. van Dam, M. Mulder, and M. M. van Paassen.** Design of an Airborne Three-Dimensional Separation Assistance Display. *IEEE Transactions on Systems, Man, and Cybernetics, part A: Systems and Humans*, 41(6), 863–875, 2011. ISSN 1083-4427. doi:10.1109/TSMCA.2010.2093890.
- [17] **K. J. Vicente and J. Rasmussen.** Ecological Interface Design: Theoretical Foundations. *IEEE Transactions on Systems, Man, and Cybernetics*, 22(4), 589–606, 1992.
- [18] **C. M. Burns and J. R. Hajdukiewicz.** *Ecological Interface Design*. CRC Press LLC, FL: Boca Raton, 2004. ISBN 0415283744.
- [19] **J. J. Gibson.** The Theory of Affordances. *Perceiving, Acting and Knowing: Toward an Ecological Psychology*, pp. 67–82, 1977.
- [20] **J. J. Gibson.** *The Ecological Approach to Visual Perception*. Houghton Mifflin, 1979. ISBN 0-89859-959-8.
- [21] **K. Christoffersen, C. N. Hunter, and K. J. Vicente.** A Longitudinal Study of the Effects of Ecological Interface Design on Deep Knowledge. *International Journal of Human-Computer Studies*, 48, 729–762, 1998.
- [22] **E. J. Bass and A. R. Pritchett.** Human-Automated Judge Learning: A Methodology for Examining Human Interaction With Information Analysis Automation. *IEEE Transactions on Systems, Man, and Cybernetics, part A: Systems and Humans*, 38(4), 759–776, 2008.
- [23] **M. S. T. Carpendale, D. J. Cowperthwaite, and F. D. Fracchia.** Extending Distortion Viewing from 2D to 3D. *Computer Graphics and Applications, IEEE*, 17(4), 42–51, 1997.
- [24] **M. St John, M. B. Cowen, H. S. Smallman, and H. M. Oonk.** The Use of 2D and 3D Displays for Shape-Understanding versus Relative-Position Tasks. *Human Factors*, 43(1), 79–98, 2001.

- [25] **S. R. Ellis, M. W. McGreevy, and R. J. Hitchcock.** Perspective Traffic Display Format and Airline Pilot Traffic Avoidance. *Human Factors*, 29(4), 371–382, 1987.
- [26] **A. L. Alexander, C. D. Wickens, and D. H. Merwin.** Perspective and Coplanar Cockpit Displays of Traffic Information: Implications for Maneuver Choice, Flight Safety, and Mental Workload. *The International Journal of Aviation Psychology*, 15, 1–21, 2005.
- [27] **L. C. Thomas and C. D. Wickens.** Display Dimensionality, Conflict Geometry, and Time Pressure Effects on Conflict Detection and Resolution Performance Using Cockpit Displays of Traffic Information. *The International Journal of Aviation Psychology*, 16(3), 321–342, 2006.
- [28] **S. N. Roscoe.** Airborne Displays for Flight and Navigation. *Human Factors*, 10(4), 321–332, 1968.
- [29] **C. D. Wickens.** The When and How of Using 2-D and 3-D Displays for Operational Tasks. In: *Proceedings of the Human Factors and Ergonomics Society*, pp. 403–406, 2000.
- [30] **M. L. Bolton, E. J. Bass, and J. R. Comstock.** Spatial Awareness in Synthetic Vision Systems: Using Spatial and Temporal Judgments to Evaluate Texture and Field of View, 2007.
- [31] **M. W. McGreevy and S. R. Ellis.** The Effect of Perspective Geometry on Judged Direction in Spatial Information Instruments. *Human Factors*, 28(4), 439–456, 1986.
- [32] **M. L. Bolton and E. J. Bass.** Using Relative Position and Temporal Judgments to Identify Biases in Spatial Awareness for Synthetic Vision Systems. *The International Journal of Aviation Psychology*, 18(2), 183–206, 2008.
- [33] **J. M. Hoekstra.** *Designing for Safety: The Free Flight Air Traffic Management Concept*. Ph.D. thesis, Delft University of Technology, The Netherlands, 2001.
- [34] **C. D. Wickens, J. Helleberg, and X. Xu.** Pilot Maneuver Choice and Workload in Free Flight. *Human Factors and Ergonomics*

- Society Annual Meeting Proceedings*, 44(2), 171–188, 2002. doi: 10.1518/0018720024497943.
- [35] **C. L. A. Steens, S. B. J. van Dam, M. M. van Paassen, and M. Mulder.** Comparing Situation Awareness for Two Airborne Separation Assistance Interfaces. In: *AIAA Guidance, Navigation and Control Conference and Exhibit*. Honolulu (HI), 2008.
- [36] **J. Ellerbroek, M. M. van Paassen, and M. Mulder.** Evaluation of a Separation Assistance Display in a Multi-Actor Experiment. *IEEE Transactions on Human-Machine Systems*, submitted, 2011.
- [37] **J. K. Kuchar and L. C. Yang.** A Review of Conflict Detection and Resolution Modelling Methods. *IEEE Transactions on Intelligent Transportation Systems*, 1(4), 179–189, 2000.
- [38] **R. Ghosh and C. J. Tomlin.** Maneuver Design for Multiple Aircraft Conflict Resolution. In: *Proceedings of the American Control Conference*, pp. 672–676. Chicago (IL), 2000.
- [39] **J. M. Hoekstra, R. N. H. W. van Gent, and R. C. J. Ruigrok.** Designing for Safety: the Free Flight Air Traffic Management Concept. *Reliability Engineering and System Safety*, 75, 215–232, 2002.
- [40] **L. Pallottino, E. M. Feron, and A. Bicchi.** Conflict Resolution Problems for Air Traffic Management Systems Solved With Mixed Integer Programming. *IEEE Transactions on Intelligent Transportation Systems*, 3(1), 3–11, 2002. ISSN 15249050. doi:10.1109/6979.994791.
- [41] **D. J. Wing, R. A. Vivona, and D. A. Roscoe.** Airborne Tactical Intent-Based Conflict Resolution Capability. In: *9th AIAA Aviation, Technology, Integration, and Operations*, 2009.
- [42] **C. Meckiff and P. Gibbs.** PHARE Highly Interactive Problem Solver. Tech. Rep. 273/94, Eurocontrol, 1994.
- [43] **V. Battiste, W. W. Johnson, N. H. Johnson, S. Granada, and A. Q. V. Dao.** Flight Crew Perspective on the Display of 4D Information for En Route and Arrival Merging and Spacing. *Human-Computer Interaction: Interaction Platforms and Techniques*, pp. 541–550, 2007.

- [44] **W. R. Knecht**. Testing a Multidimensional Nonveridical Aircraft Collision Avoidance System. *Human Factors*, 50(4), 565–575, 2008. doi: 10.1518/001872008X288600.
- [45] **E. R. Tufte**. *Envisioning Information*. Cheshire, CT: Graphics Press, 1990. ISBN 978-0961392116.
- [46] **S. K. Ojha**. *Flight Performance of Aircraft*. AIAA Education Series, 1995. ISBN 978-1563471131.
- [47] **Radio Technical Commission for Aeronautics**. Final Report of the RTCA Board of Directors' Select Committee on Free Flight. Tech. rep., RTCA, 1995.
- [48] **Federal Aviation Administration and Eurocontrol**. Principles of Operation for the Use of Airborne Separation Assurance Systems. Tech. Rep. PO-ASAS-V7.1, Federal Aviation Authorities - Eurocontrol, 2001.
- [49] **S. B. J. van Dam, M. Mulder, and M. M. van Paassen**. The Use of Intent Information in an Airborne Self-Separation Assistance Display Design. In: *AIAA Guidance, Navigation, and Control Conference and Exhibit*, 2009.
- [50] **J. D'Engelbronner, M. Mulder, M. M. van Paassen, S. de Stigter, and H. Huisman**. The Use of the Dynamic Solution Space to Assess Air Traffic Controller Workload. In: *AIAA Guidance, Navigation, and Control Conference and Exhibit*, 2010.
- [51] **G. A. Mercado-Velasco, M. Mulder, and M. M. van Paassen**. Analysis of Air Traffic Controller Workload Reduction Based on the Solution Space for the Merging Task. In: *AIAA Guidance, Navigation, and Control Conference and Exhibit*, 2010.
- [52] **R. A. Paielli**. Modeling Maneuver Dynamics in Air Traffic Conflict Resolution. *Journal of Guidance Control and Dynamics*, 26(3), 407–415, 2003.
- [53] **S. B. J. van Dam, M. Mulder, and M. M. van Paassen**. Airborne Self-Separation Display with Turn Dynamics and Intruder Intent-Information. In: *IEEE International Conference on Systems, Man and Cybernetics*. IEEE, Montreal, Canada, 2007.

- [54] **U.S. Department of Transportation and Federal Aviation Administration.** Introduction to TCAS II Version 7.1, 2011.
- [55] **D. D. Woods.** Visual Momentum: a Concept to Improve the Cognitive Coupling of Person and Computer. *International Journal of Human-Computer Studies*, 21, 229–244, 1984.

Part II

Evaluation

Evaluating the co-planar display concept

This chapter presents the results from two experiments that were conducted to evaluate the co-planar display concept introduced in Chapter 4. In both experiments, the co-planar display concept is compared with a display that is very similar, but lacks the visualization of the interaction between projection planes. The first experiment concerns an active conflict resolution task, that investigates how operator performance and behavior are influenced by the visualization. The second experiment consisted of a passive situation awareness assessment. Together, these experiments cover each of the three main categories of situation awareness measures: Explicit, implicit, as well as subjective methods are used to assess situation awareness.

- Paper title** Experimental Evaluation of a Co-planar Airborne Separation Display
- Authors** J. Ellerbroek, K. C. R. Brantegem, M. M. van Paassen, N. de Gelder, M. Mulder
- Published in** IEEE Transactions on Human-Machine Systems, Vol. 43, No. 3, May 2013, pp. 290–301

Abstract: *Two experiments, an active conflict resolution task and a passive situation awareness assessment, were conducted that compared two versions of a constraint-based co-planar airborne separation assistance display. A baseline display showed a maneuver space based on two-dimensional projections of traffic and performance constraints. A second augmented display also incorporated cutting-planes that take the dimension orthogonal to the projection into account, thereby providing a more precise visualization of traffic constraints. Results showed that although pilots performed well with either display, the augmented display scored consistently better in terms of performance, efficiency of conflict resolutions, the amount of errors in initial resolutions, and the level of situation awareness compared to the baseline display. On the other hand, more losses of separation were found with the augmented display, as pilots tried to maximize maneuvering efficiency according to the precision with which constraints were visualized.*

5-1 Introduction

In an ongoing study on the design of a three-dimensional separation assistance interface, a constraint-based co-planar display was proposed that presents constraints on maneuvering in a ‘velocity action space’, that is overlaid on traditional moving-map displays [1]. The co-planar display is a combination of previous single-plane presentations [2, 3], with additional visualization of the interactions that exist between these planes. The evaluation of this display is the topic of this paper.

To meet the demands set by current plans for highly-automated conflict resolution [4, 5], such a self-separation interface should enable pilots to monitor separation, select and apply resolution advisories, but also judge the functioning of the separation assurance automation. This means that although automation will provide resolutions, pilots will ultimately be responsible for the validity of those resolutions. Several studies argue that this requires transparent and understandable functioning of automation [6–9]. The interface should provide a window to the reasoning and functioning of the automation, to ensure proper situation awareness (SA), and to keep pilots “in-the-loop” [10–12].

The constraint-based displays proposed in this study aim to improve pilots’ understanding of automated resolutions, by helping them understand how different elements in the work environment interact, and shape the possibilities for conflict resolution. These data invariably form the premise

on which automation bases its actions, and are therefore essential when automation functioning needs to be judged.

The focus of an evaluation study of such a display should therefore lie on how the elements of the display affect the pilot's awareness and understanding of the traffic situation. In the current study, two experiments are presented to serve this purpose. An active conflict resolution experiment was performed to evaluate how operator performance and behavior are influenced by the visualization. The second experiment consisted of a passive situation awareness assessment, and a questionnaire. The methods that were used to assess SA are also presented in this paper.

In both these experiments, two displays were compared that are very similar, and differ only in the visualization of interactions of constraints. The resulting comparison should illustrate the main addition in the co-planar concept, that sets it apart from its two-dimensional predecessors, i.e., visualization of the interactions that exist between planes of projection. Although the 'baseline' display condition will lack certain information compared to the 'augmented' co-planar display, there are no other, more equal alternatives to compare the co-planar concept with. Other existing display concepts either only show explicit resolution advisories, or show only one dimensional constraints, and are therefore even less detailed than the baseline condition in this study [13–16]. Although some degree of bias is unavoidable in this kind of comparison, the experiments were designed to minimize this effect.

The work presented in this paper will employ this comparison to focus on the effect of the additional interaction visualizations on the performance, behavior, and situation awareness of pilots in the task of airborne self-separation. The following section introduces the co-planar display. Section 5-3 discusses the topic of situation awareness measurement methods, and presents the methods that were used in this study. Sections 5-4-5-7 describe an active conflict resolution experiment and its results, and a passive situation awareness assessment and its results, respectively. The paper ends with a discussion on the results, and conclusions from the experiments.

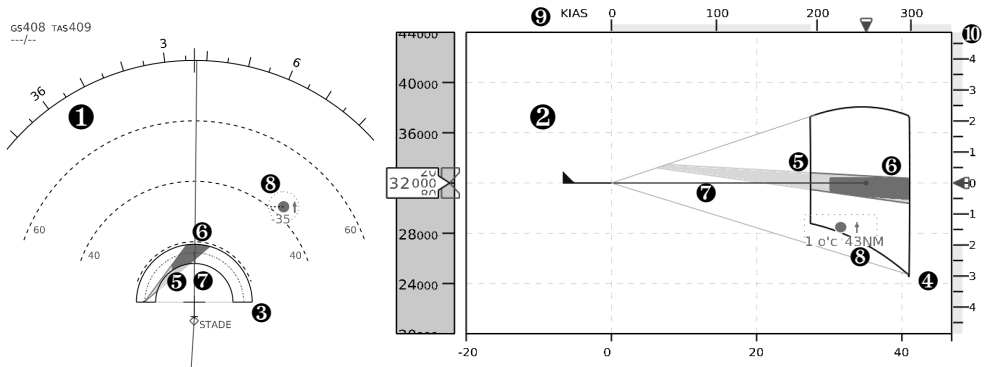


Figure 5.1: Concept for a co-planar separation assistance display. This figure shows a HSD (❶) and a VSD (❷), with added separation assistance overlays. Relative intruder locations are indicated using TCAS-like symbology (❸). ❹ and ❺ are the horizontal and vertical State-Vector Envelope, respectively. ❻ is the reduced forbidden area on both on the HSD and the VSD. ❼ is the projected forbidden area on both displays. ❽ represents the ownship state vector.

5-2 The interface

Figure 5.1 illustrates the co-planar display concept that was evaluated in this study. It consists of a concept for a self-separation interface, that presents separation-related constraints and relations on a co-planar display [1]. Important elements of the display are numbered in the figure, and will be described in the remainder of this section. This display concept is part of an ongoing study on the design of a three-dimensional separation assistance interface, that uses work-domain analysis tools to identify constraints and relations relevant to the separation task [17].

In this display concept, the three-dimensional traffic situation is visualized in two orthogonal, two-dimensional views: a top-down view (❶), and a side view (❷). Both views present a classical ownship-centered moving map, that shows spatial information such as the planned route and the relative positions of other aircraft (❸). In addition, constraints on ownship maneuvering are shown on both displays through velocity action-space* overlays

*The term 'velocity action-space' refers to the vector space containing all possible velocity vectors. The State-Vector Envelope describes the reachable subset of this vector space [1].

(④, ⑤). These overlays are referred to as State-Vector Envelopes (SVEs) in the remainder of this text.

The horizontal SVE (④) shows the horizontal maneuver space, in terms of track angle and airspeed. The boundaries of this action space are determined by the aircraft performance limits: The aircraft minimum and maximum operating speeds result in the concentric circular boundaries of the SVE. The vertical SVE (⑤) shows a vertical maneuvering space, in terms of airspeed and vertical speed. Similar to the horizontal SVE, the boundaries of the vertical SVE are also determined by aircraft performance limits. The vertical edges of the SVE result from the limits on aircraft airspeed. The curved edge at the top of the vertical SVE visualizes the maximum obtainable steady climb at each velocity. The bottom edge indicates steady descent at idle thrust for each velocity. The area within these envelopes describes all reachable velocity vectors.

Intruder aircraft that are within detection range will reduce the available maneuver space in the horizontal and vertical SVEs. The reduced forbidden areas (RFAs) (⑥) give the most precise representation of these constraints, because they incorporate the influence of the conflict geometry perpendicular to the respective projection plane [1]. On the Horizontal Situation Display (HSD), a RFA gives the constraints imposed by an intruder on ownship track angle and airspeed (⑧), for the current value of ownship vertical speed. On the Vertical Situation Display (VSD), a RFA gives intruder-imposed constraints on ownship airspeed and vertical speed (⑨), for the current ownship heading. The RFAs result from the intersection between a flat cutting plane, and the three-dimensional forbidden area: a compound of two slanted conical shapes, aligned with the top and bottom of the intruder protected zone. The shapes that result from this intersection range from circles, to ovals, to open-ended hyperbolic curves.

The projected forbidden areas (⑦) are shown in combination with the RFAs, and provide several SA-related cues, as well as an outer limit on the shape and size of the RFA, when a flight parameter perpendicular to the corresponding projection plane is modified [1, 18].

Conflict urgency is explicitly indicated on the display using intruder symbology similar to the existing Traffic Collision Avoidance (TCAS) system [19]. In addition, conflict urgency is also indicated using color coding

for all of the display elements that correspond to one intruder. This means that the aircraft symbols on both displays, as well as the forbidden area triangles and RFAs on both displays are colored according to the urgency of the conflict between ownship and the corresponding intruder.

5-3 Measuring situation awareness

The topic of situation awareness has stirred much debate in the past two decades. Several different definitions have been proposed, as well as varying methods aimed at measuring SA. In his review report, Uhlarik provides an extensive comparison of these definitions and methods [20].

The current work will employ Endsley's levels of situation awareness, which are a part of her definition of SA. She proposed that "Situation awareness is the perception of elements in the environment within a volume of time and space, the comprehension of their meaning, and the projection of their status in the near future" [21].

Endsley's definition differentiates between three levels: The first level of SA describes the *perception* of the status, attributes, and dynamics of relevant elements in the environment. The second level is the *comprehension* of the significance of the level 1 elements on the operator goals. The ability to *project* the future state of the elements in the environment forms the third level of SA.

Although Uhlarik argues that the use of Endsley's model to describe SA has its limitations [20], the distinction between levels of SA is very valuable when assessing to what extent pilots utilize higher level information on the display, and how they relate this information to functional goals. As suggested by Flach, these levels of SA will therefore be used to categorize observed behavior in the experiment, rather than using an SA model to explain behavior [20, 22].

Most studies differentiate between three main categories of SA measurement methods: explicit methods, implicit methods, and subjective methods [20]. Explicit methods require subjects to report relevant parameters from memory, implicit methods infer level of SA from performance measures, and subjective methods ask subjects to self-rate their situation awareness. Each

category of measurement method has its benefits and drawbacks, which is why Uhlarik argues for the use of multiple methods to ensure validity of results [20]. This study will therefore use methods from each category to assess SA.

Current explicit SA measures either require subjects to recall specific events after an experiment run is finished, or assess situation awareness on-line, while the experiment is running. A downside of retrospective methods (measuring after the actual run) is that the measurement is only as accurate as the memory of the pilot. That is, in an experiment with long runs, retrospective measurements are subject to forgetfulness and false recollections. On-line methods, on the other hand, can influence the pilot task being performed in the experiment. By having participants attend to particular information on the interface, these measures can cause participants to behave differently than they would otherwise [20, 23].

To mitigate the downsides of these methods, participants in this study will each perform two experiments, that separate the explicit from the implicit SA measurements. In the main experiment, subjects actively resolve conflict situations in a real-time simulated environment. The results from this experiment will be used to analyze resolution strategies, performance, and safety metrics. The performance measures will be used as implicit indicators of level of SA. In an additional passive experiment, subjects are presented with static conflict situations, each accompanied with a set of time-limited, multiple-choice SA questions, that are centered around Endsley's levels of SA. The resulting measures will be used to compare the display variants in terms of how they influence situation awareness. In a final post-experiment questionnaire pilots are given the opportunity to self-rate their situation awareness. By separating the explicit SA assessment from the active experiment, behavior in the main experiment no longer runs the risk of being directed by particular SA queries, and the explicit measurements are not hampered by the drawbacks of retrospective SA assessments.

5-4 Experiment I: Active conflict resolution

To evaluate the co-planar display concept, a traffic separation experiment was performed, where pilots were placed in conflict situations with a loss

of separation in the medium to short term future (3–5 min). Each session consisted of a continuous presentation of four consecutive conflict scenarios, that needed to be resolved manually, with the aid of a co-planar separation assistance display. Traffic conflicts were always between a single human actor, and simulated conflicting traffic.

5-4-1 Apparatus and aircraft model

The experiment was performed on the Apero flight simulator of the National Aerospace Laboratory (NLR). The Apero is a fixed-base flight simulator, featuring five high-resolution touch screens, and a large (52 inch) screen that provides the outside visual. The left-hand seat, primary display showed a conventional Airbus Primary-Flight Display (PFD) and the co-planar HSD/VSD display concept. The copilot display was disabled during the experiment. The middle vertical screen showed the Electronic Centralized Aircraft Monitor (ECAM) instruments. The touch screens on the pedestal showed several instruments, such as the Multifunction Control and Display Units (MCDU's) and the radios.

Pilots controlled the aircraft through an Airbus style Flight Control Unit (FCU), located on the glare shield above the center touchscreen. An Electronic Flight Instrument System (EFIS) panel situated to left of the FCU allowed pilots to switch between display modes and change the display range. On the pedestal, a trackball was available to select and highlight intruder information on the co-planar display.

The aircraft model that was used during the experiment was a proprietary nonlinear six degree of freedom Airbus A320 model, developed at the NLR. Intruder aircraft were modeled by point-mass models[24]. Model coefficients for these point-mass models were obtained from EUROCONTROL's BADA aircraft database [25]. The experiment was conducted with zero wind, and no turbulence. Although wind conditions will impact maneuverability, these effects were considered out of scope for the current evaluation. The own aircraft flew at altitudes between flight level FL220 and flight level FL320. This flight level range was chosen so that airspeed and vertical speed still had usable margins between minimum and maximum operating speed, and between maximum climb and descent rates, respectively.

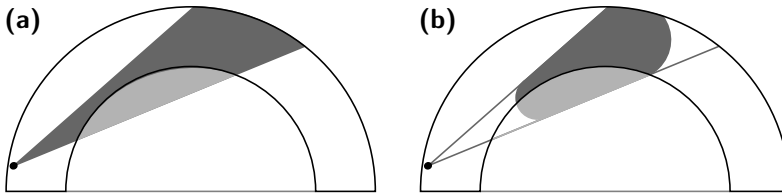


Figure 5.2: The horizontal SVE for the baseline **(a)** and the augmented display **(b)**. The baseline display shows two dimensional projections of constraints (called forbidden areas (FA)). The augmented display gives more precise constraints (called reduced forbidden areas (RFAs)) that take the dimension orthogonal to the projection into account. The differences on the VSD are similar to the differences on the HSD. The two display conditions are otherwise equal.

5-4-2 Independent variables

Throughout the experiment, two independent variables were varied. *Display type* was a factor with two levels: on the co-planar separation assistance display, the RFAs could be either present or absent, see Figure 5.2. Here, the display without RFAs was used as a baseline condition. The second factor was *conflict geometry*, which featured six levels. Scenarios differed in *phase of flight*, and *difficulty*. The phase of flight was either climb, cruise, or descent. A further distinction was made between *simple* and *difficult* scenarios. Simple conflicts always featured only one intruder, whereas in difficult scenarios, three intruders were present in each scenario. Table 5.1 gives a summary of these scenarios.

Table 5.1: Conflict geometries experiment I.

	intruder	Climb	Cruise	Descent
Simple	ac 1	200/64/-8	270/-35/7	120/-44/0*
	ac 1	25/69/0	100/-40/8	100/-74/5*
Difficult	ac 2	210/-21/5	20/-15/6	60/-34/-8*
	ac 3	138/24/0	270/59/-10	280/-54/8*

*Values are: $\Delta\chi$ [$^{\circ}$], Δh [$\times 100ft$], V/S [$\times 100ft/min$]

5-4-3 Experiment design and procedure

The experiment was designed as a within-subjects repeated-measures, where factors *display type* and *conflict geometry* were varied. The *display type* factor was introduced to illustrate the effect of the additions that the co-planar display concept features compared to the original two-dimensional separation displays. The *conflict geometry* factor was divided in phases of flight (climb, cruise, and descent), and subdivided in simple and difficult scenarios. In the simple scenarios, pilots were not expected to benefit substantially from the RFA visualization. Only in more difficult scenarios it was expected that the advantages of the RFA visualization would become noticeable. This resulted in 12 conditions ($2 \times 3 \times 2$).

After a briefing on the experiment and the functioning of the separation display, subjects performed approximately one hour of training. The experimenter would end the training session based on observed performance, and the subject's answers to informal scenario-related questions. To avoid memorizing effects, but still reach a stable level of performance and sufficient understanding of the information presented by the separation assistance interface, separate example scenarios were used for training. During the experiment, conflict scenarios were presented in a randomized block design, and conflict geometries were mirrored between display conditions. Trials were combined in four blocks of four sequential conflict scenarios. Each block started with a climb from flight level FL220 to flight level FL320, at 1,000 ft/min, followed by a cruise segment, and then a descent back to flight level FL220, again at 1,000 ft/min. Each block featured one conflict in the climb segment, two conflicts in the cruise segment, and one conflict in the descent segment. Starting times were different for each conflict to make it less evident for pilots when to expect each new conflict. A block lasted about 40 minutes.

The *display type* factor was kept constant over two blocks: first two blocks with one display, then two blocks with the other. The order of presentation for the display types was varied evenly over the subjects. In all conflict scenarios, multiple options in both the horizontal and vertical plane were available to solve the conflict situation, although not all options were equally fast and efficient. Intruder aircraft never maneuvered in order to solve a conflict situation, instead they just kept following their initial path.

5-4-4 Subjects and instructions to subjects

Seventeen experienced glass-cockpit pilots participated in the experiment, all male. Experience in terms of flight hours per pilot ranged from 3,000 to 21,000 hours ($\mu=10,000$). None of these subjects had any previous experience with constraint-based displays. Subjects were asked to perform an experiment, where they should resolve traffic conflicts in unmanaged airspace. They were informed that the results would be used to evaluate a concept for a three-dimensional co-planar separation display. They were also informed that intruder aircraft would not participate in the resolution of conflicts.

In a written guide pilots received beforehand, and in a short presentation prior to the experiment, pilots were briefed on the geometrical concepts behind the display, how to use the display, and on the experimental setup. To ensure safe flight, pilots' first and foremost priority was to avoid a loss of separation at all times. When safety is ensured, pilots could explore their resolution options to optimize for efficiency. They were instructed to use the cues from the forbidden area to determine an efficient solution [18], and that their aim should be to apply a resolution that is appropriate, given the current phase of flight (i.e., climb, descent or cruise).

5-4-5 Dependent measures

Dependent measures for this experiment consisted of several objective measures. *Resolution strategy* was measured in terms of own aircraft velocity vector change dimensions, which could be any combination of a change in heading, speed and vertical speed. Path deviation, initial reaction time, and resolution duration were used as measures of *performance*. The path deviation metric differentiates between horizontal and vertical maneuvers: For horizontal maneuvers, the path deviation was characterized by the additional distance flown. In case of a vertical maneuver during the climb or descent phase, the mean deviation from the prescribed vertical speed was used. For cruise conflicts, the maximum altitude deviation from the cruising level was measured. Pilot reaction time (the time between the start of a conflict and the first selection of a resolution maneuver) and the total time of the resolution maneuver (the time between leaving and rejoining the reference

trajectory) were used as metrics that allow for comparison between vertical and horizontal maneuvers. *Safety* was measured in terms of minimum separation, and the occurrence of losses of separation.

5-4-6 Experiment hypotheses

Several studies involving manual (horizontal) conflict resolutions found that pilots prefer single-axis maneuvers, keeping velocity constant [18, 26–28]. It was therefore hypothesized that the majority of the maneuvers would be either heading-only, or vertical speed-only (H1-1). It was also hypothesized that the resolution dimension would depend on phase of flight, i.e., that climb and descent conflicts would be solved vertically and cruise conflicts would be solved horizontally (H1-2).

Differences between the baseline display and the augmented display were only expected during difficult scenarios (scenarios with multiple intruder aircraft, which are both off-level and off-track). It was therefore hypothesized that performance would be improved with the augmented display in difficult scenarios (H1-3). Because the RFAs show more precise constraints than the projected forbidden areas, it was also hypothesized that they would result in smaller separation distances at the Closest Point of Approach (CPA) (H1-4), as previous studies showed that the precision with which constraints are presented is used by pilots to optimize their efficiency [18, 29]. The number of separation violations was hypothesized to be low, regardless of display type (H1-5).

5-5 Experiment I: Results

Kolmogorov-Smirnov tests on the ratio data results revealed that for none of the cases a normality assumption could be made (altitude deviations, response times and resolution times, $p < 0.001$ in each case). Therefore, only non-parametric tests were used: the Wilcoxon Signed-Rank test (test statistic z) for metrics based on ratio data that did not depend on the chosen evasive maneuver (e.g., pilot response time), and the Wilcoxon rank sum test (test statistic W) for all other metrics based on ratio data. Pearson's chi squared test (test statistic χ^2) was used for categorical metrics. Effects

were considered significant at a probability level $p \leq 0.05$, where p is the probability that the null hypothesis is true.

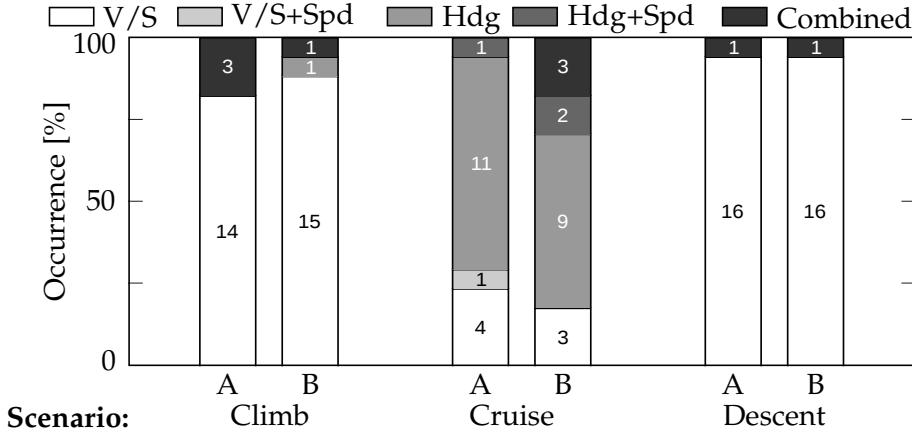


Figure 5.3: Solution strategy for simple conflicts, sorted by scenario and display type (A = augmented, B = baseline) along the abscissa. The scale on the ordinate axis gives the occurrence in percent of the total per scenario, the absolute values are indicated inside the bars.

5-5-1 Resolution strategy

The resolution maneuvers in the experiment can be grouped by the flight parameters that were changed to resolve each conflict. The available maneuver options are heading, speed and vertical speed (V/S) changes. Although a resolution maneuver can consist of any possible combination of these parameters, speed-only maneuvers were never observed, and three-way combinations were rare. Therefore, Figure 5.3 and Figure 5.4 show resolution strategy divided into five levels: *vertical maneuvers (with and without speed)*, *horizontal maneuvers (with and without speed)*, and *combined horizontal and vertical maneuvers*. Maneuver selection will depend on conflict geometry, aircraft performance limitations, phase of flight, and personal or airline preference.

Figure 5.3 shows the maneuver choice for the simple cruise, climb and descent scenarios. Each of these scenarios featured a conflict with a single intruder. The majority of the maneuvers for the climb and descent scenarios were V/S-only, regardless of display type (82% - 94%). With one exception, the direction of the change in V/S was always the same: the climb conflict

was always solved by increasing the rate of climb, and the descent conflict by decreasing the rate of descent. These choices correspond to the smallest available state change for the current conflict, an efficiency strategy given to the subjects during the briefing. They can, however, also be an indication of a preference for ‘staying high’, to optimize for fuel efficiency.

Although the spread in solution strategy was larger than in the climb and descent scenarios, the majority of the resolutions in the simple cruise scenario was still heading only (baseline display 53%, augmented 65%). As was hypothesized (hypothesis H1-2), phase of flight was an important factor when deciding on a solution strategy. Comparison between the cruise scenario and the vertical scenarios showed a significant difference in resolution decisions ($\chi^2(2) = 56.9$, $p < 0.001$). Comparison between displays did not reveal significant effects for simple conflicts.

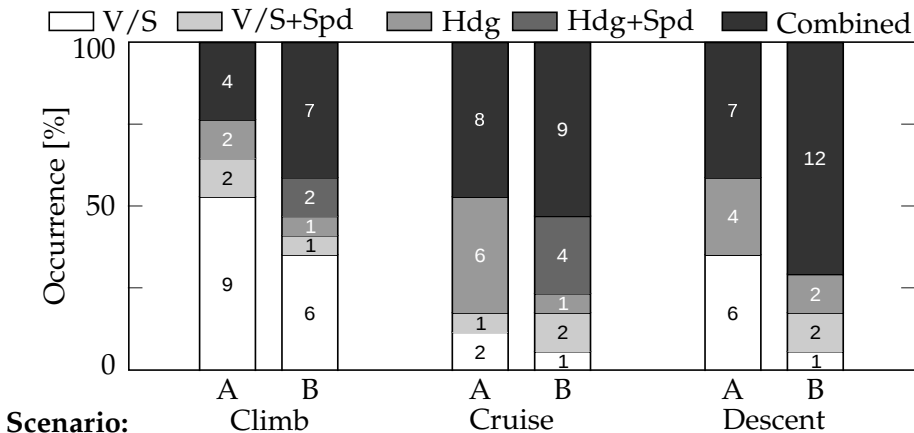


Figure 5.4: Solution strategy for difficult conflicts, sorted by scenario and display type (A = augmented, B = baseline) along the abscissa. The scale on the ordinate axis gives the occurrence in percent of the total per scenario, the absolute values are indicated inside the bars.

Figure 5.4 shows the maneuver choice for the difficult cruise, climb and descent scenarios. These scenarios each featured multiple intruders, of which only one was causing a conflict with ownship. In these scenarios, intruder aircraft were all off-level and off-track, making the maneuver space presented on the augmented display significantly different from the presentation on the baseline display. On the baseline display, this resulted

in a considerable portion of the SVEs being colored, which increases the perceived severity of the conflict.

In terms of resolution strategy, the difference between the displays is visible in the number of multi-axis resolutions (V/S+SPD, HDG+SPD, or combined), which were used significantly more often with the baseline display: 77% for the baseline display, compared to 43% for the augmented display, for the climb, cruise, and descent scenario combined ($\chi^2(1) = 11.8$, $p = 0.001$). Most of these multi-axis resolutions were sequential maneuvers, rather than a single combined maneuver, regardless of display type. In other words, pilots often changed their minds after an initial resolution. The high number of multi-axis resolutions, therefore, doesn't necessarily refute the hypothesis of single-axis maneuver preference (H1-1), as the initial resolution maneuver often was single-axis. It is likely that lack of training plays a large role in this result. The difference between displays in the number of multi-axis resolutions can also be indicative of reduced situation awareness with the baseline display.

Based on pilot comments during the experiment, the multi-axis maneuvers can be classified into two categories. For the baseline display, the most often heard comment was that a pilot realized that he had made a wrong initial maneuver. This was either a maneuver that did not resolve the conflict, or a maneuver that resulted in a very inefficient resolution. A second category of maneuvers were from pilots that attempted to increase efficiency, by maneuvering in an additional direction.

Phase of flight also significantly influenced maneuver strategy in the difficult scenarios ($\chi^2(2) = 6.3$, $p = 0.04$). The cruise conflict was solved horizontally (32.4%) almost twice as much as vertically (17.6%). Similarly, the climb and descent scenarios were more often solved vertically (39.7%) than horizontally (16.2%).

5-5-2 Safety

The separation between aircraft at the closest point of approach, compared to the minimum safe distance, was used as a measure of safety. To allow for comparison between horizontal and vertical separation, each measured

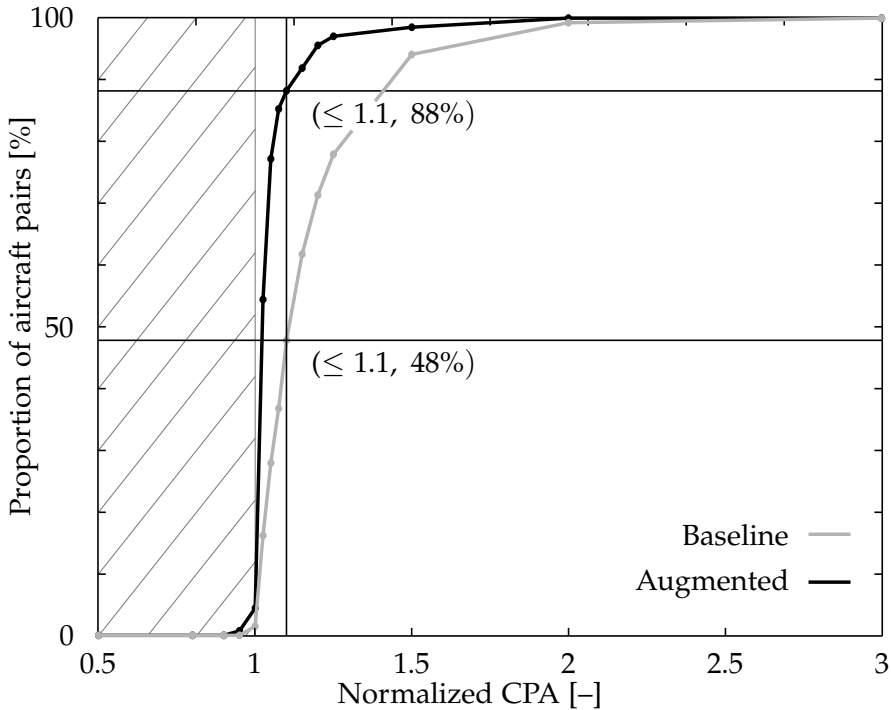


Figure 5.5: Cumulative distribution graph of normalized minimum separation values. Minimum separation occurs at the closest point of approach, which is indicated as a ratio of the separation minimum along the abscissa. The number of aircraft is indicated along the ordinate axis, counted in percent of the total number of aircraft. The hatched area on the left of the graph indicates the values of CPA that violate the minimum separation constraint.

value is normalized by their respective separation minimum (5 *nmi* horizontal, and 1,000 *ft* vertical separation). For each measured CPA, the largest* of both normalized separation values was used. Figure 5.5 shows a cumulative distribution graph of the normalized CPA values, for the augmented and baseline displays.

*For example, if vertical separation is equal to zero, but horizontal separation is much larger than the separation margin, then both aircraft are still safely separated. The largest normalized separation value is therefore the most relevant parameter.

The separation minimum was violated in eight out of 272 measured trials, twice with the baseline display, and six times with the augmented display. In all eight cases, this occurred during a premature return to the nominal track, after resolving the conflict. In all cases, the incursion was minimal (all within 10% of the separation minimum, and 6 less than 1%). A common practice that was observed in this, but also in previous experiments with a constraint-based display [18, 29], was that after resolving a conflict, pilots are inclined to optimize their performance by returning to their nominal state as soon as possible, in small steps, while staying as close as possible to the edge of the forbidden area. In these situations, a judgment error can easily result in a (small) violation of the separation constraint. The difference between displays in the number of losses of separation was not significant ($\chi^2(1) = 2.1$, $p = 0.15$), but does illustrate that the more restrictive constraints presented by the baseline display act as an added safety margin for this kind of behavior.

5-5-3 Performance

Figure 5.5 also shows that, especially with the augmented display, pilots often came within close distance of the protected zone of the other aircraft. With the augmented display, 88% came closer than 1.1 times the separation minimum, versus 48% for the baseline display. In terms of performance, this is a strong indication that pilots use the precise visualization of constraints to optimize the efficiency of their resolution. The difference in CPA distance between displays was significant ($z = -7.22$, $p < 0.001$), supporting hypothesis H1-4.

Because a direct comparison between path deviation of a horizontal maneuver and path deviation of a vertical maneuver does not make much sense, results for this performance metric will be divided in horizontal maneuvers and vertical maneuvers. For horizontal maneuvers, the path deviation was characterized by the additional distance flown. In case of a vertical maneuver during the climb or descent phase, the mean deviation from the prescribed vertical speed was used. For cruise conflicts, the maximum altitude deviation from the cruising level was also measured.

As climb and descent scenarios were mostly solved with a change in vertical speed, the mean deviation from the prescribed vertical speed was used

to observe differences in performance between displays for vertical conflicts. Although there is a consistent trend of the augmented display performing better than the baseline display, this difference was only significant in the difficult descent scenario ($W = 24$, $p = 0.024$).

There are several possible reasons for the lack of significance in the remaining scenarios. First, because performance penalties of a speed change, a heading change and a vertical speed change are difficult to compare directly, the data can only be compared per maneuver category. This reduces the sample size, and therefore also the statistical power. Second, several times during the experiment it was observed that with the baseline display, pilots readjusted their resolution to a point inside the forbidden area, as soon as they realized that that particular state change was sufficient for conflict resolution. Although initially this resolution is only visualized with the RFAs, these solutions are also indirectly visualized during the state change. The color of the forbidden area communicates the urgency of a conflict, where a white forbidden area indicates a non-conflicting intruder. A pilot can therefore break off a maneuver as soon as the forbidden area turns white.

Cruise conflicts were solved 14 times out of 68 with a change in vertical speed. Although the mean deviation from the prescribed vertical speed did not reveal a significant difference, the maximum altitude deviation did differ significantly between display types, where the altitude deviation was always smaller with the augmented display ($W = 62$, $p = 0.029$). This is also an indication that pilots exploit the precise constraint visualization to optimize maneuver efficiency [18].

For horizontal maneuvers, the path deviation did not reveal a significant effect for any of the scenarios. The difficult descent and climb scenarios did show a consistent trend of the augmented display performing better than the baseline display, but contained too few samples to provide sufficient statistical power. Although on average, performance was almost equal between display types for horizontal resolutions of the simple cruise scenario, the spread was much larger for resolutions using the baseline display. Similar to the visualization of the vertical constraints, the horizontal baseline display also indirectly visualizes the constraints of the RFA. The differences in spread indicate that although pilots are able to use this indirect visualization, they do so less consistently than with the augmented display.

Table 5.2: Mean reaction and resolution times.

Display × scenario	Baseline	Augmented
Simple	$\mu_{react} = 12.0$ [s]	$\mu_{react} = 11.5$ [s]
	$\mu_{reso} = 22.4$ [s]	$\mu_{reso} = 20.2$ [s]
Difficult	$\mu_{react} = 20.4$ [s]	$\mu_{react} = 15.1$ [s]
	$\mu_{reso} = 42.3$ [s]	$\mu_{reso} = 33.2$ [s]

Reaction time and resolution duration are measures that can be considered independent of the maneuver dimension, and can therefore be used as overall metrics to compare the baseline and augmented displays in simple and difficult conflict scenarios. From these measures, resolution duration is a measure of performance of a maneuver, and reaction time can be used as an indication of the difficulty experienced by pilots. Table 5.2 shows the mean reaction times and resolution durations for both displays in the simple and difficult scenarios. As hypothesized (H1-3), both these measures show significant effects of display type for the difficult conflict scenarios, but not for the simple conflict scenarios. For the simple conflict geometries, the two display variants show comparable maneuver constraints. It is therefore not expected that difficulty and resolution performance vary significantly between display types. For difficult scenarios, results for the augmented display show significantly shorter reaction times ($z = -2.32$, $p = 0.021$), and significantly shorter resolution durations ($z = -2.53$, $p = 0.012$).

5-6 Experiment II: Passive SA assessment

In addition to the active conflict resolution task, a SA assessment was conducted to obtain explicit measures of SA. In this experiment, pilots were shown four static conflict scenarios, on both display variants. For each scenario, SA was probed with a timed questionnaire.

5-6-1 Apparatus

The SA assessment was performed on a single computer with a 17 inch display. The left half of the screen showed a static version of the co-planar display. Questions and multiple-choice answers were shown on the right

half of the screen. A countdown timer indicated remaining time for each question. Pilots could select answers using a regular computer mouse.

5-6-2 Independent variables

Throughout the SA assessment, two independent variables were varied. Display type was a factor with two levels, which were equal to the display variants in the active experiment. The second factor was conflict geometry. Conflicting aircraft could be either on- or off-track, and either on- or off-level, resulting in four levels (2×2), see Table 5.3.

Table 5.3: Conflict geometries experiment II.

	intruder	On-level	Off-level
On-track	ac 1	180/0/0	180/60/-17 *
	ac 2	0/0/0	180/-25/5 *
Off-track	ac 1	300/0/0	30/30/-10 *
	ac 2	75/0/0	200/20/-2.5*

*Values are: $\Delta\chi$ [$^{\circ}$], Δh [$\times 100ft$], V/S [$\times 100ft/min$]

5-6-3 Experiment design and procedure

The SA assessment followed immediately after the active experiment. It consisted of a time-limited SA query. Subjects were shown static conflict scenarios, each accompanied with thirteen time-limited multiple-choice questions regarding the geometry of the conflict, and regarding possible resolutions. At the beginning of each new scenario, subjects were given thirty seconds prior to the first question, to analyze the new conflict situation. During the questions the co-planar display remained visible, i.e., the screen was not blanked. After the assessment, subjects were asked to fill in a questionnaire.

Similar to the active experiment, the SA assessment was designed as a within-subjects repeated-measures, where factors *display type* and *conflict geometry* were varied. Again, the augmented display was compared against a baseline display, resulting in two levels for the *display type* factor. The *conflict geometry* factor had four levels. Scenarios were always with two intruding aircraft, of which only one was causing a conflict with ownship. Conflicting

Table 5.4: Situation awareness grade categorization and interpretation.

Grade	Answer	Certainty	Interpretation
0	Incorrect	Sure	Misinformed
1	Incorrect	Unsure	Uninformed
2	Correct	Unsure	Guess/partially informed
3	Correct	Sure	Well informed

aircraft were either on- or off-track, and either on- or off-level, resulting in four different conflict geometries. Pilots were expected to benefit more from the RFA visualization when conflicting aircraft are increasingly off-track and off-level. This resulted in 8 conditions (2×4).

5-6-4 Subjects and instructions to subjects

The same seventeen subjects participated in this second experiment. Subjects were asked to study a set of conflict scenarios, and answer a set of geometry and conflict-resolution related multiple-choice questions. After the assessment, subjects were asked to fill in a form with questions relating to their opinion about several elements of the display. There was also opportunity for personal comments and suggestions.

5-6-5 Dependent measures

Dependent measures for this experiment are related to the SA questions, and a post-experiment questionnaire. The SA questions relate to easily identifiable information such as relative intruder position and intruder velocity, but some questions also required the subject to use information cues to predict the outcome given the current situation. The questions were categorized using Endsley's levels of awareness [21]. The subject's certainty of his answer was recorded together with the answers, following Hunt's method of measuring knowledge [30]. Using this method, the answers from the SA assessment are graded, and categorized into four groups, see Table 5.4. The resulting scores were averaged per pilot per level, resulting in three average SA scores per condition, for each pilot. The response time was also recorded for each answer.

The work-domain analysis that preceded the display design identifies relevant elements and relationships within the work-domain, which are arranged by level of abstraction [1, 17]. Consequently, relevant SA questions can also be based on this analysis. As a result, level 1 questions relate to conflict geometry (such as intruder location and velocity), and level 2 questions relate to principal resolution options (can a speed, vertical speed, or heading change solve the conflict). Level 3 questions for instance require subjects to evaluate different solutions in terms of efficiency, and choose the best of a set of solutions.

Measures from the post-experiment questionnaire consisted of usefulness ratings for several individual elements of the display, and comparisons between the displays in terms of clutter, intuitiveness, SA, and workload.

5-6-6 Experiment hypotheses

Because SA level 1 questions relate to elements that are directly perceivable on both displays, it was hypothesized that the SA score for level 1 questions would be very high, regardless of display type (H2-1). Since the augmented display visualizes more higher-level information and relationships, it was also hypothesized that the SA scores between displays would diverge increasingly, with higher SA levels (H2-2). An interaction with scenario was expected for this effect, as the difference between displays becomes increasingly pronounced for scenarios with off-level or off-track intruders (H2-3).

Results for the response time were expected to show an interaction between scenario and question SA level (H2-4). Because the augmented display reveals relationships in scenarios that are off-level or off-track, which the baseline display does not show, questions that relate to this information (i.e., level 3 SA questions) should be quicker to evaluate when using the augmented display.

5-7 Experiment II: Results

Similar to the first experiment, a normality assumption could not be made for any of the ratio data (reaction times, $p < 0.05$ for all SA levels). A Friedman two-way ANOVA (test statistic χ^2) was therefore used to evaluate main effects of the display factor. The Wilcoxon Signed-Rank test (test statistic z)

Table 5.5: Comparison between display types of the SA scores.

Level × scenario	SA Level 1	SA Level 2	SA Level 3
Main effect	$\chi^2(1) = 0.4$ $p = 0.540$ ○	$\chi^2(1) = 10.7$ $p = 0.001$ **	$\chi^2(1) = 20.7$ $p < 0.001$ **
On-level/On-track	$z = -0.378$ $p = 0.705$ ○	$z = -0.556$ $p = 0.579$ ○	$z = -1.633$ $p = 0.102$ ○
On-level/Off-track	$z = -1.000$ $p = 0.317$ ○	$z = -1.016$ $p = 0.309$ ○	$z = -1.173$ $p = 0.241$ ○
Off-level/On-track	$z = -1.000$ $p = 0.317$ ○	$z = -1.885$ $p = 0.059$ ○	$z = -2.362$ $p = 0.018$ *
Off-level/Off-track	$z = -0.136$ $p = 0.892$ ○	$z = -3.430$ $p < 0.001$ **	$z = -3.084$ $p = 0.002$ **

** significant; * marginally significant; ○ not significant.

was used to evaluate the effect of display per scenario. With a Bonferroni correction of 5* for the SA scores, results were considered significant at a probability level $p \leq 0.01$. Results with a probability level $0.01 < p \leq 0.05$ were considered marginally significant. Response time results were only analyzed in terms of main effects, resulting in a Bonferroni correction of 2. Here, results were considered significant at a probability level $p \leq 0.025$.

5-7-1 Situation awareness scores

The situation awareness scores from the experiment were grouped using Endsley's three levels of awareness [21], and are shown in Figure 5.6, for each combination of display type and scenario. These SA scores will depend

*A Bonferroni correction implies that the significance level is divided by the number of tests on a particular set of data. For these results this was one main effects test, and four post-hoc tests (one for each scenario level).

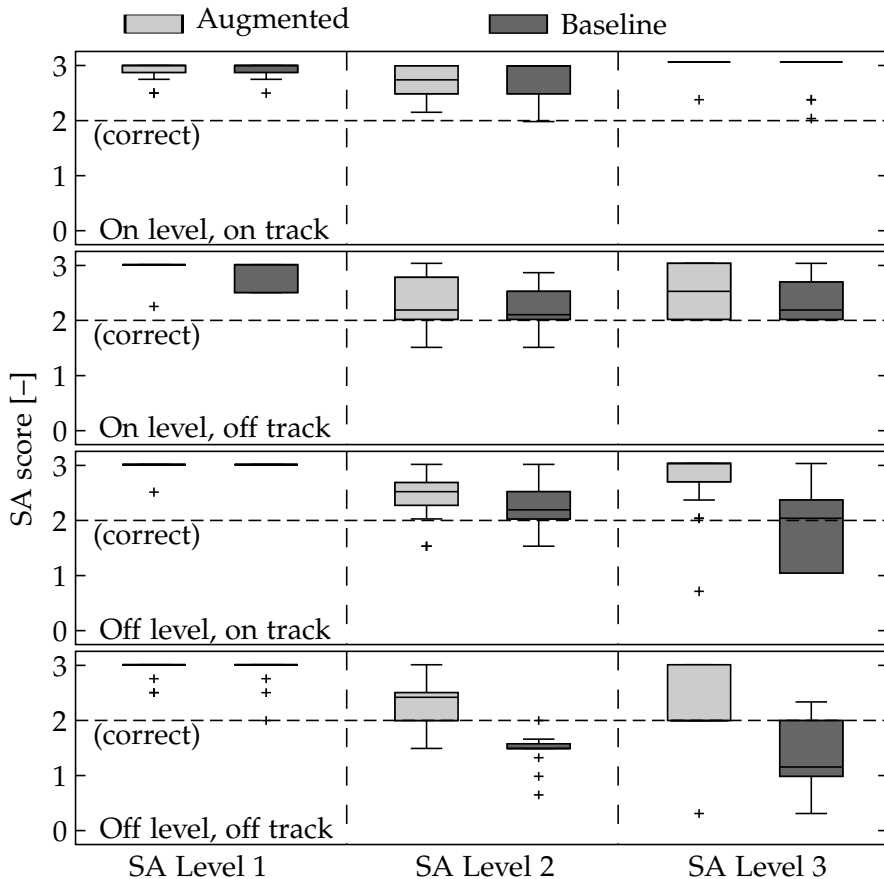


Figure 5.6: SA scores, averaged per pilot, and sorted by display type, scenario, and SA level. The three columns correspond to the three SA levels. The four rows each correspond to a scenario, as indicated in the bottom-left corner of each row. The scale on the ordinate axis gives the SA score, see Table 5.4.

on conflict geometry and accuracy of the visualization, but also on other factors that influence the buildup of SA, such as attention and workload.

As hypothesized (H2-1), the first column in Figure 5.6 shows that the majority of the subjects (92 - 100%) managed to achieve the highest SA score for level one questions, regardless of scenario or display. A comparison between display types for SA level one therefore also did not reveal any significant effects, see the first column in Table 5.5.

A main effects analysis (see Table 5.5) showed that, as hypothesized (H2-2), display becomes a significant factor for SA scores at awareness levels two and three: As can be seen in Figure 5.6, subjects scored consistently lower with the baseline display. A post-hoc analysis revealed that this effect increases when scenarios become increasingly off-level and off-track: Table 5.5 shows that the effect of display is only significant for level two and level three scores in the off-level and off-track scenario. This supports hypothesis H2-3, which stated that scenario type would influence situation awareness scores between displays.

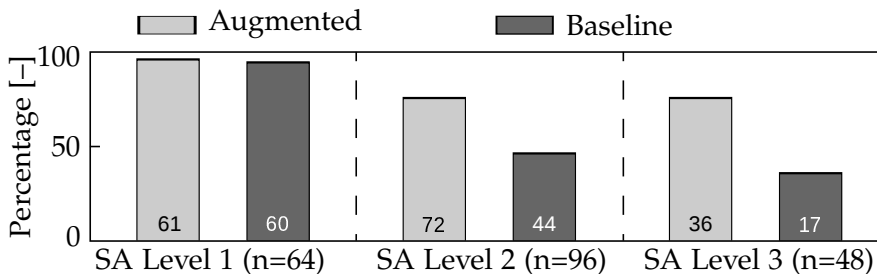


Figure 5.7: Percentage of correct and sure answers for the off-track and off-level scenario, grouped per display type and SA level. The columns in the figure table correspond to the three SA levels. The scale on the ordinate axis gives the amount of correct and sure answers, in percent of the total per display type per SA level. Absolute counts are indicated in the bottom of each bar.

Figure 5.7 illustrates the percentage of correct and sure answers, at each SA level, for the off-track and off-level scenario. According to Hunt, only these answers correspond with usable knowledge [30]. Figure 5.7 shows that, although the augmented display scores consistently higher than the baseline display, subjects still could not maintain perfect SA with the augmented display, despite the more accurate visualization. This can be—at least partly—caused by lack of training, combined with the inherent complexity of the separation problem.

5-7-2 Response time

Figure 5.8 shows the response times for the SA questions, averaged per pilot, for each combination of display type and scenario. It can be seen that although a trend in favor of the augmented display is visible in the data, it is markedly less pronounced than the effect observed for the SA score results.

Table 5.6: Effects of display and scenario on response times.

	SA Level 1	SA Level 2	SA Level 3
Display	$\chi^2(1) = 1.1$ $p = 0.300$ ○	$\chi^2(1) = 0.04$ $p = 0.851$ ○	$\chi^2(1) = 0.19$ $p = 0.187$ ○
Scenario	$\chi^2(3) = 27.3$ $p < 0.001$ ★★	$\chi^2(3) = 16.2$ $p = 0.001$ ★★	$\chi^2(3) = 10.9$ $p = 0.012$ ★★

★★ significant; ★ marginally significant; ○ not significant.

A main effects test therefore also did not reveal a significant effect of the display factor, see Table 5.6.

The response time results show larger variation between scenarios and SA levels. The response time increases with increasing conflict complexity, as well as with increasing SA level. A main effects test showed that the effect of scenario is significant for all levels of SA, see Table 5.6. These results therefore indicate that difficulty is a determining factor for response time, but that the augmented display does not enable subjects to evaluate complex situations more quickly.

5-7-3 Post-experiment questionnaire

The post-experiment questionnaire allowed subjects to give an overall rating of each display in terms of usability, and to express their preference for either display in terms of clutter, intuitiveness, situation awareness, and workload. They were also asked to rate the usefulness of several individual elements of the display. Although the sample size of 17 subjects is too small to obtain reliable results for such subjective data, these results can be used to highlight persistent trends and opinions.

Both in the overall display ratings and the display preference questions, the augmented display scored consistently better than the baseline display. An often-heard comment was that subjects could better relate information between the two displays with the augmented display, than with the baseline display. Aside from preference with regard to clutter, subjects preferred

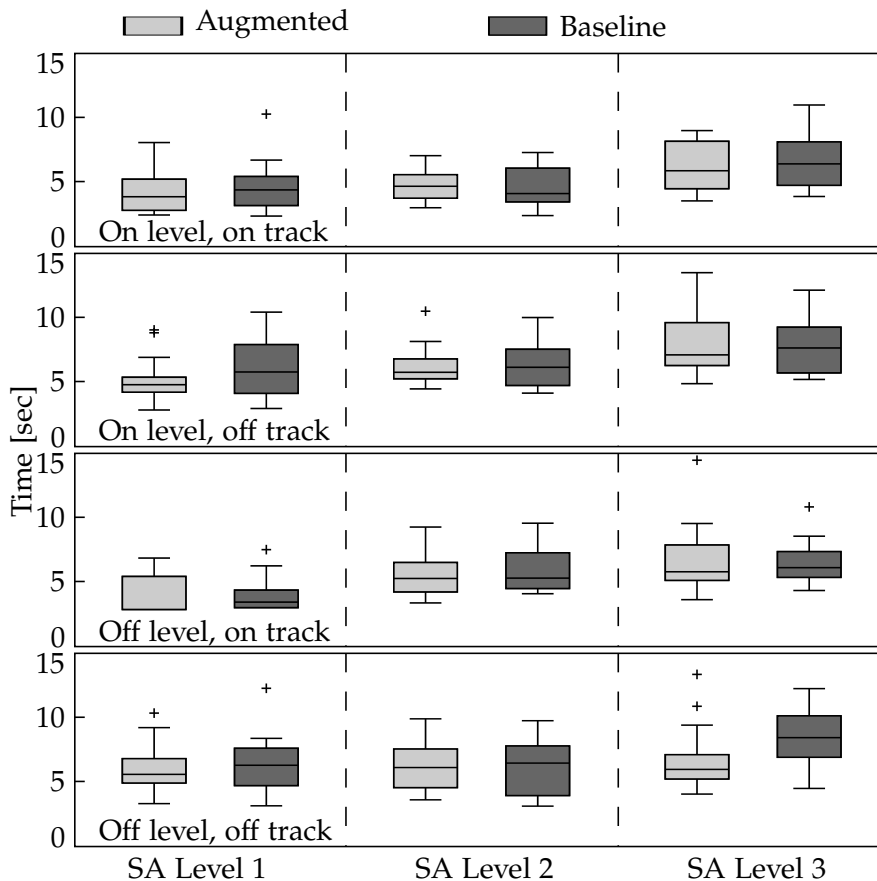


Figure 5.8: Response times, averaged per pilot, and sorted by display type, scenario, and SA level. The three columns correspond to the three SA levels. The four rows each correspond to a scenario, as indicated in the bottom-left corner of each row. The scale on the ordinate axis gives the response time in seconds.

the augmented display almost without exception (94-100%). Preference for the augmented display with regard to clutter was slightly lower (76%). Here, several subjects indicated that they did not prefer either display. One pilot remarked that while the RFAs in the augmented display increase clutter, it was ‘good clutter’. This is consistent with Tufte’s views on the use of visual details (“To clarify, add detail”) [31]. Most pilots mentioned, though, that some form of de-cluttering would be essential in high-density traffic situations (i.e., more than the 3 intruders in the current experiment). In terms of

SA, subjects mentioned that the RFAs allowed for a quicker assessment of the consequences of specific resolutions.

When asked to rate the usefulness of individual elements of the display, the majority of the subjects assigned the highest rating to the more conventional intruder symbols. The intruder symbols on the VSD, however, were mostly rated lower than the same symbols on the HSD. This is an indication that even though subjects have a very positive attitude towards the new display, and the novel visualizations, they remain biased towards appreciating familiar functionality.

Most subjects also used the opportunity to give one or more suggestions for future design iterations of the co-planar display concept. A suggestion that was prompted by almost every subject was to add the ability to zoom in on the SVEs (especially on the HSD, where it was smallest in the current simulation). An other repeated suggestion related to the addition of intent information: subjects indicated that they would appreciate the ability to see where intruders that are climbing or descending would level off, and the consequences of the own aircraft leveling off at a certain altitude. Finally, several subjects were interested to know how the concept would function when all aircraft in a conflict would use such an interface, a set-up that has already been investigated in an earlier experiment for purely horizontal maneuvers [18].

5-8 Discussion

The displays in this study are designed to help a pilot understand the reasoning behind automated decisions, by showing constraints and relationships within the work domain. This work domain information invariably forms the premise on which automation bases its actions, and is therefore also invaluable to pilots when they need to judge the automation's functioning. Although this experiment did not feature automated conflict resolution, and can therefore not be used to evaluate interaction between human and automation, the pilots' resolution decisions do give insight in how the information on the display is used by pilots, and how it affects their SA.

The objective measures presented in this paper show several trends. An effect that is seen in several other studies was that many resolution maneuvers were single-axis. Current results showed, however, that this effect diminished for more difficult scenarios. It can be argued that this was mostly a training issue, as pilot comments during the experiment often indicated that an erroneous initial resolution choice was made. Several pilots also mentioned in the post-experiment questionnaire that more training would be required to be able to understand and properly use the interface. Occasionally, pilots also initiated a multi-axis maneuver 'just to see what happens', which can be considered an artifact of volunteer test subjects in an experiment. In some cases pilots indicated that they made a multi-axis maneuver to improve efficiency. Path deviation measurements, however, showed that this was never the result.

Although difficult scenarios resulted in more multi-axis maneuvers, this effect did depend on display configuration, where multi-axis maneuvers were made more often with the baseline display. Since many of the multi-axis maneuvers were corrections of an erroneous initial single-axis maneuver, this can be an indication that, with the same (limited) level of training, pilots performed better with the augmented display. They made fewer errors, indicating a beneficial effect on traffic awareness of the augmented display.

As hypothesized (H1-2), phase of flight had a significant effect on resolution choice, regardless of scenario difficulty. This preference can be seen as the result of a procedural constraint (i.e., phase of flight) that is however not directly visible on the display. This indicates that pilots can use the presented constraints, and apply them to other rules and procedures. This is classified by Rasmussen as Rule Based Behavior [32]. Ideally, the interface should support pilots at all levels of cognitive behavior, while not forcing them to control at a higher level than necessary [33].

A persistent result found in this experiment, and earlier experiments with a constraint-based display, is that after reaching a conflict-free state, the majority of the subjects returned to their original track in several small steps, following the edge of the constraint area as closely as possible [18, 29]. This behavior can be attributed to showing precise constraints: when maneuver limits are visualized with high precision, human operators will use

that precision to maximize their efficiency. As a result, the majority of the CPA's stay within 110% of the separation margin (augmented 88%, baseline 48%). This 'hunting' behavior, however, also gives rise to judgment errors, and consequently also losses of separation, which occurred 8 times in the experiment. Although the incursions were very small, this is still an undesired side effect of showing precise constraints. Another possible influential factor in this behavior relates to the perceived severity of a violation. A minimal incursion of a separation limit will be judged differently than for example a violation of the minimum airspeed limit. As a result, pilots may permit the occasional (minor) loss of separation, in order to increase efficiency.

The experiments in this study compared two displays, where the main difference between the two was the accuracy of the presented constraints. Where the augmented display presented precise constraints, the baseline display was more conservative. Because the color of a forbidden area communicates the state of conflict (white areas indicate non-conflicting intruders), subjects were able to find resolutions with the baseline display that were still inside of the presented constraints. Several subjects who started the experiment with the baseline display, sometimes applied this same strategy with the augmented display (searching for solutions within a constraint area). With the RFAs, however, this is never a valid option. This type of mode or strategy confusion can become an issue in comparative experiments, where levels of an independent factor lie very close to each other. This effect should be taken into account for such experiments.

The SA assessment revealed that display becomes a significant factor in complex scenarios, for high-level SA probes. These scenarios consist of off-track and off-level geometry, which reveal the difference between the basic triangular forbidden areas and the RFAs. In these situations, even though the baseline display and the augmented display present the same *type* of information (horizontal and vertical maneuvering constraints), they differ in the *accuracy* of that information. Although the extra information that is hidden in the baseline display can still be derived to some extent, this requires additional cognitive work. The fact that response time was not influenced by display type (even though pilots indicated in the post-experiment questionnaire that the RFAs allowed them to quicker assess the consequences of resolution maneuvers), however, indicates that subjects used the presented

constraints on both displays in the same way. The differences in SA scores therefore mostly relate to the accuracy of the constraints.

Although the augmented display scores consistently higher than the baseline display, SA scores still drop with higher SA levels. This is in line with a notion put forward by Vicente, who states that ecological interfaces were never intended to be used by untrained operators [34]. Proper training is therefore an important issue for these concepts and their evaluation. The fact that many subjects assigned the highest usefulness ratings to the more classical TCAS symbols can therefore also indicate that they do not fully understand what information is required to perform the new task of conflict resolution, and what this means for the requirements on the visualization of this information. Nevertheless, resolution performance was high, even with insufficiently trained subjects. Because these kinds of displays make several complex relationships directly perceivable, they relieve pilots from cognitive work. This transforms tasks that ordinarily require SA at the projection level to simple tasks of perception and observation, allowing pilots to perform well, despite insufficient training.

In comparison with the baseline display, the augmented display reveals more properties and relations that are inherent to the work-domain. In the search for a display that properly supports pilots' SA, the trade-off will always be between showing more information on the one hand, and maintaining a clear, understandable and uncluttered display on the other hand. The results in this study show that performance and SA benefit from the improved accuracy of the constraint visualizations, and that pilot behavior is consistent with previous evaluations of constraint-based displays. Together with the preference ratings from the post-experiment questionnaire, these results also give no indication that this increased accuracy forms a problem in terms of display clutter. Nevertheless, future design iterations should continue to focus on the trade-off between information density and clutter.

5-9 Conclusions

An experiment was conducted to evaluate a concept for a constraint-based co-planar self-separation display. The display shows performance and traffic constraints on maneuvering, as well as interactions between the two planar

projections. A comparison was made between this concept and a baseline display that did not show these interactions, in an active conflict resolution experiment, and a passive SA assessment.

Results showed that although pilots performed well with either display, performance was consistently better with the augmented display: resolutions were more efficient, pilots made fewer errors in their initial resolutions, and situation awareness scores were higher. Similar to previous studies, a preference for single-axis maneuvers was found, although this effect was smaller for difficult scenarios.

A persistent effect observed with this and other constraint-based displays is that pilots use the precision of the constraint visualization to optimize their efficiency. This type of behavior sometimes leads to over-optimization, and can cause minor losses of separation.

5-10 Bibliography

- [1] **J. Ellerbroek, K. C. R. Brantegem, M. M. van Paassen, and M. Mulder.** Design of a Co-Planar Airborne Separation Display. *IEEE Transactions on Human-Machine Systems*, 43(3), 277–289, 2013. doi: 10.1109/TSMC.2013.2242888.
- [2] **S. B. J. van Dam, M. Mulder, and M. M. van Paassen.** Ecological Interface Design of a Tactical Airborne Separation Assistance Tool. *IEEE Transactions on Systems, Man, and Cybernetics, part A: Systems and Humans*, 38(6), 1221–1233, 2008.
- [3] **F. M. Heylen, S. B. J. van Dam, M. Mulder, and M. M. van Paassen.** Design and Evaluation of a Vertical Separation Assistance Display. In: *AIAA Guidance, Navigation, and Control Conference and Exhibit*. Honolulu (HI), 2008.
- [4] **Radio Technical Commission for Aeronautics.** Airborne Conflict Management: Application Description V2.5. Tech. Rep. RTCA SC-186, Federal Aviation Authorities, 2002.
- [5] **SESAR Consortium.** SESAR Definition Phase D3: The ATM Target Concept. Tech. Rep. DLM-0612-001-02-00, Eurocontrol, 2007.

- [6] **D. A. Norman.** The “Problem” of Automation: Inappropriate Feedback and Interaction, not “Over-Automation”. *Philosophical Transactions of the Royal Society of London*, 327(1241), 585–593, 1990. ISSN 0962-8436. doi: 10.1098/rstb.1990.0101.
- [7] **N. B. Sarter** and **D. D. Woods.** Pilot Interaction With Cockpit Automation: Operational Experiences With the Flight Management System. *The International Journal of Aviation Psychology*, 2(4), 303–321, 1992. doi:10.1207/s15327108ijap0204_5.
- [8] **G. Lintern, T. Waite,** and **D. A. Talleur.** Functional Interface Design for the Modern Aircraft Cockpit. *The International Journal of Aviation Psychology*, 9(3), 225–240, 1999.
- [9] **A. M. Bisantz** and **A. R. Pritchett.** Measuring the Fit Between Human Judgments and Automated Alerting Algorithms: A Study of Collision Detection. *Human Factors*, 45(2), 266–280, 2003.
- [10] **S. W. A. Dekker.** On the Other Side of Promise: What Should We Automate Today? In: **D. Harris**, ed., *Human Factors for Civil Flight Deck Design*, pp. 141–155. Ashgate Pub Ltd, 2004.
- [11] **T. Inagaki.** Design of Human–Machine Interactions in Light of Domain-Dependence of Human-Centered Automation. *Cognition, Technology & Work*, 8(3), 161–167, 2006.
- [12] **A. Q. V. Dao, S. Brandt, V. Battiste, K. P. Vu, T. Strybel,** and **W. W. Johnson.** The Impact of Automation Assisted Aircraft Separation on Situation Awareness. In: *Human Interface and the Management of Information. Information and Interaction*, pp. 738–747. Springer, 2009.
- [13] **C. Meckiff** and **P. Gibbs.** PHARE Highly Interactive Problem Solver. Tech. Rep. 273/94, Eurocontrol, 1994.
- [14] **R. Azuma, H. Neely, M. Daily,** and **M. Correa.** Visualization of Conflicts and Resolutions in a “Free Flight” Scenario. In: *Proceedings of IEEE Visualization*, pp. 433–436, 1999.
- [15] **J. M. Hoekstra, R. N. H. W. van Gent,** and **R. C. J. Ruigrok.** Designing for Safety: the Free Flight Air Traffic Management Concept. *Reliability Engineering and System Safety*, 75, 215–232, 2002.

- [16] **R. Canton, M. Refai, W. W. Johnson, and V. Battiste.** Development and Integration of Human-Centered Conflict Detection and Resolution Tools for Airborne Autonomous Operations. In: *International Symposium on Aviation Psychology*, pp. 115–120, 2005.
- [17] **J. Ellerbroek, M. Visser, S. B. J. van Dam, M. Mulder, and M. M. van Paassen.** Design of an Airborne Three-Dimensional Separation Assistance Display. *IEEE Transactions on Systems, Man, and Cybernetics, part A: Systems and Humans*, 41(6), 863–875, 2011. ISSN 1083-4427. doi: 10.1109/TSMCA.2010.2093890.
- [18] **J. Ellerbroek, M. M. van Paassen, and M. Mulder.** Evaluation of a Separation Assistance Display in a Multi-Actor Experiment. *IEEE Transactions on Human-Machine Systems*, submitted, 2011.
- [19] **Radio Technical Commission for Aeronautics.** Minimal Operational Performance Standards for Traffic Alert and Collision Avoidance System 2 (TCAS2) Airborne Equipment. Tech. rep., Federal Aviation Authorities, 2002.
- [20] **J. Uhlarik and D. A. Comerford.** A Review of Situation Awareness Literature Relevant to Pilot Surveillance Functions. Tech. Rep. DOT/FAA/AM-02/3, Federal Aviation Authorities, 2002.
- [21] **M. R. Endsley.** Toward a Theory of Situation Awareness in Dynamic Systems. *Human Factors*, 37(1), 32–64, 1995.
- [22] **J. M. Flach.** Situation Awareness: Proceed with Caution. *Human Factors*, 37(1), 149–157, 1995.
- [23] **A. M. McGowan and S. P. Banbury.** Evaluating Interruption-Based Techniques using Embedded Measures of Driver Anticipation. In: **S. P. Banbury and S. Tremblay**, eds., *A Cognitive Approach to Situation Awareness: Theory and Application*, pp. 176–192. Ashgate, 2004. ISBN 978-0-7546-4198-8.
- [24] **D. M. Henderson.** *Applied Cartesian Tensors for Aerospace Simulations*. American Institute of Aeronautics and Astronautics, 2006. ISBN 1-56347-793-9.

- [25] **A. Nuic, D. Poles, and V. Mouillet.** BADA: An Advanced Aircraft Performance Model for Present and Future ATM Systems. *International Journal of Adaptive Control and Signal Processing*, 24(10), 850–866, 2010.
- [26] **J. M. Hoekstra.** *Designing for Safety: The Free Flight Air Traffic Management Concept*. Ph.D. thesis, Delft University of Technology, The Netherlands, 2001.
- [27] **C. D. Wickens, J. Helleberg, and X. Xu.** Pilot Maneuver Choice and Workload in Free Flight. *Human Factors and Ergonomics Society Annual Meeting Proceedings*, 44(2), 171–188, 2002. doi: 10.1518/0018720024497943.
- [28] **A. L. Alexander, C. D. Wickens, and D. H. Merwin.** Perspective and Coplanar Cockpit Displays of Traffic Information: Implications for Maneuver Choice, Flight Safety, and Mental Workload. *The International Journal of Aviation Psychology*, 15, 1–21, 2005.
- [29] **C. Borst, M. Mulder, and M. M. van Paassen.** Design and Simulator Evaluation of an Ecological Synthetic Vision Display. *Journal of Guidance, Control and Dynamics*, 33(5), 1577–1591, 2010. doi:10.2514/1.47832.
- [30] **D. P. Hunt.** The Concept of Knowledge and How to Measure It. *Journal of Intellectual Capital*, 4(1), 100–113, 2003.
- [31] **E. R. Tufte.** *Envisioning Information*. Cheshire, CT: Graphics Press, 1990. ISBN 978-0961392116.
- [32] **J. Rasmussen.** Skills, Rules, Knowledge; Signals, Signs, Symbols, and Other Distinctions in Human Performance Models. *IEEE Transactions on Systems, Man, and Cybernetics*, 13, 257–266, 1983.
- [33] **K. J. Vicente and J. Rasmussen.** Ecological Interface Design: Theoretical Foundations. *IEEE Transactions on Systems, Man, and Cybernetics*, 22(4), 589–606, 1992.
- [34] **K. J. Vicente.** *Cognitive Work Analysis Toward Safe, Productive and Healthy Computer-Based Work*. Lawrence Erlbaum Associates Mahwah, NJ, 1999.

Implicit coordination in manual airborne separation

Most of the concepts that preceded this research, as well as the concepts presented in this thesis, are evaluated one way or another, with a number of professional pilot subjects, who are asked to resolve conflicts with simulated traffic. Because conflicts are resolved in a decentralized fashion, however, coordination between actors in each conflict is no longer trivial, especially when manual conflict resolution is concerned. This chapter, therefore, describes an experiment that evaluates the horizontal separation assistance display concept described in Chapter 2, in a set of conflict scenarios where all aircraft in each conflict were controlled by actual pilots.

- Paper title** Evaluation of an Airborne Separation Assistance Display in a Multi-Actor Experiment
- Authors** J. Ellerbroek, M. M. van Paassen, M. Mulder
- Submitted to** IEEE Transactions on Systems, Man and Cybernetics, part A

Abstract: *In the past, several cockpit display concepts have been developed, as aids in the task of airborne self-separation. In several of these concepts, the interface helps the pilot solve the conflict, as opposed to automation providing an explicit resolution. Especially in the absence of automated resolutions, (implicit) interaction between the actors in a conflict becomes an important factor. An experiment was conducted to evaluate an EID-inspired, constraint-based separation assistance display, where all aircraft in each conflict were controlled by pilot subjects. In the experiment, several conflict scenarios have been evaluated, where coordination between pilots could either follow implicitly from the conflict geometry presented by the interface, or require additional, explicit rules (“rules of the air”) to be solved in a coordinated fashion. Similar to previous studies, results showed a considerable preference for single-axis maneuvers. Also, difficulties with implicit coordination occurred for conflict geometries that do not clearly fall into a single category of coordination rules.*

6-1 Introduction

Current ATM concepts for unmanaged airspace propose that aircraft should fly completely predetermined four-dimensional trajectories. Automated systems should provide resolution advisories for traffic (or other) conflicts that may result from uncertainties that arise during the en-route part of flight [1, 2]. In this situation, the pilot’s task will be one of monitoring separation, and selecting and applying resolution advisories, provided by the automation. He should, however, be able to judge the fidelity of a proposed resolution, and be able to intervene in case the automation fails.

Furthermore, because conflicts will be resolved in a decentralized fashion, determining the resolution to a conflict will require coordination between the actors in that conflict. This means that for automated, as well as for manual conflict resolution, predictability of decisions will be essential to guarantee an acceptable level of safety. In situations where there is no opportunity for negotiation, implicit coordination will be required, e.g., by following a predetermined set of rules that dictate which aircraft should maneuver (or both), and how they should maneuver. In worst-case scenarios, pilots will have to manually determine resolution maneuvers, for instance when the automation has failed, or for other reasons that make pilots decide to resolve a conflict manually. This poses limits on the complexity of

the coordination rules. For automated resolution advisories, high rule complexity can make it difficult for pilots to understand the rationale behind resolution advisories, potentially resulting in non-conformance and distrust of the system [3–5].

For adequate situation awareness, proper interaction with automated systems, and for reliable interaction between actors in a conflict, it is therefore necessary for regulation and automation to be transparent and understandable to the human operator [6–9]. The work presented in this paper is part of an ongoing study on the design of a separation assistance interface that can fulfill this role [10–12]. The display concepts developed in this study try to support the pilot, by showing the implications of other traffic for the affordances of ownship locomotion, and how they relate to constraints that result from ownship performance limits.

By going beyond visualizations that relate only to the automation logic, these displays help pilots gain deeper knowledge of the functions and relations within the work domain [13, 14]. These displays should provide support in routine as well as unforeseen situations, where the pilot may have to rely on his own problem-solving skills to resolve a conflict.

The work presented in this paper will focus on the coordination rules that can be used with these display concepts, in multi-actor resolution of traffic conflicts. An experiment was defined to evaluate coordination behavior in worst-case scenarios, in which pilots have to resort to manual determination of conflict resolutions. In the experiment, a constraint-based separation assistance display was available to the pilots to evaluate conflicts in the horizontal plane, and to determine resolution maneuvers. The following section will present the interface, illustrate how it can be used, and provide a set of coordination rules that can be used with the display. The third and fourth sections describe the experiment and the results of this experiment, respectively. The paper concludes with a discussion on the findings, and plans for future work.

6-2 The interface

This study is part of an ongoing research towards the design of a constraint-based separation assistance display, that can present all the relevant properties of the three-dimensional, spatio-temporal separation problem. This study adopts an Ecological Interface Design (EID) inspired approach [15, 16], where work-domain analysis tools such as the Abstraction Hierarchy are used to identify constraints and relations on multiple levels of abstraction [13, 14]. Ideally, a visual representation of these constraints and relations should act as an *external mental model* of the complex traffic system.

Three interface concepts have thus far been proposed. Each of these concepts presents a two-dimensional projection of the traffic constraints, on a relatively traditional cockpit display [10–12]. For the current study, the first of these interface concepts was used, which is restricted to navigation in the horizontal plane: it only visualizes horizontal constraints, and only of obstacles that are on, or close to the own flight level. The remainder of this section gives a brief description of the display, and illustrates how it is used.

6-2-1 Functional presentation of constraints

For travel planning and avoidance in the horizontal plane, several relevant constraints can be identified. These constraints fall broadly into two categories: constraints that are internal to the own aircraft, and constraints that are external to the own aircraft [10, 12]. The internal constraints relevant to separation relate to the various limitations on the performance of the aircraft. These are the maximum turn rates, and the maximum and minimum aircraft operating speeds.

In addition to own aircraft limitations, the maneuver space is further constrained by external factors such as weather, terrain, other traffic, and the boundaries of the unmanaged airspace. For airborne separation, the focus obviously lies on the constraints imposed by other traffic. These traffic constraints are shaped by a minimum horizontal and vertical separation between any two aircraft, that should be adhered to at all times. With common values of 5 nautical miles horizontal, and 1,000 feet vertical separation, this results in a flat, three-dimensional disc around each aircraft, that should remain clear of other traffic [17, 18]. Intrusion of this space is referred to as a

loss of separation. A conflict is defined as a future loss of separation, within a certain observation time span (e.g., 5 minutes).

In cruise flight, pilots control their aircraft by manipulating velocity, track angle, and altitude settings, using the autopilot, or by modifying the planned route in the Flight Management System. A modern glass cockpit supports horizontal trajectory planning through the Navigation Display (ND), which shows a horizontal projection of task-relevant information such as the planned route, terrain, weather, and other traffic. Although this visualization does identify the elements of the airspace that constrain the maneuver options of the aircraft, it does not meaningfully show how they shape the space for operator actions.

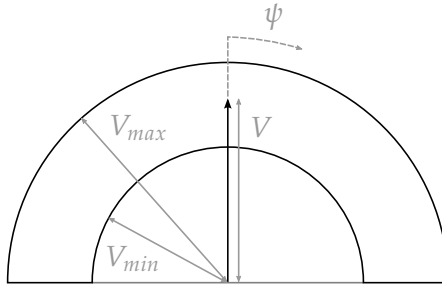


Figure 6.1: The State-Vector Envelope is a vector space that represents combinations of velocity (V) and heading (ψ) that can be obtained by ownship. The minimum (V_{min}) and maximum (V_{max}) obtainable airspeed constraints give it its ring-shaped appearance.

The interface concept employed in this study tries to achieve this by combining the existing spatial representation of airspace elements, with a *velocity action space*, that relates own aircraft velocity and heading to the identified internal and external constraints [10]. This action space is essentially a vector space that contains all possible velocity vectors (i.e., all combinations of velocity and heading). Because of several constraints, only a certain subset of this vector space represents obtainable, conflict-free velocity vectors. For instance, the minimum and maximum obtainable airspeeds reduce the available action space to a ring-shaped area, see Figure 6.1.

Figure 6.2 shows how the traffic separation constraints can be expressed in a velocity space. In this figure, \mathbf{V}_{rel} represents the motion of ownship,

relative to the intruder aircraft:

$$\mathbf{V}_{rel} = \mathbf{V}_{own} - \mathbf{V}_{int} \quad 6.1$$

The figure also shows that when the relative path of ownship intersects with the minimum separation circle, separation will eventually be lost, with a minimum separation of d_{CPA} . It can also be seen that the area between the two lines tangent to the intruder separation circle represents an instantaneous, complete set of relative velocities that result in an eventual loss of separation. In the remainder of this paper, this area is referred to as a *forbidden area*, or *FA*.

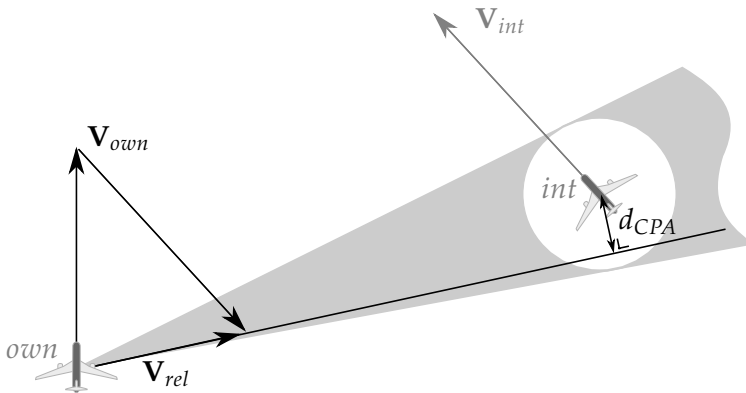


Figure 6.2: Traffic separation constraints can be expressed in a velocity action space, through observation of the relative motion between two aircraft. All relative paths of ownship, that intersect with the separation circle of the intruder aircraft, eventually lead to a loss of separation. Hence, the area between the two lines tangent to the intruder separation circle represents an instantaneous, complete set of conflicting relative velocities. In this figure, *own* is the observed aircraft, and *int* the intruder. \mathbf{V}_{own} is the observed aircraft velocity vector, \mathbf{V}_{int} is the intruder velocity vector, \mathbf{V}_{rel} is the relative velocity vector, and d_{CPA} is the distance at the closest point of approach.

A disadvantage of this relative velocity representation, however, is that it is hard for pilots to relate a velocity constraint zone expressed in *relative space*, to the affordances for control of their own aircraft in *absolute space*. This relation can be made visible by translating the forbidden area and relative velocity vector by the intruder velocity vector. This would be equivalent to adding \mathbf{V}_{int} on both sides of the equal sign in Equation (6.1): the equation

is still valid, but the relation between the ownship velocity vector and the relative velocity forbidden area is made explicit.

The resulting visualization shows all horizontal maneuver options, under the assumption that maneuver dynamics and duration can be neglected. For short-term conflicts this assumption is no longer valid, and maneuver duration needs to be taken into account [19]. The current concept, therefore, compensates for turn duration by calculating the forbidden area legs at time $t_{cur} + t_{turn}$. Here, t_{turn} is the maneuver duration for the heading solution that corresponds to the respective forbidden area leg. A new relative position is extrapolated using the current aircraft velocities, which in turn is used to calculate the corrected position for the forbidden area leg.

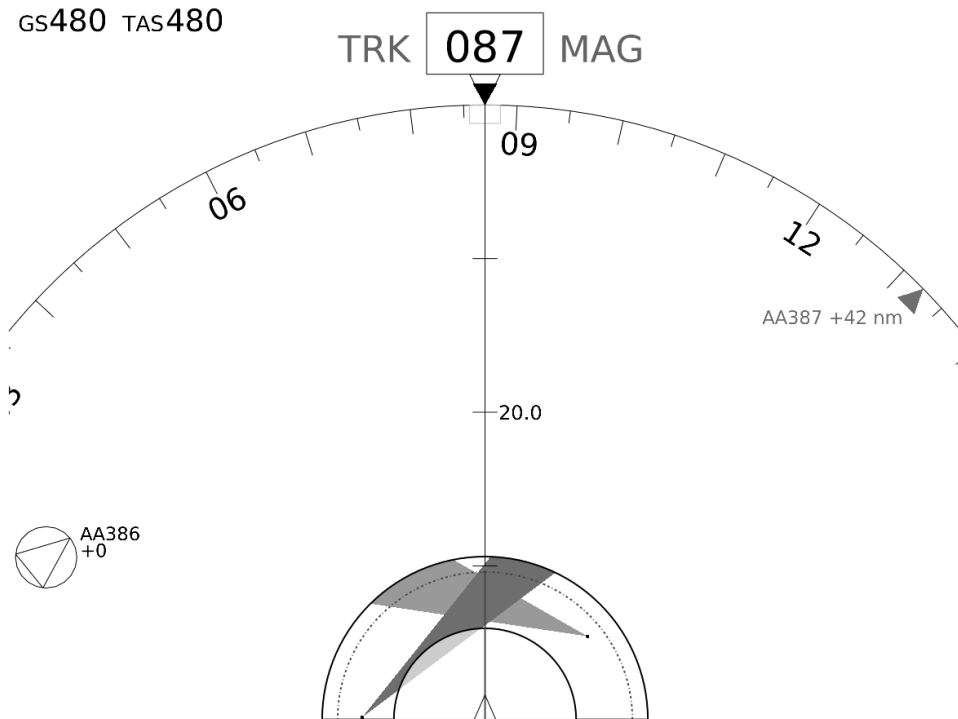


Figure 6.3: The horizontal separation assistance display is based on a classical navigation display, with an added separation assistance overlay. The overlay provides a functional presentation of the affordances for aircraft airspeed and track angle using a horizontal projection of the three-dimensional velocity-vector affordance space.

6-2-2 Using the interface

Figure 6.3 shows how the velocity action-space overlay is presented on a Navigation Display (ND). The action space, bounded by the velocity limits of the aircraft, shows forbidden areas for detected aircraft at, or close to the own flight-level. The forbidden areas work in a cumulative fashion: selecting a 'clear' area solves all detected conflicts, without creating a new conflict.

Several properties of the conflict geometry can be derived from the forbidden area, see Figure 6.4. The width of the forbidden area reveals spatial proximity, and the rate of expansion or contraction of the area is indicative of the closure rate: when ownship and intruder are on a convergent track, the opening angle of the forbidden area will increase with time (Figure 6.4 (a)). The direction of the bisector of the forbidden area is equal to the relative bearing of the corresponding intruder aircraft (Figure 6.4(b)). These properties also provide a strong link with the existing intruder aircraft symbology on the ND.

The location of the tip of each forbidden area provides information about the relevant velocities in a conflict. The location of the tip of the forbidden area corresponds to the intruder velocity vector (Figure 6.4(c)). Its distance from the velocity space center is determined by the intruder true airspeed, and its direction is given by the difference in track angle between ownship and intruder. Also, the relative velocity vector can be derived by imagining a vector between the tip of the forbidden area and the tip of the ownship velocity vector (Figure 6.4(d)).

6-2-3 Implicit coordination for manual control

For implicit coordination between actors in a conflict to function consistently well, a set of rules must be defined that keeps pilots from selecting opposing resolutions. These rules may be based on extensions of the visual flight rules [20], but in most cases, a cooperative resolution can also be derived from the conflict geometry, see Figure 6.5. This type of coordination is related to the conflict solution that results in *minimum path deviation*.

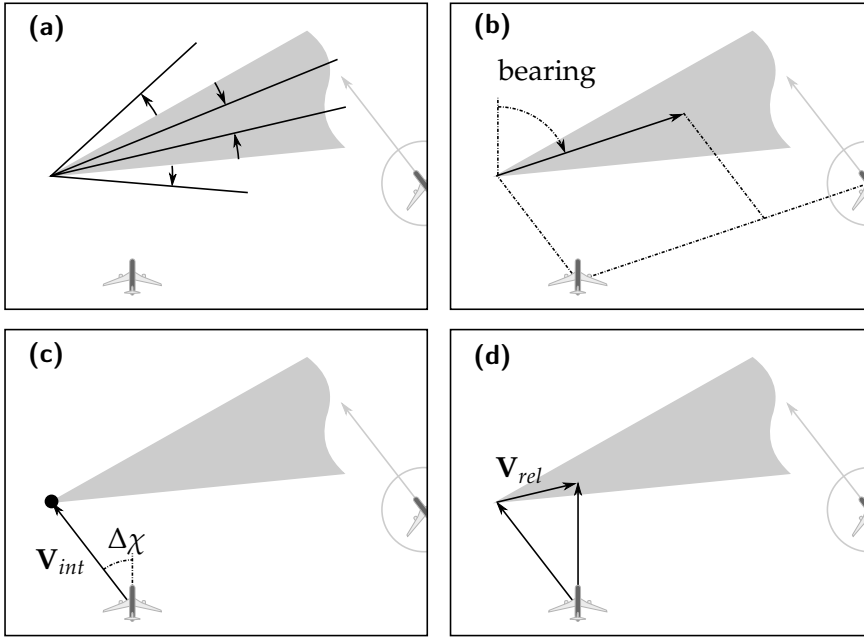


Figure 6.4: Some examples of basic properties of the conflict geometry that can be derived from the forbidden area. **(a):** The width of the forbidden area is directly related to the distance between ownship and the intruder. **(b):** The direction of the bisector of the forbidden area corresponds to the relative bearing of the intruder aircraft. **(c):** The location of the tip of the forbidden area corresponds to the intruder velocity vector. Its distance from the velocity space center is determined by the intruder true airspeed, and its direction is given by the difference in track angle between ownship and intruder. **(d):** The vector that can be constructed between the tip of the forbidden area and the tip of the ownship velocity vector corresponds to the relative velocity vector.

Consider the nominal aircraft position at time t :

$$\mathbf{x}(t) = \mathbf{x}_0 + \int_{t_0}^t \mathbf{V}_{orig}(t) dt \tag{6.2}$$

The path deviation for a maneuver can be derived from the difference between maneuver and original velocities:

$$\Delta x = \int_{t_0}^{t_1} |\mathbf{V}_{sol}(t) - \mathbf{V}_{orig}(t)| dt = \int_{t_0}^{t_1} |\Delta \mathbf{V}_{sol}(t)| dt \tag{6.3}$$

Using Equation (6.3), it can be shown that the path deviation is minimized by minimizing $\Delta \mathbf{V}_{sol}$.

Figure 6.5 shows a traffic conflict with two aircraft, and the derivation of their velocities relative to each other. The circles visualize the horizontal separation margin around each aircraft, and the areas between the triangle lines tangent to each circle show the conflicting values for each relative velocity vector. In this figure, $\Delta\mathbf{V}_{sol}$ is the vector distance between \mathbf{V}_{rel} and the nearest forbidden area leg. The shortest distance is found when $\Delta\mathbf{V}_{sol}$ is taken perpendicular to the forbidden area leg [10, 21]. Figure 6.5 also illustrates that, as long as \mathbf{V}_{rel} is closer to one leg than to the other, a single optimum for $\Delta\mathbf{V}_{sol}$ can be found, and that both aircraft share this optimum. Therefore, implicit coordination is guaranteed when the optimum is selected as a resolution.

An additional set of rules is required for situations where there is no unique geometrically optimal solution. These are situations where the distances between the relative velocity vector and either forbidden area leg are equal: The relative velocity vector lies exactly along the forbidden area bisector, which means that $d_{CPA} = 0$, and the aircraft in conflict are on a collision course. For the experiment, the following ‘rules of the air’ were used for

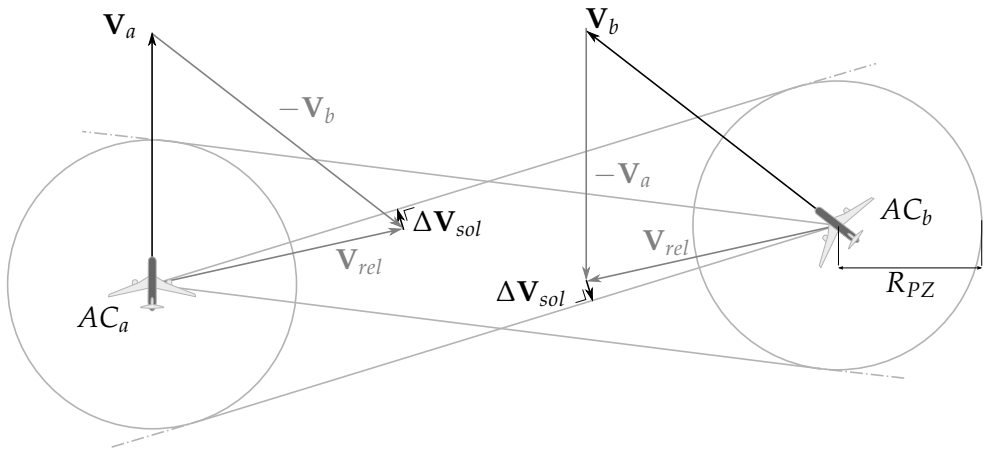


Figure 6.5: Geometrically optimal solutions guarantee implicit coordination, for all conflict geometries with the exception of collision courses. Because of the rotational symmetry of forbidden areas of both aircraft, selecting the optimal solution for aircraft AC_a will always be complementary to the geometrically optimal solution for aircraft AC_b .

these situations: aircraft being overtaken have the right of way and overtaking aircraft must remain clear by altering heading to the right. When two aircraft are approaching each other head on, they must both alter heading to the right.

For conflict geometries with a small, non-zero expected CPA distance, the distances between the relative velocity vector and both forbidden area legs are nearly (but not exactly) equal. This can make the choice between the optimal solution and applying rules of the air ambiguous for pilots. This issue will be addressed in the experiment.

Because the separation assistance display presents the pilot with a velocity action space that is based on the conflict geometry, it can support both coordination strategies. Geometrically optimal solutions can be selected using the display, by changing speed and heading to move the speed vector to the nearest conflict zone leg. Also, selecting a velocity vector to the left, or to the right of a conflict area is analogous to passing the intruder aircraft to the left or the right. Ownship will pass in front of the intruder when the velocity vector crosses the respective forbidden area on the display.

6-3 Experiment

To evaluate the coordination of manual resolution maneuvers between actors in traffic conflicts in unmanaged airspace, a multi-actor traffic separation experiment was performed. To obtain analyzable pilot responses, as well as the interactions between those responses, pairs of pilots were placed in two-aircraft traffic conflict situations, with a loss of separation in the near to short term future. Each session consisted of a continuous presentation of five consecutive conflict scenarios, that needed to be resolved manually, with the aid of a constraint-based separation assistance display. Traffic conflicts were always between two human actors, and were designed using parameters *conflict angle*, *time to first loss of separation*, and *CPA distance*, see Figure 6.6.

6-3-1 Apparatus and aircraft model

The experiment was performed on two physically separated, fixed-base pilot stations. Each setup featured two LCD screens: one showing a Primary

Flight Display, the other showing a Navigation Display with separation assistance overlays. Participants could control display settings and auto-pilot heading and speed modes through physical Electronic Flight Instrument System (EFIS) selector and Mode Control panels.

The aircraft models employed in the simulation were low-order, quasi-linear models of a Boeing 707-300, and an Airbus A330, see Table 6.1. The model coefficients were obtained from EUROCONTROL's BADA aircraft database [22]. The differences between these two aircraft that are relevant to the experiment are the difference in cruise speed, and the difference in speed margins. The difference in cruise speed influences conflict geometry, and the reduced speed margin for the Airbus can limit the resolution possibilities.

The simulation was run in real-time, at an update rate of 100 Hz. The experiment was conducted with zero wind, and no turbulence. Flight level FL250 was used as cruise altitude. Although this is lower than usual in most commercial flights, this flight level was chosen so that airspeed still had a usable margin between stall speed and maximum operating speed.

6-3-2 Experiment design and procedure

The experiment was designed as a within-subjects repeated-measures, where factors *aircraft model* and *conflict geometry* were varied. The *aircraft model* factor was introduced to illustrate the effect of a reduced speed margin on the availability of (optimal) resolution options. Because every aircraft type suffers from reduced speed margins at increasing altitude (stall speed and critical mach number converge with increasing altitude), speed margins are an important factor for conflict resolutions at cruise altitude.

The conflict geometry was designed based on three factors: conflict angle, time to first loss of separation, and the distance between the two aircraft

Table 6.1: Relevant data for the aircraft models in the experiment.

		Boeing 707-300	Airbus A330
TAS _{min}	[kts]	282.4	331.1
TAS _{max}	[kts]	530.1	471.5
TAS _{cruise}	[kts]	485.0	432.0

at the closest point of approach, see Figure 6.6. Here, the conflict angle determines the shape and orientation of the forbidden area, and the magnitude of the closing speed between the two aircraft. Varying conflict angle between scenarios, therefore, is a way to minimize memorizing/learning effects between scenarios. The distance at the CPA, d_{CPA} , determines whether a unique optimal solution to the conflict can be found ($d_{CPA} \neq 0$), or whether coordination based on an additional set of rules is required ($d_{CPA} = 0$). The time to first loss of separation varied between 3 - 5 minutes, which meant a medium to high level of urgency for each conflict scenario.

Each of the conflicts was designed with two participating aircraft. Five levels of conflict angle were combined with four levels of CPA distance, where each conflict angle could be combined with either a zero or a certain non-zero value for d_{CPA} , see Table 6.2. The resulting experiment design is not full factorial, which means that not all effects can be unambiguously attributed to one factor. Ideally an experiment design should be full factorial, but timing constraints made this impossible.

Table 6.2: Geometry parameter combinations.

Conflict angle [°]	0	25	90	180	225
CPA distance [<i>nmi</i>]	0/1	0/2	0/3	0/1	0/2

All experimental conditions consisted of conflict situations between two aircraft, that were both manually controlled, by a pilot subject using the constraint display. This meant that each experiment session required two subjects. These subjects were invited and briefed separately, were kept apart in two part-task simulator rooms, and were not informed that the conflicting aircraft were controlled by a second participating pilot.

After a briefing on the experiment and the functioning of the separation display, subjects performed approximately one hour of training. To avoid learning effects, but still reach a stable level of performance and sufficient understanding of the information presented by the separation assistance interface, separate example scenarios were used for training.

The measurement phase consisted of 10 conditions, presented in a randomized block design. Subjects performed each scenario in both aircraft,

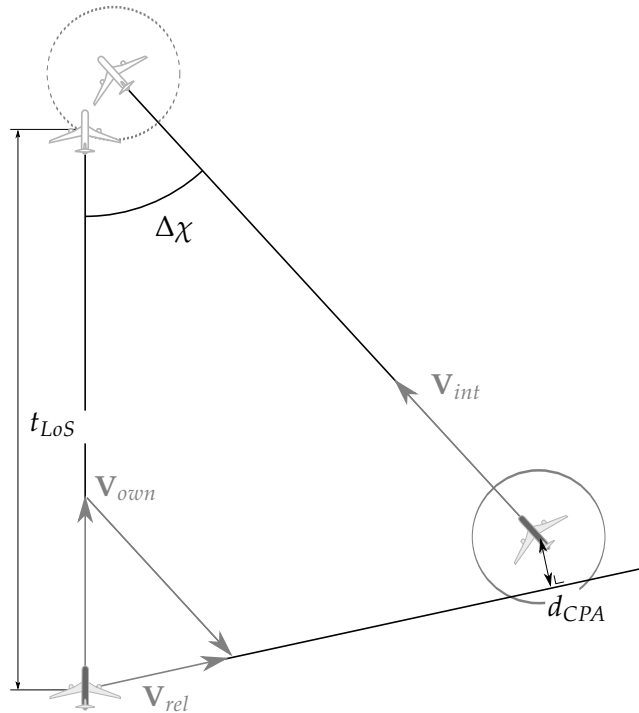


Figure 6.6: The conflict geometry for each scenario is defined by three parameters: conflict angle $\Delta\chi$, time to first loss of separation t_{LoS} , and the distance between the two aircraft at the closest point of approach d_{CPA} . The conflict angle is the angle between intruder and ownship tracks. The time to first loss of separation determines the initial distances in the conflict. The distance at the CPA determines how close the two aircraft will pass each other should neither aircraft maneuver.

resulting in 20 measurement trials per subject. The trials were combined in blocks of five sequential conflict scenarios. This meant that for each set of five scenarios, all participating aircraft were present in the same simulated airspace, during the course of the five trials, and that the simulation did not halt until after all five conflicts were resolved. Aircraft that did not participate in the current conflict were placed at different flight levels, to avoid previous and future conflicts having an effect on the affordance space of the current trial. Each of these blocks lasted approximately 50 minutes.

To ensure that conflicts occurred in the exact geometry that they were designed, aircraft belonging to future conflicts were continuously shifted

Table 6.3: Rules and strategies for conflict resolution.

-
1. Safety has the main priority: Ensure sufficient separation at all times.
 2. Avoid resolutions that result in parallel tracks.
 3. If available, apply the geometrically optimal solution.
 4. When a unique optimal solution is not available, apply rules of the air:
 - 4a. An aircraft being overtaken has right of way and the overtaking aircraft must remain clear by altering heading to the right.
 - 4b. When two aircraft are approaching each other head on they must both alter heading to the right.
 - 4c. Aircraft from the right have the right of way. Remain clear by passing behind that aircraft.
-

from their nominal path, based on the maneuvers of the ownship. This did not lead to a visible effect on the pilot's display. After each conflict, pilots were instructed to return to their initial heading and speed. After each trial, subjects were asked to fill in a short questionnaire concerning their resolution decision.

6-3-3 Subjects and instructions to subjects

Sixteen experienced glass-cockpit pilots participated in sets of two, 15 male, and one female. Experience in terms of flight hours per pilot ranged from 2,000 to 16,700 hours. Subjects were asked to perform an experiment, where they should resolve traffic conflicts in unmanaged airspace. They were informed that the results would be used to evaluate a concept for a separation assistance interface. To avoid "gaming" effects, (e.g., pilots creating, or prolonging conflicts on purpose), pilots were not informed that there was a second participant, and that they were, in fact, flying against a human "opponent". Instead, they were told that during the measurements, intruder aircraft could participate in the resolution of a conflict, by using certain automated logic.

Prior to the experiment, pilots received a short briefing on the geometrical concepts behind the display, how to use the display, and on the experimental setup. An important aspect of this briefing was to instruct the pilot on the rules and strategies for conflict resolution, see Table 6.3. To ensure safe flight, pilots' first and foremost priority was to avoid a loss of

separation at all times. When safety is ensured, pilots could explore their resolution options to optimize for efficiency.

They were instructed to use the cues from the forbidden area to determine an efficient solution. First, the tip of the triangle should be avoided, as solutions close to the tip result in (near) parallel tracks. Second, pilots were instructed to apply the geometrically optimal solution. As was described in the previous section, the geometrically shortest way out of the forbidden area is used as the optimal solution. Other considerations, such as fuel efficiency, were not taken into account, because they are variable and difficult to determine, but also because the geometrical optimum can be used for implicit coordination. When such a geometrical optimum is not available, pilots were instructed to apply rules of the air.

6-3-4 Dependent measures

Dependent measures for this experiment consisted of several objective and several subjective measures. Objective measures were the *solution choice per pilot* in terms of vector change dimensions (heading and speed), and applied tactic (optimal state change vs. rule of the air), and the level of cooperation between pilots. *Safety* was measured in terms of minimum separation, and path deviation and the initial reaction time were used as measures of *performance*. These measures were constructed from recorded time histories of parameters position, heading, and selected speed and heading.

The initial pilot actions per scenario were identified manually by reviewing time traces of each run. The initial selections were used to determine vector change dimensions, minimum separation, reaction times, and the level of cooperation. After each conflict scenario, pilots were asked to select on a form which tactic they applied. These responses were manually compared to the pilot actions that were identified from the time traces. Subjective measures consisted of verbal Situation Awareness (SA) questions during the experiment, and a post-experiment questionnaire. The situation awareness questions relate to easily identifiable information such as relative intruder position and intruder velocity, but some questions also required the subject to use information cues to predict the outcome given the current situation. The subject's certainty of his answer was recorded together with the answers, following Hunt's method of measuring knowledge [23].

6-3-5 Experiment hypotheses

Several studies involving manual (horizontal) conflict resolutions found that pilots prefer single-axis maneuvers, keeping velocity constant [18, 24–26]. It was therefore hypothesized that the majority of the maneuvers would be heading-only. It was also hypothesized that conflict geometries with a small, non-zero expected CPA distance result in the largest amount of opposing resolutions, as the choice between the optimal solution and applying rules of the air is less clear for such conflicts. Conflict geometries where $d_{CPA} = 0$ were assumed to result in more coordination based on the rules of the air, whereas conflict geometries with large expected CPA distances will mostly be solved implicitly, where pilots use the shortest-way-out principle.

In the current display concept, the edge of the state-vector envelope is determined by the own aircraft maximum operating speed. Forbidden areas are only shown within this boundary. It can therefore happen that when a relatively slow aircraft gets into conflict with a faster aircraft, a large part of the resulting forbidden area will be hidden outside the SVE, see Figure 6.7. In these situations, the bearing and relative heading of such an intruder

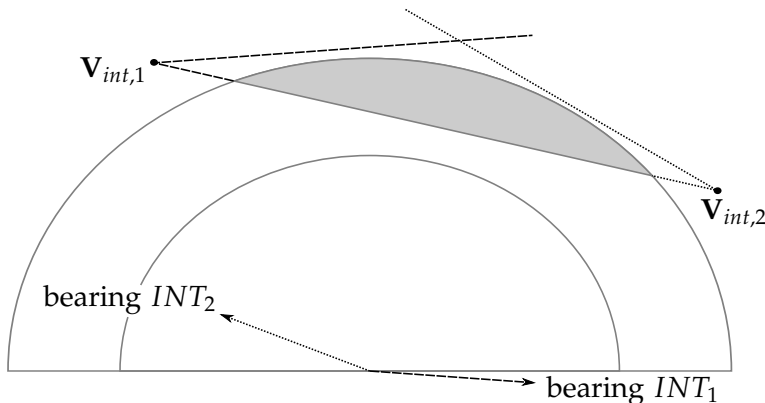


Figure 6.7: Forbidden areas that correspond to intruder aircraft with a velocity greater than the ownship maximum velocity have their tips hidden in the current SVE concept. Because of this, bearing and relative heading of these intruders cannot be unambiguously derived from the forbidden areas alone.

cannot be unambiguously derived from the FA's alone. It was therefore hypothesized that pilots would perform worse in these situations, with fewer coordinated resolutions, and less efficient maneuvers for the slower aircraft.

6-4 Results

Aside from path deviation and minimum separation, all of the measures from the experiment are non-parametric. Solution choice, cooperation level, and applied tactic are categorical data, and the results from the SA questionnaire are ordinal. These data types require statistical methods that make fewer assumptions, but often also require larger sample sizes.

Because of this fact, but also because of the uneven distribution of the outcomes of some of the measures in this experiment, none of the measures provided enough statistical power. No conclusions could therefore be made on the significance of the following results.

Table 6.4: Percentages maneuver choice.

None	17 %	Heading only	69 %
Speed only	4 %	Heading and speed	11 %

6-4-1 Solution type and level of cooperation

The resolution maneuvers in the experiment can be grouped by the flight parameters that were changed to resolve each conflict. For horizontal conflict resolution the available maneuver options are heading and speed changes. Therefore, solution choice is a categorical measure with four levels: *no action*, *heading only*, *speed only*, and *combined heading and speed*. The selection of a maneuver will depend on conflict geometry, aircraft performance limitations, phase of flight, and personal or airline preference.

Table 6.4 shows the maneuver choice average for the entire experiment. As was hypothesized, the majority of the resolution maneuvers was heading only (almost 70 %), which can be attributed to personal or airline preference [18]. Figure 6.8 shows the maneuver choice sorted by conflict angle and aircraft type. Because CPA distance and rules of the air only influence the direction of a maneuver, it can be assumed that differences in solution choice

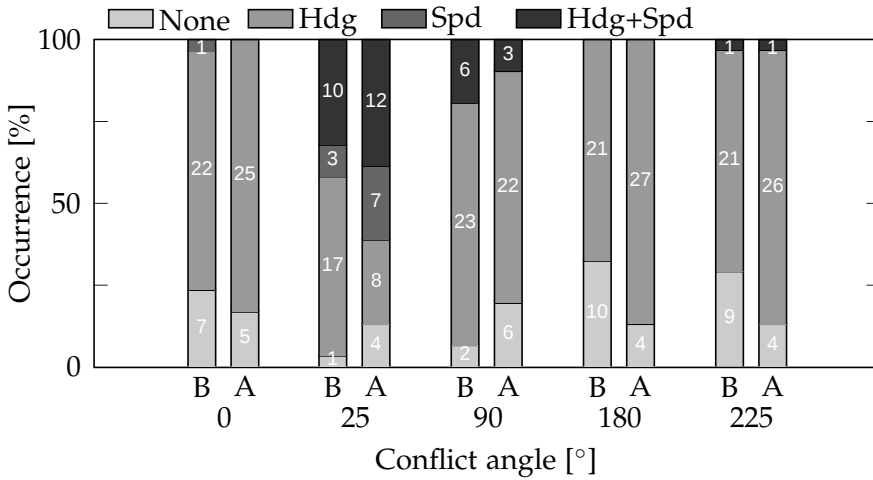


Figure 6.8: Maneuver dimensions sorted by conflict angle and aircraft type (*B* = B707, *A* = A330) along the abscissa. The scale on the ordinate axis gives the occurrence of each solution type in percent of the total per conflict angle / aircraft type pair, the absolute values are indicated inside the bars.

depend mostly on conflict angle. This was also observed in the measured data. For conflict angles 0°, 180°, and 225° this figure shows that (nearly) no speed maneuvers were used. These conflict angles result in (near) head-on or parallel (take-over) courses. In these situations, speed changes have no effect other than speeding or delaying a loss of separation, and only heading changes can be used to resolve such conflicts.

A notable exception to the preference for heading resolutions is found in the 25° conflict angle scenarios, especially for the A330 (61% of the resolutions involved a speed change). In this situation, large heading changes are required to resolve the conflict. Also, for the A330, the max. speed line hides the tip of the intruder triangle, making it difficult to detect intruder intent, and impossible to determine the correct coordination rule. Giving way to the intruder by slowing down might then indeed be considered the safest course of action.

Figure 6.9 shows the rule types applied, as reported by the subjects, sorted by CPA distance. If the pilots had followed the rules in Table 6.3 flawlessly, the first column ($d_{CPA} = 0$) would have been 90 % rules of the air, and 10 % none (the latter percentage is because in one of the scenarios

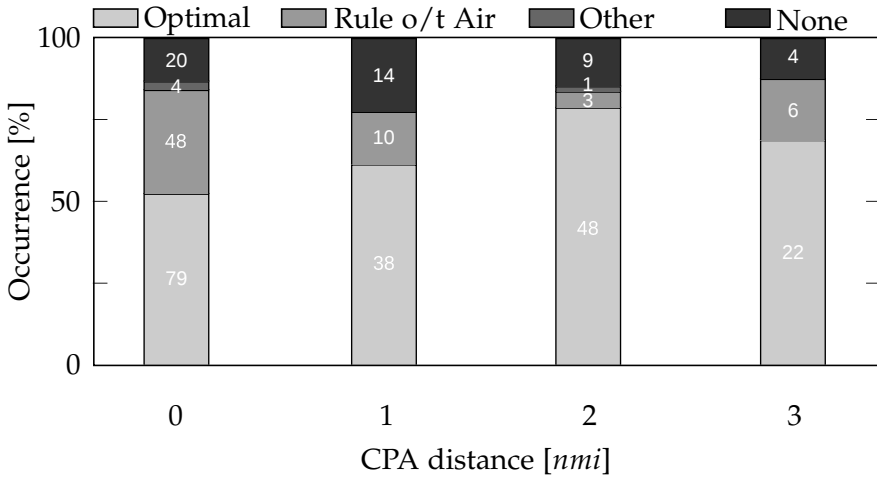


Figure 6.9: Resolution rule sorted by CPA distance along the abscissa. The scale on the ordinate axis gives the occurrence of each solution type in percent of the total per CPA distance, the absolute values are indicated inside the bars.

the applicable rule of the air was a priority rule, forcing one of the aircraft to give way to the other aircraft). The remaining columns would have been 100 % optimal. In the experiment, a more even distribution of rules was reported. Due to the short time in which the experiment was performed, lack of training is probably the main cause of this difference. The results in Figure 6.9, however, do show the expected trend: the rules of the air were applied most often in the conflicts where $d_{CPA} = 0$, and the geometrically optimal solution was applied more often with increasing d_{CPA} .

The level of cooperation between pilots is shown, grouped by CPA distance in Figure 6.10, and averaged in Figure 6.11. Figure 6.11 shows that pilots selected opposing solutions in 16% of the measured trials. Especially in small-scale experiments like these, this can be a matter of insufficient training. It can, however, also be an indication of a weakness of the interface. The most prominent cause for the opposing solutions was that (at least) one of the pilots applied the wrong rule: 93% for scenarios where $d_{CPA} = 0$, and 45% for scenarios where $d_{CPA} \neq 0$, see Figure 6.11. For all values of d_{CPA} , errors where the wrong rule is applied can be an indication that pilots could not reliably retrieve the required information from the display.

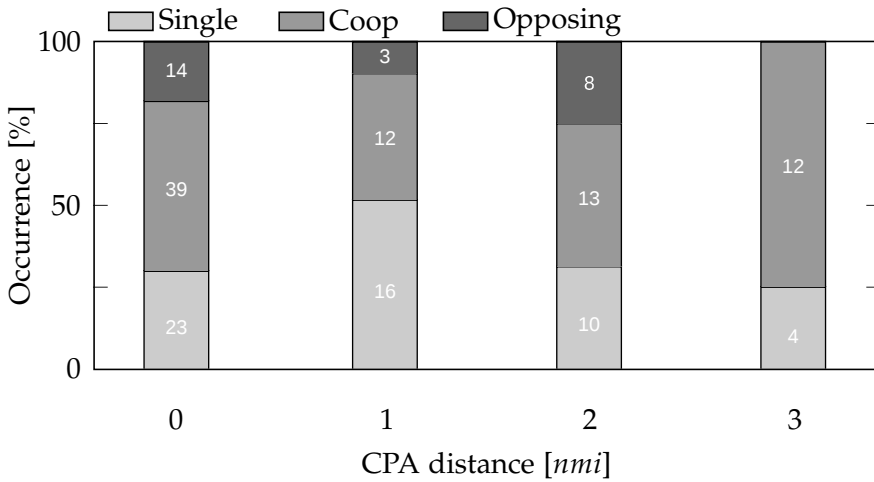


Figure 6.10: Level of cooperation between pilots sorted by conflict CPA distance along the abscissa. The scale on the ordinate axis gives the occurrence in percent of the total per conflict CPA distance, the absolute values are indicated inside the bars.

In other cases, the correct rule was applied, but an error was made while evaluating the rule (7% for $d_{CPA} = 0$, and 55% for $d_{CPA} \neq 0$).

In scenarios where $d_{CPA} = 0$, the direction of the maneuver depends on a previously stored ‘rule of the air’. Therefore, when a wrong maneuver is made in such a scenario, it is because the pilot did not remember the applicable rule correctly. For scenarios where $d_{CPA} \neq 0$, the rule requires the direction of the maneuver to be derived from the display. In such scenarios, an erroneously applied rule can also be an indication that pilots could not retrieve the required information from the display.

50% of the measured trials were solved cooperatively. Figure 6.10 shows that this occurred most frequently for scenarios with the largest conflict CPA distance. In situations where d_{CPA} is large, the velocity vector of ownship is close to the edge of the forbidden area belonging to the conflict. The optimal solution (the shortest way out of the triangle) is clearly visible on the interface, and guarantees implicit coordination when both parties strive for minimum path deviation. The scenarios with the smallest, non-zero CPA distance showed the lowest percentage of cooperation. In these situations,

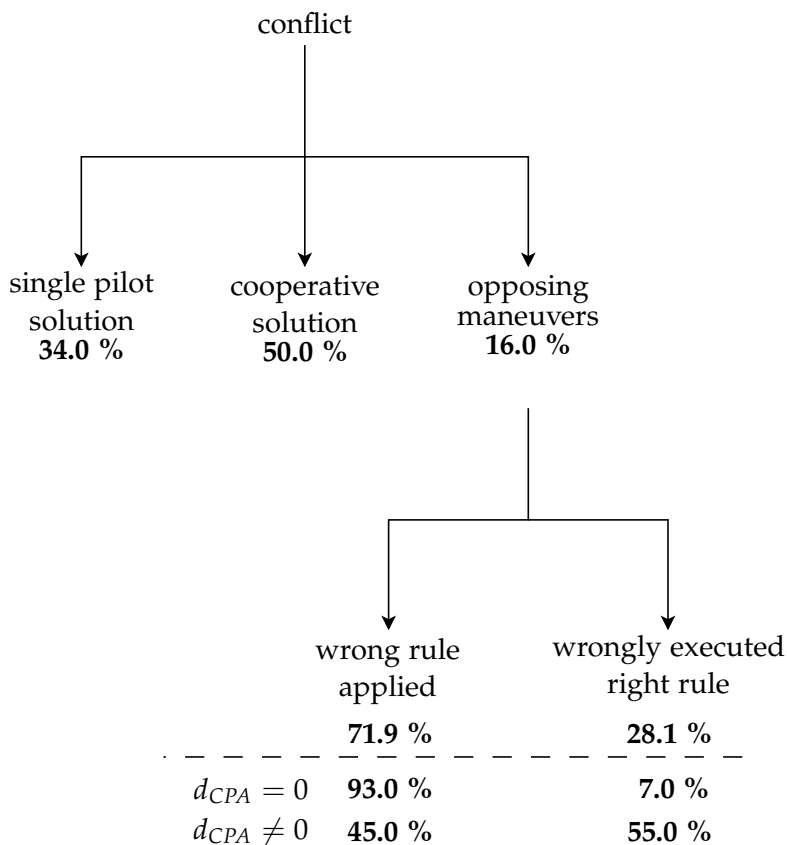


Figure 6.11: Conflict scenario outcome diagram for initial resolution maneuvers. The occurrences per outcome are indicated in percent of the total on that level of the diagram.

the optimal solution is less evident, and the choice between applying the optimal solution or applying the rules of the air becomes less clear.

Table 6.5: Opposing solution frequency per conflict angle.

Conflict angle [°]	0	25	90	180	225
Percentage opposing [%]	20	29	6	10	16

Table 6.5 shows how often opposing solutions were selected, grouped by scenario conflict angle. Each percentage gives the occurrence of opposing

solutions, compared to the total number of runs at the corresponding conflict angle. Although these outcomes are also influenced by the differences in CPA distance, still two notable observations can be made. First, the smallest percentage of opposing resolutions was found for scenarios with conflict angle $\Delta\chi = 90^\circ$, also in the runs where $d_{CPA} = 0$. This can be an indication that for some conflict geometries, such as situations where an intruder is approaching at a right angle, the traffic geometry is more evident from the forbidden area visualization than with other conflict geometries. Second, the largest percentage of opposing resolutions was found for scenarios with conflict angle $\Delta\chi = 25^\circ$, regardless of CPA distance. As was hypothesized, this is the result of the situation illustrated in Figure 6.7. For the pilot controlling the slower Airbus A330, it was impossible to derive conflict geometry from the forbidden area in these conflicts. This made it more difficult to identify the correct maneuver, which resulted in more opposing maneuvers.

6-4-2 Safety

The minimum separation was used as a measure of safety, by comparing the measured value to the defined separation minimum. Figure 6.12 shows a cumulative distribution graph of these minimum separation values. The separation minimum was violated in 3 out of 160 measured trials. In all three cases, this occurred during a premature return to nominal heading and speed, and in all cases, the incursion was minimal (less than 200 meters). A common practice that was observed in this, but also in previous experiments with a constraint-based display [27], was that after resolving a conflict, pilots are inclined to optimize their performance by returning to their nominal state as soon as possible, in small steps, while staying as close as possible to the edge of the forbidden area. In these situations, a judgment error can easily result in a (small) violation of the separation constraint.

6-4-3 Performance

Figure 6.12 also shows that in more than 75% of the conflict scenarios, pilots came within half a nautical mile distance of the protected zone of the other aircraft. In terms of performance, this is a strong indication that pilots use the precise visualization of constraints to optimize the efficiency of their resolution, together with the optimization behavior described above. Reaction

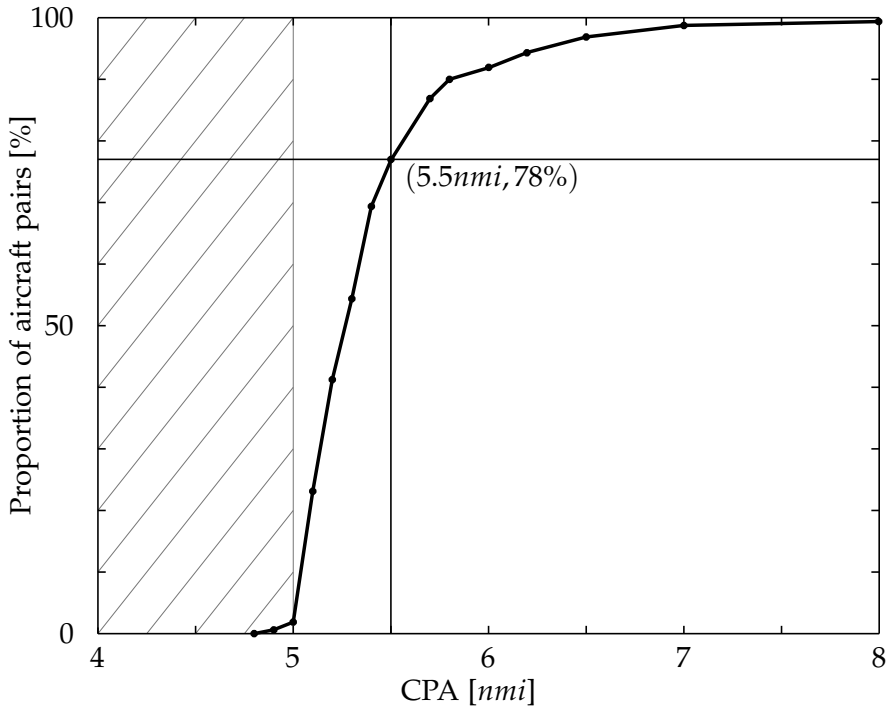


Figure 6.12: Cumulative distribution graph of minimum separation values. Minimum separation occurs at the closest point of approach, which is indicated in nautical miles along the abscissa. The number of aircraft is indicated along the ordinate axis, counted in percent of the total number of aircraft. The hatched area on the left of the graph indicates the values of CPA that violate the minimum separation constraint.

time was also used as a measure of performance, but showed no significant variation across conditions.

Figure 6.13 shows a cumulative distribution graph of the measured path deviation, as a percentage of the theoretically minimal path deviation. When, for example, one pilot solves a conflict, using the exact geometrically optimal solution, his path deviation score would be 100% the theoretically minimal path deviation. However, when two pilots solve a conflict cooperatively, each using the optimal solution, their path deviation score would be 50%, since each of the pilots would provide half of the required vector change.

The data in Figure 6.13 have been divided by solution type, i.e., single-pilot (dark-gray), cooperative (light gray), and opposing solutions (gray).

For the single-pilot solutions it can be seen that only a small percentage was solved close to the optimal solution (14.3%). The majority of the single-pilot solutions (83.3%), however, do stay within 150% of that value. Graphs per single run of the path deviation as a function of time (not shown in this paper) reveal that this efficiency is achieved by multiple corrections of the flight-path vector, after the initial resolution: by closely following the edge of the forbidden area with the own velocity vector, pilots often tried to optimize their efficiency.

The charts for cooperative solutions in Figure 6.13 show that in more than 50% of the cooperative runs, pilots managed to divide the path deviation between them, although not always equally: 40.0% of the maneuvers resulted in a path deviation smaller than half of the single-pilot minimum. In these cases, the second pilot was forced to make an unequally large contribution to the conflict resolution to avoid a loss of separation. Interestingly, also the opposing maneuvers show a high percentage of path deviations smaller than half the single-pilot optimum (41.3%). In these situations, after having identified that an opposing resolution was selected, only one of the pilots makes the necessary adjustment to resolve this problem, allowing the other pilot to immediately revert to his original course.

6-4-4 Situation awareness

As a subjective measure, pilots were given random questions from a set of traffic awareness questions during the experiment. Most questions were answered correctly, with two notable exceptions. When asked whether the other aircraft was slower or faster than the own aircraft, pilots gave more unsure and wrong answers in conflict scenarios where the tip of the conflict zone (which also indicates the tip of the intruder velocity vector) was not visible on the display. Another question that was often answered wrongly was whether or not the other aircraft participated in the resolution maneuver. This cue is visible from the movement of the conflict zone on the display, which can be difficult for pilots to see without extra visual cues. Results from the post-experiment questionnaire also identify this as the most important issue with the display.

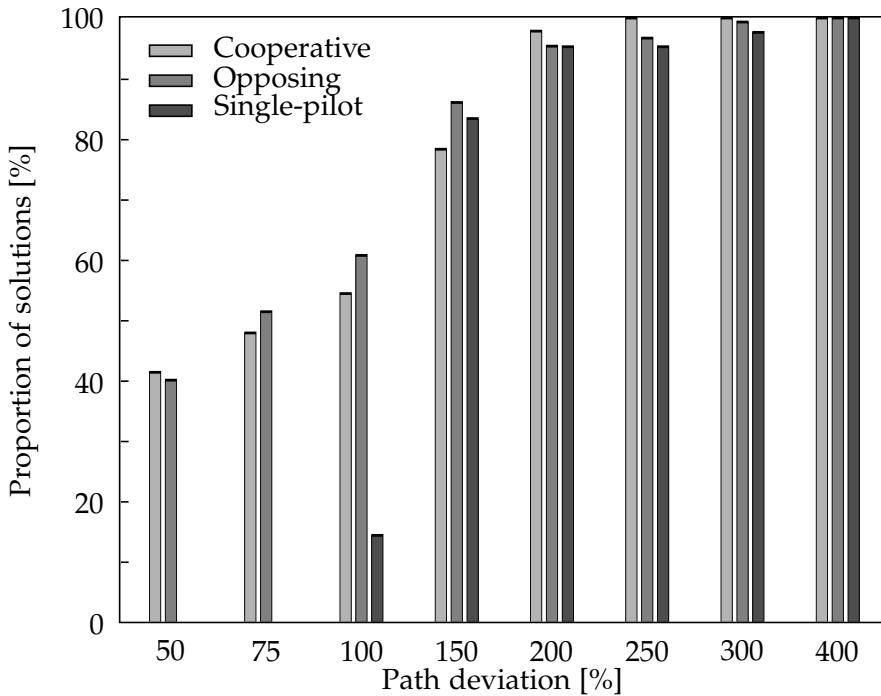


Figure 6.13: Cumulative distribution graph of path deviation, compared to the optimal solution, for single-pilot solutions, cooperative solutions, and opposing solutions. Eight groups along the abscissa indicate the ratio between the measured path deviation, and the theoretical minimum path deviation, in percent. In each group, the length of a bar indicates the amount of solutions that resulted in a path deviation equal or smaller than the path deviation for that group. Values along the ordinate axis indicate the amount of solutions, as a percentage of the total amount of solutions for the three solution types.

6-5 Discussion

The goal of this multi-actor traffic separation experiment was to evaluate coordination between actors when manually resolving traffic conflicts in unmanaged airspace. Although several studies in the past considered multi-actor airborne separation, either in simulations or human-in-the-loop experiments [28–31], they did not consider specific coordination rules, or manual conflict resolution.

In the experiment, pilots made use of a constraint-based separation assistance display, and were provided a set of rules that, when followed correctly,

implicitly lead to coordinated resolution maneuvers. These rules were a combination of applying the optimal solution that could be derived from the interface, and applying “rules of the air”, based on extensions of the visual flight rules [20].

Although this means that most of the results specifically relate to the display and this set of rules, the conclusions that can be drawn from these results should be viewed in a broader perspective. The importance of implicit coordination also applies to conflict avoidance automation, and since the aircrew will always be ultimately responsible for the safety of a maneuver, there will be limits on the complexity of automated resolution logic. This interaction between humans and automation therefore requires a thorough analysis of how these new tasks should be allocated between humans and automation, and how the human actors can interact, and share their decision-making with the automation [6, 7, 32].

In the experiment, sixteen pilots participated, in pairs of two. Each pilot performed all scenarios in both the B707-300 aircraft and the A330. However, because after switching aircraft, it is still the same pair of pilots that provide the data, these two data sets cannot be regarded as independent. Regrettably, even when this dependency is neglected, none of the measures provided enough statistical power. The reason for this is that most of the measurements are either categorical or ordinal, with uneven expectations for the outcome per category. These data types require statistical methods that make fewer assumptions, and require larger sample sizes. Sufficient statistical power for these data, therefore, would require a sample size closer to 50 groups, or 100 pilots, possibly even more. The hypotheses that were made in this study can therefore not be proved or refuted with significant results, but will be compared to the results in a qualitative manner.

Recorded time histories of parameters position, heading, and selected speed and heading were used to construct measures of solution choice and the level of cooperation between pilots. Averages of selected speed and heading showed that, similar to earlier experiments, pilots preferred keeping velocity constant. Table 6.4 shows that 69 % of the resolution maneuvers only involved a heading change. This supports the hypothesis that the majority of maneuvers would be heading-only. Figure 6.11 shows that 50 % of

the scenarios were solved cooperatively. Figure 6.10 shows that cooperative solutions occurred most often for scenarios with the largest CPA distance.

It was also hypothesized that conflict geometries with small non-zero CPA would result in the largest amount of opposing resolutions, because the choice between the optimal solution and applying rules of the air is less clear for such conflicts. This ambiguity is also a function of the distance between ownship and intruder: with increasing distance, the forbidden area becomes narrower, up to the point that display resolution makes it impossible to see how the own velocity vector is positioned within the forbidden area. Because of the greater distance, however, the urgency of the conflict will be low, and the odds of a simultaneous maneuver will be small.

The largest percentage of opposing solutions was observed for scenarios where $d_{CPA} = 2\text{nm}$. This is already a significant CPA distance, which should benefit implicit coordination by selection of the geometrically optimal solution. This was, however, also the scenario with conflict angle $\Delta\chi = 25^\circ$, which is a more likely reason for the large amount of opposing resolutions. Because the experiment was not designed full factorial, it was not possible to separate these effects. The hypothesis that small-CPA conflicts would result in the largest amount of opposing resolutions could therefore not be unambiguously concluded from the results.

The scenarios with conflict angle $\Delta\chi = 25^\circ$ was added to illustrate the effect of a forbidden area that is for the most part hidden (including the tip of the triangle) by the edges of the state-vector envelope. This can occur when an intruder aircraft approaches on a near-parallel course (small $\Delta\chi$), and is flying faster than the maximum operating speed of ownship. This causes a large part of the forbidden area to be hidden by the edges of the state-vector envelope, and the bearing and relative heading of such an intruder cannot be unambiguously inferred from the forbidden areas alone. As was hypothesized, these scenarios resulted in the largest amount of opposing resolutions.

Also, a large number of solutions that were made in the slower aircraft (the A330) were more inefficient, with the most speed changes. Figure 6.7 illustrates that when an aircraft gets into conflict with an aircraft that is flying faster than the own maximum operating speed, it can happen that

much of the geometry of the forbidden area is hidden outside the state-vector envelope, which can result in inefficient resolutions. Results from the situation awareness questions also show that pilots had the most difficulty judging intruder airspeed in these scenarios. This was the only prominent effect that could be discerned from the *aircraft model* factor.

For scenarios with zero CPA distance it was hypothesized that most of the maneuvers would be based on the rules of the air, while scenarios with large CPAs would result in a high number of maneuvers based on the geometrically optimal solution. Figure 6.9 shows that for the experiment, this distinction is not that clear-cut. A large percentage of the resolutions was reported as a geometrically optimal solution, regardless of CPA distance. Although the rules of the air were applied most often in the zero-CPA scenarios, the differences are too small to either prove or disprove the corresponding hypotheses.

Minimum separation was considered as a measure of safety. Similar to earlier experiments with a constraint-based display, results from the experiment show that after reaching a conflict-free state, the majority of the subjects returned to their original track in several small steps, following the edge of the forbidden area as closely as possible. This behavior can be attributed to showing precise constraints: when maneuver limits are visualized with high precision, human operators will use that precision to maximize their efficiency. As a result, 78 % of the CPA's stay within 110 % of the separation margin. This 'hunting' behavior, however, also gives rise to coordination problems, and consequently also losses of separation, which occurred 3 times in the experiment. Although the incursions were small (less than 200 meters), this is still an unwanted side effect of showing precise constraints.

In addition, performance was measured in terms of path deviation. Figure 6.13 shows that more than 80 % of the resolution maneuvers were performed with a path deviation smaller or equal to 150 % of the path deviation that could be obtained by applying the optimal solution. As most of the maneuvers were heading-only, this can be regarded as an indication of the path deviation penalty of a heading-only maneuver, compared to the smallest state change maneuver. Note, however, that this difference is greatly

influenced by the geometry of the conflict. Figure 6.13 also shows that cooperative solutions divide path deviation, but not always evenly. Also, many of the opposing maneuvers end up being solved by only one of the pilots.

The in-flight situation awareness queries, and the post-experiment questionnaire revealed the most important issues with the display in its current form. Although subjects answered most SA questions almost flawlessly for the majority of the scenarios, certain conflict geometries proved more difficult. As was hypothesized, scenarios where a large part of the forbidden area is hidden by the edges of the state-vector envelope make it difficult or even impossible to extract relevant information on conflict geometry from the forbidden area. This was also clearly visible in the results from SA questions that related to intruder speed, location, and maneuvering. Together with the SA queries, results from the post-experiment questionnaire identify poor visibility of intruder maneuvering as the most important issue with the display. Information on the maneuvering of the intruder is not instantly visible on the display: it can only be inferred from the translation of the forbidden area on the display, which can be difficult to discern. In addition, the target state of the intruder is not known before the end of the maneuver.

6-6 Future work and recommendations

In the experiment, sixteen pilots participated, in pairs of two. For practical reasons, this is already a considerable amount of subjects. However, because of the nature of most of the measurements, sufficient statistical power in the data requires a sample size closer to 50 groups, or 100 pilots, possibly even more. Because an experiment of this magnitude is difficult to realize, a follow-up study has been initialized that employs pilot decision models in a Monte-Carlo simulation, in an effort to identify the influence of behavioral characteristics on separation coordination and safety.

Future work on the display will focus on dealing with shortcomings of the display that were identified in the current study, such as guaranteed visibility of all the cues of the forbidden areas, and the possibilities for visualization of intruder maneuvering during resolutions. An issue that could be addressed by a future experiment is a study of coordination rules in case of multi (more than two) aircraft conflicts.

6-7 Conclusions

A multi-actor aircraft separation experiment was performed, to evaluate the coordination of manual resolution maneuvers between actors in traffic conflicts in unmanaged airspace. Similar to previous studies, results from the experiment showed a preference for single-axis, heading-only maneuvers. Difficulties with implicit coordination between actors in a conflict occurred for conflict geometries that do not clearly fall into a single category of coordination rules.

Two safety issues were identified for the separation assistance display. Subjective measurement results identify poor visibility of intruder maneuvering as the most important shortcoming of the display. Second, because constraints are visualized precisely, pilots are inclined to use this precision to optimize their efficiency, which sometimes leads to over-optimization. This type of behavior is characteristic to constraint-based displays. Of the 160 recorded conflicts, three resulted in a minor loss of separation. In each of these situations, the conflict was solved correctly, but an incursion occurred during the return to the nominal track, as a result of over-optimization.

This study also showed one of the limits of a piloted simulator study. When trying to evaluate decision behavior and safety aspects of airborne separation, sample sizes are required that go far beyond practical limits for these kind of experiments.

6-8 Bibliography

- [1] **Radio Technical Commission for Aeronautics.** Airborne Conflict Management: Application Description V2.5. Tech. Rep. RTCA SC-186, Federal Aviation Authorities, 2002.
- [2] **SESAR Consortium.** SESAR Definition Phase D3: The ATM Target Concept. Tech. Rep. DLM-0612-001-02-00, Eurocontrol, 2007.
- [3] **R. Schild and J. K. Kuchar.** Operational Efficiency of Maneuver Coordination Rules for Airborne Separation Assurance System. In: *3rd USA/Europe Air Traffic Management R&D Seminar Napoli*. Naples, Italy, 2000.

-
- [4] **J. D. Lee** and **N. Moray**. Trust, Control Strategies and Allocation of Function in Human-Machine Systems. *Ergonomics*, 31(10), 1243–1270, 1992.
- [5] **R. Parasuraman** and **V. Riley**. Humans and Automation: Use, Misuse, Disuse, Abuse. *Human Factors*, 39(2), 230–253, 1997.
- [6] **D. A. Norman**. The “Problem” of Automation: Inappropriate Feedback and Interaction, not “Over-Automation”. *Philosophical Transactions of the Royal Society of London*, 327(1241), 585–593, 1990. ISSN 0962-8436. doi: 10.1098/rstb.1990.0101.
- [7] **N. B. Sarter** and **D. D. Woods**. Pilot Interaction With Cockpit Automation: Operational Experiences With the Flight Management System. *The International Journal of Aviation Psychology*, 2(4), 303–321, 1992. doi:10.1207/s15327108ijap0204_5.
- [8] **G. Lintern**, **T. Waite**, and **D. A. Talleur**. Functional Interface Design for the Modern Aircraft Cockpit. *The International Journal of Aviation Psychology*, 9(3), 225–240, 1999.
- [9] **A. Q. V. Dao**, **S. Brandt**, **V. Battiste**, **K. P. Vu**, **T. Strybel**, and **W. W. Johnson**. The Impact of Automation Assisted Aircraft Separation on Situation Awareness. In: *Human Interface and the Management of Information. Information and Interaction*, pp. 738–747. Springer, 2009.
- [10] **S. B. J. van Dam**, **M. Mulder**, and **M. M. van Paassen**. Ecological Interface Design of a Tactical Airborne Separation Assistance Tool. *IEEE Transactions on Systems, Man, and Cybernetics, part A: Systems and Humans*, 38(6), 1221–1233, 2008.
- [11] **F. M. Heylen**, **S. B. J. van Dam**, **M. Mulder**, and **M. M. van Paassen**. Design and Evaluation of a Vertical Separation Assistance Display. In: *AIAA Guidance, Navigation, and Control Conference and Exhibit*. Honolulu (HI), 2008.
- [12] **J. Ellerbroek**, **M. Visser**, **S. B. J. van Dam**, **M. Mulder**, and **M. M. van Paassen**. Design of an Airborne Three-Dimensional Separation Assistance Display. *IEEE Transactions on Systems, Man, and Cybernetics*,

- part A: *Systems and Humans*, 41(6), 863–875, 2011. ISSN 1083-4427. doi: 10.1109/TSMCA.2010.2093890.
- [13] **K. J. Vicente** and **J. Rasmussen**. Ecological Interface Design: Theoretical Foundations. *IEEE Transactions on Systems, Man, and Cybernetics*, 22(4), 589–606, 1992.
- [14] **C. M. Burns** and **J. R. Hajdukiewicz**. *Ecological Interface Design*. CRC Press LLC, FL: Boca Raton, 2004. ISBN 0415283744.
- [15] **K. J. Vicente**. Ecological Interface Design: Progress and Challenges. *Human Factors*, 44, 62–78, 2002.
- [16] **G. A. Jamieson**. Ecological Interface Design for Petrochemical Process Control: An Empirical Assessment. *IEEE Transactions on Systems, Man, and Cybernetics, part A: Systems and Humans*, 37(6), 906–920, 2007. doi: 10.1109/TSMCA.2007.897583.
- [17] **Radio Technical Commission for Aeronautics**. Final Report of the RTCA Board of Directors' Select Committee on Free Flight. Tech. rep., RTCA, 1995.
- [18] **J. M. Hoekstra**. *Designing for Safety: The Free Flight Air Traffic Management Concept*. Ph.D. thesis, Delft University of Technology, The Netherlands, 2001.
- [19] **R. A. Paielli**. Modeling Maneuver Dynamics in Air Traffic Conflict Resolution. *Journal of Guidance Control and Dynamics*, 26(3), 407–415, 2003.
- [20] **International Civil Aviation Organization (ICAO)**. Rules of the Air and Air Traffic Services (Doc 4444). Tech. rep., 1996.
- [21] **K. D. Bilimoria**. A Geometric Optimization Approach to Aircraft Conflict Resolution. In: *AIAA Guidance, Navigation, and Control Conference and Exhibit*. Denver (CO), 2000.
- [22] **A. Nuic**, **D. Poles**, and **V. Mouillet**. BADA: An Advanced Aircraft Performance Model for Present and Future ATM Systems. *International Journal of Adaptive Control and Signal Processing*, 24(10), 850–866, 2010.

- [23] **D. P. Hunt.** The Concept of Knowledge and How to Measure It. *Journal of Intellectual Capital*, 4(1), 100–113, 2003.
- [24] **C. D. Wickens, J. Helleberg, and X. Xu.** Pilot Maneuver Choice and Workload in Free Flight. *Human Factors and Ergonomics Society Annual Meeting Proceedings*, 44(2), 171–188, 2002. doi: 10.1518/0018720024497943.
- [25] **A. L. Alexander, C. D. Wickens, and D. H. Merwin.** Perspective and Coplanar Cockpit Displays of Traffic Information: Implications for Maneuver Choice, Flight Safety, and Mental Workload. *The International Journal of Aviation Psychology*, 15, 1–21, 2005.
- [26] **C. L. A. Steens, S. B. J. van Dam, M. M. van Paassen, and M. Mulder.** Comparing Situation Awareness for Two Airborne Separation Assistance Interfaces. In: *AIAA Guidance, Navigation and Control Conference and Exhibit*. Honolulu (HI), 2008.
- [27] **C. Borst, M. Mulder, and M. M. van Paassen.** Design and Simulator Evaluation of an Ecological Synthetic Vision Display. *Journal of Guidance, Control and Dynamics*, 33(5), 1577–1591, 2010. doi:10.2514/1.47832.
- [28] **A. Bicchi and L. Pallottino.** On Optimal Cooperative Conflict Resolution for Air Traffic Management Systems. *IEEE Transactions on Intelligent Transportation Systems*, 1(4), 221–231, 2000.
- [29] **R. Ghosh and C. J. Tomlin.** Maneuver Design for Multiple Aircraft Conflict Resolution. In: *Proceedings of the American Control Conference*, pp. 672–676. Chicago (IL), 2000.
- [30] **F. van Westrenen and J. Groeneweg.** Co-operative Conflict Resolution: An Experimental Validation Of Aircraft Self-Separation in a Classroom Environment. *The International Journal of Aviation Psychology*, 13(3), 233–248, 2003.
- [31] **L. Pallottino, V. G. Scordio, A. Bicchi, and E. Frazzoli.** Decentralized Cooperative Policy for Conflict Resolution in Multivehicle Systems. *IEEE Transactions on Robotics*, 23(6), 1170–1183, 2007.
- [32] **G. Lintern.** An Affordance-Based Perspective on Human-Machine Interface Design. *Ecological Psychology*, 12(1), 65–69, 2000.

Fast-time simulations of manual conflict resolution

This chapter presents the results of a fast-time batch simulation study, that investigated emergent features of conflict detection and resolution in unmanaged airspace. This simulation study is a follow-up of the experiment described in Chapter 6. Because the particular measures employed in this experiment required sample group sizes that well exceed a practical experiment setup, a simulation study can be used as a way to extrapolate findings to larger sample sizes.

Paper title Emergent Behavior of Decentralized CD&R in ATM
Authors J. Ellerbroek, M. M. van Paassen, M. Mulder
Presented at The 17th International Symposium on Aviation Psychology,
Dayton, Ohio, May 6–9 2013

Abstract: *The work described in this paper used simulations with a deterministic decision model for airborne separation, to investigate the influence of domain-inherent factors such as conflict geometry, aircraft performance limitations, and system delays on safety, efficiency, and other emergent properties of a decentralized airspace separation system. Each of these properties was systematically varied in fast-time batch simulations, to identify their individual contributions. Results show that coordination can be hindered by performance limitations, regardless of manual or automation implementation. It was also found that shortest-way-out methods are relatively sensitive to asymmetric data uncertainties such as a communication delay, compared to resolution methods based on the rules of the air.*

7-1 Introduction

In today's airspace, traffic increase is pushing the limits of capacity and safety. To facilitate continuing growth, new air-traffic management concepts are under development, which allow a more flexible use of airspace [1–4]. The most ambitious plans propose delegation of separation responsibility from the air-traffic controller to the aircrew, as a way to reduce controller workload and increase airspace capacity.

This shift from centralized control of aircraft separation to decentralized control results in a complex system with many degrees of freedom, and many reciprocal interdependencies between agents in the system [5]. Providing proof of the level of safety for such complex systems is traditionally done using probabilistic methods such as a fault-tree analysis, a method that has also been applied to airborne separation [6]. Brooker, however, argues that the probability estimates that are required for such an analysis, makes that although such probabilistic methods can provide an *assertion* of the degree of risk, they cannot *prove* a certain level of safety [7].

This study, instead, takes a systems approach to analyzing safety and efficiency aspects of airborne separation [8]. The current paper is part of an ongoing study, which applies a Cognitive Systems Engineering approach to the design of an airborne separation assistance interface [9–12]. The aim of this approach is to reveal and categorize the semantic structure of the work domain, in an effort to provide a common basis on which both automation

and visualization can be based [13, 14]. This structure constitutes the inescapable complexity of the airborne separation problem, which makes it an unavoidable factor in the level of safety that can be obtained.

An important contribution to the complexity of an airspace where separation responsibility is delegated, comes from the interactions between multiple autonomous agents, each having different goals and capacities. To provide a sufficient level of safety, these interactions require a robust coordination between those agents. A previous experiment was conducted to evaluate coordination between aircraft when manually resolving traffic conflicts in unmanaged airspace [15]. In the experiment, pilots made use of a constraint-based separation assistance display, and were provided a set of rules that, when followed correctly, implicitly lead to coordinated resolution maneuvers. This experiment resulted in a limited number of resolutions, from which a good impression could be formed on the behavior of the pilots in a conflict situation. Because of the nature of the dependent measures (categorical and ordinal), however, sample sizes beyond practical limits are required to obtain sufficient statistical power. A possible way to improve upon these qualitative results would be to use large-scale simulations, in an effort to generalize the findings from the (small-scale) pilot experiment.

Previously, several simulation studies have been done to test the feasibility of specific self-separation algorithms, e.g., [16–21], or to test the stability of intersecting flows of aircraft [22]. Other work investigated more generally how maneuverability is affected by the initial distance between conflicting aircraft [23], or compared coordination rules in terms of a combined cost based on minimum separation and maneuver efficiency [24]. The current study will use fast-time simulations to look more closely at how (implicit) coordination is affected by several inherent properties of the separation problem, by the shape of several coordination rules, and by particular pilot preferences that were found in previous human-subject experiments. The simulation study focuses primarily on the inherent properties of the separation problem, by only considering deterministic elements of the work domain, and without looking specifically at automation or human behavior. This should enable identification of the individual contributions of specific properties to the emergent behavior and efficiency of decentralized aircraft conflict resolution. Similar to the preceding pilot experiment, this study will only consider horizontal conflicts and resolution maneuvers.

The following section introduces the coordination rules that were used in the simulations. The third and fourth sections describe the simulation set-up, and the results of the simulations, respectively. The paper concludes with a discussion on the findings.

7-2 Coordination rules

The shift of the separation task from the ground to the aircrew implies that conflicts will be resolved in a decentralized fashion. Determining a safe resolution to a conflict will require coordination between the actors in that conflict. This means that for automated, as well as for manual conflict resolution, predictability of decisions will be essential to guarantee an acceptable level of safety. In situations where there is no opportunity for negotiation, implicit coordination will be required, e.g., by following a predetermined set of rules that dictate which aircraft should maneuver, and how they should maneuver. In worst-case scenarios, pilots will have to manually determine resolution maneuvers, for instance when the automation has failed, or for other reasons that make pilots decide to resolve a conflict manually. This poses limits on the complexity of the coordination rules. For automated resolution advisories, high rule complexity can make it difficult for pilots to understand the rationale behind resolution advisories, potentially resulting in non-conformance and distrust of the system [24–26].

Several decentralized conflict resolution methods exist which provide various levels of (implicit) coordination. The Modified Voltage Potential method provides resolutions following a ‘shortest way out’ principle, which guarantees implicit coordination for non-collision course conflicts [27, 28]. The minimum path deviation resolution that is visually apparent in the displays in this study works in a similar fashion, and also provides implicit coordination for non-collision course conflicts [15, 29]. While the Visual Flight Rules (a.k.a. the Rules of the Air) do not provide actual resolutions, they can be used to decide between sets of resolutions, in order to find a coordinated resolution [15, 30].

Other, more complex algorithms coordinate by having each agent optimize the global performance for a group of agents (the ownship and the immediate surrounding aircraft) [18, 31, 32], or rely on the availability of

knowledge of all aircraft (in the vicinity) that have already maneuvered [22]. Because these methods rely on (many) computer calculations, they do not lend themselves well for application in worst-case scenarios, i.e., where one or more of the actors in a conflict has to resort to manual conflict resolution.

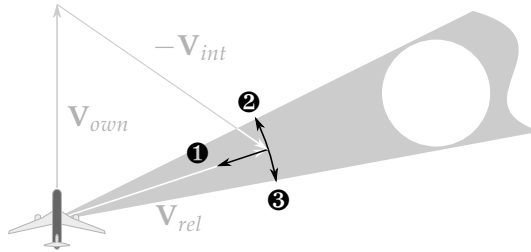


Figure 7.1: Possible directions for a resolution maneuver, expressed as changes of the relative velocity vector, \mathbf{V}_{rel} . In the horizontal plane, all possible resolution maneuvers correspond with one of three types. ❶: Reduce the magnitude of the relative velocity vector to zero, without changing its direction. This maneuver is guaranteed to be coordinated, regardless of what type of maneuver is chosen by the other actor in the conflict. However, because it results in parallel courses for the aircraft in the conflict, it results in very inefficient resolution maneuvers. ❷, ❸: Place the relative velocity vector outside one of the two legs of the constraint zone, by changing the direction of \mathbf{V}_{rel} (and, optionally, changing its magnitude). These maneuvers are implicitly coordinated when both actors choose the target state of their resolution maneuver along the same edge of the velocity constraint area.

Even though these methods vary considerably in how they determine an appropriate resolution, they all ultimately have to decide between the same options, see Figure 7.1. In the horizontal plane, all possible resolutions correspond with one of three maneuver options. The first option is to reduce the magnitude of the relative velocity vector to zero, without changing its direction. This maneuver is guaranteed to be coordinated, regardless of what type of maneuver is chosen by the other actor in the conflict. However, because it results in parallel courses for the aircraft in the conflict, it postpones, rather than resolves the conflict. The remaining two options are to place the relative velocity vector outside one of the two legs of the constraint zone, by changing the direction of \mathbf{V}_{rel} (and, optionally, changing its magnitude). These maneuvers are implicitly coordinated when both actors choose the target state of their resolution maneuver along the same edge of the velocity constraint area. In practice, therefore, a coordination rule will

always be a binary choice between two directions of change for the relative velocity vector.

The experiment preceding this study employed a combination of the rules of the air and a shortest-way-out rule, to enable implicitly coordinated maneuvers. In the experiment, pilots made use of a constraint-based separation assistance display, that provided an intuitive way to determine which coordination rule should be applied for a given conflict situation [15]. The current study will employ the same coordination rules in the fast-time simulations. The remainder of this section will illustrate how each of these rule sets can be used to provide implicitly coordinated resolutions.

7-2-1 Coordination using rules of the air

Since 1945, the *International Standards - Rules of the air* have been published by the International Civil Aviation Organization (ICAO), as an annex to the Convention on International Civil Aviation [30]. These rules of the air include general flight rules, visual flight rules and instrument flight rules. The visual flight rules include priority rules, that are comparable to priority rules for road traffic. These priority rules will also be employed in this study.

The priority rules of the air are divided into three rules:

- An aircraft being overtaken has the right of way and the overtaking aircraft must remain clear by altering heading to the right.
- When two aircraft are approaching each other head-on they must both alter heading to the right.
- Aircraft from the right have the right of way. Remain clear by passing behind that aircraft.

Figure 7.2 illustrates how the applicable rule can be determined from the conflict geometry. An aircraft is being overtaken when the intruder aircraft approaches from behind on a relative bearing no more than 70 degrees from

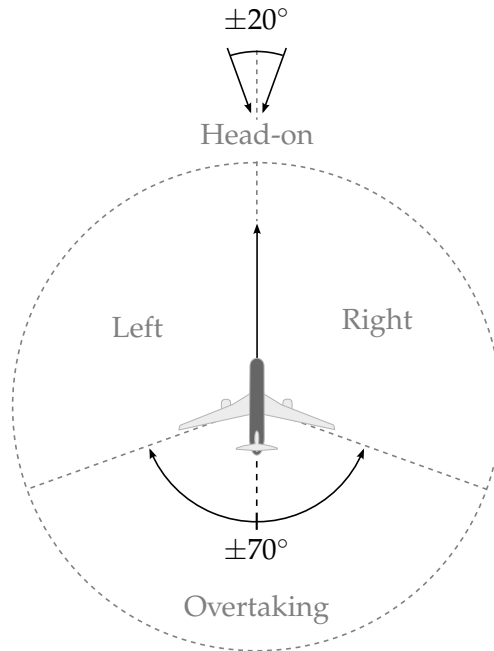


Figure 7.2: Determination of applicable rule of the air from conflict geometry. An aircraft is being overtaken when the intruder aircraft approaches from behind on a relative bearing no more than 70 degrees from the ownship track. Aircraft are approaching each other head-on when the difference in track angles is between 160 and 200 degrees. Otherwise, intruder aircraft either come from the left, in which case they have to give way to ownship, or they come from the right, and have the right of way.

the ownship track* [30]. The rules of the air also provide a rule for aircraft that are head-on, or nearly so, but do not specify when exactly this is the case. This study will assume that aircraft are approaching each other head-on when the difference in track angles is between 160 and 200 degrees. Conflicting aircraft that do not fall in any of these categories either come from the left, in which case they have to give way to the other aircraft, or they come from the right, and have the right of way.

*The range of bearings of ± 70 degrees follows from the visibility of the navigation lights of an aircraft. An aircraft's port and starboard lights are designed such, that they are not visible beyond 110 degrees to the left and right of the aircraft's plane of symmetry, respectively.

Note, that the ICAO Rules of the Air state that, aside from head-on conflicts, an aircraft that has the right of way should maintain its current heading and course. However, in a situation without explicit communication, safety requires that both actors should at least be able to maneuver, in a coordinated fashion. This means that for overtake conflicts, aircraft being overtaken can cooperatively solve the conflict by altering their course to the left. When an aircraft has an intruder coming from the left, a cooperative resolution maneuver would be to pass in front of the intruder.

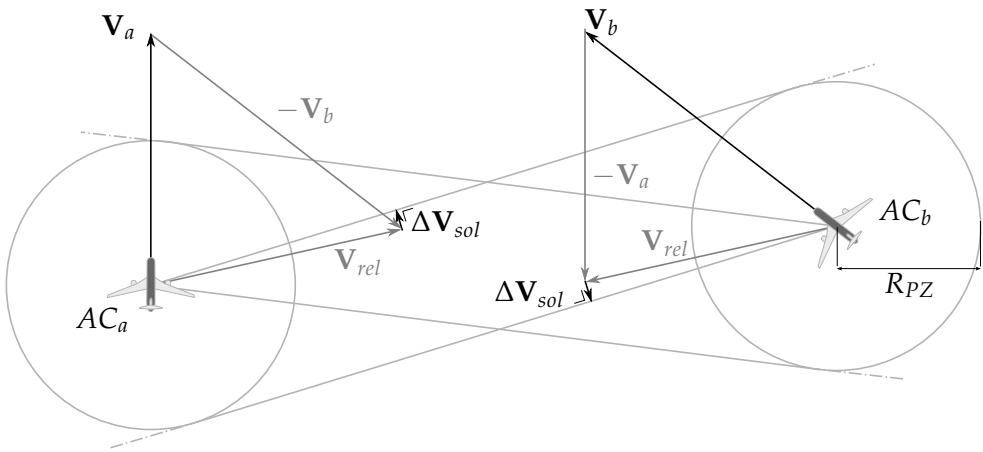


Figure 7.3: Geometrically optimal solutions guarantee implicit coordination, for all conflict geometries with the exception of collision courses. Because of the rotational symmetry of the velocity constraint areas of both aircraft, selecting the optimal solution for aircraft AC_a will always be complementary to the geometrically optimal solution for aircraft AC_b .

7-2-2 Coordination using minimum path deviation

In most cases, a cooperative resolution can also be derived from the configuration of the velocity constraints, see Figure 7.3. This type of coordination is related to the conflict solution that results in *minimum path deviation*, which can be achieved by taking the shortest way out of the velocity constraints.

Consider the nominal aircraft position at time t :

$$\mathbf{x}(t) = \mathbf{x}_0 + \int_{t_0}^t \mathbf{V}_{orig}(t) dt$$

The path deviation for a maneuver can be derived from the difference between maneuver and original velocities:

$$\Delta x = \int_{t_0}^{t_1} |\mathbf{V}_{sol}(t) - \mathbf{V}_{orig}(t)| dt = \int_{t_0}^{t_1} |\Delta \mathbf{V}_{sol}(t)| dt \quad 7.2$$

Using Equation (7.2), it can be shown that the path deviation is minimized by minimizing $\Delta \mathbf{V}_{sol}$.

Figure 7.3 shows a traffic conflict with two aircraft, and the derivation of their velocities relative to each other. The circles visualize the horizontal separation margin around each aircraft, and the areas between the triangle lines tangent to each circle show the conflicting values for each relative velocity vector. In this figure, $\Delta \mathbf{V}_{sol}$ is the vector distance between \mathbf{V}_{rel} and the nearest edge of the velocity constraint area. The shortest distance is found when $\Delta \mathbf{V}_{sol}$ is taken perpendicular to the edge of the velocity constraint area [17, 29]. Figure 7.3 also illustrates that, as long as \mathbf{V}_{rel} is closer to one leg than to the other, a single optimum for $\Delta \mathbf{V}_{sol}$ can be found, and that both aircraft share this optimum. Therefore, implicit coordination is guaranteed when the optimum is selected as a resolution.

7-2-3 Combined coordination rules

An additional set of rules is required for situations where there is no unique geometrically optimal solution. These are situations where the distances between the relative velocity vector and either edge of the velocity constraint area are equal: The relative velocity vector lies exactly along the bisector of the velocity constraint area, which means that $d_{CPA} = 0$, and the aircraft in conflict are on a collision course. The previous experiment therefore combined the minimum path deviation method with the rules of the air for conflicts where the maneuver choice is ambiguous in terms of coordination.

7-3 Simulation set-up

A simulation study was performed to investigate how implicit coordination and efficiency in decentralized CD&R are affected by several inherent properties of the separation problem, by the shape of the coordination rules, and by particular pilot preferences that were found in previous human-subject

experiments. Each of these properties was systematically varied in fast-time batch simulations, to identify their individual contributions to the emergent behavior and efficiency of decentralized aircraft conflict resolution.

7-3-1 Simulation design

The simulation was designed to evaluate conflict resolution rules and strategies, in two-aircraft scenarios, for varying conflict geometries and system delays. In the evaluation, only conflict detection and the initial conflict resolution maneuver for each aircraft were considered, additional maneuvers that might be required when initial maneuvers are conflicting were left out of the analysis. In these situations, manual pilot responses are very unpredictable, whereas specific design for resolution automation is not the focus of this study.

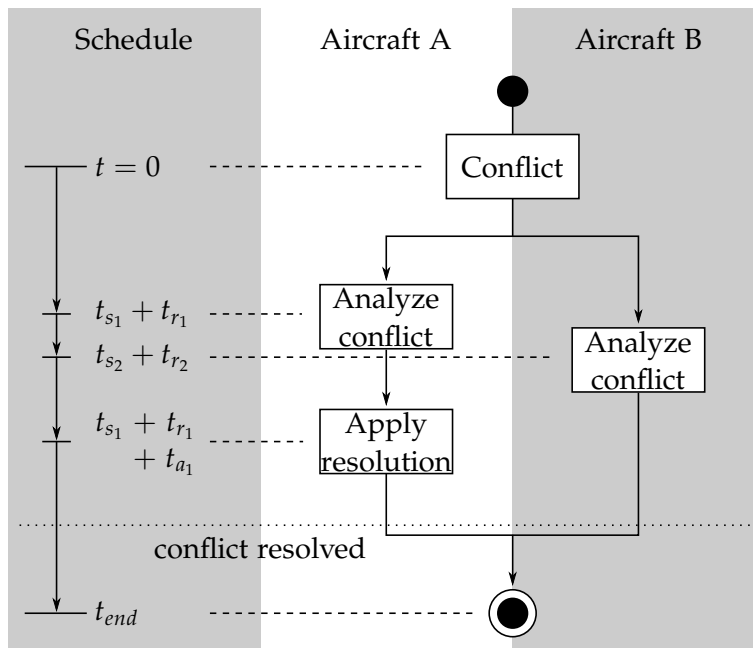


Figure 7.4: Example of a simulation run schedule. In this example, aircraft A detects the conflict first, and resolves the conflict before aircraft B has finished analyzing the conflict.

The simulator considers the process of conflict detection, resolution, and aircraft motion as a series of discrete events. In each simulation, (simulated) pilots can perform conflict detection, maneuver determination and execution events. The (simulated) time at which these events occur is determined by various latencies in the decision model. The simulator schedules the events of each simulated pilot in order of occurrence. An example of such a schedule is given in Figure 7.4. The simulator calculates updates of the aircraft states for each agent in a conflict, prior to the evaluation of each scheduled event.

Aircraft motion was modeled using a discrete-event point-mass model [33]. The model consists of analytically derived expressions for straight flight, unaccelerated turns, and accelerated turns. Transitions between maneuvers were assumed to be instantaneous (no maneuver dynamics were modeled). Model coefficients for these point-mass models were obtained from EUROCONTROL's BADA aircraft database [34]. The experiment was conducted with zero wind, and no turbulence. Although wind conditions will impact maneuverability, these effects were considered out of scope for the current evaluation. Aircraft flew at flight level FL250, because at this altitude airspeed still has usable margins between minimum and maximum operating speed. The aircraft type was randomly selected in each simulation run from a set of two possible aircraft, equal to the aircraft types used in the manned experiment. Table 7.1 shows the relevant model parameters for these aircraft.

Table 7.1: Relevant data for the aircraft models in the experiment.

		Boeing 707-300	Airbus A330
TAS_{min}	[kts]	282.4	331.1
TAS_{max}	[kts]	530.1	471.5
TAS_{cruise}	[kts]	485.0	432.0

Conflict geometries were created by systematically varying *conflict angle* ($\Delta\chi$) and *CPA distance* (d_{CPA}), and randomly varying time to loss of separation, see Figure 7.5. Here, the conflict angle determines the shape and orientation of the forbidden area, and the magnitude of the closing speed between the two aircraft. The distance at the CPA, d_{CPA} , determines how

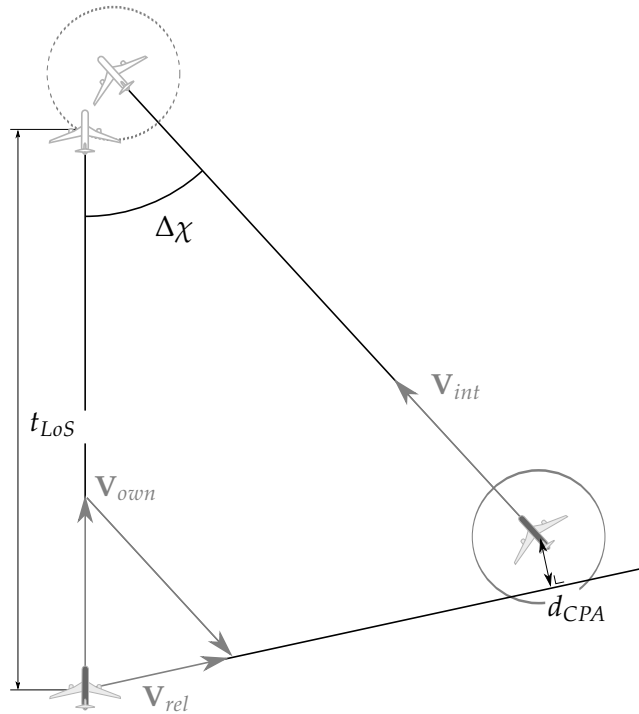


Figure 7.5: The conflict geometry for each scenario is defined by three parameters: conflict angle $\Delta\chi$, time to first loss of separation t_{LoS} , and the distance between the two aircraft at the closest point of approach d_{CPA} . The conflict angle is the angle between intruder and ownship tracks. The time to first loss of separation determines the initial distances in the conflict. The distance at the CPA determines how close the two aircraft will pass each other should neither aircraft maneuver.

the aircraft pass each other, and at what distance. The time to first loss of separation varied between 3 - 5 minutes, which meant a medium to high level of urgency for each conflict scenario.

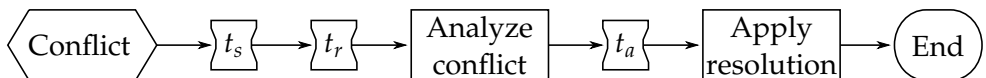


Figure 7.6: The pilot decision logic. Conflicts are detected after $t_s + t_r$ seconds (the system delay and the reaction time, respectively). Conflict analysis takes t_a seconds, after which a resolution according to the applicable coordination rule is applied.

7-3-2 Decision logic

Figure 7.6 shows how pilot decision making is modeled, from the moment that a conflict is first detected, until a resolution maneuver is selected and executed. There are three time parameters in the model: a system delay (t_s), a pilot response time latency (t_r), and a pilot analysis time duration (t_a). The system delay consists of processing delays within the Automatic Dependent Surveillance – Broadcast (ADS-B) system, as well as any communication delay that might occur. When it is assumed that broadcast ADS-B messages are based on current data (i.e., that there are no processing delays), and are always received, the system delay only depends on the message rate. An ADS-B transmitter sends one message per second, which would mean a system delay between zero and one second. In reality, not all broadcast messages will be received, resulting in larger system delays. The effects of this delay will be investigated in this study.

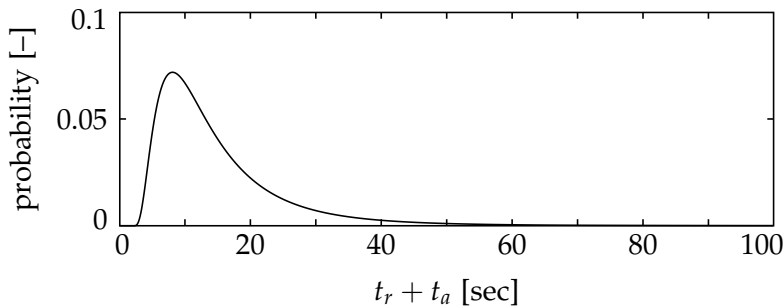


Figure 7.7: Probability density function for the combination of response time and analysis time, $t_r + t_a$. Values for this combined latency are given in seconds along the abscissa, the probability of occurrence is indicated along the ordinal axis.

Conflict Detection and Resolution (CD&R) will be just one of many tasks performed on the flight deck, which means that pilot response time can not be neglected. In addition, after detecting a conflict, pilots will also require a certain amount of time to analyze the conflict, and determine an appropriate response. For the current simulation, values for response time and analysis duration were derived from latencies measured in the previous experiment [15]. The minimum observed latency was chosen as response time, $t_r = 2$ sec; the remainder fitted a log-normal distribution ($\mu = 2.31$, $\sigma = 0.708$), see

Figure 7.7. In the simulation, values for t_a were randomly drawn from this distribution, for each pilot, in each experimental run.

The *Analyze conflict* block represents the decision-making phase, where the pilot selects a maneuver that is appropriate for the actual conflict. In the current simulation, this decision making is modeled as a completely deterministic process, based only on the applied conflict resolution rule set, and a possible maneuver dimension preference. In practice, manual conflict resolution would imply a certain percentage of error, this is, however, out of scope for the current research.

7-3-3 Independent variables

Throughout the simulation, four independent variables were varied. *Conflict geometry* was a factor that is defined by two sub-parameters: the conflict angle varied between 0 and 180 degrees, in steps of 5 degrees, and CPA distance varied between ± 4.75 nautical miles, in steps of 0.25 *nmi*. This resulted in 1443 different conflict geometries (37×39). *Resolution policy* was a factor with three levels: conflicts could be resolved cooperatively using coordination based on the Rules of the Air (R), the optimal shortest-way out (O), or a combination of both (R+O), see Section 7-2.

The system delay could vary between zero and a certain maximum. This maximum system delay was a factor that varied between 0 and 10 seconds in steps of one second, and between 10 and 60 seconds in steps of five seconds. For each run, the actual system delay value was determined separately for each aircraft using a random draw from a uniform distribution, between zero and the maximum delay. For non-zero maximum delay this meant that the aircraft in each conflict could have unequal system delays. Pilot heading-only maneuver preference was evaluated in a separate case. These simulations only considered the optimal (O) resolution policy, and only with zero system delay.

7-3-4 Dependent measures

Dependent measures for this simulation study related to maneuver strategy, level of cooperation, and the efficiency of the applied resolutions. Maneuver strategy related to the *solution type* in terms of vector change dimensions

(heading and speed). The *level of cooperation* if one or both aircraft maneuvered, and if their resolutions were cooperative. Path deviation was used as a measure of *efficiency*. All measures were constructed from simulated time histories of parameters position, heading, and selected speed and heading.

7-4 Results

7-4-1 Solution type and level of cooperation

The available resolution maneuvers for a conflict can be grouped by the flight parameters that were changed to resolve each conflict. For horizontal conflict resolution the available maneuver options are heading changes, speed changes, or a combination of the two. In general, possible factors that influence the selection of a maneuver are the conflict geometry, aircraft performance limitations, phase of flight, and personal or airline preference. In this particular case, i.e., fully deterministic simulations of different rule sets for conflict resolution, only conflict geometry in combination with the own aircraft's performance limitations will play a role.

Table 7.2: Percentages maneuver choice for a single aircraft.

Ruleset	None	HDG+SPD	HDG only	SPD only
R+O	42.7%	55.9%	1.6%	0.0%
R	29.4%	61.9%	9.4%	0.0%
O	44.4%	55.4%	0.4%	0.0%

For each of the three rule sets, after discarding those solutions that do not comply with the applicable coordination rule, and those that exceed the aircraft's performance limits, the remaining resolution possibilities are still compared based on efficiency, where the most efficient remaining maneuver is selected as a resolution to the conflict. Table 7.2 shows the maneuver choice distribution for each of the rule sets. When comparing rule set *R* to rule sets *R+O* and *O* in terms of single aircraft solutions, it can be seen that a resolution performed by only one aircraft occurs more often with the latter two rule sets than with the former. This difference results from the fact that whereas the optimal coordination rule always results in the coordinated

resolution being on the closest edge of the velocity constraint area, coordination based on the rules of the air may actually lead away from the nearest edge of the constraint area. This leads to relatively longer maneuver times for rule set R , increasing the probability that both aircraft maneuver. This is also visible in Figure 7.8(a): The percentage of single-aircraft resolutions, sorted by CPA distance, is symmetric around $d_{CPA} = 0$ for the optimal rule sets, but is increasingly reduced for more negative CPA values for the rules of the air rule set.

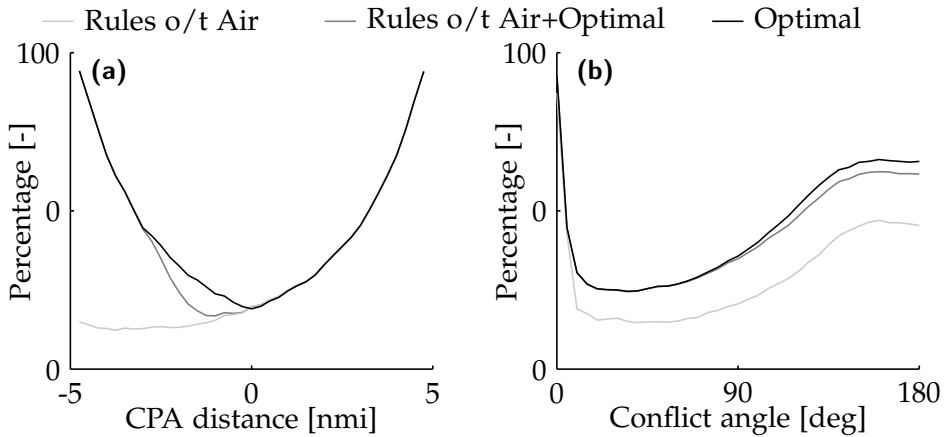


Figure 7.8: Percentage of single-aircraft maneuvers for each of the three rule sets. **(a):** Percentage of single-aircraft maneuvers versus CPA distance in nautical miles along the abscissa. **(b):** Percentage of single-aircraft maneuvers versus conflict angle in degrees along the abscissa.

Figure 7.8(b) shows the percentage of single-aircraft resolutions, sorted by conflict angle. It shows that for relatively small conflict angles (20 - 60 degrees), the percentage of single-aircraft resolutions drops noticeably. This drop coincides with an increase in speed change that is required when resolving conflicts with these geometries. Because speed changes, in general, are slower than heading changes, these resolution maneuvers take longer, making the conflict more imminent, and increasing the chances of both aircraft maneuvering.

In the remaining conflicts, both aircraft maneuvered, either cooperatively, or opposing, see Table 7.3. It can be seen that especially the percentage of opposing solutions is larger when using only rules of the air, compared

Table 7.3: Percentages level of cooperation for aircraft pairs.

Ruleset	Single	Cooperative	Opposing
R+O	42.7%	56.7%	0.6%
R	29.4%	69.1%	1.5%
O	44.4%	54.8%	0.8%

to the other two rule sets. The distribution of these opposing resolutions over the possible conflict geometries is shown for each rule set in Figure 7.9. Because the current simulation does not include pilot or data uncertainty, opposing solutions in principle only occur when the desired maneuver is obscured by a speed limit of the own aircraft, or, with the optimal rule set (*O*), in situations where $d_{CPA} = 0$. In some cases, however, with the optimal rule set, an uncoordinated solution is also selected for small non-zero d_{CPA} . In the current conflict resolution logic, possible solutions for a conflict are determined using velocity constraint areas that are corrected for maneuver duration, similar to the separation assistance display on which the optimal coordination rule is based [29]. The current implementation to correct for maneuver duration does so by looking at the smallest available heading change. In some situations it can happen that the edge of the constraint area along which the coordinated solutions lie receives a larger correction than the opposite edge, making solutions along the opposite edge seem more efficient. Because coordination is based solely on maneuver efficiency, such corrections can lead to uncoordinated solutions. This occurred in 63 out of 8,259 conflicts with opposing resolutions with the optimal rule set (0.76%).

Figure 7.9(a) shows the distribution of opposing solutions for the rules of the air rule set. Maneuvering solely on rules of the air implies that solutions on one of the edges of the velocity constraint area are immediately discarded*. Similar to the optimal rule sets, conflict geometries with moderate conflict angles (20-60°) can lead to situations where the speed solution and the combined solution on the front constraint area edge are unavailable because they would exceed the maximum speed limit. When all solutions on the opposite edge are discarded, however, this will happen twice as often.

*In the current simulation, these solutions are sometimes considered, but only when there is no reachable maneuver available on the coordinated edge of the velocity constraint area.

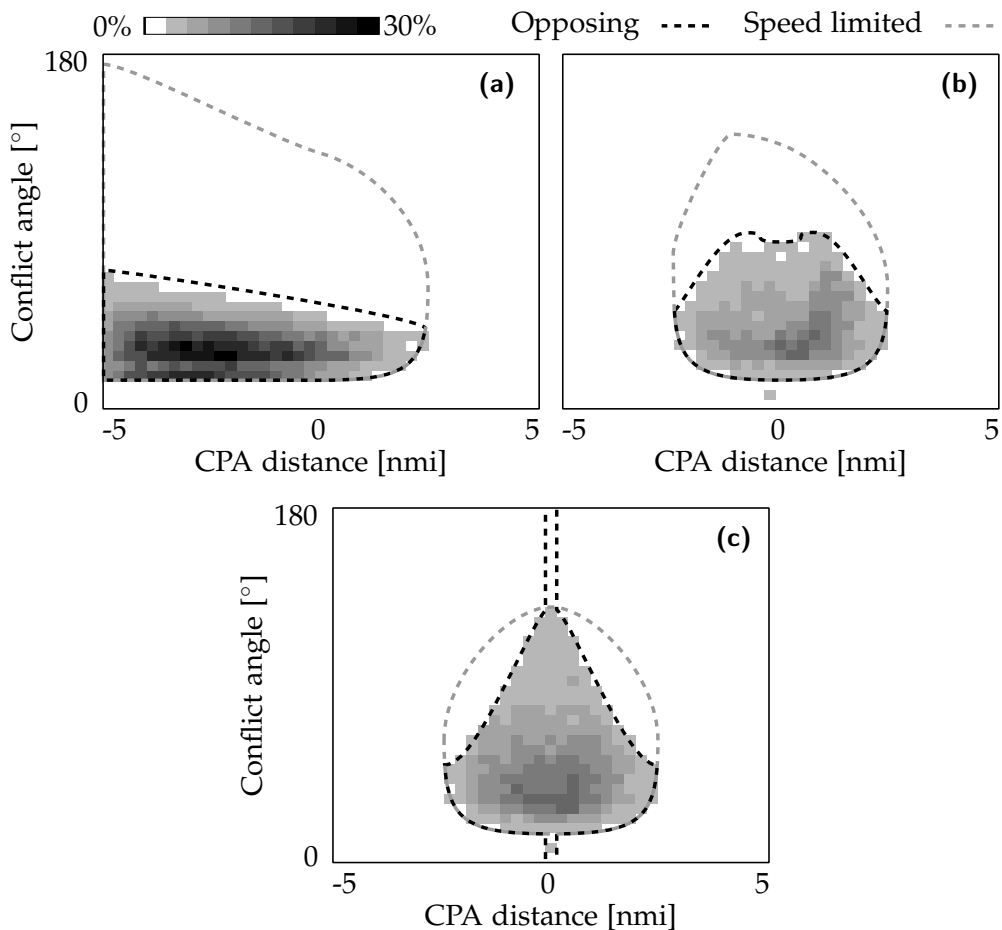


Figure 7.9: Percentage of opposing solutions for each of the three rule sets. **(a)**: Rules of the air (R), **(b)**: Rules of the air + optimal (R+O), and **(c)**: Optimal (O). The percentages are divided by CPA distance along the abscissa, and by conflict angle along the ordinal axis. The percentages are indicated between zero and thirty percent by increasing shades of gray. In each figure, a black dashed line indicates the area in which opposing maneuvers occur, and a gray dashed line indicates the area in which the preferred solution is obscured by the aircraft's speed limits.

In Figure 7.9(a), this is revealed by a large percentage of opposing solutions for small conflict angles and large negative d_{CPA} .

On the other hand, when comparing rule set R to the other rule sets for larger conflict angles, combined with smaller CPA distances, the rules of the air actually result in fewer opposing resolutions. Because the optimal rule sets (O , $R+O$) do not specifically exclude solutions on either of the edges of the velocity constraint area, a second-best solution is sometimes found on the constraint area edge opposite to the preferred solution, when the preferred solution is excluded because of a speed limit (such solutions are, however, not cooperative). For the rules of the air, when a heading solution is available on the cooperative constraint area edge, this solution will be preferred over a solution on the opposite edge. Note, however, that when both aircraft are flying at similar cruise speed, these heading maneuvers lead to a (near) parallel course, which occurred in 1.2% of the cases.

It should also be noted that according to the rules of the air, aircraft that can cooperate by passing in front of the intruding aircraft by definition have right of way, and therefore in principle do not have to maneuver. When the aircraft is in a situation where it cannot be assumed that the other aircraft will maneuver to resolve the conflict, an alternative solution could be to select the nearest solution on the top edge of the constraint area that is within the speed limit of the aircraft, leading to a slightly less parallel course. This type of maneuver was, however, not considered in the current simulation.

Figure 7.9(b) shows the distribution of opposing solutions for the combined rules of the air and optimal rule set ($R+O$). It can be seen that because the rules of the air are used here for conflicts with a small expected CPA, the number of opposing solutions for larger conflict angles is reduced, compared to the optimal rule set (Figure 7.9(c)). Instead of selecting a non-cooperative solution on the opposite constraint area edge, a heading change on the coordinated edge is used to resolve the conflict (see also the increase in heading-only solutions in Table 7.2).

Figure 7.10 shows how the percentage of opposing resolutions changes when a heading-only maneuver preference is applied in combination with the Optimal (O) rule set. When compared to Figure 7.9(c) it can be seen that opposing solutions occur in a smaller range of conflict angles, but in a wider range of CPA distances. In this case, a heading solution is always preferred

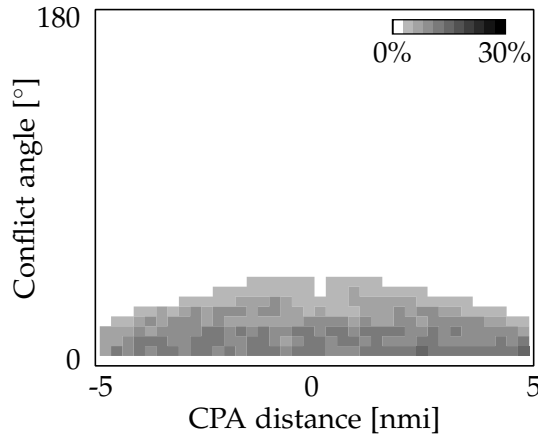


Figure 7.10: Percentage of opposing solutions for each the optimal (O) rule set, with a heading-only maneuver preference. The percentages are divided by CPA distance along the abscissa, and by conflict angle along the ordinal axis. The percentages are indicated between zero and thirty percent by increasing shades of gray.

over a solution that involves a speed change. This means that speed limits do not affect the number of opposing resolutions. The opposing maneuvers in Figure 7.10, therefore, correspond to situations where a speed change is *required* to cooperatively resolve a conflict. This occurs in situations where the intruder is flying faster than ownship, at a relative bearing close to 90 degrees (i.e., right next to ownship). This corresponds to a small (non-zero) conflict angle, as can be seen in Figure 7.10. For larger conflict angles a heading-only solution does become available. When ownship and intruder are flying at similar or equal velocity, however, these heading maneuvers can result in (near) parallel courses.

Figure 7.11 shows how the level of cooperation varies when the ADS-B message delay increases, for each of the three rule sets. The percentage of single-aircraft solutions shows similar trends with varying message delay for all three rule sets. Between zero and ten seconds message delay, each graph in Figure 7.11 shows a decrease of single-aircraft resolutions. The dominant factor in this range of message delays, is that the increasing duration of the message dropout period reduces the chances that a maneuver from the other aircraft is observed. Because of this, it is more likely that both aircraft

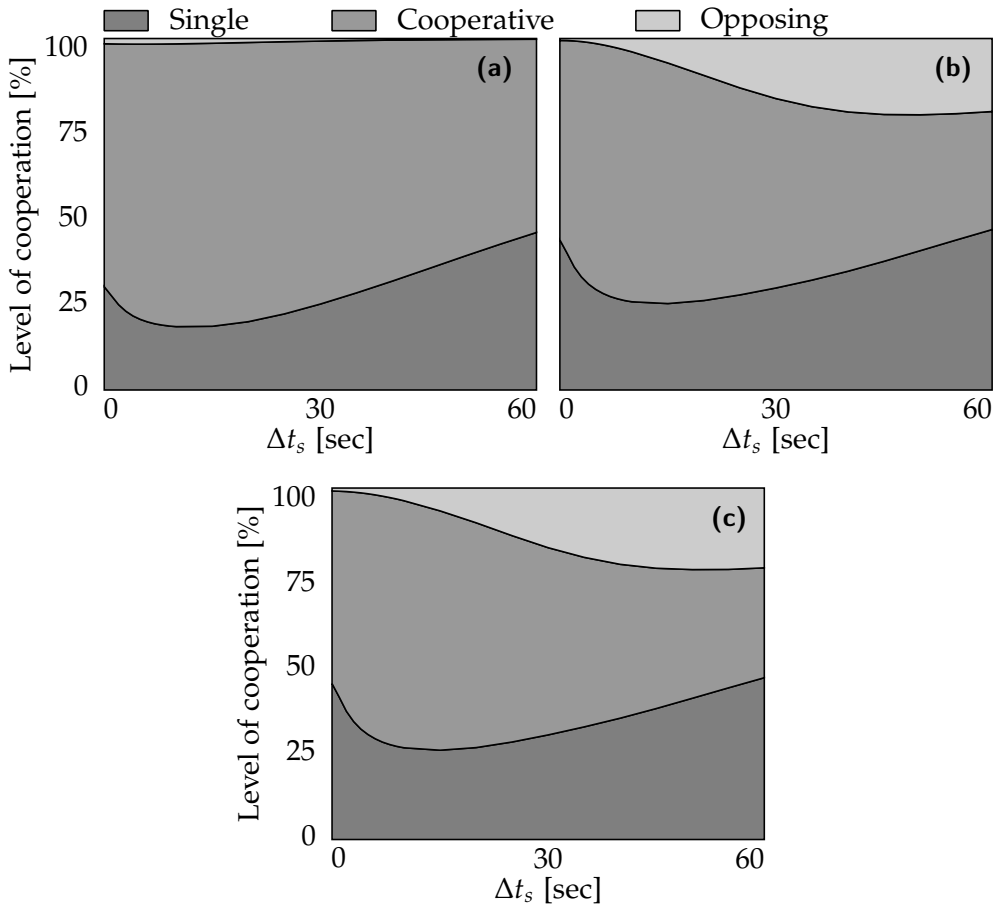


Figure 7.11: Cumulative graph of the level of cooperation for each of the three rule sets. **(a):** Rules of the air (R), **(b):** Rules of the air + optimal (R+O), and **(c):** Optimal (O). The level of cooperation varies with ADS-B message delay (Δt_s) along the abscissa.

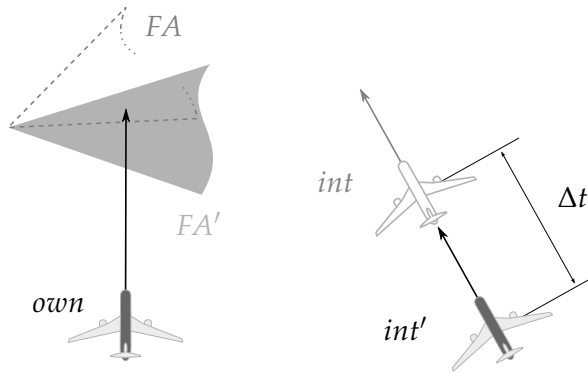


Figure 7.12: The effect of a message delay on perceived constraints. Here, *own* is the ownship, *int* is the true intruder position, and *int'* is the last broadcast position of the intruder. *FA* gives the extents of the true horizontal velocity constraints, while *FA'* represents the constraints that are calculated with the outdated ADS-B message. In this example, the employed ADS-B sample is sixty seconds too old; $\Delta t = 60$ sec.

maneuver, even though this is not necessary. The combined efficiency of the two aircraft therefore also goes down.

The downward trend of the number of single-aircraft resolutions reverses, however, when the message delay is increased beyond ten seconds. This is caused by the fact that changing the position of one aircraft in a conflict also changes the (perceived) relative position of that aircraft, and therewith the constraints that this aircraft imposes on the other aircraft in the conflict (the forbidden area rotates around its apex). Given enough delay, this can cause conflicts to go undetected. As a result, it can happen that only one aircraft detects the conflict, and only that aircraft will maneuver to resolve the conflict. For smaller delays, only conflicts with a large predicted d_{CPA} can go undetected. This range increases with increasing delay.

In contrast to the number of single-aircraft solutions, a difference between rule sets can be found in terms of opposing resolutions, when ADS-B delay is increased. Although in the ideal, zero delay case, optimal rule sets have superior performance in terms of opposing maneuvers, the Rules of the air perform better when ADS-B delays are introduced. In fact, Figure 7.11(a) shows that the proportion of opposing resolutions reduces from 1.5% to 0.2%, when the rules of the air are applied, and the ADS-B delay

is increased from zero to sixty seconds. In contrast, with the optimal rule set, the proportion of opposing resolutions shows an increase from 0.8% to a maximum of 23.2% (see Figure 7.11(c)).

With the rules of the air, a coordinated maneuver is determined largely from the relative bearing of the intruder aircraft, by distinguishing between four quadrants around ownship. This method is relatively robust against uncertainties in position. Methods that optimize for efficiency, such as the R+O and O rule sets in this study, on the other hand, are much more sensitive to small changes in relative position: Figure 7.12 shows that an error in intruder position along the intruder track rotates the velocity constraint area caused by that intruder. The optimal rule sets determine a coordinated maneuver by observing on which side of the constraint area bisector the relative velocity vector is situated. A rotation of the constraint area can therefore have influence on the selection of a coordinated maneuver.

7-4-2 Performance

Figure 7.13 shows how the mean path deviation varies with conflict angle and CPA distance, for each of the rule sets. In these graphs, exactly parallel solutions are excluded, as well as opposing solutions. Parallel courses are discarded because they never reach a point where the aircraft can return to its original track. Opposing solutions are discarded because there, the path deviation not only depends on the initial resolution maneuvers, but also on how the opposing solutions are handled.

Because the simulation doesn't include uncertain data or pilot decisions, the average path deviations for the optimal (O) rule set (Figure 7.13(c)) always correspond to the most efficient resolutions (Note, though, that the values in Figure 7.13 are an average of the single-aircraft and the cooperative resolutions). As expected, the largest path deviations occur around $d_{CPA} = 0$, and path deviations reduce symmetrically for increasing (absolute) CPA distances. Figure 7.13(c) also shows that, for a given value of d_{CPA} , path deviation doesn't vary noticeably with conflict angle.

Figure 7.13(a) shows that the path deviation for rule set R increases with increasingly negative d_{CPA} , with a trend similar to the optimal (O) rule set. An exception to this trend can be seen for conflict angles between 40 and

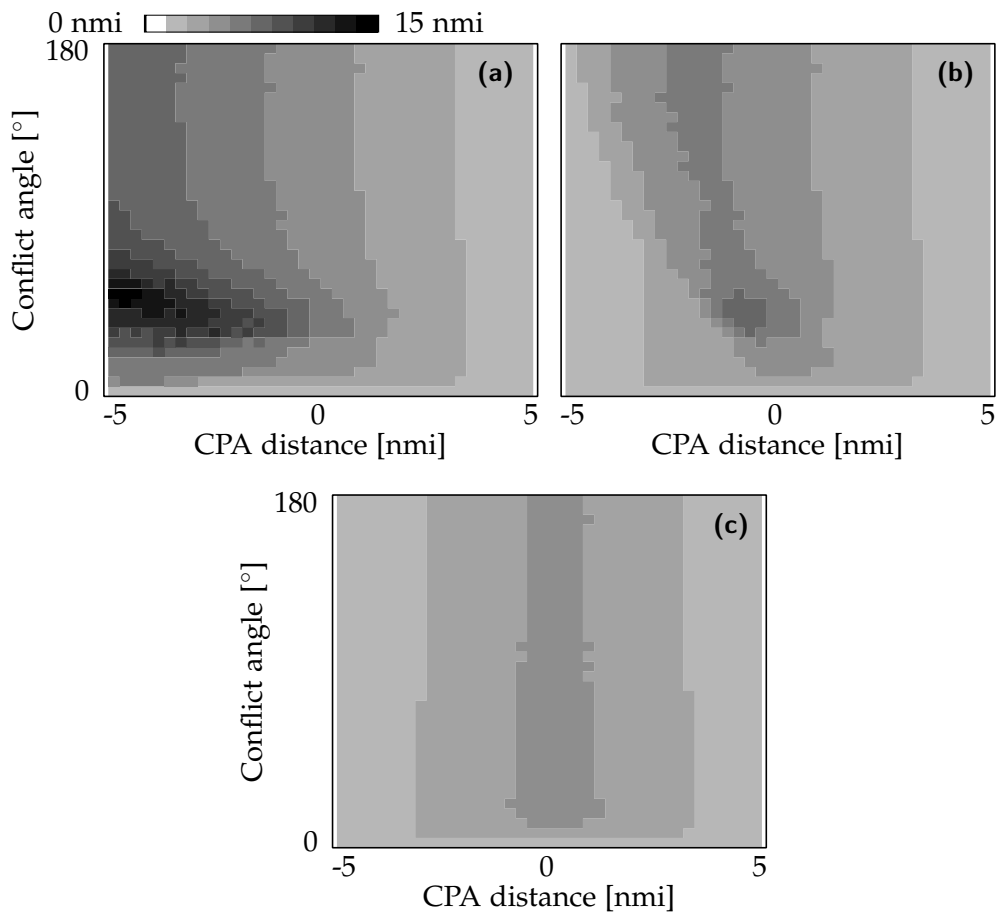


Figure 7.13: Path deviation for each of the three rule sets. **(a)**: Rules of the air (R), **(b)**: Rules of the air + optimal (R+O), and **(c)**: Optimal (O). Path deviation is divided by CPA distance along the abscissa, and by conflict angle along the ordinal axis. Path deviation is indicated between zero and fifteen nautical mile by increasing shades of gray.

80 degrees, combined with negative values for d_{CPA} . Here, average path deviation values increase up to a factor two, compared to other conflict angles. These inefficient maneuvers occur when more efficient coordinated maneuvers are obscured by the aircraft's speed limit. The only coordinated maneuver available, in this case, is a heading-only maneuver, which maneuvers the aircraft to parallel courses.

Figure 7.13(b) shows the average path deviation for the R+O rule set. For small conflict angles and small negative values for d_{CPA} , it can be seen that the less efficient rules of the air maneuvers are used for coordination. For larger conflict angles the range of CPA values for which the rules of the air are applied is increased. This effect follows from the definition of the conflict geometry in the simulation. Recall that a conflict is defined using the cruise characteristics of both aircraft, and the three parameters *conflict angle*, *expected CPA distance*, and *time to CPA*. When comparing a conflict where $\chi = 0^\circ$, and a conflict where $\chi = 180^\circ$, with equal time to CPA, the initial distance between the two aircraft is many times larger in the latter case, compared to the former. For increasing conflict angles, therefore, the width of the forbidden area decreases, and the ratio between the expected CPA distance and the opening angle of the forbidden area increases. The rules of the air are applied when the relative velocity vector is within a certain angle from the bisector of the forbidden area, which means that the rules of the air are applied for a widening range of expected CPA, for increasing conflict angle. The negative effect of the applied rule on path deviation is asymmetric around $d_{CPA} = 0$, because for $d_{CPA} > 0$, the optimal solution complies with the rules of the air, which means that the most efficient maneuver can be applied.

Figure 7.14 shows how path deviation using the Optimal strategy (O) is affected by a heading-only maneuver preference. When compared to Figure 7.13(c), it can be seen that especially for small conflict angles, path deviation is negatively affected by a heading-only maneuver preference. For such conflicts, when heading maneuvers are available at all, they are either very large, or they result in a (near) parallel course. For large conflict angles and large initial CPA distances, on the other hand, there is little to no difference between heading-only and combined maneuvers. In both these situations, the nearest heading solution and the optimal solution lie close to each other in the maneuver space, making the difference in path deviation negligible.

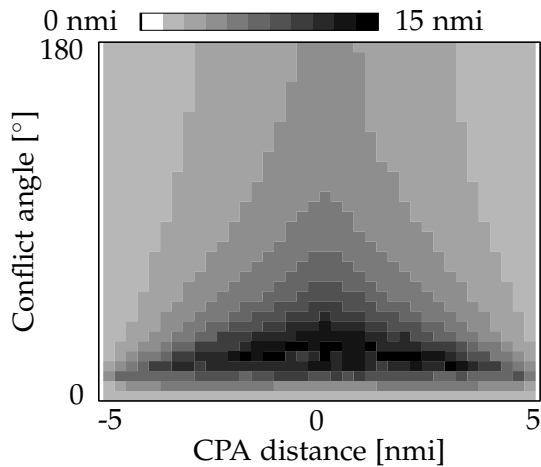


Figure 7.14: Path deviation for the Optimal (O) rule set, when a heading-only maneuver preference is incorporated.

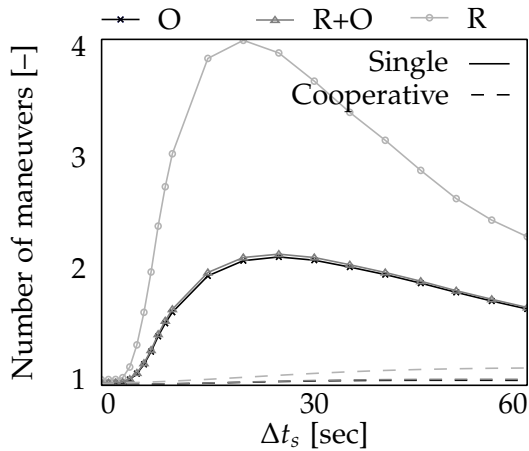


Figure 7.15: Average number of maneuvers required to resolve a conflict. The system delay in seconds is varied along the abscissa, the average number of required maneuvers is indicated along the ordinal axis. Continuous lines represent the three rule sets when only a single aircraft maneuvers. Dashed lines represent the same three rule sets when both aircraft maneuver cooperatively.

Performance in terms of path deviation did not show differences between rule sets, when ADS-B delay was varied. For all three rule sets, path deviation increased marginally (22% at most), when ADS-B delay was increased. This increase relates to the fact that the chance that an intruder maneuver can be taken into account when determining the own maneuver is reduced, when delays are introduced to the state communication. Figure 7.15 shows the average number of maneuvers that are required to resolve a conflict, for single-aircraft resolutions, and cooperative resolutions (dashed lines). It can be seen that with zero delay, the average number of maneuvers is close to one, regardless of rule set or level of cooperation (single/cooperative). When ADS-B delay is increased, however, the number of maneuvers required increases for single-aircraft resolutions. As illustrated in Figure 7.12, this can be caused by a rotation of the velocity constraints with respect to the true state. Because the true constraints are not known, it can happen that the initial maneuver does not resolve the conflict. A second possible cause is that, because the intruder aircraft is perceived as being further away than it really is, the forbidden area becomes narrower than it should be, making it an underestimation of the true constraints. This effect will be more severe when aircraft are closer together.

Compared to the single-aircraft resolutions, almost no increase in the required number of maneuvers is observed in the case of cooperative resolutions (the dashed lines in Figure 7.15). This is also caused by the fact that with non-zero delay, intruder maneuvers are less likely to be observed. As a result, the magnitude of both maneuvers in a cooperative resolution will be higher, which reduces the chance that an additional correction on the original maneuver is required. Figure 7.15 also shows that the effect of delay on the average number of required maneuvers is larger when the rules of the air are used, compared to the other two rule sets. Similar to the increase in path deviation in Figure 7.13(a), this is caused by the fact that for negative d_{CPA} , larger maneuvers are required with the rules of the air rule set.

The non-zero ADS-B delay also had an effect on the number of losses of separation, detected by the aircraft. This occurred with small conflict angles (and therefore also small relative velocities). Because the conflicts in this simulation study were designed with a constant time to loss of separation, aircraft start off close together in conflict situations with a small conflict angle. Using intruder data from only a short time earlier can then make it

seem as if there is already a loss of separation, while in fact both aircraft are still separated. In reality such situations are unlikely to occur because these kinds of overtake scenarios are detected earlier, when the aircraft are still further apart.

7-5 Discussion

The simulation study presented in this paper is part of a larger study on the design of an airborne separation assistance interface. This study applies a Cognitive Systems Engineering approach to determine what kind of information should be present on such an interface. This approach puts emphasis on the semantic structure of the work domain, as it invariably shapes the possibilities for work, regardless of whether this work is done by a human operator or an automated system. In the current study, the same focus on the inherent work domain properties is applied, in an effort to provide fundamental insights to how safety is affected by the base properties of the separation problem.

Even though the current simulations only consider deterministic properties of the separation problem, and therefore can not provide conclusive results regarding safety, they can provide useful insights. Such simulations can reveal whether emergent behavior is satisfactory, when simulated agents are all exactly acting according to procedure [35]. They also provide a structured way of identifying individual contributions of specific properties of the work domain to the emergent behavior and efficiency of decentralized aircraft conflict resolution.

The results in terms of level of cooperation in this study should therefore not be taken as percentages representative of the real system. Instead they can be used to investigate in which situations multi-agent solutions are more likely to occur, and which situations pose problems for cooperative behavior. There are, for instance, situations possible where, because of maximum speed restrictions, the only available cooperative maneuver for an aircraft would be not to maneuver at all. This has important repercussions for the safety of the system: The system would be safest if all aircraft in a conflict are individually able to resolve the conflict, each in a way that would be cooperative with the possible maneuvers of the other aircraft in the conflict.

The benefit over a priority rule, where one or more aircraft are required to maintain their original course, is that this way, the safe course of an aircraft that has right of way does not depend on the actions of another aircraft. Although this study considered certain specific coordination rules, it can be shown that for any coordination rule that does not consider specific aircraft capabilities, there exist situations where cooperative maneuvering will not be possible. A possible solution would be a priority rule where the faster aircraft in a conflict maneuvers in front of the slower aircraft.

The simulation results also showed situations where the availability of a coordinated resolution is affected by the type of coordination rule, or maneuver strategy that is applied. With the rules of the air, for instance, conflict geometries with a large negative CPA distance, combined with a moderate conflict angle ($\Delta\chi \in [20, 60]$) can only be solved cooperatively when a large speed increase is applied. In a similar conflict, the optimal rules dictate coordinated resolutions that require a much smaller state change, thus reducing the chance that a resolution is obscured by a speed limit. The optimal rules, on the other hand, are ambiguous in terms of coordination around $d_{CPA} = 0$. The range of CPA distances that can result in uncoordinated resolutions increases with asymmetric data uncertainty such as an ADS-B broadcast delay, but also when a heading-solution based method to account for maneuver dynamics (see e.g., [36]) is used to correct the shape of the velocity constraints. The heading-only preference that is found in many pilot evaluation studies can also eliminate a cooperative resolution, in conflict geometries where coordination requires at least one aircraft to increase velocity.

When coordination is based solely on the relative bearing between aircraft (e.g., rules of the air), it can happen that solutions that are actually very efficient, have to be discarded to comply with the coordination rule. In this study, the penalty in terms of path deviation was up to 7 nautical miles for medium-term conflicts (3-5 min). This method of coordination, however, also has its benefits. Compared to the optimal rule set, coordination based on the rules of the air is relatively robust against asymmetric data uncertainties such as an ADS-B delay: a small change in (perceived) relative position will only rarely result in the intruder moving from one relative bearing quadrant to another. Even when it does, the rules of the air are such that the applicable resolution options are consistent across quadrant boundaries. In contrast, when coordination is based on maneuver optimality, the

effects of small (asymmetric) relative position errors are not negligible, as was shown in Figure 7.12.

This study investigated coordination only in the horizontal plane, and only for single pairs of aircraft. Even in this simplified case, the results show that selecting a coordinated maneuver is not always trivial. When vertical geometry and maneuvering are also taken into account, the possibilities for maneuvering will obviously increase, but coordination rules will become more complex. Multi-aircraft conflicts will further increase this complexity, as the constraints in terms of coordination will go up exponentially. These issues should be the focus of future research.

7-6 Conclusions

In an effort to categorize how base properties of the airborne separation work domain affect safety and efficiency, regardless of specific CD&R automation, this simulation study took a systems approach to analyze the emergent properties of airborne separation. The result was a completely deterministic set of simulations, where base properties of conflict geometry, coordination regulation, and system delay, were varied.

Two important results were found from these simulations. First, results show that certain conflict situations exist, where aircraft speed limits make any kind of coordinated maneuver impossible, unless coordination rules take individual aircraft capabilities into account. These restrictions on cooperative maneuvering are imposed solely by the geometry of the conflict, which means that for any coordination rule that does not consider specific aircraft capabilities, there exist situations where cooperative maneuvering will not be possible.

Second, it was found that although the rules of the air relatively often result in situations where speed limits inhibit a coordinated maneuver, because of the large maneuvers that are sometimes required, they are much more robust against data uncertainties that affect only one aircraft, such as an ADS-B transmission delay. When this delay increases, shortest-way-out methods can lose coordination, because the shape of the velocity constraints is sensitive to small changes in relative position.

Even though these simulations cannot provide conclusive results regarding safety, they do provide valuable insights, which can be incorporated in the design of regulation, automation, and visualization for the future airborne separation system.

7-7 Bibliography

- [1] **JPDO**. Concept of Operations for the Next Generation Air Transportation System, Version 2.0. Tech. rep., Joint Planning and Development Office, 2007.
- [2] **Federal Aviation Administration**. Nextgen Implementation Plan 2012. Tech. Rep. March, 2012.
- [3] **SESAR Consortium**. SESAR Definition Phase D3: The ATM Target Concept. Tech. Rep. DLM-0612-001-02-00, Eurocontrol, 2007.
- [4] **SESAR Consortium**. European ATM Master Plan - Edition 2. Tech. rep., SESAR-JU, 2012.
- [5] **J. M. Flach**. Complexity: learning to muddle through. *Cognition, Technology & Work*, 2012.
- [6] **J. W. Andrews, H. Erzberger, and J. D. Welch**. Safety analysis for advanced separation concepts. *Air Traffic Control Quarterly*, 2006.
- [7] **P. Brooker**. Airborne Separation Assurance Systems: towards a work programme to prove safety. *Safety Science*, 42(8), 723–754, 2005.
- [8] **N. Leveson**. *Engineering a Safer World*. MIT Press, Boston (MA), 1 edn., 2011. ISBN 978-0-262-01662-9.
- [9] **K. J. Vicente and J. Rasmussen**. Ecological Interface Design: Theoretical Foundations. *IEEE Transactions on Systems, Man, and Cybernetics*, 22(4), 589–606, 1992.
- [10] **C. M. Burns and J. R. Hajdukiewicz**. *Ecological Interface Design*. CRC Press LLC, FL: Boca Raton, 2004. ISBN 0415283744.

- [11] **J. Ellerbroek, M. Visser, S. B. J. van Dam, M. Mulder, and M. M. van Paassen.** Design of an Airborne Three-Dimensional Separation Assistance Display. *IEEE Transactions on Systems, Man, and Cybernetics, part A: Systems and Humans*, 41(6), 863–875, 2011. ISSN 1083-4427. doi: 10.1109/TSMCA.2010.2093890.
- [12] **J. Ellerbroek, K. C. R. Brantegem, M. M. van Paassen, and M. Mulder.** Design of a Co-Planar Airborne Separation Display. *IEEE Transactions on Human-Machine Systems*, 43(3), 277–289, 2013. doi: 10.1109/TSMC.2013.2242888.
- [13] **K. J. Vicente and J. Rasmussen.** The Ecology of Human-Machine Systems II: Mediating Direct-Perception in Complex Work Domains. *Ecological Psychology*, 2(3), 207–249, 1990.
- [14] **M. H. J. Amelink.** *Ecological Automation Design, Extending Work Domain Analysis*. Dissertation, Delft University of Technology, 2010.
- [15] **J. Ellerbroek, M. Mulder, and M. M. van Paassen.** Evaluation of a Separation Assistance Display in a Multi-Actor Experiment. In: *Proceedings of the 16th International Symposium on Aviation Psychology*, 2011.
- [16] **A. Bicchi and L. Pallottino.** On Optimal Cooperative Conflict Resolution for Air Traffic Management Systems. *IEEE Transactions on Intelligent Transportation Systems*, 1(4), 221–231, 2000.
- [17] **K. D. Bilimoria.** A Geometric Optimization Approach to Aircraft Conflict Resolution. In: *AIAA Guidance, Navigation, and Control Conference and Exhibit*. Denver (CO), 2000.
- [18] **L. Pallottino, A. Bicchi, and S. Pancanti.** Safety of a decentralized scheme for free-flight ATMS using mixed integer linear programming. *Proceedings of the American Control Conference*, 2002.
- [19] **K. D. Bilimoria, K. S. Sheth, H. Q. Lee, and S. R. Grabbe.** Performance Evaluation of Airborne Separation Assurance for Free Flight. *Air Traffic Control Quarterly*, (August), 2003.
- [20] **H. A. P. Blom and G. J. Bakker.** Free flight safety risk modeling and simulation. In: *ICRAT 2006*, 2006.

- [21] **R. A. Paielli**. Evaluation of Tactical Conflict Resolution Algorithms for Enroute Airspace. *Journal of Aircraft*, 48(1), 324–330, 2011.
- [22] **Z. H. Mao, E. M. Feron, and K. D. Bilimoria**. Stability of intersecting aircraft flows under decentralized conflict avoidance rules. In: *AIAA Guidance, Navigation, and Control Conference and Exhibit*, August, 2000.
- [23] **K. D. Bilimoria, B. Sridhar, and G. Chatterji**. Effects of conflict resolution maneuvers and traffic density on free flight. In: *AIAA Guidance, Navigation and Control Conference and Exhibit*, July, 1996.
- [24] **R. Schild and J. K. Kuchar**. Operational Efficiency of Maneuver Coordination Rules for Airborne Separation Assurance System. In: *3rd USA/Europe Air Traffic Management R&D Seminar Napoli*. Naples, Italy, 2000.
- [25] **J. D. Lee and N. Moray**. Trust, Control Strategies and Allocation of Function in Human-Machine Systems. *Ergonomics*, 31(10), 1243–1270, 1992.
- [26] **R. Parasuraman and V. Riley**. Humans and Automation: Use, Misuse, Disuse, Abuse. *Human Factors*, 39(2), 230–253, 1997.
- [27] **M. Eby**. A self-organizational approach for resolving air traffic conflicts. *The Lincoln Laboratory Journal*, 1994.
- [28] **J. M. Hoekstra, R. N. H. W. van Gent, and R. C. J. Ruigrok**. Designing for Safety: the Free Flight Air Traffic Management Concept. *Reliability Engineering and System Safety*, 75, 215–232, 2002.
- [29] **S. B. J. van Dam, M. Mulder, and M. M. van Paassen**. Ecological Interface Design of a Tactical Airborne Separation Assistance Tool. *IEEE Transactions on Systems, Man, and Cybernetics, part A: Systems and Humans*, 38(6), 1221–1233, 2008.
- [30] **International Civil Aviation Organization (ICAO)**. Rules of the Air and Air Traffic Services (Doc 4444). Tech. rep., 1996.
- [31] **R. K. Menon, G. D. Sweriduk, and B. Sridhar**. Optimal strategies for free-flight air traffic conflict resolution. *Journal of Guidance Control and Dynamics*, 22(2), 202–211, 1999. doi:10.2514/2.4384.

- [32] **L. Pallottino, E. M. Feron, and A. Bicchi.** Conflict Resolution Problems for Air Traffic Management Systems Solved With Mixed Integer Programming. *IEEE Transactions on Intelligent Transportation Systems*, 3(1), 3–11, 2002. ISSN 15249050. doi:10.1109/6979.994791.
- [33] **D. M. Henderson.** *Applied Cartesian Tensors for Aerospace Simulations*. American Institute of Aeronautics and Astronautics, 2006. ISBN 1-56347-793-9.
- [34] **A. Nuic, D. Poles, and V. Mouillet.** BADA: An Advanced Aircraft Performance Model for Present and Future ATM Systems. *International Journal of Adaptive Control and Signal Processing*, 24(10), 850–866, 2010.
- [35] **A. P. Shah, A. R. Pritchett, K. M. Feigh, S. A. Kalaver, A. Jadhav, D. M. Holl, R. C. Bea, and A. Z. Gilgur.** Analyzing air traffic management systems using agent-based modeling and simulation. In: *Proceedings of the 6th USA/Europe Air Traffic Management Research and Development*. Georgia Institute of Technology, 2005.
- [36] **S. B. J. van Dam, M. Mulder, and M. M. van Paassen.** Airborne Self-Separation Display with Turn Dynamics and Intruder Intent-Information. In: *IEEE International Conference on Systems, Man and Cybernetics*. IEEE, Montreal, Canada, 2007.

Discussion and conclusions

Discussion and conclusions

This chapter combines results and conclusions from each of the preceding chapters. It aims to obtain an overarching view on the challenges of designing a situation awareness tool for airborne separation, and to illustrate how the concepts developed in this thesis face up to complex, real-world applications. This chapter also discusses the difficulties of evaluating tools designed to be used by experts, especially those created for domains that do not yet exist.

8-1 Design of an airborne separation assistance display

Since 2005, a 'master plan' for the future of the European Airspace System has been laid out, to overcome its current capacity problems [1, 2]. The most ambitious plans, which will take place beyond 2020, propose (various degrees of) delegation of separation responsibility from the air-traffic controller to the aircrew, as a way to reduce controller workload and increase airspace capacity. These plans will have far-reaching consequences for the degree of automation, both on the ground and in the cockpit. While this increase in automation is not necessarily a problem in itself, it does raise the question how tasks should be distributed, and, more importantly, how they should be coordinated between human and automated actors [3–10]. This thesis considered the changes required on the flight-deck, when separation responsibility is delegated to the aircrew.

8-1-1 Interfacing humans, automation, and work

A key observation for any change on the flight deck is that the introduction of automated systems cannot be considered in isolation: human operators and automation are not independent actors. Rather, they share a work domain, in which both operate, and adding a piece of automation will have a profound effect on the nature of the human operator's role in the system. Especially because pilots remain responsible for the proper functioning and safety of their aircraft, the level of cooperation between humans and automation will be a deciding factor for the feasibility of airborne separation.

For automation to be cooperative, it needs to be both observable and directable [7]. Observability of automation implies that the human operator is able to follow the line of reasoning in the decision making of the automated system. This interaction requires a shared representation of the situation [7, 11, 12]. More specifically, not only should the operator have insight in the functioning of the automation itself (the more traditional *dyadic* approach to interface design), humans and automation should also share a common understanding of the work domain, which is what Bennett and Flach call a *triadic* approach to interface design [13].

The purpose of this thesis, therefore, was to determine what kind of information would be required for this shared representation, and to determine how this information should be presented, such that it maximizes transparency of automation. The focus lay on the representation of work domain information, which resulted in two design concepts, presented in Chapter 3 and Chapter 4. A constraint-based approach was used, inspired by Ecological Interface Design (EID), to reveal and categorize the semantic structure of the work domain (Section 3-2), in an effort to provide a common basis on which both automation and visualization can be based [14, 15].

According to Billings [16], as long as humans remain responsible for the actions of the automation, they must also have unequivocal authority over the decision-making process of the automation. More than providing just a single resolution, that can either be accepted or ignored, the automation needs to provide means of cooperative interaction, such that the human operator can direct the solution methods of the automation. More specifically, the human operator should not be there only to resolve the anomalies in the functioning of the automation, but should be actively involved in the normal operational decision process [17]. Although this thesis does not present any automated mode of resolution, the presentation of work domain constraints in the concepts in this thesis does provide a basis for directable automation, as it provides a way to compare resolution options, and to evaluate how each of the resolutions relates to the separation problem. Because this work domain information invariably forms the premise on which automation bases its actions, presenting this information will be essential for active involvement of human operators in the decision-making process.

8-1-2 Visual form

Vicente and Rasmussen identified three dimensions that define the core of the interface design problem: *content* (what are the goal-relevant properties of the work domain?), *structure* (how are these properties related?), and *form* (what visual form should be used to represent these properties?) [14]. In EID, content and structure are determined through a work domain analysis, using tools such as the Abstraction Hierarchy (AH), developed by Rasmussen [18]. Section 3-2 presented a work domain analysis for the airborne

separation problem, that is based on previous analyses [19–22]. The resulting AH identifies productivity, efficiency, and safety as primary functional goals, and shows how they relate to several holonomic (energy equations, principles of absolute and relative locomotion, ...) and nonholonomic (separation margins, airspace structure, ...) constraints. The analysis also revealed how the relevant properties of the work domain can be categorized as being either internal, or external to the own aircraft.

Determining an appropriate visual form, however, does not have a clearly defined recipe in EID (neither, for that matter, do most, if not all, other interface design paradigms) [23, 24]. On the other hand, while in the domain of process control, the application of EID could benefit from a relatively large amount of freedom to design a radically new display, the flight-deck has a well-defined, existing ecology, where significant modifications or additions are complicated by issues such as limited display real-estate, a strict and lengthy certification process, and training issues. The existing ecology, therefore, determines the reference situation for any new cockpit display. For travel planning and avoidance, pilots already make use of the outside view and existing cockpit instruments, to perceive the affordances of the airspace. The previous separation assistance concepts, as well as the two concepts in this study, aimed to enhance this perception, by adding overlays that reveal higher-order information about the separation problem [22, 25].

The first of the two concepts that preceded this thesis, the horizontal separation assistance display, used the Horizontal Situation Display (HSD) to present the travel affordances. The second display, the vertical separation assistance display, projected the additional information on the Vertical Situation Display (VSD). Both concepts present a planar projection of the own aircraft three-dimensional maneuver space. These projections represent simplified, two-dimensional versions of the maneuver space. Because of this planar projection, both displays inescapably discard information about the three-dimensional structure. The aim of the concepts in this thesis was, therefore, to find a representation that captures as much as possible the relevant information of the multi-dimensional separation problem.

A crucial aspect in this analysis is that concessions with respect to revealing the three-dimensional structure of the separation problem are inescapable, a problem inherent to the presentation of multi-dimensional data

on a two-dimensional display [26, 27]. This thesis argued that these concessions should be motivated based on the task requirements for the resulting display. This task-oriented approach seemingly conflicts with Vicente's view, who argues that a task-based approach to display design might impede other strategies [14]. The fact that a task-based approach can have this effect can indeed clearly be seen with the one-dimensional bands visualization in initial versions of the P-ASAS system. The argument for one-dimensional bands is that current practice rarely incorporates multi-dimensional resolutions, i.e., a task-based decision. In practice, however, the automated resolution system that accompanies the bands display can generate two-dimensional solutions, which are not recognizable as valid solutions on the one-dimensional bands. Also more generally, there are conflict situations where one-dimensional resolutions either do not exist (because of a speed limit), or are very inefficient (a heading solution at equal velocities, resulting in a parallel course). In these situations, a two-dimensional maneuver can have a clear advantage over a one-dimensional maneuver.

The limiting factors of a two-dimensional screen remain a fact, however, so if the relevant work domain information can not be unambiguously presented within the dimensions of the interface, the next logical aspect to consider is what kind of tasks are performed in that work domain [28, 29]. This means that aside from the task of airborne separation itself, also the implications of interaction with existing tasks (e.g., path planning) should be examined. The horizontal and vertical display concepts preceding the work in this thesis, therefore, related airborne separation to horizontal trajectory management, and vertical path management, respectively. These concepts showed that the separation constraints can be functionally presented in two dimensions, that could be mapped onto existing situation displays [22, 25]. The constraint projections in these displays are valid, under the assumption that a conflict lies exactly in the plane of projection. When this assumption no longer holds, the projected constraints can become overly conservative. To go beyond these single planar projections, two options can be distinguished: perspective displays and co-planar displays: options that were both considered in this thesis. Chapter 3 investigated an egocentric (semi-)perspective display, whereas Chapter 4 considered a co-planar approach.

Here, the choice for a particular visualization depends on the specifics of the separation task, and in which context it is performed. From previous

studies and experiments, several arguments can be found for the use of a co-planar display. First, experiments presented in this thesis, as well as those performed in other studies, showed that pilots have a strong preference for single-axis resolution maneuvers [30–33]. Although this does not imply that one-dimensional representations should be used (the above discussion), it does argue for a co-planar over a perspective display, because only a co-planar representation provides an undistorted view on the constraints along each axis. A second argument for a co-planar display can be drawn from the design of each of the constraint-based separation assistance displays. They illustrate that traffic constraints can become complex, yet precise judgment of these constraints is valuable for safe and efficient conflict resolution. They also illustrate that the planar projections of the constraints show an intuitive relation with the absolute geometry of the conflict, which benefits situation awareness. Perspective distortion makes this relation less visible in a perspective projection, a problem that also hampered the semi-perspective display concept (Chapter 3). Although that concept employed constant-velocity cutting planes to reduce the complexity of the constraint visualization, it did not reproduce the intuitive visual relation with the spatial representation of the conflict, which is still present in the co-planar display concept.

In summary, although for the ‘perfect’ shared representation, one might argue that the interface should present an unambiguous view on the relevant constraints within the work domain, the fact that, in the case of the separation problem, part of the complexity of the work domain is due to the multi-dimensionality of the constraints, makes this difficult, if not impossible to achieve. This sets many real-world interface design challenges apart from simplified EID examples such as the DURESS micro-world [14, 34].

8-2 Experimentation and evaluation

The second part of this thesis presented two human subject evaluations of the separation assistance display concepts (Chapter 5 and Chapter 6), and the results from a fast-time simulation (Chapter 7). Each of the experiments investigated the effect of using constraint displays in terms of safety, efficiency, and situation awareness. This section will discuss several of the configuration issues for these kinds of experiments, and pervasive types of behavior for these displays.

8-2-1 Evaluating automation transparency

The displays in this thesis are designed to help a pilot understand the reasoning behind automated decisions, by showing constraints and relationships within the work domain. This focus on automation transparency, however, does not reflect in the configuration of the evaluation experiments described in this thesis. Rather, the focus of the experiments was on how the displayed information affects the pilots' situation awareness, regardless of specific implementation of automated conflict resolution. In anticipated situations, as long as automation is functioning properly, the outcome of an evaluation with explicit resolution automation would be trivial, as subjects would not be encouraged to participate in the assessment of conflict situations. An experiment with explicit resolution automation is therefore of limited value for the evaluation of a separation assistance display. It are the unanticipated situations where well-informed pilots, supported by good interfaces, prove their worth, but these are by definition impossible to evaluate. As an alternative, therefore, the interface concepts were evaluated as if automated resolution had already failed, and the pilots' resolution decisions were used to give insight in how the information on the display is used by pilots, and how it affects their situation awareness. This way, the pilots' ability to comprehend automated resolutions is evaluated by observing how well they make decisions themselves, based on the information available on the displays.

8-2-2 Evaluating an expert tool

In contrast to what many people seem to expect with the term 'ecological', EID displays are not necessarily intended to be natural, or easy to use. On the contrary, EID is aimed at complex domains, and ecological displays are designed as expert tools [24, 35, 36]. A complicating factor for the domain under analysis in this thesis, that of airborne separation, is that it represents a situation that is not currently implemented. In commercial aviation (the source of experienced test subjects), the task of separation is performed centrally (by Air-Traffic Control), not by the pilot*. An experiment that elicits expert behavior and expert opinion for the task of airborne separation will therefore be difficult to achieve.

*It should be noted that in uncontrolled airspace, separation is performed decentrally by General Aviation (GA) pilots, under visual flight rules. Because the domain under evaluation is that of unmanaged airspace, however, GA pilots were not considered as test subjects.

Situation awareness

An effect of this can, for instance, be seen in Chapter 5, where results from the evaluation of the co-planar separation display show that SA scores drop markedly with higher SA levels (i.e., Endsley's levels of *perception, comprehension, and projection* [37].), regardless of the type of visualization. Proper training is therefore an important issue for these concepts and their evaluation. The fact that many subjects assigned the highest usefulness ratings to the more classical TCAS symbols that were used in the experiment, can therefore also indicate that they do not fully understand what information is required to perform the *new* task of conflict resolution, and what this means for the requirements on the visualization of this information.

In terms of conflict resolution performance in normal situations, however, both experiments show that, regardless of training, pilots are able to use the visualizations to find efficient resolutions. Because these kinds of displays make several complex relationships directly perceivable, they relieve pilots from cognitive work. This transforms tasks that ordinarily require SA at the projection level to simple tasks of perception and observation, allowing pilots to perform well, despite insufficient training.

The measurement of situation awareness is also a factor of complexity in these kinds of experiments, as even the definition of SA is a subject of debate [38]. Explicit SA measures, for instance, either have to rely on the subjects' memory for a reliable measurement (i.e., with retrospective measurements), or they run the risk of directing the subjects' attention, when SA queries are probed on-line [38, 39]. Flach also warns that relating operator performance to their situation awareness (implicit SA measurements) can be sensitive to circular reasoning: "*How does one know that SA was lost? Because the operator responded inappropriately. Why did the operator respond inappropriately? Because SA was lost.*" [40]. In other words, a bad decision made by a pilot might have been due to a wrong interpretation of the problem (i.e., a loss of SA), or it could have been that the pilot made a bad decision, despite having an accurate picture of the situation (i.e., a decision error) [41].

An alternative explicit method was therefore introduced for the experiment in Chapter 5. To mitigate the downsides of existing methods, participants in the experiment each performed two sub-experiments, that separated the explicit from the implicit SA measurements. In the first (main)

experiment, subjects were asked to actively resolve conflict situations in a real-time simulated environment. The performance measures from this experiment were used as implicit indicators of level of SA. In an additional passive experiment, subjects were presented with static conflict situations, that were accompanied with a set of time-limited, multiple-choice SA questions, centered around Endsley's levels of SA [37]. These measures were used to compare the display variants in terms of how they influence situation awareness.

By separating the explicit SA assessment from the active experiment, behavior in the main experiment no longer runs the risk of being directed by particular SA queries, and at the same time, the explicit measurements are not hampered by the drawbacks of retrospective SA assessments. No matter how good the SA measurement method, however, attempts to measure the relevant components of situation awareness will always depend on the context in which the measurements are made [42, 43]. Predicting how a new interface would influence situation awareness in real-world situations, from measurements in a synthetic experimental environment, will therefore not always produce accurate results, even when subjects in the experiment are domain experts, and have been properly trained.

Safety

A persistent result found in the experiments presented in this thesis, but also in other experiments with a constraint-based display, is that after reaching a conflict-free state, the majority of the subjects returned to their original track in several small steps, following the edge of the constraint area as closely as possible [44]. This behavior can be attributed to showing precise constraints: when maneuver limits are visualized with high precision, human operators will use that precision to maximize their efficiency. This 'hunting' behavior, however, in some instances also led to small judgment errors, which in the current context can lead to losses of separation. Although such incursions are mostly minor (see Section 5-7), this is still an undesired side effect of showing precise constraints.

According to Rasmussen's model of 'Migration to Accidents', requirements for efficiency, and a tendency towards the least amount of effort, cause operators to seek the limits of system performance. The relative salience of

these limits on ecological displays thus provides an extra invitation for this hunting behavior [45]. Borst and Flach argue that the balance between mitigating this behavior, and maintaining flexibility, requires a balance between physical (holonomic) and intentional (non-holonomic) constraints and their representations in ecological information aids [46, 47]. Note, though, that the separation assistance displays in their current form already present a mixture of physical and intentional constraints (for example, although separation minima relate to aspects such as the turbulence wake of an aircraft, the values that are used for separation are generalized, and do not necessarily represent the physical margins). A possible modification to these displays could therefore be to differentiate explicitly between the physical and the intentional part of each constraint [48].

Coordination

If conflicts are to be resolved in a decentralized fashion, coordination between the actors in each conflict will be required to guarantee safe separation. This means that for automated, as well as for manual conflict resolution, predictability of decisions will be essential to guarantee an acceptable level of safety. The experiment in Chapter 6 and the fast-time simulations in Chapter 7 were designed to observe how implicit coordination between actors is influenced by factors such as the definition of the coordination rules, the geometry of a conflict, and the variability from sources such as pilot preferences and uncertainties within the system.

A systematic evaluation of these factors is difficult, as the problem of coordination is complex, both in terms of dimensionality and in terms of interdependence [49]. The problem is multi-dimensional in the traditional sense (i.e., separation is a four-dimensional problem), but also in terms of solution space complexity, when multiple (> 2) actors are involved in a conflict. Furthermore, the interdependence of constraints is reciprocal, i.e., the constraints for several actors, or even the various constraints for one actor change, depending on how one actor decides to resolve a conflict. The experiment in Chapter 6 showed that due to this variability, a large number of subjects (± 100) are required to obtain statistically significant results. On the other hand, results from fast-time simulations of a behavioral model depend largely on the accuracy of the pilot decision model. The large variability of

the interactions between pilots can result in emerging behavior that is hard to predict. This makes that many aspects of the model remain a best guess.

Nevertheless, the experiment and fast-time simulation studies produced two important findings. First, in the simulation study it was shown that for any coordination rule that does not consider specific aircraft capabilities, there exist situations where cooperative maneuvering will not be possible. In these cases, the only available cooperative maneuver for the slower aircraft in a conflict would be not to maneuver at all. This has important repercussions for the safety of the system: The system would be safest if all aircraft in a conflict are individually able to resolve the conflict, each in a way that would be cooperative with the possible maneuvers of the other aircraft in the conflict. This way, the safe course of an aircraft that has right of way does not depend on the actions of another aircraft.

A second observation related to the comparison between the optimal coordination rule, and the rules of the air. In some situations, the rules of the air result in maneuvers that require large speed increases, which increases the chance that a resolution is obscured by a speed limit. The optimal rules, on the other hand, are ambiguous in terms of coordination around the bisector of the velocity constraints. The range of conflict situations that can result in uncoordinated resolutions increases with asymmetric data uncertainty such as an ADS-B broadcast delay, but also when a heading-solution based method to account for maneuver dynamics (see e.g., [50]) is used to correct the shape of the velocity constraints. Together, these findings stress the importance of coordination, both from a human factors perspective, and for the design of conflict resolution automation.

8-3 Limitations and recommendations

The research in this thesis has been limited to self-separation in unmanaged airspace, under idealized conditions. This means that interactions with other limiting factors within the work domain, such as weather and terrain, have been left out of the equation. In the current plans for the future air space system, self-separation is intended to be performed only in the cruise phase. It can therefore be justified that terrain is not taken into account. Weather, however, can be a significant factor in airborne separation: bad weather cells

can restrict large parts of the available airspace, and the presence of wind can skew the internal aircraft maneuver limits. Adding to the complexity is the fact that weather is not always a rigid constraint, as bad weather cells do not always completely inhibit aircraft from moving through the area [41]. For future design iterations it should therefore be considered to include additional types of constraints, to increase the real-world applicability of the display.

Even though the future trajectories of the own aircraft, as well as those of other aircraft, can significantly influence maneuver constraints, the concepts in this study present only state-based short term constraints. The applicability of this method will depend on the situations in which the separation display will be used, and how the final concepts for four-dimensional trajectory planning will be implemented. For instance in situations where the aircraft trajectory is managed by manipulating trajectory points, pilots might benefit more from a constraint visualization that relates directly to such modifications [51, 52].

The traffic scenarios in the experiments are also not always representative of real-world situations. Conflicts are on a shorter timescale, and relative orientations are designed to provide measurable results, and sometimes also to elicit specific behavior. The experiment in Chapter 6, for instance, evaluates coordination between aircraft when manually resolving conflicts, even though conflict resolution in unmanaged airspace will most likely be highly automated. The importance of *implicit* coordination, however, also applies to conflict resolution automation, to be able to guarantee a sufficient level of safety. Also, since the aircrew will always be ultimately responsible for the safety of a maneuver, there will be limits on the complexity of automated resolution logic.

In both experiments presented in this thesis, visualizations on the displays are created using perfect data. In real-life situations, however, the data used in displays is uncertain, for instance due to sensor noise. On the one hand, Vicente argues that because constraints are so easy to perceive, operators might confuse the displayed state of the work domain with its true state [23, 53]. Borst and Flach, on the other hand, argue that, provided that the mapping of the work domain on the interface is sufficiently complete, the visualizations of the relationships between measured data makes errors

in one of these parameters more salient, not less so [46]. In the context of airborne separation displays, the salience of such display uncertainties will sometimes depend on the magnitude of the error (for instance, an intruder aircraft flying well below the minimum velocity will be easier to detect than the same aircraft with a measured velocity that is just a few knots off), and will be more salient when the data can be related to another reference (such as a constraint). This becomes more difficult for data that have no confining context (such as position errors and the communication delays in Chapter 7). Future experiments are therefore recommended that can evaluate the separation assistance display in off-normal situations, i.e., situations where the accuracy of data cannot be guaranteed, as well as other system malfunctions or emergency situations.

8-4 Conclusions

Since 2005, a plan for the future of the European Airspace System has been laid out, to overcome current and future capacity problems. Long-term plans propose delegation of separation responsibility from the controller to the aircrew, as a way to reduce controller workload and increase airspace capacity. These plans acknowledge the importance of human-centered automation and transparency through visualization, and state that a display of traffic information should be present in the cockpit. Most existing concepts, however, do not go beyond showing elementary traffic information, in combination with explicit automation commands. The concepts and experiments in this thesis show that it is possible to improve upon these displays by showing how the own aircraft maneuverability is affected by proximate traffic and performance limits, and how the various resulting elements on the display relate to each other. The aim of this method is to create a shared representation, between human operators and automation, that facilitates proper interaction between automated and human actors.

Because displays confine visualization possibilities to a two-dimensional form, concessions with respect to revealing the three-dimensional structure of the separation problem are inescapable. From the analysis in this thesis it was concluded that a co-planar representation is preferred over a perspective display, as it presents an undistorted view on the traffic situation and

resulting constraints, and because it retains an intuitive view on the many relationships between constraints and elements within the work domain. The co-planar display was also considered preferable because it conforms more to existing tasks and interfaces on the flight-deck.

Results from evaluations of the concepts showed that, despite the lack of experience with the task of self-separation and with the novel display, pilots performed well, and were able to use the visualizations to apply their own preferences and rules to the resolution of traffic conflicts. It was, however, also found that the visualization of precise constraints sometimes leads pilots to migrate towards working at the limits of that system, in an effort to increase performance. This behavior sometimes gives rise to judgment errors, which can lead to minor losses of separation. Both manned and simulation experiments also showed that coordination of maneuvers between aircraft should play an important role in the design of interface and automation, especially when data cannot be considered perfect.

8-5 Bibliography

- [1] **SESAR Consortium.** SESAR Definition Phase D3: The ATM Target Concept. Tech. Rep. DLM-0612-001-02-00, Eurocontrol, 2007.
- [2] **SESAR Consortium.** European ATM Master Plan - Edition 2. Tech. rep., SESAR-JU, 2012.
- [3] **D. A. Norman.** The “Problem” of Automation: Inappropriate Feedback and Interaction, not “Over-Automation”. *Philosophical Transactions of the Royal Society of London*, 327(1241), 585–593, 1990. ISSN 0962-8436. doi: 10.1098/rstb.1990.0101.
- [4] **N. B. Sarter and D. D. Woods.** Pilot Interaction With Cockpit Automation: Operational Experiences With the Flight Management System. *The International Journal of Aviation Psychology*, 2(4), 303–321, 1992. doi:10.1207/s15327108ijap0204_5.
- [5] **R. Parasuraman and V. Riley.** Humans and Automation: Use, Misuse, Disuse, Abuse. *Human Factors*, 39(2), 230–253, 1997.

- [6] **G. Lintern.** An Affordance-Based Perspective on Human-Machine Interface Design. *Ecological Psychology*, 12(1), 65–69, 2000.
- [7] **K. Christoffersen** and **D. D. Woods.** How To Make Automated Systems Team Players. In: **E. Salas**, ed., *Advances in Human Performance and Cognitive Engineering Research*, vol. 2, chap. 1, pp. 1—12. Elsevier, 2002. ISBN 0-7623-0864-8.
- [8] **A. M. Bisantz** and **A. R. Pritchett.** Measuring the Fit Between Human Judgments and Automated Alerting Algorithms: A Study of Collision Detection. *Human Factors*, 45(2), 266–280, 2003.
- [9] **B. Hilburn**, **R. Parasuraman**, **P. Jha**, and **K. McGarry.** Emerging Human Factors Issues in Future Air Traffic Management, 2006.
- [10] **A. Q. V. Dao**, **S. Brandt**, **V. Battiste**, **K. P. Vu**, **T. Strybel**, and **W. W. Johnson.** The Impact of Automation Assisted Aircraft Separation on Situation Awareness. In: *Human Interface and the Management of Information. Information and Interaction*, pp. 738–747. Springer, 2009.
- [11] **H. H. Clark** and **S. E. Brennan.** Grounding in communication. *Perspectives on socially shared cognition*, 13(1991), 127–149, 1991. ISSN 14726920. doi:10.1016/S0921-8890(98)00023-2.
- [12] **K. Höök.** Steps to take before intelligent user interfaces become real. *Interacting with Computers*, 12(4), 409–426, 2000. ISSN 09535438. doi:10.1016/S0953-5438(99)00006-5.
- [13] **K. B. Bennett** and **J. M. Flach.** *Display and interface design: Subtle science, exact art.* CRC Press, 2011. ISBN 978-1420064384.
- [14] **K. J. Vicente** and **J. Rasmussen.** The Ecology of Human-Machine Systems II: Mediating Direct-Perception in Complex Work Domains. *Ecological Psychology*, 2(3), 207–249, 1990.
- [15] **M. H. J. Amelink.** *Ecological Automation Design, Extending Work Domain Analysis.* Dissertation, Delft University of Technology, 2010.
- [16] **C. E. Billings.** *Aviation Automation: The Search for a Human-Centered Approach.* CRC Press, 1 edn., 1996. ISBN 0805821279.

- [17] **C. E. Billings.** Human-Centered Aviation Automation: Principles and Guidelines. *Nasa Technical Memorandum*, (February), 1996.
- [18] **J. Rasmussen.** The Role of Hierarchical Knowledge Representation in Decision Making and System Management. *IEEE Transactions on Systems, Man, and Cybernetics*, 15(2), 234–243, 1985.
- [19] **M. M. van Paassen.** Functions of Space and Travellers. In: *Proceedings of 18th European Annual Conference on Human Decision Making and Manual Control*. Faculty of Aerospace Engineering, Delft University of Technology, 1999.
- [20] **R. M. de Neef and M. M. van Paassen.** Functional Modeling of Airspace. In: *Conference on Human Decision Making and Manual Control*. Orsted DTU, Automation, 2001.
- [21] **M. M. van Paassen, M. Mulder, and S. B. J. van Dam.** Cognitive Work Analysis for Vehicle Locomotion - Aircraft Short-Term Path Planning. In: *IFAC/IFIP/IFORS/IEA Symposium: Analysis, Design and Evaluation of Human Machine Systems*, vol. 46, p. 5. Faculty of Aerospace Engineering, Delft University of Technology, Atlanta GA, 2004.
- [22] **S. B. J. van Dam, M. Mulder, and M. M. van Paassen.** Ecological Interface Design of a Tactical Airborne Separation Assistance Tool. *IEEE Transactions on Systems, Man, and Cybernetics, part A: Systems and Humans*, 38(6), 1221–1233, 2008.
- [23] **K. J. Vicente.** Ecological Interface Design: Progress and Challenges. *Human Factors*, 44, 62–78, 2002.
- [24] **C. M. Burns and J. R. Hajdukiewicz.** *Ecological Interface Design*. CRC Press LLC, FL: Boca Raton, 2004. ISBN 0415283744.
- [25] **F. M. Heylen, S. B. J. van Dam, M. Mulder, and M. M. van Paassen.** Design and Evaluation of a Vertical Separation Assistance Display. In: *AIAA Guidance, Navigation, and Control Conference and Exhibit*. Honolulu (HI), 2008.
- [26] **M. S. T. Carpendale, D. J. Cowperthwaite, and F. D. Fracchia.** Extending Distortion Viewing from 2D to 3D. *Computer Graphics and Applications, IEEE*, 17(4), 42–51, 1997.

- [27] **M. St John, M. B. Cowen, H. S. Smallman, and H. M. Oonk.** The Use of 2D and 3D Displays for Shape-Understanding versus Relative-Position Tasks. *Human Factors*, 43(1), 79–98, 2001.
- [28] **C. M. Burns and K. J. Vicente.** Model-Based Approaches for Analyzing Cognitive Work: A Comparison of Abstraction Hierarchy, Multilevel Flow Modeling, and Decision Ladder Modeling. *International Journal of Cognitive Ergonomics*, 5(3), 357–366, 2001. ISSN 10886362. doi: 10.1207/S15327566IJCE0503_13.
- [29] **G. A. Jamieson, C. A. Miller, W. H. Ho, and K. J. Vicente.** Integrating Task- and Work Domain-Based Work Analyses in Ecological Interface Design: A Process Control Case Study. *IEEE Transactions on Systems, Man, and Cybernetics, part A: Systems and Humans*, 37(6), 887–905, 2007. doi:10.1109/TSMCA.2007.904736.
- [30] **J. M. Hoekstra.** *Designing for Safety: The Free Flight Air Traffic Management Concept*. Ph.D. thesis, Delft University of Technology, The Netherlands, 2001.
- [31] **C. D. Wickens, J. Helleberg, and X. Xu.** Pilot Maneuver Choice and Workload in Free Flight. *Human Factors and Ergonomics Society Annual Meeting Proceedings*, 44(2), 171–188, 2002. doi: 10.1518/0018720024497943.
- [32] **A. L. Alexander, C. D. Wickens, and D. H. Merwin.** Perspective and Coplanar Cockpit Displays of Traffic Information: Implications for Maneuver Choice, Flight Safety, and Mental Workload. *The International Journal of Aviation Psychology*, 15, 1–21, 2005.
- [33] **C. L. A. Steens, S. B. J. van Dam, M. M. van Paassen, and M. Mulder.** Comparing Situation Awareness for Two Airborne Separation Assistance Interfaces. In: *AIAA Guidance, Navigation and Control Conference and Exhibit*. Honolulu (HI), 2008.
- [34] **K. J. Vicente.** Cognitive work analysis: Implications for microworld research on human-machine interaction. In: *IEEE International Conference on Systems, Man and Cybernetics*, vol. 4, pp. 3432–3436, 1995.

- [35] **K. J. Vicente** and **J. Rasmussen**. Ecological Interface Design: Theoretical Foundations. *IEEE Transactions on Systems, Man, and Cybernetics*, 22(4), 589–606, 1992.
- [36] **K. J. Vicente**. *Cognitive Work Analysis Toward Safe, Productive and Healthy Computer-Based Work*. Lawrence Erlbaum Associates Mahwah, NJ, 1999.
- [37] **M. R. Endsley**. Toward a Theory of Situation Awareness in Dynamic Systems. *Human Factors*, 37(1), 32–64, 1995.
- [38] **J. Uhlarik** and **D. A. Comerford**. A Review of Situation Awareness Literature Relevant to Pilot Surveillance Functions. Tech. Rep. DOT/FAA/AM-02/3, Federal Aviation Authorities, 2002.
- [39] **A. M. McGowan** and **S. P. Banbury**. Evaluating Interruption-Based Techniques using Embedded Measures of Driver Anticipation. In: **S. P. Banbury** and **S. Tremblay**, eds., *A Cognitive Approach to Situation Awareness: Theory and Application*, pp. 176–192. Ashgate, 2004. ISBN 978-0-7546-4198-8.
- [40] **J. M. Flach**. Situation Awareness: Proceed with Caution. *Human Factors*, 37(1), 149–157, 1995.
- [41] **C. Borst**. *Ecological Approach to Pilot Terrain Awareness*. Dissertation, Delft University of Technology, 2009.
- [42] **D. D. Woods**. Paradigms for intelligent decision support. In: **E. Hollnagel**, **G. Mancini**, and **D. D. Woods**, eds., *Intelligent decision support in process environments*, chap. 11. Springer-Verlag New York, Inc., New York, NY, 1986. ISBN 0-387-13922-2.
- [43] **N. B. Sarter** and **D. D. Woods**. Situation Awareness - A Critical But Ill-Defined Phenomenon. *The International Journal of Aviation Psychology*, 1(1), 45–57, 1991.
- [44] **C. Borst**, **M. Mulder**, and **M. M. van Paassen**. Design and Simulator Evaluation of an Ecological Synthetic Vision Display. *Journal of Guidance, Control and Dynamics*, 33(5), 1577–1591, 2010. doi:10.2514/1.47832.
- [45] **J. Rasmussen**. Risk Management In A Dynamic Society : A Modelling Problem. *Safety Science*, 27(2), 183–213, 1997.

- [46] **C. Borst** and **J. M. Flach**. Ecological Interface Design: Twenty Years and Counting. *in preparation*, 2013.
- [47] **J. R. Hajdukiewicz**, **C. M. Burns**, **K. J. Vicente**, and **R. G. Eggleston**. Work Domain Analysis for Intentional Systems. In: *Proceedings of the Human Factors and Ergonomics Society Annual Meeting*, vol. 43, pp. 333–337, 1999. ISSN 1071-1813. doi:10.1177/154193129904300343.
- [48] **J. Comans**, **C. Borst**, **M. M. van Paassen**, and **M. Mulder**. Risk Perception in Ecological Information Systems. In: *Proceedings of the 17th International Symposium on Aviation Psychology*. Dayton (OH), 2013.
- [49] **J. M. Flach**. Complexity: learning to muddle through. *Cognition, Technology & Work*, 2012.
- [50] **S. B. J. van Dam**, **M. Mulder**, and **M. M. van Paassen**. Airborne Self-Separation Display with Turn Dynamics and Intruder Intent-Information. In: *IEEE International Conference on Systems, Man and Cybernetics*. IEEE, Montreal, Canada, 2007.
- [51] **B. J. A. Van Marwijk**, **C. Borst**, **M. A. Mulder**, **M. Mulder**, and **M. M. Van Paassen**. Supporting 4D Trajectory Revisions on the Flight Deck : Design of a Human-Machine Interface. *The International Journal of Aviation Psychology*, 21(1), 35–61, 2011. ISSN 10508414. doi: 10.1080/10508414.2011.537559.
- [52] **R. Klomp**, **M. M. van Paassen**, **C. Borst**, and **M. Mulder**. Joint Human-Automation Cognition through a Shared Representation of 4D Trajectory Management. In: **D. Schaefer**, ed., *Proceedings of the SESAR Innovation Days*. EUROCONTROL, Braunschweig, Germany, 2012.
- [53] **O. St-Cyr**. Impact of sensor noise magnitude on emergent features of ecological interface design. In: *Human Factors and Ergonomics Society Annual Meeting Proceedings*, vol. 50, pp. 319–323. Human Factors and Ergonomics Society, 2006.

Appendices

Horizontal and vertical projected constraints

A-1 Defining a conflict

Figure A.1 illustrates a generic traffic situation with ownship and one intruder. Here, ownship and intruder will be in conflict when the ownship relative velocity vector ($\mathbf{V}_{rel} = \mathbf{V}_{own} - \mathbf{V}_{int}$), is pointed towards the intruder protected zone, i.e., if the ownship relative track crosses the intruder protected zone.

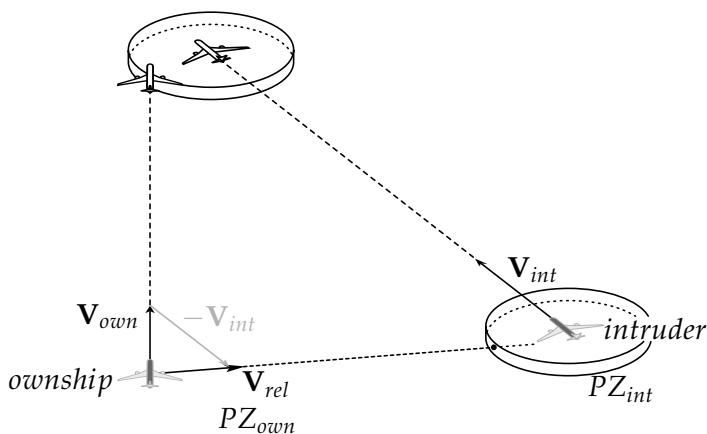


Figure A.1: Example conflict situation.

In the experiments in Chapter 5 and Chapter 6, horizontal conflicts are defined using parameters *conflict angle* (CA), *distance at closest point of approach* (d_{CPA}), *time to (horizontal) loss of separation* ($t_{los,hor}$), the *ownship track angle* (χ_{own}), and the *ground speed of both aircraft* ($V_{GS,own}$, $V_{GS,int}$), see Figure A.2.

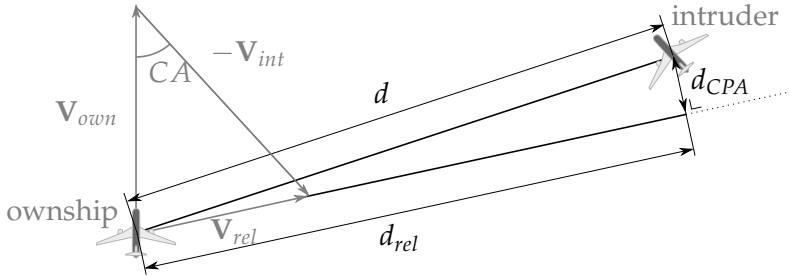


Figure A.2: Parameters used to define a horizontal conflicting traffic situation.

From these parameters, first the velocity vectors for ownship and intruder are calculated:

$$\begin{aligned} \mathbf{V}_{own} &= V_{GS,own} \cdot \begin{pmatrix} \cos \chi \\ \sin \chi \end{pmatrix}, \\ \mathbf{V}_{int} &= V_{GS,int} \cdot \begin{pmatrix} \cos (\chi_{own} - CA) \\ \sin (\chi_{own} - CA) \end{pmatrix}. \end{aligned} \quad \text{A.1}$$

The relative velocity vector ($\mathbf{V}_{rel} = \mathbf{V}_{own} - \mathbf{V}_{int}$), is then used in combination with the time to horizontal loss of separation to calculate the length of the relative distance vector:

$$d_{rel} = t_{los,hor} \cdot |\mathbf{V}_{rel}| + \sqrt{R_{PZ}^2 - d_{CPA}^2}, \quad \text{A.2}$$

with R_{PZ} the radius of the intruder protected zone. Using the property that d , d_{CPA} , and d_{rel} form a right triangle, the relative distance vector of the intruder position relative to the ownship is determined as:

$$\mathbf{x}_{rel} = \begin{bmatrix} d_{rel} & d_{CPA} \\ -d_{CPA} & d_{rel} \end{bmatrix} \cdot \frac{\mathbf{V}_{rel}}{|\mathbf{V}_{rel}|}. \quad \text{A.3}$$

For vertically oriented conflicts, the vertical speed of both aircraft (VS_{own} , VS_{int}), and either the vertical distance between ownship and intruder (Δh),

or the time to vertical loss of separation times the difference in vertical speed ($t_{los,ver} \cdot (VS_{own} - VS_{int}) \pm h_{PZ}$), should be added as vertical components of Equation (A.1), and Equation (A.3), respectively.

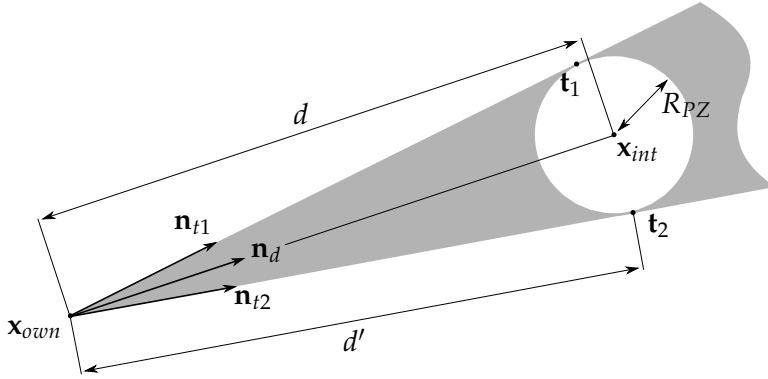


Figure A.3: Relevant parameters for horizontal traffic constraints.

A-2 Derivation of the horizontal forbidden area

The unit vectors for the direction of the lines that span the horizontal forbidden area can be determined from Figure A.3. The lines are tangent to the intruder protected zone, therefore, they are simply the projections of distance vector $\mathbf{d} = d \cdot \mathbf{n}_d = \mathbf{x}_{int} - \mathbf{x}_{own}$ onto the line through \mathbf{x}_{own} , tangent to the intruder protected zone:

$$d' = d \cdot \mathbf{n}_d \cdot \mathbf{n}_t. \quad \text{A.4}$$

Here, d' is the projected \mathbf{d} , which equals $d' = \sqrt{d^2 - R_{PZ}^2}$. The unit vectors \mathbf{n}_{t1} and \mathbf{n}_{t2} can be determined by rotating \mathbf{n}_d using rotation matrix R , which is defined as:

$$R = \begin{bmatrix} \sqrt{1 - \left(\frac{R_{PZ}}{d}\right)^2} & \frac{R_{PZ}}{d} \\ -\frac{R_{PZ}}{d} & \sqrt{1 - \left(\frac{R_{PZ}}{d}\right)^2} \end{bmatrix}. \quad \text{A.5}$$

Using R , the tangent vectors can be calculated:

$$\mathbf{n}_{t1} = R\mathbf{n}_d, \quad \text{A.6}$$

$$\mathbf{n}_{t2} = R^T\mathbf{n}_d. \quad \text{A.7}$$

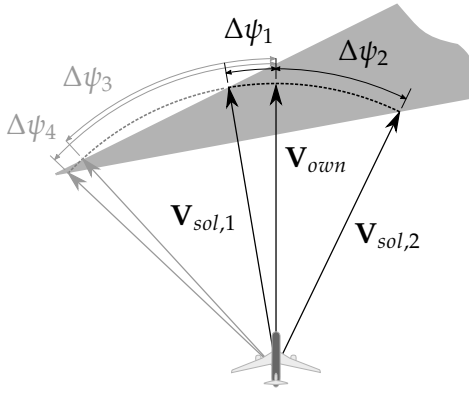


Figure A.4: Heading maneuver solutions in a traffic conflict.

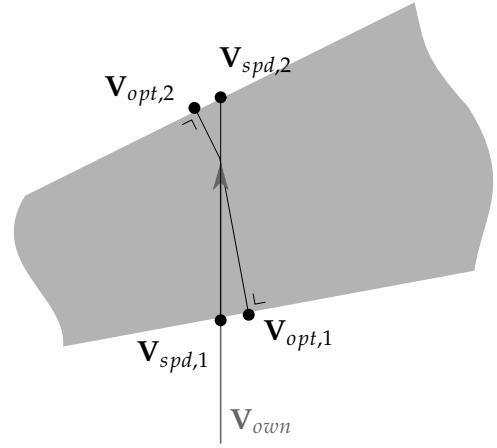


Figure A.5: Speed solutions and geometrically optimal solutions.

A-3 Horizontal resolution maneuvers

When conflicts and conflict-free states are observed for a certain fixed ownship velocity magnitude $|\mathbf{V}_{own}|$, transitions between conflicting and conflict-free headings are marked by the intersections of the legs of the forbidden area and the circular set of vectors for ownship velocity at constant magnitude $|\mathbf{V}_{own}|$, see Figure A.4. Each line-circle intersection equation can have either zero, one, or two solutions. Together, these can result in, respectively, zero, one, or two heading ranges that generate a conflict.

These intersections can be determined by substituting the general line equation into the general circle equation: The general equation for a line:

$$\mathbf{x} = \mathbf{x}_0 + t \cdot \mathbf{n}. \quad \text{A.8}$$

The general equation for a circle or a sphere:

$$\|\mathbf{x} - \mathbf{c}\|^2 = r^2. \quad \text{A.9}$$

Substituted gives:

$$\|\mathbf{x}_0 + t \cdot \mathbf{n} - \mathbf{c}\|^2 = r^2. \quad \text{A.10}$$

Or, expanded and rearranged:

$$t^2 \cdot (\mathbf{n}^2) + t \cdot (2 \cdot \mathbf{n} \cdot (\mathbf{x}_0 - \mathbf{c})) + (\mathbf{x}_0^2 + \mathbf{c}^2 - 2 \cdot \mathbf{x}_0 \cdot \mathbf{c} - r^2) = 0. \quad \text{A.11}$$

Because \mathbf{n} is a unit vector, this simplifies to:

$$t^2 + t \cdot (2 \cdot \mathbf{n} \cdot (\mathbf{x}_0 - \mathbf{c})) + (\mathbf{x}_0^2 + \mathbf{c}^2 - 2 \cdot \mathbf{x}_0 \cdot \mathbf{c} - r^2) = 0. \quad \text{A.12}$$

Solving for t :

$$t = \frac{- (\mathbf{n} \cdot (\mathbf{x}_0 - \mathbf{c})) \pm \sqrt{(\mathbf{n} \cdot (\mathbf{x}_0 - \mathbf{c}))^2 - (\mathbf{x}_0^2 + \mathbf{c}^2 - 2 \cdot \mathbf{x}_0 \cdot \mathbf{c} - r^2)}}{2}. \quad \text{A.13}$$

The discriminant, $\Delta = (\mathbf{n} \cdot (\mathbf{x}_0 - \mathbf{c}))^2 - (\mathbf{x}_0^2 + \mathbf{c}^2 - 2 \cdot \mathbf{x}_0 \cdot \mathbf{c} - r^2)$, determines the amount of solutions.

1. $\Delta < 0$: There are no real roots, and therefore no intersections between the circle and the line.
2. $\Delta = 0$: There is exactly one root: in this case the line is tangent to the circle.
3. $\Delta > 0$: There are two roots, the line intersects the circle twice.

For the heading solutions from Figure A.4, the following substitutions can be made: $r = \|\mathbf{V}_{own}\|$, $\mathbf{c} = (0, 0)$, $\mathbf{x}_0 = \mathbf{V}_{int}$, $\mathbf{n} = \mathbf{n}_t$, and $t = \|\mathbf{V}_{rel}\|$. Then:

$$\|\mathbf{V}_{rel}\| = - (\mathbf{n}_t \cdot \mathbf{V}_{int}) \pm \sqrt{(\mathbf{n}_t \cdot \mathbf{V}_{int})^2 - \mathbf{V}_{int}^2 + \|\mathbf{V}_{own}\|^2}. \quad \text{A.14}$$

The corresponding relative and ownship velocity vectors can now be determined:

$$\mathbf{V}_{rel} = \|\mathbf{V}_{rel}\| \cdot \mathbf{n}_t, \quad \text{A.15}$$

$$\mathbf{V}_{own} = \mathbf{V}_{rel} + \mathbf{V}_{int}. \quad \text{A.16}$$

Figure A.5 shows horizontal solutions where only speed is varied, and geometrically optimal solutions that result in the minimum path deviations. The geometrically optimal solutions can be calculated using the dot product between the relative velocity vector and the respective forbidden area leg:

$$\mathbf{V}_{rel,sol} = (\mathbf{V}_{rel} \cdot \mathbf{n}_t) \cdot \mathbf{n}_t, \quad \text{A.17}$$

$$\mathbf{V}_{own,sol} = \mathbf{V}_{int} + \mathbf{V}_{rel,sol}. \quad \text{A.18}$$

Speed solutions can be calculated using the following equation:

$$(\mathbf{V}_{int} + V_{rel,sol} \cdot \mathbf{n}_t) \times \mathbf{V}_{own} = \mathbf{V}_{own,sol} \times \mathbf{V}_{own}. \quad \text{A.19}$$

Because $\mathbf{V}_{own,sol}$ and \mathbf{V}_{own} are parallel, the cross product between these vectors is equal to zero. This reduces Equation (A.19) to:

$$(\mathbf{V}_{int} + V_{rel,sol} \cdot \mathbf{n}_t) \times \mathbf{V}_{own} = 0, \quad \text{A.20}$$

$$V_{rel,sol} = \frac{-\mathbf{V}_{int} \times \mathbf{V}_{own}}{\mathbf{n}_t \times \mathbf{V}_{own}}. \quad \text{A.21}$$

The corresponding ownship solution vector can now be calculated:

$$\mathbf{V}_{own,sol} = V_{rel,sol} \cdot \mathbf{n}_t + \mathbf{V}_{int}. \quad \text{A.22}$$

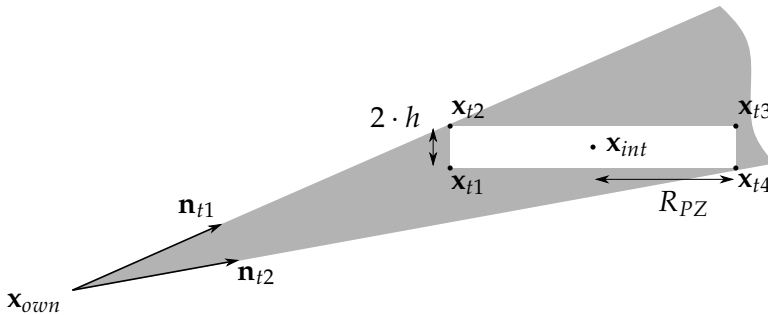


Figure A.6: Relevant parameters for vertical traffic constraints.

A-4 Derivation of the vertical forbidden area

Figure A.6 shows relevant parameters for the vertical forbidden area. These constraints should apply to ownship's vertical maneuvering for the current ownship heading, which means that the vertical forbidden area corresponds with a vertical projection of the three-dimensional forbidden area. When viewed from the side, the intruder protected zone is rectangular, with a width of two times the horizontal separation minimum, and a height of two times the vertical separation minimum. Relative to ownship, the four

corners of this projection are located as follows:

$$\mathbf{x}_t = \mathbf{x}_{int} - \mathbf{x}_{own} \pm \begin{pmatrix} R_{PZ} \\ 0 \end{pmatrix} \pm \begin{pmatrix} 0 \\ h \end{pmatrix}, \quad \text{A.23}$$

$$\mathbf{n}_t = \mathbf{x}_t / |\mathbf{x}_t|. \quad \text{A.24}$$

From these four vectors, the two vectors are selected that have the widest angle between them.

Constant-speed constraints

The concept in Chapter 3 presents two types of constraint areas combined in a single integrated display. One constraint area presents traffic constraints on ownship maneuvering for constant ownship velocity, the other area represents constraints on intruder relative velocity for constant relative velocity magnitude. Both these constraint areas are derived using the intersection between the three-dimensional forbidden area and a sphere of constant velocity. This appendix will derive an analytical expression for the three-dimensional forbidden area, and will derive the cone-sphere intersection equations.

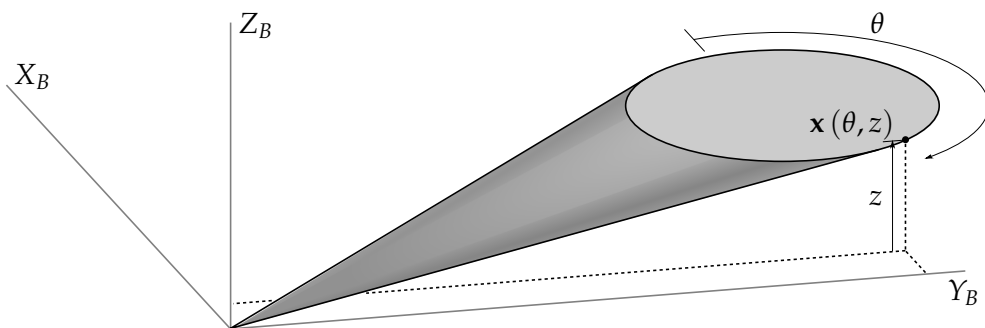


Figure B.1: A three-dimensional slanted cone. Any point along this cone can be described by an angular coordinate along the circular cross-section of the cone, θ , and a vertical coordinate, z .

B-1 Parametric description of three-dimensional traffic constraints

The three-dimensional forbidden area can be seen as a construct of two slanted cones, connected by straight sections. Both cones have their apex at the ownship position, and their curvature is aligned with the upper and lower circles of the intruder protected zone. Equation (B.1) gives an analytical expression for a point $\mathbf{x}_{FA}(\theta, z)$ on a slanted cone, see also Figure B.1:

$$\begin{aligned} \mathbf{x}_{FA}(\theta, z) &= \mathbf{V}_{int} + z \cdot \begin{pmatrix} (dx + R_{PZ} \cos \theta) (dz \pm h_{PZ})^{-1} \\ (dy + R_{PZ} \sin \theta) (dz \pm h_{PZ})^{-1} \\ 1 \end{pmatrix} \\ &= \mathbf{V}_{int} + z \cdot \mathbf{R}_c(\theta). \end{aligned} \quad \text{B.1}$$

Here, $(dx; dy; dz) = \mathbf{x}_{rel}$ is the relative distance vector between ownship and the intruder, h_{PZ} is the height of the intruder protected zone, and z and θ are the two free equation parameters, representing the vertical coordinate along the cone, and the angular coordinate along a protected zone circle, respectively.

B-2 Constant-ownspeed constraints

A sphere with the current ownship velocity as its radius can be described as follows:

$$\mathbf{x}^2 = V_{own}^2. \quad \text{B.2}$$

Substituting Equation (B.1) into Equation (B.2) gives:

$$(\mathbf{V}_{int} + z \cdot \mathbf{R}_c)^2 = V_{own}^2, \quad \text{B.3}$$

$$\mathbf{R}_c^2 \cdot z^2 + 2\mathbf{V}_{int} \cdot \mathbf{R}_c \cdot z + \mathbf{V}_{int}^2 - V_{own}^2 = 0. \quad \text{B.4}$$

Solving for z yields:

$$z = \frac{-\mathbf{V}_{int} \cdot \mathbf{R}_c \pm \sqrt{(\mathbf{V}_{int} \cdot \mathbf{R}_c)^2 - \mathbf{R}_c^2 (V_{int}^2 - V_{own}^2)}}{\mathbf{R}_c^2}. \quad \text{B.5}$$

Using this equation, values for z can be obtained as a function of the other free parameter, θ . The Cartesian coordinates for each point on the intersection can be found by substituting the values for z and θ into Equation (B.1).

B-3 Constant relative speed constraints

The relative speed constraints are derived in a similar manner, but with a different equation for the three-dimensional forbidden area (the forbidden area for the relative speed constraints isn't translated over the intruder speed, and is observed from the intruder side), and a different radius for the speed sphere equation. The relative speed forbidden area can be defined as follows:

$$\begin{aligned} \mathbf{x}_{FA,rel}(\theta, z) &= z \cdot \begin{pmatrix} (-dx + R_{PZ} \cos \theta) (-dz \pm h_{PZ})^{-1} \\ (-dy + R_{PZ} \sin \theta) (-dz \pm h_{PZ})^{-1} \\ 1 \end{pmatrix} \\ &= z \cdot \mathbf{R}_{c,rel}. \end{aligned} \tag{B.6}$$

Substituting this equation into Equation (B.2), where V_{own}^2 is replaced by V_{rel}^2 gives:

$$z^2 \cdot \mathbf{R}_{c,rel}^2 = V_{rel}^2. \tag{B.7}$$

Solving for z yields:

$$z = \sqrt{\frac{V_{rel}^2}{\mathbf{R}_{c,rel}^2}}. \tag{B.8}$$

Again, the Cartesian coordinates for each point on the intersection can be found by substituting the values for z and θ into Equation (B.6).

Horizontal and vertical reduced constraints

The co-planar concept presented in Chapter 4 uses cutting planes to determine more precise traffic constraints for horizontal and vertical conflict resolution. Constraints derived using these cutting-plane methods are still valid when a conflict cannot be purely defined in the horizontal plane ($\Delta h = 0$, $VS_{own} = 0$, $VS_{int} = 0$), or the vertical plane ($\Delta\chi = 0$, $\Delta y = 0$). The initial concept for this co-planar display uses a conical (constant climb angle) cutting plane to derive the horizontal reduced constraints, the final concept substitutes this with a horizontal, flat cutting plane (constant vertical speed). Main reasons are that the resulting shapes are more consistent and intuitive, and that constant vertical speed maneuvers are more common. This appendix will, however, present both methods, as well as the vertical cutting plane method.

C-1 Horizontal reduced constraints using a conical cutting plane

Equation (C.1) gives an analytical description of a straight cone, with its apex at $(0, 0)$, which can be used to represent the constant flight-path angle speed-heading zone, see Figure C.1:

$$(\mathbf{x} \cdot \mathbf{e}_3)^2 = \mathbf{x}^2 \cdot \sin^2 \gamma.$$

C.1

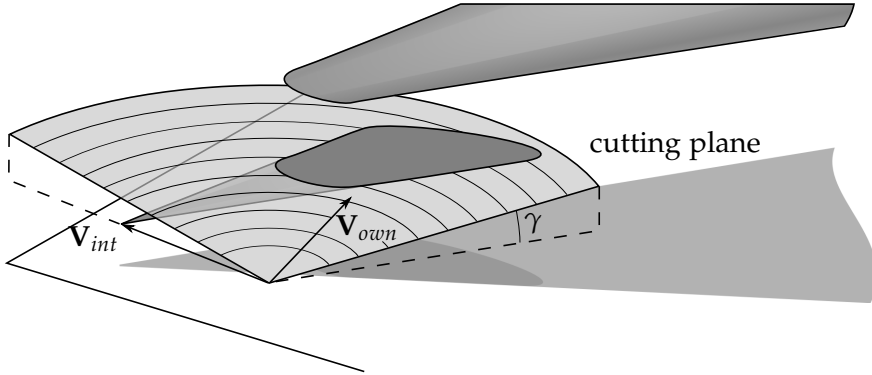


Figure C.1: The horizontal reduced constraint area in one of the initial concepts was given by the intersection of the three-dimensional constraint area, and a conical cutting plane.

Here, \mathbf{e}_3 is the vertical unit vector $\mathbf{e}_3 = (0, 0, 1)$. Substituting Equation (B.1) into Equation (C.1) gives:

$$((\mathbf{V}_{int} + z\mathbf{R}_c) \cdot \mathbf{e}_3)^2 = (\mathbf{V}_{int} + z\mathbf{R}_c)^2 \sin^2 \gamma, \quad \text{C.2}$$

$$(\mathbf{V}_{int} \cdot \mathbf{e}_3 + z)^2 = (\mathbf{V}_{int} + z\mathbf{R}_c)^2 \sin^2 \gamma. \quad \text{C.3}$$

Or, rewritten as a quadratic equation for z :

$$\begin{aligned} 0 &= (1 - \sin^2 \gamma \mathbf{R}_c^2) z^2 + 2\mathbf{V}_{int} \cdot (\mathbf{e}_3 - \sin^2 \gamma \mathbf{R}_c) z \\ &+ ((\mathbf{V}_{int} \cdot \mathbf{e}_3) - \sin^2 \gamma \mathbf{V}_{int}^2). \end{aligned} \quad \text{C.4}$$

Solving for z yields:

$$z = \frac{-b \pm \sqrt{b^2 - ac}}{a}, \quad \text{C.5}$$

where $a = 1 - \sin^2 \gamma \mathbf{R}_c^2$, $b = \mathbf{V}_{int} \cdot (\mathbf{e}_3 - \sin^2 \gamma \mathbf{R}_c)$, and $c = (\mathbf{V}_{int} \cdot \mathbf{e}_3) - \sin^2 \gamma \mathbf{V}_{int}^2$. Using this equation, values for z can be obtained as a function of the other free parameter, θ (See Figure B.1 and Equation (B.1) for an illustration of z and θ). Although the quadratic equation can have two solutions, only one of them will be valid at a time. The corresponding conjugate

value represents the same point on a mirrored cone, that is in the opposite direction of the intruder. The Cartesian coordinates for each point on the intersection can be found by substituting the values for z and θ into Equation (B.1).

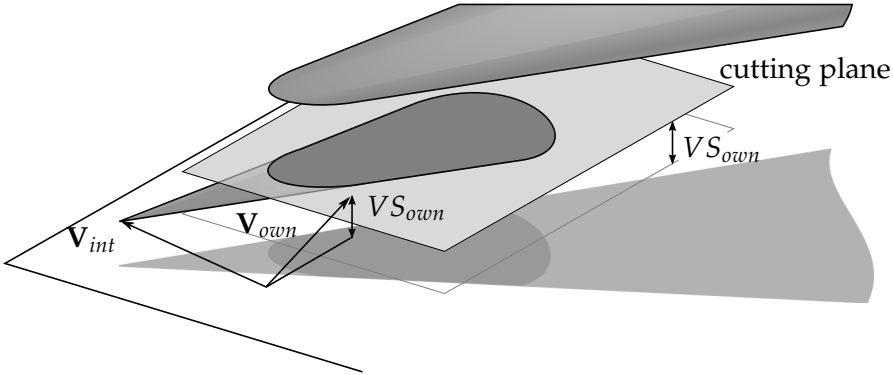


Figure C.2: The horizontal reduced constraint area is given by the intersection of the three-dimensional constraint area, and a horizontal cutting plane, offset vertically by the ownship vertical speed. The horizontal reduced area illustrates exact constraints on horizontal maneuvering, also for conflicts with non-zero relative vertical distances and velocities.

C-2 Horizontal reduced constraints using a flat cutting plane

An analytical description for the reduced constraints using a flat horizontal cutting plane, as shown in Figure C.2, are derived in a similar manner. Equation (C.6) gives an analytical description of a horizontal, flat cutting plane:

$$\mathbf{e}_3 \cdot (\mathbf{x} - \mathbf{V}_{own}) = 0. \tag{C.6}$$

Substituting Equation (B.1) into Equation (C.6) gives:

$$\mathbf{e}_3 \cdot (\mathbf{V}_{int} + z\mathbf{R}_c - \mathbf{V}_{own}) = 0. \tag{C.7}$$

Solving for z yields:

$$z = \mathbf{e}_3 \cdot (\mathbf{V}_{own} - \mathbf{V}_{int}). \tag{C.8}$$

Again, the Cartesian coordinates for each point on the intersection can be found by substituting the values for z and θ into Equation (B.1).

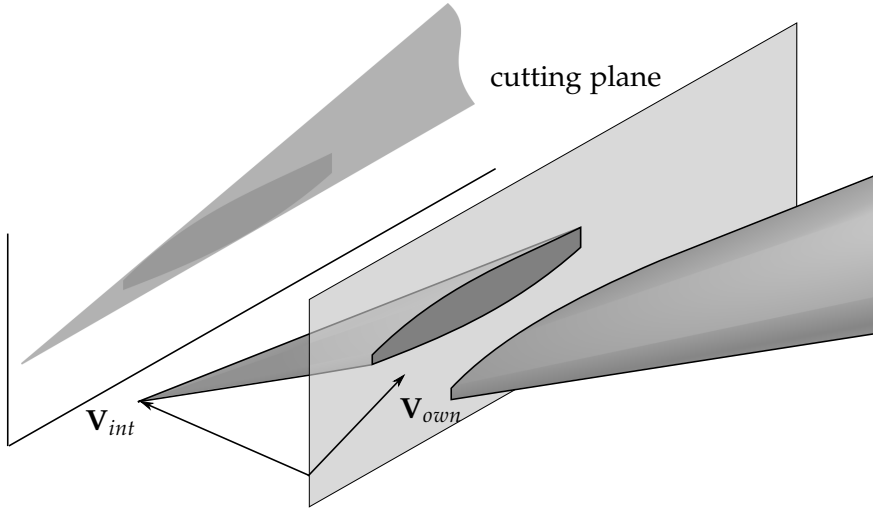


Figure C.3: The vertical reduced constraint area is given by the intersection of the three-dimensional constraint area, and a vertical cutting plane, aligned with the ownship track. The vertical reduced area illustrates exact constraints on vertical maneuvering, also for conflicts with non-zero cross-track distances and velocities.

C-3 Vertical reduced constraints using a flat cutting plane

Equation (C.9) gives an analytical description of a vertical, flat cutting plane (illustrated in Figure C.3), that is aligned with the ownship track:

$$\mathbf{n}_{V_{own}} \cdot \mathbf{x} = 0. \quad \text{C.9}$$

Here, $\mathbf{n}_{V_{own}}$ is the normal vector of the ownship velocity vector, \mathbf{V}_{own} . Substituting Equation (B.1) into Equation (C.9) gives:

$$\mathbf{n}_{V_{own}} \cdot (\mathbf{V}_{int} + z \cdot \mathbf{R}_c) = 0. \quad \text{C.10}$$

Solving for z yields:

$$z = \frac{\mathbf{n}_{V_{own}} \cdot \mathbf{V}_{int}}{\mathbf{n}_{V_{own}} \cdot \mathbf{R}_c}. \quad \text{C.11}$$

Again, values for z can be obtained as a function of the other free parameter, θ . The Cartesian coordinates for each point on the intersection can be found by substituting the values for z and θ into Equation (B.1).

Discrete event maneuver equations

This appendix describes the maneuver equations that are used in the discrete event simulations in Chapter 7. Analytical expressions are derived for a point-mass model for the following situations: unaccelerated straight flight, accelerated straight flight, turns, and accelerated turns. All of the derived equations assume an absence of wind. In the simulations, these equations are used in combination to calculate complete horizontal aircraft trajectories at discrete points in time.

D-1 Straight flight

The most basic situation is one where the aircraft is flying straight, at a constant velocity. The change in position as a function of time then only depends on the current velocity and the aircraft heading:

$$\mathbf{x}(t) = \mathbf{x}(t_0) + V_{TAS} \cdot \Delta t \cdot \begin{pmatrix} \cos \psi \\ \sin \psi \end{pmatrix}. \quad \text{D.1}$$

When there is a change in velocity, an acceleration term is added:

$$\mathbf{x}(t) = \mathbf{x}(t_0) + \left(V_{TAS} + \frac{1}{2}a\Delta t \right) \cdot \Delta t \cdot \begin{pmatrix} \cos \psi \\ \sin \psi \end{pmatrix}. \quad \text{D.2}$$

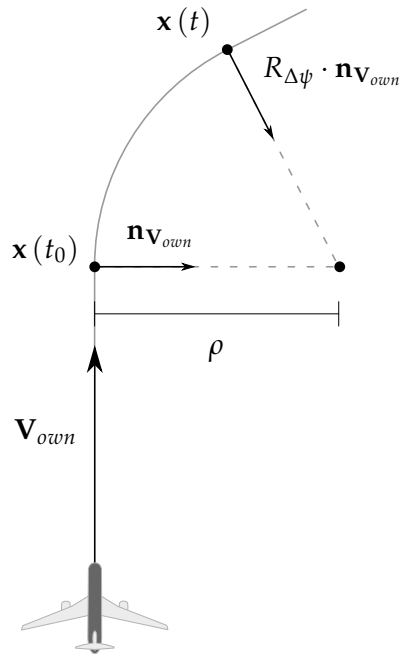


Figure D.1: Relevant parameters for an unaccelerated turn maneuver.

D-2 Unaccelerated turns

In an unaccelerated turn, the aircraft position depends not only on velocity, but also on the turn radius (ρ) and the turn rate ($\dot{\psi}$), which, in turn, both depend on bank angle and airspeed [1]:

$$\rho = \frac{V_{TAS}^2}{g \tan \phi'} \quad \text{D.3}$$

$$\dot{\psi} = \frac{g \tan \phi}{V_{TAS}} \quad \text{D.4}$$

Figure D.1 shows how the aircraft position at time t can be constructed using the following equation:

$$\mathbf{x}(t) = \mathbf{x}(t_0) + \rho \cdot (1 - R_{\Delta\psi}) \cdot \mathbf{n} \mathbf{v}_{own} \quad \text{D.5}$$

Here, $\mathbf{n}_{V_{0\text{own}}}$ is the initial track normal, and $R_{\Delta\psi}$ a rotation matrix corresponding to the change in heading:

$$R_{\Delta\psi} = \begin{bmatrix} \cos(\dot{\psi}\Delta t) & -\sin(\dot{\psi}\Delta t) \\ \sin(\dot{\psi}\Delta t) & \cos(\dot{\psi}\Delta t) \end{bmatrix}. \quad \text{D.6}$$

D-3 Accelerated turns

In an accelerated turn, turn radius and turn rate are no longer constant, but change with the changing velocity [1]:

$$\rho(t) = \frac{(V_0 + at)^2}{g \tan \phi}, \quad \text{D.7}$$

$$\dot{\psi} = \frac{g \tan \phi}{V_0 + at}. \quad \text{D.8}$$

The heading change as a function of time can be derived by integrating Equation (D.8):

$$\begin{aligned} \Delta\psi(t) &= g \tan \phi \int_0^t \frac{1}{V_0 + at} dt \\ &= \frac{g \tan \phi}{a} \left| \ln(V_0 + at) \right|_0^t \\ &= \frac{g \tan \phi}{a} \ln \left(\frac{V_0 + at}{V_0} \right). \end{aligned} \quad \text{D.9}$$

Rearranging Equation (D.7) and substituting it in Equation (D.9) gives the turn radius as a function of $\Delta\psi$:

$$\rho(\Delta\psi) = \frac{V_0^2}{g \tan \phi} e^{\frac{2a\Delta\psi}{g \tan \phi}}. \quad \text{D.10}$$

The aircraft position as a function of $\Delta\psi$ is then defined as:

$$\begin{aligned}
 \mathbf{x}(\Delta\psi) &= \mathbf{x}(t_0) + \int_0^{\Delta\psi} \rho(\psi) \cdot -\frac{d\mathbf{nv}_{own}}{d\psi} d\psi \\
 &= \mathbf{x}(t_0) + \int_0^{\Delta\psi} \rho(\psi) \begin{pmatrix} \sin \psi \\ -\cos \psi \end{pmatrix} d\psi \\
 &= \mathbf{x}(t_0) + \frac{V_0^2}{g \tan \phi} \cdot \int_0^{\Delta\psi} e^{\frac{2a\psi}{g \tan \phi}} \begin{pmatrix} \sin \psi \\ -\cos \psi \end{pmatrix} d\psi.
 \end{aligned} \tag{D.11}$$

Integration by parts gives:

$$\begin{aligned}
 \mathbf{x}(\Delta\psi) &= \mathbf{x}(t_0) \\
 &\quad - \frac{V_0^2 g \tan \phi}{4a^2 + g^2 \tan^2 \phi} \cdot e^{\frac{2a\psi}{g \tan \phi}} \begin{pmatrix} \cos \psi - \frac{2a}{g \tan \phi} \sin \psi \\ \sin \psi + \frac{2a}{g \tan \phi} \cos \psi \end{pmatrix} \Big|_0^{\Delta\psi} \\
 &= \mathbf{x}(t_0) \\
 &\quad + \frac{V_0^2 g \tan \phi}{4a^2 + g^2 \tan^2 \phi} \cdot \left(I - e^{\frac{2a\Delta\psi}{g \tan \phi}} \cdot R_{\Delta\psi} \right) \cdot \begin{pmatrix} 1 \\ \frac{2a}{g \tan \phi} \end{pmatrix}.
 \end{aligned} \tag{D.12}$$

When the aircraft heading at $t = t_0$ is not equal to zero, $\Delta\mathbf{x}(\Delta\psi)$ needs to be rotated over the initial heading:

$$\begin{aligned}
 \mathbf{x}(\Delta\psi) &= \mathbf{x}(t_0) + \frac{V_0^2 g \tan \phi}{4a^2 + g^2 \tan^2 \phi} \\
 &\quad \cdot R_{\psi_0} \cdot \left(I - e^{\frac{2a\Delta\psi}{g \tan \phi}} \cdot R_{\Delta\psi} \right) \cdot \begin{pmatrix} 1 \\ \frac{2a}{g \tan \phi} \end{pmatrix}.
 \end{aligned} \tag{D.13}$$

D-4 Bibliography

- [1] S. K. Ojha. *Flight Performance of Aircraft*. AIAA Education Series, 1995. ISBN 978-1563471131.

Abbreviations

1-D	One-dimensional
2-D	Two-dimensional
3-D	Three-dimensional
4-D	Four-dimensional
A	Augmented
ADS-B	Automatic Dependent Surveillance – Broadcast
AH	Abstraction Hierarchy
ANOVA	Analysis of Variance
ANSP	Air Navigation Service Provider
APERO	Avionics Prototyping Environment for Research and Operations
ASAS	Airborne Separation Assistance System
ATC	Air-Traffic Control
ATCo	Air Traffic Controller
ATM	Air-Traffic Management
B	Baseline
BADA	Base of Aircraft Data
CD&R	Conflict Detection and Resolution
CDTI	Cockpit Display of Traffic Information
CPA	Closest Point of Approach
CSD	Cockpit Situation Display
ECAM	Electronic Centralized Aircraft Monitor
EFB	Electronic Flight Bag

EFIS	Electronic Flight Instrument System
EID	Ecological Interface Design
EMD	Expected Miss-Distance
FA	Forbidden Area
FAA	Federal Aviation Administration
FCU	Flight Control Unit
FL	Flight Level
FMS	Flight-Management System
FPA	Flight-Path Angle
FPV	Flight-Path Vector
GA	General Aviation
HDG	Heading
HIPS	Highly Interactive Problem Solver
HSD	Horizontal Situation Display
IAS	Indicated Airspeed
LoS	Line of Sight
LoS	Loss of Separation
MCDU	Multifunction Control and Display Unit
MCL	Maximum Climb Thrust
MCP	Mode Control Panel
MCT	Maximum Continuous Thrust
MTO	Maximum Takeoff Thrust
MVP	Modified Voltage Potential
NASA	National Aeronautics and Space Administration
ND	Navigation Display
NextGen	Next Generation Air Transportation System
NLR	National Aerospace Laboratory
P-ASAS	Predictive Airborne Separation Assurance System
PFD	Primary Flight Display
PZ	Protected Zone
RAT	Route Analysis Tool
RFA	Reduced Forbidden Area
SA	Situation Awareness
SESAR	Single European Sky ATM Research
SESAR-JU	Single European Sky ATM Research Joint Undertaking
SPD	Speed
SRK	Skills, Rules, and Knowledge

SVD	Synthetic Vision Display
SVE	State-Vector Envelope
TAS	True Airspeed
TBO	Trajectory-Based Operations
TCAS II	Traffic Collision Avoidance System II
TCP	Trajectory Change Point
V/S	Vertical Speed
VSD	Vertical Situation Display

Symbols

AC_n	Aircraft n
C_{D_0}	Drag-coefficient at zero lift
D	Drag
D_{proj}	Constraint area projection distance
K	Lift-dependent drag coefficient
PZ'_{int}	Projected intruder protected zone
PZ_{int}	Intruder protected zone
PZ_{own}	Ownship protected zone
R	Rotation matrix
R_{PZ}	Protected zone radius
S	Wing surface
S'_{own}	Projected flight-path vector constraint area
S_{own}	Flight-path vector constraint area
T	Thrust
T_{max}	Maximum thrust
T_{min}	Minimum thrust
V	Velocity
V_{TAS}	True airspeed
V_{max}	Maximum velocity
V_{min}	Minimum velocity
W	Wilcoxon rank sum test statistic
W	Weight
Δh	Altitude offset

a	Acceleration
d	Distance
d'	Projected distance
d_{CPA}	Distance at closest point of approach
g	Gravitational acceleration
h_{PZ}	Protected zone height
int	Intruder aircraft
int'	Virtual intruder aircraft
own	Own aircraft
p	Probability that the zero hypothesis is true
t	Time
t_c	Time to collision
t_{CPA}	Time until closest point of approach
t_{PZ}	Time until loss of separation
t_{TCP}	Time until trajectory change point
t_{cur}	Current time
t_{turn}	Turn duration
x	Horizontal screen coordinate
y	Vertical screen coordinate
z	Wilcoxon signed rank test statistic
\mathcal{V}_{FA}	Three-dimensional forbidden area
$\Delta\chi$	Track angle offset
$\Delta\chi$	Relative track
$\Delta\psi$	Relative heading
$\Delta\psi$	Heading maneuver offset
γ	Flight-path angle
γ_E	Total energy angle
θ	Vertical visual range
μ	Mean
ρ_{SSL}	Air density at sea level
σ	Density difference dependent on altitude
ϕ	Bank angle
ϕ	Horizontal visual range
χ^2	Chi-squared statistic
χ	Track angle
$\dot{\psi}$	Turn rate
\mathbf{R}_c	Slanted cone direction coefficient vector

\mathbf{V}_{TAS}	True airspeed vector
\mathbf{e}_3	Vertical unit vector
\mathbf{n}_d	Normalized distance vector
\mathbf{n}_{ti}	Normalized forbidden area leg vector
$\mathbf{n}\mathbf{v}_{own}$	Own velocity vector normal
$\mathbf{V}_{int,post}$	Post-TCP intruder velocity vector
$\mathbf{V}_{int,pre}$	Pre-TCP intruder velocity vector
\mathbf{V}_{int}	Intruder velocity vector
\mathbf{V}_{opt}	Optimal solution velocity vector
\mathbf{V}_{own}	Ownship velocity vector
$\mathbf{V}'_{rel,int}$	Projected relative intruder velocity vector
$\mathbf{V}_{rel,int}$	Relative intruder velocity vector
\mathbf{V}_{rel}	Relative velocity vector
\mathbf{V}_{sol}	Solution velocity vector
\mathbf{V}_{spd}	Speed solution velocity vector
\mathbf{x}_i	Intruder position vector
\mathbf{x}_o	Ownship position vector
\mathbf{x}_{rel}	Relative position vector

Vliegtuig Conflictoplossing in Drie Dimensies

Joost Ellerbroek

De opkomst van automatisering in de luchtvaart is van grote invloed geweest op zowel de aard van de taken in de cockpit, als op de eisen die worden gesteld aan de bemanning. Alhoewel deze invoering van automatisering een onmiskenbare verbetering heeft teweeggebracht op het gebied van efficiëntie en veiligheid, heeft deze ook geresulteerd in een toename van complexiteit op het vliegdek. Buiten de elementaire vliegvaardigheden moeten piloten nu ook in staat zijn om het functioneren van hun geautomatiseerde systemen te controleren. Dit vereist een weloverwogen afstemming van taken tussen mens en de automatisering, alsmede dat geautomatiseerde systemen hun functioneren op een transparante wijze communiceren naar de mens. In de huidige situatie kunnen deze aspecten echter niet altijd worden gegarandeerd.

Het werk in dit proefschrift richt zich op het concept van gedecentraliseerde separatie tussen vliegtuigen, uitgevoerd vanaf het vliegdek. Deze vorm van separatie maakt deel uit van zowel Europese als Amerikaanse plannen voor de toekomst van de structuur van het luchtruim. Een dergelijk systeem kan op twee manieren worden geïmplementeerd: ofwel wordt

de verantwoordelijkheid voor de separatie tussen vliegtuigen gedeeltelijk gedelegeerd naar de vliegtuigbemanning, ofwel krijgt de bemanning volledige autonomie in het behouden van veilige separatie ten opzichte van alle nabije vliegtuigen. Een dergelijk systeem zou de werklast voor de luchtverkeersregelaar moeten verminderen, met als gevolg de mogelijkheid tot vergroting van de capaciteit van het luchtruim. Deze plannen zullen aanzienlijke gevolgen hebben voor de mate van automatisering, zowel op de grond als op het vliegdek.

Om de bemanning te ondersteunen met de separatietaak stellen de huidige plannen nieuwe automatisering voor, welke zowel in conflictdetectie als in expliciete adviezen voor conflictoplossing voorziet. De taken van de bemanning zullen daarbij in principe bestaan uit het controleren van de werking van de automatisering en het selecteren en toepassen van de resoluties die worden aangeboden door de automatisering. De bemanning zal echter te allen tijde eindverantwoordelijkheid dragen voor veilige separatie met andere vliegtuigen en voor het correct functioneren van de automatisering. Het behouden van een centrale rol voor de mens speelt daarom een prominente rol in alle plannen voor de toekomst van het luchtruim.

Met de hoge mate van automatisering, welke wordt benadrukt in de vernieuwingsplannen voor het luchtruim, wordt het belangrijker dan ooit dat automatisering en instrumentatie transparant functioneren en een hoog niveau van toestandsbewustzijn bevorderen. Alhoewel automatisering de vliegveiligheid en de werkdruk van de vliegtuigbemanning ten goede kan komen, kan het ook een vermindering teweegbrengen van de betrokkenheid van de bemanning in het besluitvormingsproces, met een vermindering van toestandsbewustzijn als gevolg. Ironisch genoeg vormt de invoering van dergelijke automatisering op deze manier een belemmering voor een piloot om weloverwogen te oordelen over het functioneren van diezelfde automatisering. Het werk in dit proefschrift is daarom gericht op onderzoek naar welke informatie nodig zou zijn voor een juiste interactie tussen de bemanning en de automatisering. Ook richt het zich op hoe deze informatie moet worden gepresenteerd, zodanig dat het de transparantie van de automatisering verhoogt en een goed toestandsbewustzijn voor de piloot bevordert.

Een belangrijk aspect van de problemen met betrekking tot de transparantie van geautomatiseerde systemen is dat, ongeacht de specifieke uitvoering van een geautomatiseerd systeem, de complexiteit van het systeem van gedecentraliseerde separatie als geheel, evenals dat van het automatische systeem zelf, direct gerelateerd is aan de complexiteit van het werkdomein waarin het systeem moet functioneren. Inzicht in het werkdomein is dus noodzakelijk om enige vorm van automatisering te kunnen begrijpen. Voor separatie geldt dat dit werkdomein kan worden gekenmerkt als een complex, open systeem, onderhevig aan meerdimensionale en vaak nauw gerelateerde eigenschappen van verscheidene objecten in het luchtruim. Al deze objecten bewegen ten opzichte van elkaar, elk met individuele randvoorwaarden en doelen.

In dit proefschrift wordt betoogd dat het vastleggen in een functionele representatie van de informatie die inherent is aan het werkdomein de basis moet vormen voor automatiseringssystemen voor separatie. Om dit te bereiken is een methode toegepast die zich richt op het tonen van beperkingen en relaties in het werkdomein. Deze methode, geïnspireerd op de ecologische interface ontwerpmethode (Eng. Ecological Interface Design, EID), kan worden gebruikt om een basis te bieden voor een systeem van transparante interactie tussen mens en automatisering. Deze methode is erop gericht de structuur van het werkdomein zichtbaar te maken. Ook zou het, samen met het verschaffen van een basis voor een automatiseringsontwerp, een interface moeten kunnen opleveren die transparantie van automatisering bewerkstelligt en die de bemanning ondersteunt in het opbouwen en onderhouden van hun toestandsbewustzijn.

Een grondige analyse van het werkdomein is vooraf gegaan aan de interface ontwerpen in dit proefschrift. Deze analyse identificeerde functionaliteiten, beperkingen en relaties tussen de verschillende elementen in het werkdomein. De Abstractie Hiërarchie (AH) was een belangrijk hulpmiddel in deze analyse. De hiërarchische structuur en de nadruk op de relaties en afhankelijkheden tussen de elementen op elk niveau en tussen niveaus maken de AH een waardevol instrument om de structuur van het werkdomein te bepalen. Als gevolg helpt de AH om te bepalen welke informatie nodig is voor een passende interactie tussen de piloten en de separatieautomatisering. De overgang van een dergelijke analyse naar een effectief ontwerp voor

een interface blijft echter een belangrijke uitdaging bij deze methode. Vergelijkbaar met andere interface ontwerpmethodes levert EID geen duidelijk omschreven recept voor het bepalen van een passende visuele representatie. Samen met voortschrijdend inzicht van experimenten en onderzoek betekent dit dat de stap van een werkdomeinanalyse naar een effectief ontwerp geen instantane transitie is, maar een transitie waar analyse, ontwerp en evaluatie elkaar volgen in een iteratief proces.

De nieuwe cockpit displays die gepresenteerd zijn in dit proefschrift moeten daarom ook worden gezien in het licht van de concepten die aan dit proefschrift vooraf gingen. Al deze voorgangers zijn tweedimensionale displays, die vlakke projecties presenteren van de driedimensionale bewegingsruimte van het eigen vliegtuig, in combinatie met de meer traditionele horizontale en verticale situatiedisplays. Deze projecties vertegenwoordigen vereenvoudigde tweedimensionale versies van de manoeuvreringsruimte. De toegepaste vlakke projectie maakt dat beide displays onvermijdelijk informatie van het driedimensionale probleem verbergen. Het doel van de concepten in dit proefschrift was daarom ook om een representatie te creëren die de relevante gegevens van het multidimensionale separatieprobleem zo goed mogelijk weergeeft.

Om te bepalen hoe de complexiteit van dit multidimensionale probleem het beste gereduceerd kan worden, beschouwt dit proefschrift tevens welke andere taken worden uitgevoerd in het werkdomein. Dit betekent dat afgezien van de separatietaak zelf, ook de implicaties van de interactie met bestaande taken (bijvoorbeeld routeplanning) werden onderzocht. De twee resulterende concepten nemen twee fundamenteel verschillende benaderingen van het visualisatie probleem. Het eerste concept presenteert een egocentrische (semi-)perspectief weergave, terwijl voor het tweede concept een tweevlakkige aanpak werd gevolgd. De uiteindelijke vergelijkende analyse tussen deze twee concepten beargumenteert een voorkeur voor het tweevlakkige display, op basis van twee argumenten. Allereerst toonden experimenten beschreven in dit proefschrift, evenals die uitgevoerd in andere studies, aan dat piloten een sterke voorkeur hebben voor éénassige oplossingsmanoeuvres. Hoewel dit niet betekent dat eendimensionale representaties moeten worden gebruikt, pleit het wel voor een tweevlakkige weergave boven een weergave met nagebootst perspectief, omdat van deze twee mogelijkheden enkel de tweevlakkige weergave een onverstoord overzicht biedt op

de beperkingen langs elke as. Een tweede argument voor een tweevlakkelig display volgt uit het ontwerp van beide separatiedisplays. Beide weergaves illustreren dat de representatie van de beperkingen als gevolg van ander verkeer complex kan worden, terwijl een nauwkeurig oordeel van deze beperkingen waardevol is voor het veilig en efficiënt oplossen van conflicten. Tevens tonen de vlakke projecties van de beperkingen een intuïtieve relatie met de absolute geometrie van het conflict, wat het toestandsbewustzijn ten goede komt.

Ondanks dat bij het ontwerp van de displayconcepten de nadruk lag op transparantie van automatisering, werd in de experimenten vooral gekeken naar handmatige conflictoplossing. De redenen hiervoor zijn dat in normale omstandigheden de evaluatie van een ondersteuningsdisplay voor een automatiseringssysteem triviaal zal zijn, omdat proefpersonen in een dergelijke configuratie niet worden aangemoedigd om deel te nemen in de beoordeling van conflictsituaties. Het zijn juist de onverwachte situaties waarin goed geïnformeerde piloten, ondersteund door goede interfaces, hun toegevoegde waarde bewijzen. Deze situaties zijn echter per definitie onmogelijk te evalueren. Als alternatief werden de interface concepten geëvalueerd in een nagebootste omstandigheid waar het geautomatiseerde systeem niet juist meer functioneert. In de analyse van deze experimenten werden de beslissingen van de proefpersonen gebruikt om inzicht te verkrijgen in de manier waarop de informatie op het display wordt gebruikt door piloten en hoe het display het toestandsbewustzijn van de piloten beïnvloedt. Op deze manier wordt het vermogen van de piloten om geautomatiseerde resoluties te begrijpen geëvalueerd door te observeren hoe goed ze besluiten zelf maken, op basis van de beschikbare informatie op de displays.

Uit de resultaten van deze evaluaties blijkt dat, ondanks de beperkte trainingsduur van de proefpersonen, ze in staat zijn om de visualisaties te gebruiken om efficiënte resoluties te vinden. Omdat deze displays een aantal complexe relaties direct waarneembaar maken ontdoen ze piloten van verscheidene cognitieve taken. Dit reduceert taken die op kennis gebaseerde probleemoplossing vereisen tot eenvoudige waarnemingstaken waar piloten hun basisvaardigheden en vooraf gedefinieerde regels kunnen toepassen, om zo conflicten veilig en efficiënt op te lossen. Dit maakt dat piloten goed kunnen presteren, zelfs met een beperkte hoeveelheid training.

De resultaten onthullen ook een persistente vorm van gedrag, waarbij de meerderheid van de proefpersonen na het bereiken van een conflictvrije toestand terug tracht te keren naar de oorspronkelijk geplande route in meerdere kleine stappen, waarbij de rand van het beperkingsgebied zo dicht mogelijk wordt gevolgd. Dit gedrag kan worden toegeschreven aan de precisie van de weergegeven beperkingen: wanneer grenzen op manoeuvreerbaarheid gevisualiseerd worden met hoge precisie zal een menselijke bestuurder die precisie gebruiken om de efficiëntie van de oplossing te maximaliseren. Deze vorm van optimalisatie kan echter in sommige gevallen ook leiden tot kleine fouten, die in de huidige context kunnen leiden tot schending van de separatieminima.

Het moet echter wel opgemerkt worden dat elke poging tot het meten van de relevante bestanddelen van het gedrag, de efficiëntie van oplossingen en het toestandsbewustzijn van piloten altijd afhankelijk zal zijn van de context waarin de metingen worden gedaan. Het voorspellen van de invloed van nieuwe interfaces op het toestandsbewustzijn in realistische situaties uit metingen in een synthetische experimentele omgeving zal dus niet altijd correcte resultaten opleveren, zelfs wanneer goed opgeleide domein experts gebruikt zijn als proefpersonen in het experiment. Ondanks deze beperkingen en ondanks het soms minder gewenste gedrag van piloten in de experimenten is het bemoedigend dat, zelfs met een zeer beperkte hoeveelheid training, piloten in staat zijn om de interfaces te gebruiken om zich meer bewust te worden van hun omgeving. Ook is het bemoedigend dat de piloten deze kennis kunnen gebruiken om de taak van conflictoplossing uit te voeren, waarbij ze hun conflictoplossingen weten te optimaliseren, maar vooral ook dat ze effectief kunnen redeneren over de conflicten die ze tegenkomen. Dit soort diepgaand begrip van het werkdomein zal essentieel zijn voor een transparante interactie tussen mens en de automatisering.

Acknowledgments

Back in high-school I never would have guessed that I would be defending a doctoral thesis some fifteen years later. In fact, the question whether I should attend university was still very much a question to me back then. In retrospect (of course) I am very happy to have made that decision, and would like to thank my parents for the unquestionable support they gave (and still give) their children in the decisions they have to make. I am, of course, also very grateful to my friends and the rest of my family, my brother and sisters, my wife Simone, and my sons Bram and Thomas: they are the ones that show you what life is really about.

During my masters study Max Mulder (my promotor) proposed an internship position for me at the Max Planck Institute for Biological Cybernetics. I still don't quite understand why he thought of that combination, but apparently he saw something in me that I myself did not quite know yet. It was at the MPI where I got enthusiastic about academic research. Max, thank you for that opportunity, your contagious enthusiasm about research, and the many fun meetings, hilarious conference visits, and for defying the *meedraaiende tegenwind* with me.

I would also like to thank my co-promotor, René *–the guru–* van Paassen. You can drop by René's office any time, and ask for a minute, he rarely lets you leave with fewer than ten. René, thank you for not just solving my problems, but for helping me solve those problems myself.

I may have lost a couple of teeth, and gained a good amount of bruises, but I still greatly enjoyed playing squash with my squash buddies Coen, Erik-Jan, Peter, Paul, Deniz, and on occasion Hans, René, Liguó, and Pieter. Alwin, thanks for all the chats, the *klusadvies*, and all your help with my various home improvement projects. I would also like to thank my other colleagues: Olaf, first my M.Sc. supervisor, now my roomie, Daan, Rita, Herman, Jan, Clark, Laurens, Wouter, Thomas, Joost, Frank, Ferdinand, Henk, Andre, and many more. We've had some great discussions in the coffee corner, and excellent conference visits, barbeque's, poker nights, basketball games, and other events. I would also like to thank my 'part-time' colleagues at the NLR, Frank, Nico, and Michiel, for the lunch walks, the chats, and for your help with my experiment.

Finally I would like to thank the many M.Sc. students I have worked with. I think I have been very lucky with a lot of very good students, that collaborated in my Ph.D. research. In chronological order the students whose M.Sc. work I have been involved with: Folkert, Gijs, Mark, Gert-Jan, Ties, Wim, Remco, Jasper, Pieter, Joris, Koen, Jochem, Wouter, Jeroen, Reinier, and Bram. I've had a lot of fun with each of you, in meetings, (preparing) experiments, and the *ingenieurs examens*. It has been a great time!

Joost Ellerbroek

Pijnacker, May 2013

Biography

Joost Ellerbroek was born on 11 April 1980 in Boskoop, The Netherlands. From 1992 to 1999 he attended the Groene Hart Lyceum in Alphen aan den Rijn, where he obtained his Atheneum diploma.

In 1999 he enrolled as a student at the Faculty of Aerospace Engineering at Delft University of Technology. As a part of his masters program, he performed an internship at the Max Planck Institute for Biological Cybernetics in Tübingen, Germany, where he prepared and performed a motion cueing experiment that investigated the effect of helicopter lateral and roll motion cues on pilot control performance. In June 2007 he obtained his M.Sc. degree in Aerospace Engineering at the Control and Simulation division. His thesis work investigated the effect of lateral and yaw-rotational motion cues on human control behavior in a helicopter hovering task.

Before starting his Ph.D. research in December 2008, he worked for a year as researcher and software developer at the Control and Simulation division of the Faculty of Aerospace Engineering at Delft University of Technology. His Ph.D. research, described in this thesis, involved the development and evaluation of a three-dimensional airborne separation assistance display.

Joost is currently assistant professor at the Faculty of Aerospace Engineering at Delft University of Technology, following a tenure track program. He is still involved in airborne separation projects, as well as other studies related to cognitive systems engineering and human-centered automation.

